SEISMIC EFFECTS ON STRUCTURES SUPPORTED ON PILES EXTENDING THROUGH DEEP SENSITIVE CLAYS

to

California State Division of Highways
under
State of California Standard Agreement
No. 14247

by

R. A. Parmelee
J. Penzien
C. F. Scheffey
H. B. Seed
G. R. Thiers

University of California
Institute of Engineering Research
August 1964

FOREWORD

This report is submitted to the California State Division of Highways in fulfillment of State of California Standard Agreement No. 14247.

The investigation was conducted under the general supervision and technical responsibility of J. Penzien, C. F. Scheffey, and H. B. Seed, Department of Civil Engineering, University of California, Berkeley, California.

TABLE OF CONTENTS

ACKNOWLEDGEMENTS

The authors wish to express their appreciation and sincere thanks to the many individuals who contributed to the completion of the general investigation reported herein; especially to Mr. A. Shah, Mr. M. Venkatesan, and Mr. I. King who wrote the digital computer programs, to Mr. K. L. Lee who participated in the soil testing program, to Dr. V. Jenschke who developed the response spectra program, and to Mr. A. Chopra and Mr. G. Wang who participated in the generation of basic response data and in the preparation of material for this report.

The authors also wish to thank Mr. John Kozak of the California State Division of Highways for his advice and encouragement on all phases of the program.

Finally the authors wish to express their appreciation to the California State Division of Highways and the U. S. Bureau of Public Roads whose financial support made this investigation possible.

The IBM-7090 digital computer used in the analysis was operated by the University of California Computer Center.

NOTATION

a	=	acceleration in dynamics test;
a_n	=	single amplitude of acceleration;
B	=	pile radius;
C	=	damping coefficient;
C_θ	=	rotational damping coefficient of pile cap;
C_i^b	=	damping coefficient of the pier at level i;
C_i^c	=	interaction creep coefficient of the clay medium at level i;
C_i^d	=	interaction damping coefficient of the clay medium at level i;
c_i	=	damping coefficient;
c	=	vertical distance of concentrated load below the boundary surface of the half-space;
$\bar{c}$	=	vertical distance from the boundary surface to the mid-height of the interval over which the uniform load acts;
c_i^c	=	creep coefficient of layer i of the clay medium;
c_i^d	=	damping coefficient of layer i of the clay medium;
d_i	=	vertical distance from base of foundation medium to mid-height of level i of the clay medium;
d_n	=	overall height of the clay medium;
D	=	creep coefficient;
$E(z)$	=	modulus of elasticity of the clay medium at depth z;
E_{os}, E_{1s} E_{2s}	=	static moduli of elasticity;
E_{od}, E_{1d} E_{2d}	=	dynamic moduli of elasticity;

e_i = vertical distance from top of clay medium to mid-height of level i of the pier system;

F_i^s = interaction force in the bi-linear hysteresis type of spring element at layer i of the clay medium;

F_{iy}^s = yielding value of interaction spring force at level i of the clay medium;

f_i^s = force in the bi-linear hysteresis type of spring element at layer i of the clay medium;

G = shear modulus of the clay medium;

g = acceleration of gravity;

h = half height of discrete layer of the clay medium

I_n = rotary moment of inertia of pile cap;

K_{ie} = elastic spring constant for concentrated interaction spring at level i;

K_θ = rotational spring constant of pile cap;

k' = Winkler continuous spring constant for a single pile;

k'' = Winkler continuous spring constant for a pile group;

k_{iy}^a = stiffness influence coefficient of piles at layer i;

k_{iy}^b = stiffness influence coefficient of the pier at level i;

M_i = $M_i^e + M_i^p$ = total mass at level i;

M^d = mass of the bridge deck and girders;

M_i^e = effective mass of the clay medium at level i;

M_i^p = mass of the piles at level i;

M_n = mass of pile cap;

m = number of discrete masses in the idealized bridge and pier system;

m_i = lumped mass of clay medium at discrete point i;

m_i^b = mass of bridge pier at level i;

n = number of discrete masses in the idealized clay system;

P = concentrated horizontally applied load;

p = intensity of uniform line loading;

q = ultimate compressive strength of clay;

Q = number of piles per group;

R_1, R_2 = magnitudes of principle position vectors;

r, θ, z = cylindrical coordinates;

S_i = axial load carried by the piers at level i;

T_i = axial load carried by the piles at level i;

U_i^r = relative displacement of the pile group at level i;

U_i^s = displacement of interaction spring at level i;

u_x = horizontal displacement in the x direction as produced by loading acting in the x direction;

u_i^r = relative displacement of mass i of the clay medium;

u_i^s = displacement of the spring element associated with mass i of the clay medium;

$\ddot{u}_g$ = earthquake ground acceleration;

W^p = weight of single pier per foot of height;

γ = unit weight of clay medium;

γ_s = principal shear strain;

δ_i = soil test displacement;

δ_{rs} = Kronecker delta;

ϵ_1 = major principal compression strain;

$\dot{\epsilon}_i$ = strain rate of clay medium at level i;

θ = angle of rotation of the pile cap about horizontal axis;

κ_i = stress influence function at level i;

λ = damping ratio;

λ_s = shear wave length of clay medium;

ν = Poisson's ratio;

ρ = mass density of clay medium;

σ_d = principal compression stress difference, $\sigma_1 - \sigma_3$;

σ_1 = major principal stress in compression test;

σ_3 = minor principal stress in compression test;

σ_x = component of normal stress in the x direction;

τ = principal shear stress; and

ψ_i = displacement influence function at level i.

LIST OF FIGURES

List of Figures (continued)

List of Figures (Continued)

ABSTRACT

A general method of determining the dynamic response to seismic disturbances of structures when supported on long piles extending through deep sensitive clays is presented. This method accounts for the interaction effects between the superstructure and its pile foundations and the interaction effects between the pile foundations and their surrounding clay media. The method is applied to a specific bridge structure presently being designed by the California State Division of Highways which is to be erected at the Elkhorn Slough site.

An extensive soil testing program was conducted using undisturbed clay samples taken from the Elkhorn Slough site; the results of this program are reported. The testing techniques used to determine the non-linear hysteretic stress-strain relations, the damping characteristics, and the creep characteristics of the clay are described in considerable detail.

The dynamic response of the specific bridge-pile-clay system, when subjected to the N-S component of the 1940 El Centro ground acceleration, is presented in graphical form and its significance with respect to design questions is analyzed.

INTRODUCTION

The improvement of modern traffic systems requires in certain localities that major bridges be constructed across coastal estuaries which, when located in active seismic regions, present an extremely difficult design problem due to the poor foundation conditions usually present. Under such conditions, the bridge piers are normally supported on piles driven through a deep layer of relatively weak material to a penetration in the underlying firm material deemed sufficient to carry the superimposed loads by friction or by point bearing.

The California State Division of Highways is presently designing a bridge approximately 3000 feet in length to be erected across Elkhorn Slough which is located near Monterey, California. At this bridge site a surface layer of saturated soft to firm gray silty clay is present which varies in depth from approximately 50 feet at the proposed bridge abutment locations to approximately 120 feet midway between these locations. A very shallow layer of water covers the clay layer and a well compacted sand lies below the clay layer. In order to aid the State Division of Highways in carrying out a rational design of a bridge-pile structural system for this site, the investigation reported herein was undertaken to determine the interaction effects between the bridge structure and its supporting piles and between the supporting piles and the clay medium when subjected to a prescribed strong motion earthquake excitation.

METHODS OF ANALYSIS

General

The purpose of this section is to present a general method for investigating the seismic effects on bridges which are supported on long piles extending through deep sensitive clays. The analysis is separated into two parts, namely (1) the determination of the dynamic response of the clay medium alone when excited through its lower boundary by a prescribed horizontal seismic motion, and (2) the determination of the interaction of the entire structural system, including the piles, with the moving clay medium. Application of the method to a specific bridge structure now being designed by the California State Division of Highways is presented in considerable detail.

Dynamic Response of Clay Medium

The first part of the general analysis is the determination of the dynamic response of the clay medium alone without any bridge structure being present. Since the deformations produced in this medium by a horizontal excitation are essentially pure shear, the real system will be represented by the idealization shown in Fig. 1. It is necessary in this case to use a discrete parameter system due to the non-linearities and hysteresis effects involved in the shear stress-strain relations for the clay medium. Thus, the basic idealized system consists of a series of discrete masses connected by non-linear linkages which resist relative lateral shearing deformation.

Since the clay medium is assumed to be of infinite extent in the horizontal plane and of constant depth, the discrete properties of the

mathematical model may be based on a column of clay having a unit cross sectional area and a height equal to the depth of the clay layer. Using this column as the physical system, its mass will be lumped at discrete points uniformly spaced as shown in Fig. 1. Thus,

$$m_1 = m_2 = - - - = m_{n-1} = \frac{2\gamma h}{g} \tag{1a}$$

$$m_n = \frac{\gamma h}{g} \tag{1b}$$

in which γ is the unit weight of clay medium, g denotes the acceleration of gravity, and 2h is the vertical spacing of the discrete masses. The number of discrete masses (n) is selected of sufficient magnitude so that the response of the idealized model to any prescribed strong motion earthquake input will adequately represent the response of the continuous system.

Each of the linkages connecting adjacent pairs of masses consists of a bilinear hysteresis type spring having the idealized force-displacement characteristics as shown in Fig. 2 and a non-linear dashpot placed in parallel, which are in turn placed in series with a second non-linear dashpot. These three linkage components represent the elasto-plastic, damping, and creep properties, respectively, of the clay medium. Based on the discrete parameter model (Fig. 1), the non-linear coupled differential equations of motion which define the dynamic response of the clay medium are the following:

$$m_i \ddot{u}_i^r + c_i^d \dot{u}_i^s - c_{i+1}^d \dot{u}_{i+1}^s + f_i^s h_i\left(\frac{t}{T}\right) - f_{i+1}^s h_{i+1}\left(\frac{t}{T}\right) = -m_i \ddot{u}_g \tag{2}$$

and

$$c_i^c\left(\dot{u}_i^r - \dot{u}_{i-1}^r - \dot{u}_i^s\right) - c_i^d \dot{u}_i^s - f_i^s h_i\left(\frac{t}{T}\right) = 0 \tag{3}$$

for $i = 1,2. \ . \ .,n$, in which

$$c_i^c \equiv \left[c_i^{co} + c_i^{c'} \left| \dot{u}_i^r - \dot{u}_{i-1}^r - \dot{u}_i^s \right| + c_i^{c''}\left(\dot{u}_i^r - \dot{u}_{i-1}^r - \dot{u}_i^s\right)^2\right] f_i\left(\frac{t}{T}\right) \tag{4}$$

and

$$c_i^d \equiv \left[c_i^{do} + c_i^{d'} \left| \dot{u}_i^s \right| \right] g_i\left(\frac{t}{T}\right) \qquad (5)$$

Note that the time dependent coefficients c_i^c and c_i^d ($i = 1,2,\ldots,n$) as defined by Eqs. 4 and 5 and the spring force terms given in Eqs. 2 and 3 include the dimensionless time functions $f_i(t/T)$, $g_i(t/T)$, and $h_i(t/T)$, respectively. These functions will be defined so that they equal unity at time zero and decay with time thereafter in such a way that changes in clay characteristics due to remolding can be included in the dynamic analysis. These changes in characteristics are undoubtedly dependent on the entire past history of response. However, the appropriate history dependency is extremely difficult to establish. The dimensionless time functions as well as the constants appearing in Eqs. 4 and 5 can be determined only by extensive laboratory tests performed on clay samples taken from the bridge site. A discussion of these specific tests and their interpretation towards establishing the preceding characteristics of the clay medium are presented in a subsequent section of this report.

In the proposed analysis, the clay medium is excited through its lower boundary by a prescribed horizontal acceleration ($\ddot{u}_g$) of the foundation medium which is assumed to be time dependent only, i.e., space variations in the horizontal direction of motion are ignored. This excitation is represented by the term ($-m_i\ddot{u}_g$) on the right side of Eq. 2. Ground accelerations as recorded by the Coast and Geodetic Survey, U.S. Dept. of Commerce (USC&GS) for several past strong motion earthquakes are used as the prescribed inputs. Solutions of the coupled differential Eqs. 2 and 3 are obtained assuming zero initial conditions and using known step-by-step methods of analysis.[4]

Dynamic Response of the Bridge Structural System

The specific bridge structural system used in this investigation is shown schematically in Fig. 3. This system included the bridge itself, the supporting piers, and the piles. The dynamic response of this entire bridge structural system in the direction of the longitudinal axis of the bridge which results from its interaction with the clay and foundation media is determined using the idealized discrete parameter system shown in Fig. 4. This idealized system characterizes a typical longitudinal section of the bridge structure which is located between two transverse expansion joints.

Since there are two distinct types of pile groupings in the bridge structural system being considered, namely a single row grouping and a multiple row grouping, it is necessary that the lumped mass M^d representing the rigid deck girder mass be connected to the foundation medium by two separate but parallel discrete parameter systems having somewhat different properties. The discrete parameters which characterize this idealized structural system are the following:

(1) a single mass M^d representing the mass of the bridge deck and girders,

(2) masses m_i^b ($i = 1,2,- - -, m-1$) representing the mass of the piers,

(3) stiffness influence coefficients k_{ij}^b, $k_{i\theta}^b$ ($i,j, = 1,2,- - -,m$) representing the elastic force characteristics of the piers,

(4) stiffness influence coefficients $k_{\theta j}^b$, $k_{\theta\theta}^b$ ($j = 1,2,- - -,m$) representing the elastic moments which are applied to the pile caps by the piers,

(5) linear viscous dashpots having constant coefficients C_i^b ($i = 1,2,---, m$) which represent damping present in the piers and bridge deck,

(6) mass M_n representing the mass of a pile cap which has rotary moment of inertia equal to I_n,

(7) a linear rotational spring (spring constant K_θ) representing the elastic moment resistance to a rotation of the pile cap at the tower as produced by the resulting axial forces developed in the pile grouping,

(8) linear viscous dashpot having constant coefficient C_θ which represents damping due to rotational motion of the pile cap,

(9) stiffness influence coefficients k^a_{ij}, $k^a_{i\theta}$ ($i = 1,2,---,n$; $j = 1,2,---,n-1$) representing the elastic force characteristics of the piles,

(10) stiffness influence coefficients $k^a_{\theta j}$, $k^a_{\theta\theta}$ ($j = 1,2,---,n-1$) representing the elastic moments which are applied to the pile caps by the piles,

(11) bi-linear hysteresis type springs representing the interaction forces F^s_i (excluding damping) between the clay medium and piles which have characteristics similar to those represented in Fig. 2,

(12) masses M_i ($i = 1,2,---,n-1$) representing the mass of the piles which include an effective mass of the clay medium (M^e_i: $i=1,2,---,n-1$) resulting from the relative motion caused by interaction,

(13) non-linear time dependent viscous dashpots having the variable coefficients C^c_i ($i = 1,2,---,n$) which represent the creep properties of the clay medium resulting from its interaction with the piles,

(14) non-linear time dependent viscous dashpots having the variable coefficient C^d_i ($i = 1,2,---,n$) which represent the damping characteristics of the clay medium resulting from the elastic deformations produced by interaction with piles, and

(15) axial forces S_i ($i = 1,2,---,m$) representing the vertical imposed loads carried by the piers, and axial forces T_i ($i = 1,2,---,n$) representing the vertical imposed loads carried by the piles.

Referring to Fig. 4, the idealized model will be excited simultaneously at its base by the prescribed horizontal acceleration $\ddot{u}_g$ of the foundation

medium and at each level i (i = 1,2,---,n) by a known support acceleration time history u_i^t which represents the acceleration time history of the clay medium at level i assuming no interaction with the bridge structure (see Fig. 1). The coupled non-linear differential equations of motion which govern the response of this idealized bridge structural system are the following:

$$\left[M_i\right]\left\{\ddot{U}_i^r\right\} + \left[C_i^d\right]\left\{\dot{U}_i^s\right\} + \left[F_i^s\right] + \left[k_{ij}^a\right]\left\{U_i^r - \frac{d_i}{d_n}U_n^r\right\} + \left(\theta - \frac{U_n^r}{d_n}\right)\left\{k_{i\theta}^a\right\} + \left[T_{ij}\right]\left\{U_i^r\right\} = -\ddot{u}_g\left[M_i\right]\left\{I\right\} + \left[M_i^e\right]\left\{\ddot{u}_i^t\right\} \tag{6}$$

$$\left[m_i^b\right]\left\{\ddot{U}_i^b + \ddot{U}_n^r\right\} + \left[C_i^d\right]\left\{\dot{U}_i^b\right\} + \left[k_{ij}^b\right]\left\{U_i^b\right\} + \theta\left\{k_{i\theta}^b\right\} + \left[S_{ij}\right]\left\{U_i^b\right\} = -\ddot{u}_g\left[m_i^b\right]\left\{I\right\} \tag{7}$$

$$M_n\ddot{U}_n^r + C_n^d\dot{U}_n^s + F_n^s + \langle k_{nj}^a\rangle\left\{U_i^r - \frac{d_i}{d_n}U_n^r\right\} + k_{n\theta}^a\left(\theta - \frac{U_n^r}{d_n}\right) + \langle k_{0j}^b\rangle\left\{U_i^b\right\} + \frac{T_n}{d_n - d_{n-1}}U_{n-1}^r - \left(\frac{T_n}{d_n - d_{n-1}} + \frac{S_i}{e_i}\right)U_n^r + \frac{S_1}{e_1}\left(U_n^r + U_i^b\right) = -\ddot{u}_g M_n + M_n^e\ddot{u}_n^t \tag{8}$$

$$M^d\left(\ddot{\bar{U}}_m^b + \ddot{U}_n^r\right) + \bar{C}_m^d\dot{\bar{U}}_m^b + \langle\bar{k}_{mj}^b\rangle\left\{\bar{U}_i^b\right\} + \langle\bar{\bar{k}}_{mj}^b\rangle\left\{\bar{\bar{U}}_i^b\right\} + \bar{\theta}\bar{k}_{m\theta}^b + \bar{\bar{\theta}}\bar{\bar{k}}_{m\theta}^b + \frac{\bar{S}_m\left(\bar{U}_{m-1}^b - \bar{U}_m^b\right)}{\bar{e}_m - \bar{e}_{m-1}} + \frac{\bar{\bar{S}}_m\left(\bar{\bar{U}}_{m-1}^b - \bar{\bar{U}}_m^b\right)}{\bar{\bar{e}}_m - \bar{\bar{e}}_{m-1}} = -\ddot{u}_g M_d \tag{9}$$

$$I_n\ddot{\theta} + \langle k^b_{\theta j}\rangle \left\{U^b_i\right\} + k^b_{\theta\theta}\theta + \langle k^a_{\theta j}\rangle \left\{U^r_i - \frac{d_i}{d_n} U^r_n\right\} + k^a_{\theta\theta}\left(\theta - \frac{U^r_n}{d_n}\right)$$

$$+ K_\theta\theta + C_\theta\dot{\theta} = 0 \qquad (10)$$

$$\left[C^c_i\right]\left\{\dot{U}^r_i - \dot{U}^s_i\right\} - \left[C^d_i\right]\left\{\dot{U}^s_i\right\} - \left[F^s_i\right] = \left[C^c_i\right]\left\{\dot{u}^t_i - \dot{u}_g\right\} \qquad (11)$$

and

$$\bar{U}^r_n + \bar{U}^b_m = \bar{\bar{U}}^r_n + \bar{\bar{U}}^b_m \qquad (12)$$

Matrix Eq. 6 represents the horizontal force equilibrium equations of motion for masses M_1, M_2,---,M_{n-1} of pile group 1; thus, giving (n-1) individual equations. Similarly, Eq. 7 represents the horizontal force equilibrium equations of motion for masses m^b_1, m^b_2,---,m^b_{m-1}; therefore, giving an additional (m-1) individual equations. The horizontal force equilibrium equation of motion for masses M_n is given by Eq. 8. Similar equations to those given by Eqs. 6, 7, and 8 must be written for corresponding masses in pile group 2. In addition the equation of motion for mass M^d must be written as given by Eq. 9. Note that in this equation (also Eq. 12) a bar is placed above those quantities representing pile group 1 and a double bar is placed above those quantities representing pile group 2.

The horizontal forces included in the above equations are inertia, damping, interaction, transverse, shear, net horizontal components of axial loads, and effective seismic loads. Eq. 10 is the moment equilibrium equation of motion for mass M_n. In addition to these equilibrium equations of motion, it is necessary that force balance be maintained throughout each individual linkage system representing the pile-clay interaction characteristics. The required equation which satisfies this condition for pile group 1

is matrix Eq. 11. A similar equation must, of course, be written for pile group 2. The final equation which must be written to satisfy the condition of continuity of horizontal displacement at mass M^d for pile groups 1 and 2 is given by Eq. 12.

The preceding differential equations of motion contain numerous time dependent coefficients which permit non-linearities to be present in the creep and damping characteristics of the clay medium and which also permit changes in these characteristics due to remoulding. These variable coefficients are defined in a similar manner to those given by Eqs. 4 and 5 and may be represented as follows:

$$C_i^c = \left[C_i^{co} + C_i^{c'} \left| \dot{U}_i^r - \dot{U}_i^s - \dot{u}_i^r \right| + C_i^{c''} \left(\dot{U}_i^r - \dot{U}_i^s - \dot{u}_i^r \right)^2 \right] F_i \left(\frac{t}{T} \right) \qquad (13)$$

and

$$C_i^d = \left[C_i^{do} + C_i^{d'} \left| \dot{U}_i^s \right| \right] G_i \left(\frac{t}{T} \right) \qquad (14)$$

The dimensionless time functions as well as the constants appearing in Eqs. 13 and 14 will be determined by considering the results of laboratory tests performed on clay samples taken from the bridge site. Many of these functions and constants are of identical form and magnitude, respectively, in the final analysis of the general problem. All of the previously coupled differential equations of motion representing the bridge structural system are solved numerically assuming zero initial conditions.

Evaluation of Discrete Parameters of Bridge Structural System

(1) Mass M^d - This quantity represents the total mass of the barrier railings, deck slab, girders and diaphragms between the transverse expansion joints (510 ft), plus the mass of the piers over the height $(e_m - e_{m-1})/2$.

(2) Masses $\bar{m}_i^b$ and $\bar{\bar{m}}_i^b$ - Thses masses are defined as follows:

$$\bar{m}_i^b = 2 \frac{W^p}{g} \left(\frac{\bar{e}_{i+1} - \bar{e}_{i-1}}{2} \right) \tag{15a}$$

$$\bar{\bar{m}}_i^b = 3 \frac{W^p}{g} \left(\frac{\bar{\bar{e}}_{i+1} - \bar{\bar{e}}_{i-1}}{2} \right) \tag{15b}$$

in which W^p denotes the weight of single pier per foot of height.

(3) Stiffness Influence Coefficients $\bar{k}_{ij}^b$ and $\bar{\bar{k}}_{ij}^b$ $(i,j = 1,2,---,m,\theta)$ - These coefficients are obtained by standard methods of structural analysis, i.e., by inverting a flexibility coefficient matrix representing the pier elastic properties. In the evaluation of the flexibility coefficient matrix, for the case of longitudinal motion, the top of the pier is allowed to translate but not rotate; whereas, the bottom is assumed to be pinned.

(4) Damping Coefficients $\bar{C}_i^b$ and $\bar{\bar{C}}_i^b$ - These coefficients define viscous damping forces for the bridge super structure which are assumed proportional to the velocity of their respective masses relative to the base of the pier. All damping coefficients are based on a percentage of critical damping of the system.

(5) Masses $\bar{M}_n$ and $\bar{\bar{M}}_n$ - These masses represent the total mass of the pile caps for pile groups 1 and 2, respectively, plus a contribution from the piers to a height of $e_1/2$, and a contribution from the piles to a depth of $(d_n - d_{n-1})/2$.

(6) Rotary Mass Moments of Inertia $\bar{I}_n$ and $\bar{\bar{I}}_n$ - These terms represent the combined mass rotary moments of inertia of the pile caps for groups 1 and 2, respectively.

(7) Spring Constant $\bar{K}_\theta$ - Because of the multiple row grouping of the piles at the tower piers there will be an elastic resistance to rotation of

the pile cap due to the axial forces developed in the piles a result of this rotation. This resistance to rotation is expressed by the rotational spring constant $\bar{K}_\theta$.

(8) Damping Coefficients $\bar{C}_\theta$ and $\bar{\bar{C}}_\theta$ - The rotational damping of the pile caps is due to the dissipation of energy resulting from the axial loads which are induced in the piles and piers as caused by a rotation of the pile cap, plus a contribution to the frictional resistance of the clay medium to this same rotation.

(9) Stiffness Influence Coefficients $\bar{k}^a_{ij}$ and $\bar{\bar{k}}^a_{ij}$ $(i,j = 1,2,---,n,\theta)$ - These stiffness coefficients are obtained by inverting the flexibility matrices for pile groups 1 and 2, respectively. In determining the flexibility coefficients, pinned end conditions are specified for the piles.

(10) Bi-linear Hysteresis Spring Forces $\bar{F}^s_i$ and $\bar{\bar{F}}^s_i$ - These forces are assumed to be related to their respective displacements $\bar{U}^s_i$ and $\bar{\bar{U}}^s_i$ as shown in Fig. 2.

The fundamental expression used in the evaluation of the elastic spring constants $\bar{K}_{ie}$ and $\bar{\bar{K}}_{ie}$ is the following Mindlin equation[5] which gives the x component of displacement as produced by a single concentrated force P located at any arbitrary point (0,0,c) within an isotropic half-space, and acting in the x direction:

$$u_x(x,y,z) = \frac{P(0,0,c)}{16\pi(1-\nu)G}\left\{\frac{3-4\nu}{R_1} + \frac{1}{R_2} + \frac{2cz}{R_2^3} + \frac{4(1-\nu)(1-2\nu)}{R_2+z+c}\right.$$

$$\left. + x^2\left[\frac{1}{R_2^3} + \frac{3-4\nu}{R_2^3} - \frac{6cz}{R_2^5} - \frac{4(1-\nu)(1-2\nu)}{R_2(R_2+c+z)^2}\right]\right\} \qquad (16)$$

in which ν equals Poisson's ratio, and c equals the z distance of the load below the surface xy boundary plane, and

$$R_1^2 \equiv x^2 + y^2 + (z - c)^2; \quad R_2^2 \equiv x^2 + y^2 + (z + c)^2$$

It is assumed in the dynamic analysis that no transfer of water takes place in the saturated clay medium during the earthquake. Therefore, it is reasonable to use a Poisson's ratio ν of 1/2. Thus $G = E/3$ which reduces Eq. 16 to

$$u_x(x,y,z) = \frac{3P(0,0,c)}{8\pi E}\left\{\frac{1}{R_1} + \frac{1}{R_2} + \frac{2cz}{R_2^3} + x^2\left[\frac{1}{R_1^3} + \frac{1}{R_2^3} - \frac{6cz}{R_2^5}\right]\right\} \qquad (17)$$

or, in cylindrical coordinates

$$u_x(r,\theta,z) = \frac{3P(0,0,c)}{8\pi E}\left\{\frac{1}{\left[r^2 + (z-c)^2\right]^{1/2}} + \frac{1}{\left[r^2 + (z+c)^2\right]^{1/2}} + \frac{2cz}{\left[r^2 + (z+c)^2\right]^{3/2}} + r^2\cos^2\theta\left[\frac{1}{\left[r^2 + (z-c)^2\right]^{3/2}} + \frac{1}{\left[r^2 + (z+c)^2\right]^{3/2}} - \frac{6cz}{\left[r^2 + (z+c)^2\right]^{5/2}}\right]\right\} \qquad (18)$$

Due to a singularity which exists at the point of application of the load (0,0,c), deflections must be considered at finite distances from this point. Since the displacements of interest are those at the boundaries of the piles, i.e. $r = B$, this singularity does not cause difficulty. From Eq. 18 it can be seen that the deflection at a constant radius r is a function of the angle θ. Therefore, it is necessary to obtain a weighted average deflection in the x direction at this radius using an averaging process with respect to the coordinate y. Thus, for radius B, a weighted average deflection is defined as

$$u_x(B,z) = \int_0^B u_x(B,\theta,z)\,dy = \int_0^{\pi/2} u_x(B,\theta,z)\cos\theta\,d\theta \qquad (19)$$

Substituting Eq. 18 into Eq. 19 gives

$$u_x(B,z) = \frac{3P(0,0,c)}{8\pi E}\left\{\frac{1}{R_1} + \frac{1}{R_2} + \frac{2cz}{R_2^3} + \frac{2}{3}B^2\left[\frac{1}{R_1^3} + \frac{1}{R_2^3} - \frac{6cz}{R_2^5}\right]\right\} \qquad (20)$$

in which

$$R_1 \equiv \left[B^2 + (z-c)^2\right]^{1/2} \; ; \; R_2 \equiv \left[B^2 + (z+c)^2\right]^{1/2}$$

When subjected to a displacement in the elastic range, a pile encounters a continuously distributed loading over its length as caused by the resistance of the clay medium. This loading can be approximated by assuming the intensity of loading as uniformly distributed along the length of the pile within each height interval 2h but that the intensity varies from one interval to the next. The general expression for the weighted average deflection at radius B as caused by a uniformly distributed loading acting over the height of one interval is obtained by substituting the intensity of loading $p(0,0,\bar{c}\pm h)$ between points $(\bar{c} - h)$ and $(\bar{c} + h)$ for the concentrated load $P(0,0,c)$ in Eq. 20 and integrating with respect to c over this interval. Thus, there is obtained

$$u_x(B,z)_{avg} = \frac{3p(0,0,\bar{c}\pm h)}{8\pi E}\left\{\sinh^{-1}\frac{\bar{c}+h-z}{B} - \sinh^{-1}\frac{\bar{c}-h-z}{B} + \sinh^{-1}\frac{\bar{c}+h+z}{B}\right.$$

$$- \sinh^{-1}\frac{\bar{c}-h+z}{B} + \frac{2}{3B^2}\left[\frac{B^2(\bar{c}+h) - 2B^2z + (\bar{c}+h)z^2 + z^3}{\left[B^2 + (\bar{c}+h+z)^2\right]^{1/2}}\right.$$

$$\left.\left. - \frac{B^2(\bar{c}-h) - 2B^2z + (\bar{c}-h)z^2 + z^3}{\left[B^2 + (\bar{c}-h+z)^2\right]^{1/2}}\right] - \frac{2}{3}\left[\frac{z - (\bar{c}+h)}{\left[B^2 + (\bar{c}+h-z)^2\right]^{1/2}}\right.\right.$$

$$- \frac{z - (\bar{c}-h)}{\left[B^2 + (\bar{c}-h-z)^2\right]^{1/2}} \Bigg] + \frac{4}{3} \left[\frac{B^2 z + (\bar{c}+h)\, z^2 + z^3}{\left[B^2 + (\bar{c}+h+z)^2\right]^{3/2}} \right.$$

$$\left. - \frac{B^2 z + (\bar{c}-h)\, z^2 + z^3}{\left[B^2 + (\bar{c}-h+z)^2\right]^{3/2}} \right] \Bigg\} \qquad (21)$$

in which $\bar{c}$ is the vertical distance from the boundary surface to the mid-height of the interval over which the load acts.

The Mindlin theory permits one to completely characterize an elastic half-space. However, to use this theory in the determination of the discrete elastic spring constants as previously defined for the idealized bridge structural system, it is necessary that numerous simplifying assumptions be made so that the problem at hand is amenable to solution. To recognize the appropriate simplifying assumptions which can be made without altering appreciably the basic characteristics of the structural system, one must understand the basic characteristics of the previously mentioned theory of the half-space. To demonstrate one very important characteristic, Eq. 21 has been plotted in dimensionless form in Figs. 5 and 6 for $h/\bar{c}$ ratios of 0.08 and 1.00, respectively. Fig. 5 demonstrates the fact that the displacement $u_x(B,z)_{avg}$ decays very rapidly with distance from the loaded region in the vertical direction, i.e., along the z axis. Similar rapid decay rates in the displacement field are also present along the x and y axes. This same rapid decay phenomenon may also be seen in Fig. 6 at the base of the loaded region. It is important to note, for subsequent considerations, that displacements $u_x(B,z)_{avg}$ produced by the loaded conditions of Fig. 6 are reasonably constant over most of the loaded region except for a very narrow region near its base, i.e. at $z = 2c$, and for a very narrow region near the surface, i.e., at $z = 0$.

From the preceding analysis of the plots shown in Figs. 5 and 6, one may conclude that (1) the displacement of a point along the axis of loading within an elastic half-space is produced primarily by loading which is present in the immediate vicinity of the point being considered and (2) the displacement of this point is not influenced greatly by its vertical position in the half-space, i.e., its z coordinate, unless it is located very near the surface. Due to these characteristics of the half-space, one can approximate the pile-clay medium interaction effects by a method similar to the classical "beam on elastic foundation" theory. This theory assumes that the reaction force per unit length along a foundation at a given location can be represented by the expression ku in which u is the deflection of the foundation and k is a constant usually called the modulus of the foundation. This constant, therefore, is the reaction per unit length when the deflection is unity. The simple assumption that the continuous reaction intensity at a point along the foundation is proportional to the deflection at that point only is commonly known as the Winkler assumption and has been proven to be very satisfactory in practical cases. Therefore, it is considered appropriate for the pile-clay medium interaction problem being considered in this investigation.

Consider now the determination of a Winkler continuous spring constant $k'(z)$ which the clay medium provides for a single pile of length d_n at depth z. This spring constant is easily obtained by applying the uniform line loading of intensity p as shown in Fig. 6 to the half-space and determining the resulting deflections $u_x(B,z)_{avg}$ as shown in this same Fig. By definition of the spring constant, one may state that

$$k'(z) \cong \frac{p}{u_x(B,z)_{avg}} \tag{22}$$

in which $u_x(B,z)_{avg}$ is given by Eq. 21. Substituting Eq. 21 into Eq. 22 gives

$$k'(z) = \frac{8\pi E(z)}{3} \left\{\text{from Eq. 21 with } \bar{c} = h = \frac{d_n}{2}\right\}^{-1} \qquad (23)$$

Note that Eq. 21 was derived for an elastic half-space in which the modulus E does not vary with location. Due to the rapid decay phenomenon previously discussed, this expression can be applied, however, with little loss of accuracy, to a clay medium where the modulus E varies slowly with depth provided the constant E is replaced by E(z). Thus, Eq. 23 reflects this substitution.

Consider now the determination of an appropriate Winkler continuous spring constant, say k"(z), for a pile group of length d_n consisting of Q individual piles. For typical spacings of piles within a group some interaction effects between individual piles are present and should be accounted for in determining k"(z). Due to these interaction effects between piles within a group, one can state the following inequality, i.e.,

$$k''(z) \leq Q\, k'(z) \qquad (24)$$

For the case where pile spacings are very large, no appreciable interaction effects would be present and as a result the pile group spring constant k"(z) would simply be equal to Qk'(z).

The loading which will now be considered as applied to the clay medium for the determination of k"(z), is similar to that shown in Fig. 6 except that this same line loading of intensity power depth d_n will be applied to the clay medium along each of the intended axes of piles within the group. It is necessary here to determine the horizontal x component of displacement of the clay medium along each axis and average these displacements for any level z.

The entire displacement field (x component) for a single line loading

of the type defined previously is obtained by substituting p dc for P(0,0,c) in Eq. 17 and integrating with respect to c over the interval $0 < c < d_n$. This results in the expression

$$u_x(x,y,z,) = \frac{3p}{8\pi E(z)} \left\{ \sinh^{-1} \frac{d_n + z}{(x^2 + y^2)^{1/2}} + \sinh^{-1} \frac{d_n - z}{(x^2 + y^2)^{1/2}} \right.$$

$$+ \frac{1}{x^2 + y^2} \left[- \frac{2x^2 z d_n (d_n + z)}{\left[x^2 + y^2 + (d_n + z)^2\right]^{3/2}} \right.$$

$$+ \frac{4x^2 z^2 (d_n + z)}{(x^2 + y^2)\left[x^2 + y^2 + (d_n + z)^2\right]^{1/2}} + \frac{x^2(d_n + z) - 2z\left[y^2 + z(d_n + z)\right]}{\left[x^2 + y^2 + (d_n + z)^2\right]^{1/2}}$$

$$\left. \left. + \frac{x^2(d_n - z)}{\left[x^2 + y^2 + (d_n - z)^2\right]^{1/2}} + \frac{2z\left[(x^2 + y^2)\, y^2 - (x^2 - y^2)\, z^2\right]}{(x^2 + y^2)\left[x^2 + y^2 + z^2\right]^{1/2}} \right] \right\} \qquad (25)$$

in which the x and y coordinates have their origin at the point of application of the load.

It should be noted that Eq. 21 represents a weighted average displacement of points on a circle of radius B which lies on a horizontal plane at level z and whose center is at the location of the horizontal load; whereas, Eq. 25 represents the displacement at an arbitrary point (x,y,z) in which $(x^2 + y^2)^{1/2} > B$. In using the latter mentioned expression, it will be assumed that the deflection of point (x,y,z) which is some distance removed from the points of application of the loading, adequately represents the weighted average deflection of points on a circle of radius B whose center is located at this same point.

Using Eqs. 21 and 25, one can obtain the horizontal x component of

displacement of any vertical axis (intended pile axis) within the clay medium at level z due to a single line static loading of intensity p applied to the clay medium over the interval $0 < z < d_n$. By moving this same line loading to each of the Q intended pile axes within the group and using Eqs. 21 and 25 in each case, one obtains Q x Q displacement functions each of which may be denoted as $u_{rs}(z)$ where r,s = 1,2,. . .,Q. Thus, an individual displacement function $u_{rs}(z)$ is defined as the horizontal displacement of the clay medium along axis r due to the line loading which is placed along axis s. Referring to Eqs. 21 and 25, these displacement functions may be expressed in equation form as follows: For the case $r \neq s$

$$u_{rs}(z) = \frac{3p}{8\pi E(z)} \left\{ \sinh^{-1} \frac{d_n + z}{(R_{rs})^{1/2}} + \sinh^{-1} \frac{d_n - z}{(R_{rs})^{1/2}} + \frac{1}{R_{rs}} \right.$$

$$\left[- \frac{2x_{rs}^2 z d_n (d_n + z)}{\left[R_{rs} + (d_n + z)^2\right]^{3/2}} + \frac{4x_{rs}^2 z^2 (d_n + z)}{R_{rs}\left[R_{rs} + (d_n + z)^2\right]^{1/2}} + \frac{x_{rs}^2 (d_n + z) - 2z\left[y_{rs}^2 + z(d_n + z)\right]}{\left[R_{rs} + (d_n + z)^2\right]^{1/2}} \right.$$

$$\left. \left. + \frac{x_{rs}^2 (d_n - z)}{\left[R_{rs} + (d_n - z)^2\right]^{1/2}} + \frac{2z\left[R_{rs} y_{rs}^2 - (x_{rs}^2 - y_{rs}^2) z^2\right]}{R_{rs}\left[R_{rs} + z^2\right]^{1/2}} \right] \right\} \qquad (26)$$

in which $R_{rs} \equiv x_{rs}^2 + y_{rs}^2 \geq B^2$, and x_{rs} and y_{rs} are the x and y coordinates, respectively, of axis r when the origin of these coordinates coincides with the s axis.

$$r = 1,2,. . .,Q; \quad s = 1,2,. . .,Q \qquad r \neq s$$

and Q is the number of intended piles in the group under consideration. For the case r = s

$$u_{ss}(z) = \frac{3p}{8\pi E(z)} \left\{ \sinh^{-1} \frac{d_n + z}{B} + \sinh^{-1} \frac{d_n - z}{B} + \frac{4}{3} \frac{B^2 z + z^2(d_n + z)}{\left[B^2 + (d_n + z)^2\right]^{3/2}} \right.$$

$$+ \frac{2}{3B^2} \left[\frac{B^2(d_n - 2z) + z^2(d_n + z)}{\left[B^2 + (d_n + z)^2\right]^{1/2}} + \frac{B^2(d_n - z)}{\left[B^2 + d_n - z)^2\right]^{1/2}} \right.$$

$$\left. \left. - \frac{z^3 - B^2 z}{\left[B^2 + z^2\right]^{1/2}} \right] \right\} \qquad (27)$$

It is now necessary to obtain the average displacement of all Q axes within the pile group, say $u(z)_{avg}$, which by definition may be expressed as

$$u(z)_{avg} = \frac{1}{Q} \sum_{r = 1,2,\ldots}^{Q} \sum_{s = 1,2,\ldots}^{Q} u_{rs}(z) \qquad (28)$$

Using Eqs. 26 and 27, Eq. 28 may be written as

$$u(z)_{avg} = \frac{3p}{8\pi E(z) Q} \left[\sum_{r=1,2,\ldots}^{Q} \sum_{s=1,2,\ldots}^{Q} (1 - \delta_{rs}) \left\{ \text{from Eq. 26} \right\} \right.$$

$$\left. + \sum_{s=1,2,\ldots}^{Q} \left\{ \text{from Eq. 27} \right\} \right] \qquad (29)$$

where the Kronecker delta term δ_{rs} is defined as $\delta_{rs} \equiv \begin{cases} 0 & r \neq s \\ 1 & r = s \end{cases}$

The Winkler spring constant k"(z) for the pile group is now defined as

$$k"(z) = \frac{Qp}{u(z)_{avg}} \qquad (30)$$

Substituting Eq. 29 into Eq. 30 gives

$$K"(z) = \frac{8\pi Q^2 E(z)}{3} \text{ (from Eq. 29)}^{-1} \qquad (31)$$

The bridge structural system between expansion joints as shown in Fig. 3 contains two multiple row pile groups directly under the tower and 3 single row groups. Using Eq. 31, the spring constant k"(z) for one multiple row group and one single row group may be obtained. Denoting these functions as $k''_1(z)$ and $k''_2(z)$, respectively, the entire bridge structural system under consideration will experience under longitudinal motion a lateral foundation modulus of $2k''_1(z)$ for the combined multiple row pile groupings and $3k''_2(z)$ for the combined single row pile groupings.

Considering that the dynamic analysis is based on a discrete parameter system as shown in Fig. 4, the continuous spring systems just determined must be lumped into concentrated springs. Thus, lumping the continuous springs over each interval of height 2h, gives the following elastic spring constants K_{ie} for the concentrated spring at level i which characterize the system shown in Fig. 4:

$$\bar{K}_{ie} = 4hk''_1(z_i) \tag{32a}$$

$$\bar{\bar{K}}_{ie} = 6hk''_2(z_1): \quad i=1,2,\ldots,n-1 \tag{32b}$$

and

$$\bar{K}_{ne} = 2hk''_1(z_n) \tag{33a}$$

$$\bar{\bar{K}}_{ne} = 3hk''_2(z_n) \tag{33b}$$

The yield values of the interaction spring forces $\bar{F}^s_{iy}$ and $\bar{\bar{F}}^s_{iy}$ as represented by F^s_{iy} in Fig. 2 are determined by multiplying the ultimate lateral bearing pressure q_f which the clay medium is capable of exerting on a pile by their respective total projected pile areas, i.e.,

$$\bar{F}^s_{iy} = 4q_f\, Bh\bar{Q} \tag{34a}$$

$$\bar{\bar{F}}^s_{iy} = 4q_f\, Bh\bar{\bar{Q}} \tag{34b}$$

in which $\bar{Q}$ and $\bar{\bar{Q}}$ represent the total number of piles represented by Pile Groups 1 and 2, respectively. Previous investigations[6] indicate the ultimate lateral bearing pressure q_f is approximately equal to $7.5c_s$ in which c_s is the soil cohesive strength, or ultimate shear strength as measured by a standard triaxial test. Since the above interaction yield force values are based on ultimate shear strength of the soil, the slopes $\bar{K}_{ip}$ and $\bar{\bar{K}}_{ip}$ of the force-displacement relations, as represented by K_{ip} in Fig. 2 are considered to be essentially zero. However, small but finite values are actually assigned to these quantities in the numerical analysis for stability reasons.

(11) Masses $\bar{M}_i$ and $\bar{\bar{M}}_i$ - The idealized discrete masses $\bar{M}_i$ and $\bar{\bar{M}}_i$, as represented by M_i in Fig. 4, are obtained by summing the total mass of the piles (or pile groups) being represented in interval i and adding an effective mass of the clay medium resulting from the relative motion caused by interaction. Thus, it may be stated that

$$M_i = M_i^p + M_i^e \; ; \quad i = 1,2,\ldots, n-1 \tag{35}$$

where M_i^p represents the combined pile masses while M_i^e represents contributions from the clay medium.

Since the effective mass M_i^e is entirely the result of interaction effects, it is convenient to separate this motion (Fig. 7) into two distinct types as shown in Figs. 8 and 9, namely, one type, where the pile group is forced to displace with the moving clay medium without interaction and a second type, where the pile group is forced to interact with an undisturbed clay medium.

In Figs. 7-10, three reference lines (OA'', OA' and OA) are used to locate the structural system relative to the foundation medium. Line OA''

represents points along a vertical axis within the clay medium in its completely undisturbed state and also represents the axis of the pile group in its initial position. Line OA' represents the displaced position of the line OA'' due to the dynamic response of the clay medium with no interaction being present while line OA is the displaced position of OA'' with interaction present.

It is quite apparent that there exists a set of dynamic loads which, if applied to the entire pile-pier-bridge structural system, would produce motion resulting in no interaction with the clay medium. This type of motion is represented in Fig. 8 where only the applied loads P_i on the pile masses are shown. It is easily established that these loads are represented by the expression

$$P_i = M_i^p (\ddot{u}_g + \ddot{u}_i^r) + < k_{ij}^a > \left\{u_i^r - \frac{d_i}{d_n} u_n^r\right\} + (\theta' - \frac{u_n^r}{d_n}) k_{i\theta}^a + < T_{ij} > \left\{u_i^r\right\} \quad (36)$$

Since no interaction is present in this case, its contribution to M_i^e is zero.

To determine the true motion of the real structural system shown in Fig. 7, one must combine the motion of Fig. 8 with that of Fig. 9. This latter case properly accounts for all interaction effects; thus, making it possible to determine M_i^e.

The motion of the real system in Fig. 9 must be exactly the same as the idealized system shown in Fig. 10. To be equivalent it is a necessary condition that the total kinetic energy in any interval i be the same in each case. This condition results in the equation

$$\frac{1}{2}(M_i^p + M_i^e)(\dot{U}_i^r - \dot{u}_i^r)^2 \cong \frac{1}{2} M_i^p (\dot{U}_i^r - \dot{u}_i^r)^2 + \frac{(\dot{U}_i^r - \dot{u}_i^r)^2}{2} \int_{\bar{c}_i - h}^{\bar{c}_i + h} \int_{-\infty}^{\infty} \int_{-\infty}^{\infty}$$

$$(\psi_u^2 + \psi_v^2 + \psi_w^2)\, dm \quad (37)$$

or

$$M_i^e \cong \int_{\bar{c}_i - h}^{\bar{c}_i + h} \int_{-\infty}^{\infty} \int_{-\infty}^{\infty} (\psi_u^2 + \psi_v^2 + \psi_w^2)\, \rho(x,y,z)\, dx\, dy\, dz \qquad (38)$$

in which $\psi_u = \psi_u(x,y,z)$, $\psi_v = \psi_v(x,y,z)$, and $\psi_w(x,y,z)$ represent the displacement fields within the clay medium in the x,y, and z directions, respectively, when subjected to the interaction forces of all piles within an intended pile group but normalized so that the relative displacement $(U_i^r - u_i^r)$ equals unity.

With the effective masses M_i^e $(i = 1,2,---,n)$ now known, consider the equilibrium equation of motion of mass M_i as shown by the idealized system in Fig. 10. This equation of motion is

$$M_i (\ddot{U}_i^r - \ddot{u}_i^r) + C_i^d U_i^s + K_i U_i^s + < k_{ij}^a > \left\{ (U_i^r - u_i^r) - \frac{d_i}{d_n} (U_n^r - u_n^r) \right\}$$

$$+ \left(\theta - \theta' - \frac{(U_n^r - u_n^r)}{d_n}\right) k_{i\theta}^a + < T_{ij} > \left\{ U_i^r - u_i^r \right\} = -P_i \qquad (39)$$

Substituting Eq. (36) into (38), rearranging, and writing for $i = 1,2,---,n-1$ gives the equation

$$\left[M_i \right] \left\{ \ddot{U}_i^r \right\} + \left[C_i^d \right] \left\{ \dot{U}_i^s \right\} + \left[K_i \right] \left\{ U_i^s \right\} + \left[k_{ij}^a \right] \left\{ U_i^r - \frac{d_i}{d_n} U_n^r \right\}$$

$$+ \left(\theta - \frac{U_n^r}{d_n}\right) \left\{ k_{i\theta}^a \right\} + \left[T_{ij} \right] \left\{ U_i^r \right\} = -\ddot{u}_g \left[M_i \right] + \left[M_i^e \right] \left\{ \ddot{u}_i^t \right\} \qquad (40)$$

which is identical with the form of Eq. 6.

In the strict sense the displacement field in any layer can not be expressed as a space dependent function multiplied by a time dependent function. This means that the effective mass as given by Eq. (38) is time dependent; however, due to the decay phenomenon as shown in Fig. 5 the variation in time is not large. Another important factor which must be

considered is that the computer time which would be required to evaluate an effective mass at all of the discrete points for each cycle of the iteration would be prohibitive. Consequently, it was necessary to calculate each effective mass for a fixed space distribution of the interaction loads. This procedure yields an effective mass which is independent of time; however, this method is assumed to be adequate for the purposes of this investigation since the interaction response of the clay-structural system is insensitive to variations in the values of the effective masses.

The loading which was used for the evaluation of the effective mass was uniformly distributed along the intended axes of the piles from a distance β_i below the mid-plane of layer i to a distance α_i above the mid-plane, i.e. from the depth $(\bar{c}_i - \alpha_i)$ to the depth $(\bar{c}_i + \beta_i)$. The necessary intensity of loading to be applied along each of the intended pile axes which will produce a unit relative displacement $(U_i^r - u_i^r = 1)$ of the intended pile group was established by means of a procedure similar to that used to evaluate the spring constants of the pile groups, and is given by

$$p_i^* = \frac{8\pi E(\bar{c}_i)}{3}\,\eta_i \qquad (41)$$

in which

$$\eta_i = Q\left[\sum_{r=1,2,\cdots}^{Q}\sum_{s=1,2,\cdots}^{Q}(1-\delta_{rs})\left\{\ln\left[\frac{4h(n-i)+\beta_i}{R_{rs}^{1/2}}+\sqrt{\frac{\langle 4h(n-i)+\beta_i\rangle^2}{R_{rs}}+1}\right]\right.\right.$$

$$+\ln\left[\frac{\beta_i}{R_{rs}^{1/2}}+\sqrt{\frac{\beta_i}{R_{rs}}+1}\right]+\ln\left[\frac{\alpha_i}{R_{rs}^{1/2}}+\sqrt{\frac{\alpha_i^2}{R_{rs}}+1}\right]$$

$$\left.\left.-\ln\left[\frac{4h(n-i)-\alpha_i}{R_{rs}^{1/2}}+\sqrt{\frac{\langle 4h(n-i)-\alpha_i\rangle^2}{R_{rs}}+1}\right]\right\}\right]$$

$$+\frac{1}{R_{rs}}\left[\frac{4x_{rs}^2\,h(n-i)\left[R_{rs}+2h(n-i)\,\langle 4h(n-i)+\beta_i\rangle\right]}{\left[R_{rs}+\langle 4h(n-i)+\beta_i\rangle^2\right]^{3/2}}\right.$$

$$+\frac{16x_{rs}^2h^2(n-i)^2\,\langle 4h(n-i)+\beta_i\rangle}{R_{rs}\left[R_{rs}+\langle 4h(n-i)+\beta_i\rangle^2\right]^{1/2}}+\frac{\beta_i x_{rs}^2}{\left[R_{rs}+\beta_i^2\right]^{1/2}}$$

$$-\frac{4h(n-i)\,\langle 8h^2(n-i)^2+y_{rs}^2\rangle+\beta_i\,\langle 8h^2(n-i)^2-x_{rs}^2\rangle}{\left[R_{rs}+\langle 4h(n-i)+\beta_i\rangle^2\right]^{1/2}}+\frac{\alpha_i x_{rs}^2}{\left[R_{rs}+\alpha_i^2\right]^{1/2}}$$

$$-\frac{4x_{rs}^2\,h(n-i)\left[R_{rs}+2h(n-i)\,\langle 4h(n-i)-\alpha_i\rangle\right]}{\left[R_{rs}+\langle 4h(n-i)-\alpha_i\rangle^2\right]^{3/2}}$$

$$+\frac{4h(n-i)\,\langle 8h^2(n-i)^2+y_{rs}^2\rangle-\alpha_i\,\langle 8h^2(n-i)^2-x_{rs}^2\rangle}{\left[R_{rs}+\langle 4h(n-i)-\alpha_i\rangle^2\right]^{1/2}}$$

$$\left.-\frac{16x_{rs}^2h^2(n-i)^2\,\langle 4h(n-i)-\alpha_i\rangle}{R_{rs}\left[R_{rs}+\langle 4h(n-i)-\alpha_i\rangle^2\right]^{1/2}}\right]+Q\left\{\ln\left[\frac{4h(n-i)+\beta_i}{B}+\right.\right.$$

$$\left.\sqrt{\frac{\langle 4h(n-i)+\beta_i\rangle^2}{B^2}+1}\right]+\ln\left[\frac{\beta_i}{B}+\sqrt{\left(\frac{\beta_i}{B}\right)^2+1}\right]+\ln\left[\frac{\alpha_i}{B}+\sqrt{\left(\frac{\alpha_i}{B}\right)+1}\right]$$

$$\left.-\ln\left[\frac{4h(n-i)-\alpha_i}{B}+\sqrt{\frac{\langle 4h(n-i)-\alpha_i\rangle^2}{B^2}+1}\right]\right.$$

$$+\frac{8h(n-i)}{3}\left[\frac{B^2+2h(n-i)\langle 4h(n-i)+\beta_i\rangle}{\left[B^2+\langle 4h(n-i)+\beta_i\rangle^2\right]^{3/2}}-\frac{B^2+2h(n-i)\langle 4h(n-i)-\alpha_i\rangle}{\left[B^2+\langle 4h(n-i)-\alpha_i\rangle^2\right]^{3/2}}\right]$$

$$+\frac{2}{3}\left[\frac{\beta_i}{\left[B^2+\beta_i^2\right]^{1/2}}+\frac{\alpha_i}{\left[B^2+\alpha_i^2\right]^{1/2}}\right]+\frac{2}{3B^2}\left[\frac{4h^2(n-i)^2\langle 4h(n-i)+\beta_i\rangle-B^2\langle 2h(n-i)-\beta_i\rangle}{\left[B^2+\langle 4h(n-i)+\beta_i\rangle^2\right]^{1/2}}\right.$$

$$\left.\left.-\frac{4h^2(n-i)^2\langle 4h(n-i)-\alpha_i\rangle-B^2\langle 2h(n-i)+\alpha_i\rangle}{\left[B^2+\langle 4h(n-i)-\alpha_i\rangle^2\right]^{1/2}}\right]\right\}\Bigg]\Bigg|^{-1} \qquad (42)$$

valid for i=1,2,---,(n-1)

in which

$i = 1,2,---,n$

$r = 1,2,---,Q$

$s = 1,2,---,Q$

n = number of intervals, i.e. number of masses

h = half height of an interval

Q = number of piles in a group

B = radius of a pile

$\left.\begin{matrix} x_r \\ y_r \end{matrix}\right\}$ = coordinate distances to the axis of pile r as measured from an origin which is located at the center of gravity of the pile group.

$\left.\begin{matrix} x_{rs} = x_r - x_s \\ y_{rs} = y_r - y_s \end{matrix}\right\}$ i.e., the x and y coordinates of axis r when the origin of these coordinates coincides with the s axis.

$R_{rs} = x_{rs}^2 + y_{rs}^2$

The expression for the top layer is

$$\eta_n = Q\left|\left[\sum_{r=1,2--}^{Q}\ \sum_{s=1,2--}^{Q}(1-\delta_{rs})\left\{\ln\left[\frac{h+\beta_n}{R_{rs}^{1/2}}+\sqrt{\frac{(h+\beta_n)^2}{R_{rs}}+1}\right]\right.\right.\right.$$

$$+ \ln\left[\frac{\beta_n}{R_{rs}^{1/2}} + \sqrt{\frac{\beta_n^2}{R_{rs}} + 1}\right] + \frac{1}{R_{rs}}\left[\frac{x_{rs}^2 h\left[R_{rs} + (h/2)(h+\beta_n)\right]}{\left[R_{rs} + (h+\beta_n)^2\right]^{3/2}}\right.$$

$$+ \frac{x_{rs}^2 h^2 (h+\beta_n)}{R_{rs}\left[R_{rs}+(h+\beta_n)^2\right]^{1/2}} - \frac{h\,(h^2/2 + y_{rs}^2) + \beta_n(h^2/2 - x_{rs}^2)}{\left[R_{rs} + (h+\beta_n)^2\right]^{1/2}} + \frac{\beta_n x_{rs}^2}{\left[R_{rs} + \beta_n^2\right]^{1/2}}$$

$$\left. + \frac{h(h^2/4 + y_{rs}^2)}{\left[R_{rs} + (h/2)^2\right]^{1/2}} - \frac{x_{rs}^2 h^2 (h/2)}{R_{rs}\left[R_{rs} + (h/2)^2\right]^{1/2}}\right]\Bigg\} + Q\left\{\ln\left[\frac{\beta_n}{B} + \sqrt{\left(\frac{\beta_n}{B}\right)^2 + 1}\right]\right.$$

$$+ \ln\left[\frac{h+\beta_n}{B} + \sqrt{\left(\frac{h+\beta_n}{B}\right)^2 + 1}\right] + \frac{2}{3}\left[\frac{hB^2 + h^2/2\,(h+\beta_n)}{\left[B^2+(h+\beta_n)^2\right]^{3/2}} + \frac{\beta_n}{\left[B^2 + \beta_n^2\right]^{1/2}}\right.$$

$$\left.\left. + \frac{(h/2)^2 (h+\beta_n) - B^2(h/2 - \beta_n)}{B^2\left[B^2 + (h+\beta_n)^2\right]^{1/2}} + \frac{h/2}{\left[B^2 + (h/2)^2\right]^{1/2}} - \frac{(h/2)^3}{B^2\left[B^2 + (h/2)^2\right]^{1/2}}\right]\right\}\Bigg]\Bigg|^{-1} \tag{43}$$

where β_n is measured from $z = h/2$

Over the height of the interval (2h) which is centered at depth $\bar{c}_i$ there is only a slight variation of the displacements with respect to depth. Therefore, one can simplify the integration by assuming the displacements remain constant over the depth of the interval, and thus Eq. (38) may be written as

$$M_i^e = N \int_{\bar{c}_i - h}^{\bar{c}_i + h} \int_{-\infty}^{\infty} \int_{-\infty}^{\infty} \left[\psi_u^2 + \psi_v^2 + \psi_w^2\right] \rho(x,y,z)\, dx\, dy\, dz = N\,(2-\delta_{in})\, h\rho_i$$

$$\int_{-\infty}^{\infty}\int_{-\infty}^{\infty}\left\{\left[\psi_u(x,y,\bar{c}_i)\right]^2+\left[\psi_v(x,y,\bar{c}_i)\right]^2+\left[\psi_w(x,y,\bar{c}_i)\right]^2\right\}dx\,dy \qquad (44)$$

Note that the mass density of the clay medium has also been assumed to be constant within the interval. The factor N has been introduced to account for the number of pile groupings which constitute the idealized pile groupings of Fig. 4.

The displacement influence functions shown in Eq. 38 are evaluated as a summation of the Q displacement fields which are induced by the special normalized uniform loading along the intended axis of each pile in the group, e.g.

$$\psi_u(x,y,\bar{c}_i)=\sum_{s=1}^{Q}u_s(x,y,\bar{c}_i) \qquad (45)$$

The expression for the components of displacement on level $\bar{c}_i$ due to a single line static loading of intensity p applied to the clay medium over the interval $(\bar{c}_i-\alpha_i)$ to $(\bar{c}_i+\beta_i)$ are:

$$u_x(x,y,\bar{c}_i)=\frac{3p}{8\pi E}\left\{\sinh^{-1}\frac{2\bar{c}_i+\beta_i}{(x^2+y^2)^{1/2}}+\sinh^{-1}\frac{\beta_i}{(x^2+y^2)^{1/2}}+\sinh^{-1}\frac{\alpha_i}{(x^2+y^2)^{1/2}}\right.$$

$$-\sinh^{-1}\frac{2\bar{c}_i-\alpha_i}{(x^2+y^2)^{1/2}}+\frac{1}{x^2+y^2}\left[\frac{2x^2\bar{c}_i\left[x^2+y^2+\bar{c}_i(2\bar{c}_i+\beta_i)\right]}{\left[x^2+y^2+(2\bar{c}_i+\beta_i)^2\right]^{3/2}}\right.$$

$$\left.\left.+\frac{4x^2\bar{c}_i^2(2\bar{c}_i+\beta_i)}{(x^2+y^2)\left[x^2+y^2+(2\bar{c}_i+\beta_i)^2\right]^{1/2}}-\frac{2\bar{c}_i(2\bar{c}_i^2+y^2)+\beta_i(2\bar{c}_i^2-x^2)}{\left[x^2+y^2+(2\bar{c}_i+\beta_i)^2\right]^{1/2}}\right]\right\}$$

$$+\frac{\beta_i x^2}{\left[x^2+y^2+\beta_i^2\right]^{1/2}}+\frac{\alpha_i x^2}{\left[x^2+y^2+\alpha_i^2\right]^{1/2}}-\frac{2x^2\bar{c}_i\left[x^2+y^2+\bar{c}_i\,(2\bar{c}_i-\alpha_i)\right]}{\left[x^2+y^2+(2\bar{c}_i-\alpha_i)^2\right]^{3/2}}$$

$$-\frac{4x^2\bar{c}_i\,(2\bar{c}_i-\alpha_i)}{(x^2+y^2)\left[x^2+y^2+(2\bar{c}_i-\alpha_i)^2\right]^{1/2}}+\frac{2\bar{c}_i\,(2\bar{c}_i^2+y^2)-\alpha_i(2\bar{c}_i^2-x^2)}{\left[x^2+y^2+(2\bar{c}_i-\alpha_i)^2\right]^{1/2}}\Bigg]\Bigg\} \qquad (46)$$

$$v_x(x,y,\bar{c}_i)=\frac{3p}{8\pi E}\,\frac{xy}{(x^2+y^2)}\left\{\frac{\beta_i}{\left[x^2+y^2+\beta_i^2\right]^{1/2}}+\frac{\alpha_i}{\left[x^2+y^2+\alpha_i^2\right]^{1/2}}\right.$$

$$+\frac{(x^2+y^2+4\bar{c}_i^2)\,(2\bar{c}_i+\beta_i)}{(x^2+y^2)\left[x^2+y^2+(2\bar{c}_i+\beta_i)^2\right]^{1/2}}+\frac{2\bar{c}_i\left[x^2+y^2+\bar{c}_i\,(2\bar{c}_i+\beta_i)\right]}{\left[x^2+y^2+(2\bar{c}_i+\beta_i)^2\right]^{3/2}}$$

$$\left.-\frac{(x^2+y^2+4\bar{c}_i^2)\,(2\bar{c}_i-\alpha_i)}{(x^2+y^2)\left[x^2+y^2+(2\bar{c}_i-\alpha_i)^2\right]^{1/2}}-\frac{2\bar{c}_i\left[x^2+y^2+\bar{c}_i(2\bar{c}_i-\alpha_i)\right]}{\left[x^2+y^2+(2\bar{c}_i-\alpha_i)^2\right]^{3/2}}\right\} \qquad (47)$$

$$w_x(x,y,\bar{c}_i)=\frac{3p}{8\pi E}\,x\left\{\frac{1}{\left[x^2+y^2+\beta_i^2\right]^{1/2}}-\frac{1}{\left[x^2+y^2+\alpha_i^2\right]^{1/2}}+\frac{1}{\left[x^2+y^2+(2\bar{c}_i+\beta_i)^2\right]^{1/2}}\right.$$

$$\left.+\frac{2\bar{c}_i(\bar{c}_i+\beta_i)}{\left[x^2+y^2+(2\bar{c}_i+\beta_i)^2\right]^{3/2}}-\frac{1}{\left[x^2+y^2+(2\bar{c}_i-\alpha_i)^2\right]^{1/2}}-\frac{2\bar{c}_i(\bar{c}_i-\alpha_i)}{\left[x^2+y^2+(2\bar{c}_i-\alpha_i)^2\right]^{3/2}}\right\} \qquad (48)$$

In view of the symmetry of the layout of the piles within each grouping, and the symmetry of the displacement field, the evaluation of the effective mass can be simplified by carrying out the integration in only

one quadrant. Thus, by combining Eq. 44 with Eqs. 45-48 yields the final result

$$M_i^e = 4N\,(2-\delta_{in})\,h\rho_i\,(\eta_i)^2 \int_0^\infty\int_0^\infty \Omega(x,y,\bar{c}_i)\,dx\,dy \;;\; i=1,2,---,n \tag{49}$$

in which

$$\Omega(x,y,\bar{c}_i) = \left[(\psi_u)^2 + (\psi_v)^2 + (\psi_w)^2\right] \tag{50}$$

$$\psi_u(x,y,\bar{c}_i) = \sum_{s=1}^{Q}\left\{ \ln\left[\frac{\bar{B}}{R_s^{1/2}} + \sqrt{\frac{\bar{B}^2}{R_s}+1}\right] + \ln\left[\frac{\beta_i}{R_s^{1/2}} + \sqrt{\frac{\beta_i^2}{R_s}+1}\right]\right.$$

$$+ \ln\left[\frac{\alpha_i}{R_s^{1/2}} + \sqrt{\frac{\alpha_i^2}{R_s}+1}\right] - \ln\left[\frac{\bar{A}}{R_s^{1/2}} + \sqrt{\frac{\bar{A}^2}{R_s}+1}\right] + \frac{1}{R_s}\left[\frac{2x_s^2\bar{c}_i(R_s+\bar{c}_i\bar{B})}{V_s^3}\right.$$

$$+ \frac{4x_s^2\bar{c}_i^2\bar{B}}{R_sV_s} + \frac{\beta_i x_s^2}{T_s} - \frac{2\bar{c}_i\bar{B} + 2\bar{c}_i y_s^2 - \beta_i x_s^2}{V_s} - \frac{2x_s^2\bar{c}_i(R_s+\bar{c}_i\bar{A})}{U_s^3} - \frac{4x_s^2\bar{c}_i^2\bar{A}}{R_sU_s}$$

$$\left.\left. + \frac{2\bar{c}_i^2\bar{A} + 2\bar{c}_i y_s^2 + \alpha_i x_s^2}{U_s} + \frac{\alpha_i x_s^2}{S_s}\right]\right\} \tag{51}$$

$$\psi_v(x,y,\bar{c}_i) = \sum_{s=1}^{Q}\left(\frac{x_s y_s}{R_s}\right)\left\{\frac{\beta_i}{T_s} + \frac{\alpha_i}{S_s} + \frac{(R_s+4\bar{c}_i^2)\bar{B}}{R_sV_s} + \frac{2\bar{c}_i(R_s+\bar{c}_i\bar{B})}{V_s^3}\right.$$

$$\left. - \frac{(R_s+4\bar{c}_i^2)\bar{A}}{R_sU_s} - \frac{2\bar{c}_i(R_s+\bar{c}_i\bar{A})}{V_s^3}\right\} \tag{52}$$

$$\psi_w(x,y,\bar{c}_i) = \sum_{s=1}^{Q} x_s\left\{\frac{1}{T_s} - \frac{1}{S_s} + \frac{1}{V_s} - \frac{1}{U_s} + \frac{2\bar{c}_i(\bar{c}_i+\beta_i)}{V_s^3} - \frac{2\bar{c}_i(\bar{c}_i-\alpha_i)}{U_s^3}\right\} \tag{53}$$

$$\left.\begin{aligned} x_s &= (x - x_r) \\ y_s &= (y - y_r) \end{aligned}\right\} \; s=1,2,---,Q$$

$$\bar{A} = 2\bar{c}_i - \alpha_i$$

$$\bar{B} = 2\bar{c}_i + \beta_i$$

$$R_s = x_s^2 + y_s^2$$

$$S_s = \left[x_s^2 + y_s^2 + \alpha_i^2\right]^{1/2} = \left[R_s + \alpha_i^2\right]^{1/2}$$

$$T_s = \left[x_s^2 + y_s^2 + \beta_i^2\right]^{1/2} = \left[R_s + \beta_i^2\right]^{1/2}$$

$$U_s = \left[x_s^2 + y_s^2 + (2\bar{c}_i - \alpha_i)^2\right]^{1/2} = \left[R_s + \bar{A}^2\right]^{1/2}$$

$$V_s = \left[x_s^2 + y_s^2 + (2\bar{c}_i + \beta_i)^2\right]^{1/2} = \left[R_s + \bar{B}^2\right]^{1/2}$$

$$\bar{c}_i = 2h\,(n-i) \quad , \; i=1,2,\text{---},(n-1) \quad ; \; c_n = h/2$$

$$N = \left\{ \begin{array}{l} 2 \text{ for multiple row grouping} \\ 3 \text{ for single row grouping} \end{array} \right\} = \text{number of groupings between expansion joints}$$

Because of the singularities of the displacement functions in the neighborhood of the point at which the load is applied it will be necessary to omit evaluation of the above quantities in the area near the intended axis of a pile, i.e., in the regions for which $R_s < B^2$.

The integration of Eq. (49) will be performed by a numerical procedure, consequently it will be necessary to set finite limits for the domain of integration. The limits of this region will be established by the defining relationship

$$\Omega\,(x_i^o, y_i^o, \bar{c}_i) \equiv 0.05\;\Omega\,(B, 0, \bar{c}_i) \qquad (54)$$

Thus it is assumed that the contribution to the integral of Eq. (49)

beyond the limits x_i^o and y_i^o, as defined by Eq. (54) is small compared with the contribution within these limits, i.e.

$$\Omega\,(x_i^o + \Delta x, y_i^o + \Delta y, \bar{c}_i) \cong 0 \tag{55}$$

(12) Damping Coefficients C_i^d - It is suggested that the coefficients which represent damping effects be evaluated by equating the rate of energy dissipation resulting from elastic deformations (creep effects excluded) of the real system in their respective i intervals to the rate of energy dissipation in the damping dashpots at corresponding locations in the idealized model.

A measure of the energy dissipation per unit volume for the clay medium can be determined from free vibration tests performed on clay samples. By definition the rate of energy dissipation per unit volume of a cylindrical test specimen is

$$E_{Di} = c_i^* \frac{\dot{u}_1^2}{AL} = c_i^* \frac{(\epsilon_i L)^2}{AL} \tag{56}$$

in which A is the cross-sectional area, and L is the height of the test specimen. The total rate of energy dissipation in the clay medium within interval i is found by integrating this expression over the volume of the interval under consideration.

The total rate of energy dissipation in the damping dashpot at level i in the idealized model can be expressed in terms of the velocity of the generalized coordinate $\dot{U}_i^s$ as follows:

$$(E_{Di})_{total} = C_i^d\,(\dot{U}_i^s)^2 \tag{57}$$

For the evaluation of the damping coefficients, the time dependent stress field is assumed to be of the form

$$\sigma_x(x,y,z,t)_i = U_i^s(t)\ \kappa_i(x,y,z) \tag{58}$$

in which $\kappa_i(x,y,z)$ is a stress influence function, and is the generalized expression for the stress field which corresponds to a unit displacement at the intended location of the pile group Taking the time derivative of Eq.(58) and dividing by the modulus of elasticity for that level, yields an expression for strain-rate which can be substituted into Eq. (56). Equating the total rates of energy dissipation as given by Eqs. (56) and 57,) an expression for the creep dashpot coefficient at level i is obtained, namely

$$c_i^d = \frac{c_i^* L}{A(E_i)^2} \int_{V_i} \left[\kappa_i(x,y,z)\right]^2 dv \tag{59}$$

In view of the slight variation of the stresses with respect to depth over the height of the interval of interest, and also the symmetry of the stress field, Eq. (59) can be written in the form

$$c_i^d = 4N\ (2 - \delta_{in})\ hc_i^{**} \frac{1}{(E_i)^2} \int_0^\infty\int_0^\infty \left[\kappa_i(x,y,\bar{c}_i)\right]^2 dx\ dy \tag{60}$$

in which

$$c_i^{**} = c_i^* \frac{L}{A} \tag{61}$$

The stress influence functions are evaluated from the total stress field which is induced by the special normalized uniform loading (see Eq. 41) along the intended axis of each pile in the group, thus

$$\kappa_i(x,y,\bar{c}_i) = \sum_{s=1}^{Q} \left[\sigma_x(x,y,\bar{c}_i)\right]_s \tag{62}$$

The expression for the stress σ_x on level $\bar{c}_i$ due to a single line static loading of intensity p applied to the clay medium over the distance $(\bar{c}_i - \alpha_i)$ to $(\bar{c}_i + \beta_i)$ is

$$\sigma_x(x,y,\bar{c}_i) = \frac{px}{4\pi(x^2+y^2)} \left\{ \frac{6x^2\bar{c}_i(\bar{c}_i+\beta_i)(2\bar{c}_i+\beta_i)}{\left[x^2+y^2+(2\bar{c}_i+\beta_i)^2\right]^{5/2}} + \frac{4\bar{c}_i(y^2-x^2)+(3x^2+2y^2)\beta_i}{\left[x^2+y^2+(2\bar{c}_i+\beta_i)^2\right]^{3/2}} \right.$$

$$+ \frac{2(2\bar{c}_i+\beta_i)}{(x^2+y^2)\left[x^2+y^2+(2\bar{c}_i+\beta_i)^2\right]^{1/2}} \left[y^2+\bar{c}_i^2(3y^2-x^2) \left\{ \frac{1}{x^2+y^2+(2\bar{c}_i+\beta_i)^2} + \frac{2}{x^2+y^2} \right\} \right]$$

$$- \frac{\beta_i x^2}{\left[x^2+y^2+\beta_i^2\right]^{1/2}} \left[\frac{1}{x^2+y^2+\beta_i^2} + \frac{2}{x^2+y^2} \right] - \frac{\alpha_i x^2}{\left[x^2+y^2+\alpha_i^2\right]^{1/2}} \left[\frac{1}{x^2+y^2+\alpha_i^2} + \frac{2}{x^2+y^2} \right]$$

$$- \frac{6x^2\bar{c}_i(\bar{c}_i-\alpha_i)(2\bar{c}_i-\alpha_i)}{\left[x^2+y^2+(2\bar{c}_i-\alpha_i)^2\right]^{5/2}} - \frac{4\bar{c}_i(y^2-x^2)+(3x^2+2y^2)\alpha_i}{\left[x^2+y^2+(2\bar{c}_i-\alpha_i)^2\right]^{3/2}} - \frac{2(2\bar{c}_i-\alpha_i)}{(x^2+y^2)\left[x^2+y^2+(2\bar{c}_i-\alpha_i)2\right]^{1/2}}$$

$$\left. \left[y^2+\bar{c}_i^2(3y^2-x^2) \left\{ \frac{1}{x^2+y^2+(2\bar{c}_i-\alpha_i)^2} + \frac{2}{x^2+y^2} \right\} \right] \right\} \tag{63}$$

Combining Eq. 39 with Eqs. 60-63 yields the result

$$C_i^d = \xi_i \, c_i^{**} \tag{64}$$

in which

$$\xi_i = 4N(2-\delta_{in})\, h \left(\frac{2\eta_i}{3}\right)^2 \int_0^\infty \int_0^\infty \left[\Gamma_i(x,y,\bar{c}_i)\right]^2 dx\, dy \tag{65}$$

$$i=1,2,---,n$$

$$\Gamma_i(x,y,\bar{c}_i) = \sum_{s=1}^{Q} \frac{x_s}{R_s} \left\{ \frac{6x_s^2\bar{c}_i(\bar{c}_i+\beta_i)\bar{B}}{V_s^5} + \frac{4\bar{c}_i(y_s^2-x_s^2)-(3x_s^2+2y_s^2)\beta_i}{V_s^3} + \frac{2\bar{B}}{R_s V_s} \right.$$

$$\left[y_s^2+\bar{c}_i^2\,(3y_s^2-x_s^2) \left\{ \frac{1}{V_s^2} + \frac{2}{R_s} \right\} \right] - \frac{\beta_i x_s^2}{T_s} \left[\frac{1}{T_s^2} + \frac{2}{R_s} \right] - \frac{\alpha_i x_s^2}{S_s} \left[\frac{1}{S_s^2} + \frac{2}{R_s} \right]$$

$$- \frac{6x_s^2\bar{c}_i(\bar{c}_i-\alpha_i)\bar{A}}{U_s^5} - \frac{4\bar{c}_i(y_s^2-x_s^2) + (3x_s^2+2y_s^2)\alpha_i}{U_s^3} - \frac{2\bar{A}}{R_s U_s} \left[y_s^2 + \bar{c}_i^2\,(3y_s^2-x_s^2) \right.$$

$$\left. \left. \left\{ \frac{1}{U_s^2} + \frac{2}{R_s} \right\} \right] \right\} \tag{66}$$

The evaluation of Eq. 65 will be performed in an identical manner to the procedure used for the integration of Eq. 49, and the limits of the region of integration will be defined by the curve $f(x_i^o, y_i^o)$ as established by the relationship of Eq. 54 . As before, it will be necessary to omit evaluation of the integrand in the neighborhood of the intended axis of a pile, i.e., where $R_s < B^2$.

An expression for the strain rate at level i is obtained by dividing Eq. 58 by the modulus of elasticity of the layer, and then taking the time derivative. This yields

$$\dot{\epsilon}_x(x,y,t)_i = \dot{U}_i^s(t) \frac{\kappa_i(x,y,z)}{E_i} \tag{67}$$

In order to determine the average value of the strain rate at level i Eq. 67 is integrated over the interval and then divided by the volume of the domain of influence, thus obtaining

$$\dot{\epsilon}_x(t)_{avg} = \dot{U}_i^s(t)\, \zeta_i \tag{68}$$

where

$$\zeta_i = \frac{2\eta_i}{3A_i} \int_0^{g(x_i^o)} \int_0^{h(y_i^o)} \sigma_i(x,y,\bar{c}_i)\, dx\, dy \qquad (69)$$

A_i = the area of the domain of influence at level $z=\bar{c}_i$ as defined by the curve $f(x_i^o, y_i^o)$

The velocity of the free-vibration test specimen can be expressed as

$$\dot{u}(t) = \dot{\epsilon}(t)_{avg} L \qquad (70)$$

Consequently, by combining Eqs. 68 and 70 an expression is obtained for the velocity of the dashpot in terms of the velocity of the clay specimen

$$\dot{U}_i^s = \frac{\dot{u}(t)}{L\zeta_i} \qquad (71)$$

A particular value of the interaction damping coefficient and the velocity which is associated with it are related to the corresponding values of the test specimen by Eqs. 64 and 71. The data from these equations are plotted on a diagram of damping coefficient vs. velocity for the interaction damping dashpot at level i. A straight line is drawn on the diagram which is the best fit of the data. The intercept and slope of this line define the damping dashpot coefficients for Eq. 14.

(13) Creep Coefficients C_i^c - The coefficients which represent creep effects in the clay medium due to its interaction with a pile group is determined from an approximate strain rate field for each layer i as produced by the distributed interaction forces within that group over layer i. Since creep will take place primarily near the piles where the stresses are high, the effects on creep in layer i due to those interaction forces in neighboring layers will be neglected. The strain-rate associated with any given stress level will be determined from triaxial tests.

For purposes of determining the creep coefficient in layer i, the elastic stress field due to F_i^s will be assumed. A study of this stress field along the x-axis shows that the major principle axis is oriented reasonably close to the x axis; thus, the stress quantity $(\sigma_x - \sigma_y)$ may be compared directly with the triaxial deviator stress to obtain an approximate measure of the creep rate present at any given point. After observing the nature of the overall stress field in the vicinity of a pile group, it appears that the $(\sigma_x - \sigma_y)$ stress distribution along a single axis can be used to adequately predict the creep displacement rate of a pile group due to a given interaction loading condition. This particular x axis is oriented in the direction of motion in a horizontal plane which is located at mid-height of the particular interval i being investigated. The origin of this x-y coordinate system is coincident with the centroidal axis of the pile group. The resulting $(\sigma_x - \sigma_y)$ stress distribution along this x axis is anti-symmetric with respect to the origin; therefore, one need consider only the distribution of stress along the positive side of this axis. From triaxial test data a relationship between strain-rate and deviator stress can be obtained. Having this relationship and the $(\sigma_x - \sigma_y)$ stress distribution along the x axis for level i, a curve showing strain-rate along this axis can be determined. The area under this curve represents the velocity of the pile group at level i due to creep effects; thus,

$$C_i^c \cong F_i^s \; / \; (\dot{U}_i^r - \dot{U}_i^s) = F_i^s \; / \int_B^\infty \dot{\epsilon}_x(x;F_i^s)\, dx \qquad (72)$$

The equation for the $(\sigma_x - \sigma_y)$ stress distribution along the positive x axis which results from a uniform loading of intensity p_j applied along the intended axis of each pile of the group is given by

$$\left[\sigma_x(x,o,\bar{c}_i;p_j) - \sigma_y(x,o,\bar{c}_i;p_j)\right] = \frac{p_j}{4\pi}\,\sigma^*(x,o,\bar{c}_i) \tag{73}$$

in which

$$\sigma^*(x,o,\bar{c}_i) = \sum_{s=1}^{Q} x_s \left[\left[\left(\frac{x_s^2-y_s^2}{R_s}\right)\left\{\frac{6\bar{c}_i(\bar{c}_i+\beta_i)\bar{B}}{V_s^5} - \frac{4\bar{c}_i+\beta_i}{V_s^3} - \frac{2\bar{B}}{R_s V_s}\right.\right.\right.$$

$$\left.\left[1+2\bar{c}_i^2\left\{\frac{1}{V_s^2}+\frac{2}{R_s}\right\}\right] - \frac{\beta_i}{T_s}\left[\frac{1}{T_s^2}+\frac{2}{R_s}\right] - \frac{\alpha_i}{S_s}\left[\frac{1}{S_s^2}+\frac{2}{R_s}\right] - \frac{6\bar{c}_i(\bar{c}_i-\alpha_i)\bar{A}}{U_s^5}\right.$$

$$\left.\left.\left.+\frac{4\bar{c}_i-\alpha_i}{U_s^3} + \frac{2\bar{A}}{R_s U_s}\left[1+2\bar{c}_i^2\left\{\frac{1}{U_s^2}+\frac{2}{R_s}\right\}\right]\right\} + \left(\frac{8\bar{c}_i y_s^2}{R_s}\right)\left\{\frac{1}{V_s^3} - \frac{1}{U_s^3} + \frac{\bar{c}_i\bar{B}}{R_s V_s}\right.\right.\right.$$

$$\left.\left.\left.\left[\frac{1}{V_s^2}+\frac{2}{R_s}\right] - \frac{\bar{c}_i\bar{A}}{R_s U_s}\left[\frac{1}{U_s^2}+\frac{2}{R_s}\right]\right\}\right]\right] \tag{74}$$

It is important to note that the terms α_i and β_i in Eq. 74 do not necessarily have the same values as the α_i and β_i terms in the equations for effective mass.

Based upon the triaxial test data a relationship between strain rate and deviator stress can be extablished for each level of the clay medium, i.e.

$$\dot{\epsilon}_i = D_{1i}\sigma_{Di} + D_{2i}\,|\sigma_{Di}|\,\sigma_{Di} + D_{3i}\sigma_{Di}^3 \tag{75}$$

The velocity of the pile group at level i due to creep effects associated with loading p_j is given by the relationship

$$V_i^c(p_j) = \int_B^\infty \dot{\epsilon}_{x_i}(x;p_j)\,dx \tag{76}$$

Substituting Eqs. 73 and 75 into Eq. 76 yields

$$V_i^c(p_j) = \frac{D_{1i}p_j}{4\pi} \int_B^{x^*} \sigma^*(x,o,\bar{c}_i)\, dx + D_{2i} \left(\frac{p_j}{4\pi} \right)^2 \int_B^{x^*} \left[\sigma^*(x,o,\bar{c}_i)\right]^2 dx$$

$$+ D_{3i} \left(\frac{p_j}{4\pi} \right)^3 \int_B^{x^*} \left[\sigma^*(x,o,\bar{c}_i)\right]^3 dx \qquad (77)$$

where $\sigma^*(x,o,\bar{c}_i)$ is given by Eq. 74, and the upper limit of integration, x^*, is established by the relationship

$$\dot{\epsilon}(x^*;p_j) = 0.02\dot{\epsilon}\ (B;p_j) \qquad (78)$$

The creep dashpot coefficient at level i which is associated with the loading p_j is given by Eq. 72 which can be written in the form

$$C_i^c(p_j) = \frac{(\alpha_i + \beta_i)\ NQp_j}{V_i^c(p_j)} \qquad (79)$$

Eqs. 77 and 79 are evaluated for a series of different applied loads p_j, and the resulting values plotted on a diagram of creep coefficient vs. the velocity for the interaction creep dashpot at level i, i.e. C_i^c vs. V_i^c. The values of loading p_j which are to be employed in evaluating the m data points of the curve will be taken as the m multiples of the maximum elastic spring force, thus

$$(p_j)_i = \frac{j}{m} \left\{ \frac{F_{iy}^s}{(2-\delta_{in})\ h\ NQ} \right\} \quad ; \quad j=1,2,---,m \text{ (e.g. } m=5) \qquad (80)$$

By utilizing a curve fitting procedure on the resulting diagram it will then be possible to determine the creep dashpot coefficients for Eq. 13.

(14) Axial Forces $\bar{S}_i$, $\bar{\bar{S}}_i$, $\bar{T}_i$, $\bar{\bar{T}}_i$, - These forces represent those portions of the total dead weight of the bridge structural system which are carried by their respective members at level i. The horizontal

components t_i and t_{i+1} of the axial forces T_i and T_{i+1}, respectively, are approximated by the relations

$$t_i = \frac{T_i}{L_i} u_{i-1} - \frac{T_i}{L_i} u_i \tag{81a}$$

$$t_{i+1} = \frac{T_{i+1}}{L_{i+1}} u_i - \frac{T_{i+1}}{L_{i+1}} u_{i+1} \tag{81b}$$

Thus, the resulting horizontal component of force at mass m_i is the difference Δt_i of the preceding components, i.e.

$$\Delta t_i = -\frac{T_i}{L_i} u_{i-1} + \left(\frac{T_i}{L_i} + \frac{T_{i+1}}{L_{i+1}} \right) u_i - \frac{T_{i+1}}{L_{i+1}} u_{i+1} \tag{82}$$

Written in matrix form for i=1,2,---,n-1, Eq. 80 may be designated simply as

$$\left\{ \Delta t_i \right\} = \left[T_{ij} \right] \left\{ u_i \right\} \tag{83}$$

DETERMINATION OF SOIL PROPERTIES

General

For purposes of analysis in this investigation it was assumed that the shear stress-deformation characteristics of the clay could be represented by the model shown in Fig. 11. The elements in this model are:

(1) a non-linear elastic spring with hysteresis characteristics to represent the immediate deformation characteristics of the soil structure under cyclic loading,

(2) a viscous dashpot in parallel with the spring to represent internal damping within the soil,

and (3) a viscous element in series with the spring-dashpot combination to represent the creep behavior of the soil.

It was necessary, therefore, to develop test procedures to determine the soil parameters defining these characteristics and to establish the variation in these parameters throughout the depth of the in-situ clay layer.

Boring and Field Testing Program

The characteristics of the clay were investigated by means of 3 borings designated PS-1, PS-2 and PS-3 made along the axis of the proposed bridge location as shown in Fig. 12. The logs of these borings are shown in the soil profile along the bridge site, Fig. 13.

Undisturbed samples were recovered from the borings at the elevations shown in Fig. 14 for use in the laboratory testing program. In boring PS-1, these were obtained in 18 inch lengths by means of 6 inch diameter Shelby tubes. In borings PS-2 and PS-3 the undisturbed samples

were taken at more frequent intervals in 30 inch lengths using 2.8 inch diameter Shelby tubes.

In all cases the tubes were forced into the soil by hand or by hydraulic jack except for the bottom 15 ft. of boring PS-2 where the tubes were driven by hammer blows. The ends of the tubes were sealed with wax as soon as practicable after recovery to prevent moisture loss from the soil prior to testing.

Adjacent to each boring made to obtain undisturbed samples, a supplementary boring was made, within about 5 ft., in which field vane shear tests were made at 5 ft. intervals. The results of these tests are presented in Fig. 14.

Soil Conditions

The clay underlying the proposed site for the Elkhorn Slough Bridge is a soft to firm gray silty clay containing many seams and thin layers of silt and silty sand up to 5 ft. in thickness. The thickness of the clay deposit varies from about 50 ft. at the bridge abutments to about 120 ft. in the center portion of the bridge span.

Atterberg limits of typical samples of the clay are:

Liquid limit = 76

Plastic limit = 22

and the water content varies from an average of about 80% at Elev. -30 to an average of about 50% at Elev. -75.

Corresponding to the decrease in water content with depth the soil strength shows a general increase with depth as illustrated by the vane shear strength data in Fig. 14. A summary of all vane test data obtained at the bridge site, both in the borings made for the present investigation and in previous investigations, is presented in Fig. 15. Although there

is considerable scatter in the strength values at any elevation, the average shear strength increases from about 0.1 tons per sq.ft. at Elev. 0 to about 0.6 tons per sq.ft. at Elev. -90. The envelope enclosing most of the strength data is shown in Fig. 15.

Laboratory Strength Tests

In conjunction with the laboratory test program to determine the soil deformation characteristics, a number of unconsolidated-undrained triaxial compression tests were conducted using a confining pressure of 1.0 kg. per sq.cm. The tests were performed on 1.4 inch diameter specimens trimmed from the undisturbed samples and the stress vs strain relationships obtained in these tests are shown in Fig. 16.

A number of other specimens used for determining damping and creep characteristics were deformed only slightly during these tests and were subsequently subjected to compression tests in the same manner as the specimens trimmed from undisturbed samples. It was considered that the strengths of these specimens were only slightly affected by the prior testing procedures and provided a reasonable indication of the strengths of the undisturbed samples in the laboratory. Thus the stress vs strain relationships for these specimens are also shown in Fig. 16.

The shear strengths for all these samples, taken in each case as one half of the compression strength, are plotted versus sample depth in Fig. 17. As in the case of the vane test data, the laboratory strength tests show considerable variations in strength for samples at any one elevation but a general increase in strength with depth.

The envelope for the field vane shear strength values is also plotted in Fig. 17.

Based on the results of the laboratory and field tests it would appear

that the shear strength vs depth relationship for the clay deposit can be reasonably represented as a uniform increase from an average value of 0.08 ton per sq.ft. at Elev. 0 to 0.52 ton per sq.ft. at Elev. -90, indicated by the solid line in Fig. 17, together with a possible variation of ±50% from these values as indicated by the dashed lines. These relationships will be used later as a basis for determining the variation of deformation parameters throughout the depth of the deposit.

Determination of Shear Properties from Compression Tests

The analysis of the response of a clay layer overlying a rigid stratum or the interaction between the clay layer and piles driven into it requires a knowledge of the shear stress vs strain characteristics of the clay. In laboratory test programs it is more convenient to determine the stress vs strain relationships for soils in axial compression. However for saturated clays subjected to short term stress applications, deformations occur at constant volume and thus Poisson's ratio will be equal to 0.5. Thus it is possible to determine numerical relationships between principal stresses and strains in compression and shear with sufficient accuracy by means of the expressions:

$$\tau = \frac{\sigma_1 - \sigma_3}{2} = \frac{\sigma_d}{2} \tag{83}$$

and

$$\gamma_s = (1 + \nu)\, \epsilon_1 \tag{84}$$

where τ = principal shear stress

σ_d = principal compression stress difference, $\sigma_1 - \sigma_3$

σ_1 = major principal stress in compression test

σ_3 = minor principal stress in compression test

γ_s = principal shear strain

ϵ_1 = major principal compression strain

ν = Poisson's ratio

Substituting $\upsilon = 0.5$ in the above expressions gives

$$\tau = 0.5\sigma_d \tag{85}$$

$$\gamma_s = 1.5\epsilon_1 \tag{86}$$

Thus the shear stress vs strain behavior for the clay can readily be determined from the compression test data.

Dynamic Tests

The creep, damping and dynamic elasticity characteristics of soil specimens were determined by dynamic tests, using the apparatus illustrated in Fig. 18. A specimen of clay, 1.4 inches in diameter and about 3.5 inches high was fitted with a lucite cap and base and mounted on a rigid slab. A rigid mass M was then lowered gently onto the cap of the specimen until 10 percent of its weight was supported by the specimen and the remaining 90 percent was supported by the pulley and counterweight shown in the Figure. At a given instant the wire attaching the rigid mass to the counterweight was severed, releasing the mass onto the cap of the specimen. The accelerations of the cap of the sample due to this sudden load application were recorded by an accelerometer mounted on the cap and deformations by a linear variable differential transformer attached to the cap. Variation of acceleration and deformation with time were recorded by a Honeywell Visicorder capable of recording at frequencies up to 1000 cps.

Typical records obtained in this type of test are shown in Fig. 19. The acceleration-time curve has the general form of the damped harmonic motion shown in Fig. 20. For this type of motion the ratio of actual damping to its critical value, λ, is determined by the relationship

$$\lambda = \frac{1}{2\pi} \log \frac{a_1}{a_2} = \frac{1}{2\pi} \log \frac{a_2}{a_3} = - - - - - = \frac{1}{2\pi} \log \frac{a_n}{a_{n+1}} \qquad (87)$$

where a_1, a_2, a_3, etc. are the amplitudes of successive peaks of the response curve. Thus an average value of λ could readily be determined from the acceleration record for each test. However this procedure is only valid for reversible elastic systems and values of λ can only be determined for samples subjected to low stress levels where this type of behavior is evidenced.

The deformation vs time relationship provides a convenient means for determining the creep and dynamic elastic characteristics of the samples. By extrapolating the displacement curve to zero time an instantaneous displacement δ_1, for the specimen may be determined and subsequent deformations can be attributed to creep of the sample (See Fig. 20). Thus the progressive increase in creep movement over any desired length of time can readily be determined. The stress causing this creep is equal to the counterweight divided by the average area of the sample since creep due to the seating load has already occurred.

For the present program it was found that the rate of creep did not vary significantly over the first 10 seconds and an average rate was reasonably representative of the sample behavior over this period of time. Thus from any one test, an average rate of creep and the stress inducing it could be determined. By repeating the test on similar specimens but using masses of different magnitudes a relationship between average creep rate and applied stress can be determined as shown in Fig. 22.

Finally the dynamic stress-strain characteristics of the soil can be obtained in two ways as follows:

(a) In each test the average stress on the specimen and the instantaneous elastic deformation δ_i are determined. By conducting a

series of tests on identical specimens but using rigid masses of different magnitudes, a series of corresponding pairs of values of stress and elastic deformation can be determined and plotted to establish a dynamic elastic stress-strain relationship as shown in Fig. 31.

(b) Due to the fact mass M is large compared with the mass of the soil sample, this system will act essentially as a single degree of freedom system, i.e., no elastic waves will propagate up and down the sample during the dynamic test. Under this condition the strains will be nearly uniform throughout the specimen, thus, giving displacements which vary essentially linearly from zero at the sample base to a maximum value at the sample top. The generalized single degree of freedom system therefore consists of a mass equal to the rigid mass plus a contribution from the soil sample equal to one-third the sample mass. The spring constant of this generalized system is, of course, the spring constant of the soil sample itself. Since the accelerations of the mass at the top of the specimen are known, the resultant forces acting on the spring can be computed (as mass times acceleration) and hence the force developed at the top of the specimen at any time can be determined. The corresponding average strains of the sample at the same times can be determined from the observed record of sample displacement. Thus by plotting stress vs strain at corresponding times, dynamic stress strain curves under these conditions are outlined as shown in Fig. 34.

Damping Characteristics

Following the procedure previously described, the damping ratio, λ, developed in a number of dynamic tests on samples of different strengths was determined. The magnitude of the rigid mass used in these tests was restricted to a value such that the maximum applied stress would not exceed 15 percent of the sample strength in order that response would be controlled by the initial portion of the stress-strain relationship where reversible elastic behavior is evidenced. The average values of λ determined in those tests are plotted against the soil strength in Fig. 21.

Values of λ for the various specimens ranged from 0.08 to 0.12 and appeared to be relatively independent of strength or elevation of sample. Since the analyses are not sensitive to minor variations in damping coefficients, the average value of λ equal to 0.094 would seem to be approximate for the entire deposit of clay at the Elkhorn Slough Bridge site.

Creep Characteristics

Tests were conducted to determine the relationships between average rate of creep over a period of 10 seconds following stress application and applied stress for 3 series of samples having compressive strengths of the order of 4 psi, 10 psi and 15 psi; the results of these tests are presented in Figs. 22 - 24, respectively.

It was found that average creep rate varied considerably with the magnitude of the applied stress and with sample strength. However for samples of any given strength, the relationship between average creep rate and applied stress could be represented with reasonable accuracy by a parabolic relationship.

In representing the effects of creep in the analysis of clay-pile

interaction, it is convenient to utilize creep strain rate as the dependent variable and applied stress as the independent variable. Thus a parabola of the form

$$\dot{\epsilon} = C_1 \sigma_0 |\sigma_0| \tag{88}$$

which fits the relationships in Figs. 22 - 24 reasonably well provides a satisfactory means of representing the soil behavior. Values of C_1 which best represent the test data in Figs. 22 - 24 can readily be determined for samples of different strengths and plotted as shown in Fig. 25. Actually it is necessary to know the variation in the creep coefficient C_1 with depth in the soil mass. Since the average variation in strength with depth has already been established (Fig. 17), the relationship between the coefficient C_1 and elevation can readily be deduced as shown in Fig. 26. The range of values shown in this figure reflects the range in strength values of $\pm$ 50% at any elevation in the soil mass.

In studying the response of the clay layer alone it is convenient to include creep effects by considering stress as the dependent variable and creep strain rate as the independent variable. For this purpose the above equation might be expressed as:

$$\sigma_0 = \left(\frac{|\dot{\epsilon}|}{C_1} \right)^{1/2} \text{sign } \dot{\epsilon} \tag{89}$$

The evaluation of σ_0 using this type of equation on a computer involves considerably more time than that required by using an equivalent equation of the form:

$$\sigma_0 = C \dot{\epsilon} - D \dot{\epsilon} |\dot{\epsilon}| \tag{90}$$

which can also be used to represent the test data with an acceptable degree of accuracy. Thus in order to simplify the computer operations, the data

in Figs. 22 - 24 have also been represented by equations of the latter form and appropriate values of the constants C and D, for soil samples of different strengths, have been determined. These values are plotted as a function of soil strength in Figs. 27 and 28. Using the relationships between strength and elevation shown in Fig. 17, the corresponding variation of the coefficients C and D with elevation will be also shown in Figs. 29 and 30.

Variation in Creep and Damping Characteristics During Cyclic Loading

In order to investigate the possible variation in creep and damping characteristics of the clay during an earthquake, values of damping ratio λ and creep coefficient C were determined for specimens which had previously been subjected to a number of stress cycles causing axial strains as large as 10 percent. It was found that the resulting changes in λ and C were insufficient to warrant the inclusion of this effect in the analysis.

Dynamic Stress-Strain Characteristics

Finally the data from the impact-creep tests were used to determine the dynamic stress-strain characteristics of the samples by each of the methods described on Pg. 48.

Figure 31 shows the relationships between instantaneous elastic deformation and average stress for eight samples having compressive strengths of about 10 psi but tested using rigid masses of different magnitudes. The average relationship drawn through these points can be considered to characterize the dynamic stress-strain relationship for samples of this strength.

Similar data for tests on samples having compressive strengths of 4 psi and 15 psi are presented in Figs. 32 and 33.

The results of a computation of the variation in dynamic stress and

strain during a single test are shown in Fig. 34. The stress-strain relationships determined in this way are slightly steeper than those determined from the instantaneous deformation measured on series of samples and shown in Figs. 31 - 33. Nevertheless they are in reasonably good agreement.

Also plotted with the dynamic stress-strain relationships in Figs. 31 - 33 are the stress vs strain relationships for samples of the same strengths tested under static loading conditions using a rate of stress application of about 0.2 $kg/cm^2/min$. It may be seen that in each case the dynamic stress-strain relationship is slightly steeper than the corresponding static relationship, reflecting the additional strains due to creep which can occur during the slower rate of loading.

In the analysis of the response of the soil deposit to earthquake-induced motions it was found desirable to characterize the stress-deformation relationship of the soil at low strains. This was done by defining a secant modulus, E_o, as the ratio of axial stress to axial strain at a strain level of 0.35 percent. Within this range in the dynamic loading tests the soil exhibits little or no hysteresis effects and may be considered to be reversibly elastic. The secant modulus determined in this way from the results of a dynamic loading test is designated E_{od}.

A similar secant modulus, E_{os}, at an axial strain of 0.35 percent can also be determined from the stress-strain relationship obtained under static or slow loading conditions.

From a comparison of dynamic and static stress vs strain relationships such as those shown in Figs. 31 - 34 it was found that the dynamic modulus E_{od} was greater than the corresponding static modulus E_{os} by amounts varying from 24 to 74 percent, with an average value of about 50 percent. This

result was subsequently used to convert static load test data to corresponding dynamic test values.

Stress-Strain Relationships During Cyclic Loading

Examination of the dynamic elastic stress-strain relationships for samples such as that shown in Fig. 34 revealed that it would be necessary to incorporate a non-linear spring with hysteresis characteristics in the model of soil behavior. To determine quantitative values for the properties of such a spring required the determination of the inelastic behavior of the soil during cyclic loading in which the directions of shear stresses and strains were repeatedly reversed. Because of difficulties in making such determinations under dynamic loading conditions and in view of the fact that dynamic and static stress-strain relationships did not appear to be too different (see Figs. 31 - 34), it was decided to conduct the cyclic loading tests under static loading conditions, which permitted accurate determination of applied stresses and corresponding strains, and subsequently modify these results appropriately to determine probable dynamic behavior.

Accordingly a number of special unconsolidated-undrained triaxial compression tests were conducted on specimens, 1.4 inches in diameter and 3.5 inches high, trimmed from the undisturbed samples. In these tests the piston of the triaxial compression cell was attached to the specimen cap so that the axial stress on the specimen could be increased or decreased, as desired, throughout the test. The rate of stress application was about 0.2 kg per sq. cm. per minute.

In a typical test, the axial stress was increased progressively until the axial strain was about 3 percent at which stage the axial stress was restored to its initial value. By pulling on the piston the axial stress

was then gradually decreased until the axial extension was about 3 percent and the stress again restored to its original hydrostatic condition. It should be noted that because of the initial ambient pressure of 1.0 kg per sq.cm. acting on the specimen, the axial stress remained compressive throughout the entire loading cycle. Usually this procedure was repeated until about 10 cycles of loading had been applied.

A typical relationship between the change in axial stress and the corresponding axial strains obtained in such a test is shown in Fig. 35. In general the stress-strain relationship for the second cycle of loading differed considerably from that during the initial loading but subsequent changes in further cycles were relatively small. Furthermore it appeared that when variations in cycles were introduced -- such as limiting one or more cycles to axial compression only or to reduced amounts of axial extension, the general form of the stress-strain relationship was maintained.

For purposes of analysis it is necessary to idealize the relationships shown in Fig. 35. When strains are small, even during cyclic loading, the stress-deformation relationships will be controlled by the initial part of the first loading cycle and can be represented with a satisfactory degree of accuracy by a straight line. For axial strains up to about 0.6 percent this relationship can be approximated by the secant modulus determined at an axial strain of 0.35 percent. This modulus, for tests conducted under static loading conditions, has been designated by E_{os}.

When high strains are induced during the stress cycles, the modulus E_{os} will apply for only the first part of the first cycle and the behavior of the soil is better characterized by the average of the reasonably consistent stress-strain relationships developed during cycles 2 to 10, as

shown in Fig. 35. This behavior may be idealized as illustrated in Fig. 36. In this representation, the first cycle is ignored and the best parallelogram fitting the stress-strain relationships for subsequent cycles and conforming to the following mathematically consistent rules is established. Behavior during initial loading is assumed to be controlled by the modulus E_{1s}, until a limiting strain ϵ_{ys} is reached, at which stage further deformations are determined by the modulus E_{2s}. When the loading is reversed, behavior is again determined by the modulus E_{1s} until a strain change equal to $2\epsilon_{ys}$ has occurred at whichstage further deformations are determined by E_{2s}. On reloading the modulus E_{1s} is again operative until a strain change of $2\epsilon_{ys}$ has occurred and the modulus E_{2s} begins to control the behavior. Similar behavior is developed during subsequent loading cycles.

By this means, the cyclic stress-strain relationships of the clay under static loading conditions are represented by the moduli E_{os}, E_{1s}, E_{2s} and the yield strain ϵ_{ys}. Following the procedure described above, values for these parameters have been determined for a number of samples, of different strengths, subjected to cyclic loading tests. Although the samples used for these tests were not loaded to failure, their probable strength values could be estimated with a high degree of accuracy from the knowledge of their stress-strain behavior during initial loading and the general form of such relationships obtained in the large number of strength tests previously conducted.

Thus the values of E_{os}, E_{1s}, E_{2s}, and ϵ_{ys}could be plotted as a function of the soil strength as shown in Figs. 37 - 40. It will be seen that the moduli vary considerably with sample strength but in each case the data can be represented by a linear relationship. However, the magnitude

of ϵ_{ys} is essentially constant, regardless of the strength of the specimens, with an average value of 0.6 percent.

Using the average relationship between soil strength and elevation established previously (see Fig. 17), the data in Figs. 37 - 40 can readily be converted to determine the variation of moduli with elevation in the clay layer. The results of such a conversion are summarized in Fig. 41.

Finally it is necessary to determine the parameters determining the elastic behavior of the soil under dynamic cyclic loading conditions. A comparison of the dynamic and static stress-strain relationships during the first loading cycle indicates considerable similarity in form with the exception that the dynamic relationship is considerably steeper at low strains. (It was previously shown that the dynamic modulus at low strains is about 50 percent higher than the static modulus at the same strain.) Thus it appears reasonable to approximate the dynamic deformation behavior of the soil by parameters E_{od}, E_{1d}, E_{2d} and ϵ_{yd} corresponding to those utilized for describing the cyclic loading behavior under static stress conditions (E_{os}, E_{1s}, E_{2s}, and ϵ_{ys}), with the following relationships:

$$E_{od} = 1.5\ E_{os}$$

$$E_{1d} = 1.5\ E_{od}$$

$$E_{2d} = E_{2s}$$

$$\epsilon_{yd} = \epsilon_{ys}$$

Based on these relationships, the variations in parameters describing the dynamic elastic behavior of the soil at different elevations are presented in Fig. 42. The probable ranges in these parameters, reflecting the variations in soil conditions at any elevation, are also indicated.

Summary of Soil Properties

The clay at the Elkhorn Bridge Slough site is a soft to firm gray silty clay containing many seams and thin layers of silt and fine sand. The thickness of the clay deposit varies from about 50 ft. at the bridge abutments to about 120 ft. along the center portion of the bridge span. The average shear strength increases with depth from about 0.08 tons per sq.ft. at Elev. 0 to about 0.52 tons per sq.ft. at Elev. -90. However, at any one elevation strengths may vary as much as $\pm$50 percent from the average value.

Based on the results obtained in the soil testing program it appears that the proposed model shown in Fig. 11 can provide a reasonably adequate representation of the stress-deformation characteristics of the clay under short term cyclic loading for use in the analyses of soil or soil-structure response to earthquake-induced ground motions. At the Elkhorn Slough site reasonable values for the characteristics of the elements comprising the model would appear to be as follows:

Non-linear spring

(a) Recoverable elastic behavior at axial strains less than 0.6 percent characterized by the modulus E_{od}; values for E_{od} at various depths are shown in Fig. 42.

(b) Hysteresis behavior during cyclic loading in which axial strains exceed about 0.6 percent, which may be approximated by a stress-strain relationship of the form shown in Fig. 36 and characterized by the moduli E_{1d} and E_{2d} together with the yield strain ϵ_{yd}. Values for E_{1d} and

E_{2d} at various depths are shown in Fig. 42. The axial strain ϵ_{yd} may be assumed to be equal to 0.6 percent.

Viscous Damping Element

Damping approximating 9.4 percent of critical damping at all depths (see Fig. 21).

Creep Characteristics

For practical purposes the creep rate can be assumed constant over the first ten seconds following stress application and will vary with stress according to either of the relationships:

$$\dot{\epsilon} = C_1 \sigma_D |\sigma_D|$$

or

$$\sigma_D = C \dot{\epsilon} - D \dot{\epsilon} |\dot{\epsilon}|$$

Values of C_1, C and D to be used in these relationships will vary with depth as shown in Figs. 26, 29, and 30, respectively.

COMMENTS ON PROPOSED METHOD OF ANALYSIS

It is apparent that it is impossible to obtain a completely rigorous solution to the general problem under consideration. However, it is believed that an approximate solution sufficiently accurate for design purposes can be obtained by the methods set forth in the preceding section of this report.

To justify the methods of analysis proposed herein several of the major assumptions which have been made should be recalled. First, it has been assumed that the elastic stress and displacement fields within the clay medium can be adequately defined by a static theory, i.e. the Mindlin theory. This assumption can be justified when the characteristic wave length in the clay medium, which in this case is the shear wave length (λ_s), is long compared with the horizontal distance (D_h) across the zone of major influence resulting from interaction. This shear wave length is calculated using the relation

$$\lambda_s = \frac{1}{f}\sqrt{\frac{G}{\rho}} \tag{84}$$

in which G is the shear modulus of clay medium, ρ denotes the mass density of clay medium, and f refers to the predominant frequency of the forcing function. It is believed that this condition is reasonably well satisfied for the general problem being considered and, therefore, the use of a static theory in defining the stress and displacement fields is considered satisfactory. It should also be noted that satisfying this condition implies that the inertia forces of masses $\overline{M}_i$ and $\overline{\overline{M}}_i$ are small compared with the interaction spring forces and the elastic shear forces in the piles. Dynamic response calculations show this latter statement to be true. Thus,

the dynamic response calculations are quite insensitive to reasonably large changes in the values assigned to the effective clay masses $\bar{\bar{M}}_i^e$ and $\bar{\bar{M}}_i^e$.

The second major assumption regarding the pile-clay medium interaction was the assumption which uncoupled the interaction springs as used in the idealized system (Winkler assumption). It was only after considerable effort had been spent on a coupled system that the decision was made to simplify the problem by using uncoupled springs. The coupled system led to an extremely complicated method of analysis which would require a great deal more effort in carrying out the solution and did not seem to be justified.

Due to the transient nature of earthquake ground motion and due to its relatively short duration, creep effects are small. Therefore, the proposed approximate method of determining creep coefficients is considered satisfactory.

The effects which all of the various simplifying assumptions have on the accuracy of the general solution could be examined at great length. However, in justifying the use of these assumptions it must be remembered that all soil properties of the clay medium have very wide variations, i.e., of the order of 100% or 200%. Therefore, inaccuracies introduced in the analysis by the various assumptions made are considered acceptable.

BRIDGE STRUCTURAL SYSTEMS INVESTIGATED

The objective of the general investigation reported herein has been to develop methods for predicting seismic effects on bridges which are supported on piles extending through deep sensitive clays and to apply these methods to the bridge structure presently being designed by the California State Division of Highways for erection across Elkhorn Slough. This bridge structure is shown schematically in Fig. 3 and is also shown in considerably more detail in Fig. 43. For additional details of this design the reader is referred to Drwgs. Nos. P. 614P-39 to 48 as prepared by the California State Division of Highways. It should be realized that the design details as presented on these drawings are preliminary and may not necessarily correspond with the final design.

While the above described structure served as the basic structure being analyzed in the general investigation, a single variation in this structure was assumed for additional analysis. This variation consisted of changing the outside diameter of all piles from 54 inches to 36 inches and the inside diameter from 44 inches to 26 inches. However, the number and arrangement of piles and the superstructure design were assumed to remain unchanged.

For analysis purposes the mass of the bridge superstructure was lumped at the bridge deck level, three intermediate levels on the piers, and at the pile cap level. This lumping of mass corresponds to $m = 4$ in Fig. 4. Damping in the superstructure was assumed to be 5 percent of critical ($\xi = 0.05$) in its fundamental mode for all analyses performed.

The depth of the clay layer varies considerably along the longitudinal axis of the proposed bridge site and has a maximum depth of approximately 120 feet. Therefore, it seemed most appropriate for analysis purposes to assume the clay medium as an infinite layer horizontally having a depth of 120 feet. Two different sets of properties were used for this medium in analyzing each of the above bridge structural types. These two sets of properties, which will be referred to subsequently as Clay System No. 1 and Clay System No. 2, were established on the basis of tests performed on San Francisco Bay "mud" and Elkhorn Slough clay, respectively.

The number of samples tested in establishing the properties of Clay System No. 1, i.e., San Francisco Bay mud, was very small as these tests were performed early in the program to aid in developing experimental techniques before Elkhorn Slough samples were available. A large number of samples however were later tested in establishing the properties of Clay System No. 2, i.e., Elkhorn Slough clay. Since Clay System No. 2 represents the actual bridge site conditions, the dynamic response studies based on this clay medium are of principal importance. However, it is considered worthwhile to present the results based on Clay System No. 1 to illustrate some differences in response which can be expected with certain specific changes in clay medium properties.

The properties of Clay System No. 2 were presented in considerable detail in the preceding section of this report; therefore, no further discussion of these properties is necessary. However, it is necessary at this point in our discussion to point out the basic differences between the properties of Clay Systems 1 and 2. The important differences as they affect the dynamic response of the bridge structural systems relate to the

stress-strain relations. The response studies using Clay System No. 1 were based on only the two moduli E_{1d} and E_{2d} which varied with depth, z, as given by the relations

$$E_{1d}(z) = 142 + 8.9z$$
$$E_{2d}(z) = 60.9 - 0.45z \qquad (85)$$

where z is depth in feet and where the moduli are given in pounds per square inch. Comparing these moduli with those given for Clay System No. 2 in Fig. 42, relatively small differences are noted for E_{1d}, while significant differences are noted for E_{2d}. However, the greatest and most significant difference in the stress-strain properties of these two clay systems is the difference in yield strain ϵ_{yd}. This normal yield strain equals 0.003 for Clay System No. 1 and 0.006 for Clay System No. 2 which corresponds to shear strains γ_{yd} of 0.0045 and 0.009, respectively. Since both clay systems have essentially the same moduli E_{1d} with depth, it is quite apparent that the above yield strains represent a much weaker material for Clay System No. 1 as compared with Clay System No. 2. Other properties such as creep and damping are similar.

For analysis purposes, the mass of the clay medium was lumped at 18 equally spaced levels, i.e. n = 18, as shown in Fig. 4.

DISCUSSION OF RESULTS

Total Acceleration of Clay Medium

The recorded acceleration of the N-S component of the 1940 El Centro earthquake was used as the prescribed horizontal acceleration $\ddot{u}_g(t)$ at the base of the clay medium. Approximately 9 seconds of this acceleration-time function is shown in Fig. 44 and its standard absolute acceleration response spectrum as defined by the relation

$$AA(\omega) = \left| \sqrt{1-\xi^2}\,\omega \int_0^t \ddot{u}_g(t) e^{-\xi\omega(t-\tau)} \left[\left(1 - \frac{\xi^2}{1-\xi^2}\right) \sin \omega\sqrt{1-\xi^2}(t-\tau) + \frac{2\xi}{\sqrt{1-\xi^2}} \cos \omega\sqrt{1-\xi^2}(t-\tau) \right] d\tau \right|_{max.}$$

is shown in Fig. 45. The absolute acceleration given by Eq. 86 is simply the absolute value of the maximum total acceleration which the mass of a single degree of freedom system will experience when excited through its support by the prescribed ground acceleration $\ddot{u}_g(t)$. The spectral values obtained in accordance with this definition are plotted in Fig. 45 vs. the undamped natural frequency ω for five different values of the damping ratio ξ, i.e. $\xi = 0$, 0.02, 0.05, 0.10, and 0.20. Note that the absolute acceleration response spectral curves approach an asymptotic value, with increasing frequency ω, which corresponds with the peak acceleration in the ground motion. In the case of the N-S component of the El Centro earthquake, this peak acceleration is approximately 0.33g.

Also shown in Fig. 44 are the time histories of total horizontal acceleration produced at the surface of Clay Systems Nos. 1 and 2 when

excited at their base by the N-S component of the El Centro earthquake. Absolute acceleration response spectra for these acceleration functions are shown in Fig. 45.

The above clay surface acceleration time histories have been calculated considering the response of the clay medium alone, i.e., the bridge structural system is assumed not to be present.

Comparing the three acceleration-time functions and their absolute acceleration response spectra as shown in Figs. 44, and 45, respectively, it is quite apparent that the surface acceleration functions contain much lower frequency components than are contained in the base acceleration function. This fact shows the effectiveness with which a soft clay medium filters out the higher frequency components. The predominant circular frequencies contained in the surface motion of both clay systems are, as shown by their response spectra, in the approximate range of 8-15 radians per second. Since the stiffnesses of both clay systems are approximately the same, one could expect this peaking of response spectra in approximately the same frequency range.

Using the response spectra of Fig. 45 to indicate magnitude of seismic forces which would be developed in linear elastic structures if subjected to base accelerations corresponding to the three acceleration functions given in Fig. 44, it is apparent that these forces would be comparable for damped structures when considering the effects of the El Centro motion vs. the effects of the surface motion of Clay System No. 2. (Reasonable damping factors for reinforced concrete bridge structures are in the approximate range of 0.05 - 0.15) However, the response spectra for Clay System No. 1 would indicate considerably lower seismic forces than those indicated by the response spectra for either Clay System No. 2

or the N-S component of El Centro. This large reduction for Clay System No. 1 is undoubtedly due to the relatively large amounts of inelastic action which take place during the response of this weaker system. Very little inelastic action will take place however during the response of Clay System No. 2 due to its higher yield strength.

The maximum peak acceleration reached during the period of the earthquake input is noted to be approximately 0.30g for the surface motion of Clay System No. 2 and 0.13g for the surface motion of Clay System No. 1.

Total Longitudinal Acceleration of Bridge Deck

The total horizontal acceleration time history for the bridge deck is shown in Fig. 46 for the three different clay-pile systems analyzed, namely (1) Clay System No. 1, 54 inch O.D. piles, (2) Clay System No. 2, 54 inch O.D. piles, and (3) Clay System No. 2, 36 inch O.D. piles.

These acceleration time-histories show maximum peak values of approximately 0.6g, 1.2g, and 1.2g for systems 1, 2, and 3, respectively. Again it is quite apparent that the weaker Clay System No. 1 produces considerably lower seismic forces in the superstructure of the bridge as compared with those produced by the stronger Clay System No. 2. Note however the similarity of the accelerations produced by Clay-Pile Systems Nos. 2 and 3. This similarity shows the relatively small influence which pile stiffness has on the response of the superstructure. As will be shown subsequently, relatively small clay-pile interaction displacements result during the earthquake; therefore, the piles are forced to move generally with the moving clay medium. In other words the displacements of the

piles are controlled to a much larger degree than the clay-pile interaction forces.

It is somewhat difficult, by observing the acceleration time histories of Fig. 46, to isolate the predominant frequencies contained therein; however, it is estimated that a Fourier analysis of the two similar wave forms representing Clay System No. 2 would show predominant frequencies in a rather narrow band near a frequency of 2 cycles per second. This observation undoubtedly reflects a response of the superstructure primarily in its fundamental mode of vibration which has been calculated to be 1.7 cycles per second on the assumption of completely fixed piers at the location of the pile caps. Since the piles can not provide full fixity as assumed, the correct fundamental frequency of the superstructure should be somewhat greater than 1.7. Using a frequency of say 1.8 cycles per second (ω = 11.3 rads/sec) and a damping factor ξ of 0.05, the absolute acceleration spectral value given in Fig. 45 for Clay System No. 2 is approximately 1.25g. This acceleration level is in very close agreement with the peak acceleration of 1.2g observed for the bridge deck. Realizing that the above prediction of a peak acceleration of 1.25g using the response spectrum of Clay System No. 2 neglects the effects of interaction between piles and clay medium while the observed peak of 1.2g includes these interaction effects, one again concludes that such interaction effects have a relatively small effect on the forces developed in the superstructure. Therefore, if one is interested only in seismic effects on the superstructure, the surface motion of the clay medium as determined with no bridge structure present could be used as a direct input into the base of the bridge piers.

This analysis would, of course, not provide an indication of the forces and deformations produced in the piles.

It is of interest to compare the above peak acceleration (1.2g) of the bridge deck when Clay System No. 2 is a part of the overall system with the peak acceleration which would be produced if the El Centro ground motion was the prescribed motion at the base of the piers. This latter peak acceleration can be obtained from the acceleration spectrum shown in Fig. 45 for the N-S component of El Centro. Using a damping factor of 0.05 and the estimated fundamental circular frequency of 11.3 rads/sec, one obtains an acceleration of approximately 0.9g which is considerably lower than the 1.2g acceleration obtained with the presence of Clay System No. 2. Therefore, it is apparent that the presence of a deep layer of clay may in some cases, if it has sufficient strength and elasticity, increase the seismic forces produced in a structure built on its surface. Such an increase would, of course, become most noticeable as the fundamental frequencies of the superstructure and the clay medium come into agreement. One should be careful however in generalizing the above observation of increased response in the presence of a clay medium as in other instances where the superstructure frequency and perhaps the clay properties are different a decrease in response could easily be obtained. For example, the peak acceleration of the bridge deck is considerably lower than the peak acceleration of the El Centro ground motion when the clay medium is represented by Clay System No. 1.

Total Longitudinal Acceleration of Pile Caps

The total longitudinal acceleration time histories of the pile caps for the multiple and single row pile groupings are shown in Figs. 47 and

48, respectively. One will note peak accelerations of the order of 1.2g in the case of Clay System No. 2 for both the multiple and single row groupings and for both pile sizes. These peak values are much higher than the peak accelerations at the surface of Clay System No. 2, i.e. 0.3g, showing that these particular accelerations are sensitive to the clay-pile interaction effects. Note the presence of higher frequency components in these acceleration functions.

Deflected Shapes of Clay and Interaction Systems

The deflected positions of the clay medium as a function of depth with no bridge structure present and the deflected positions of the piles as a function of depth with the entire bridge structure present are shown in Figs. 49-54 at times T = 0, 0.5, 1.0, . . ., 8.0 secs. All curves representing clay medium displacements are identified by the letter C and all curves representing pile displacements are identified by the letter P. The vertical line in each case is the fixed reference line from which both types of displacements are measured. This reference has been established along the axis of the pile group at time T = 0. Therefore, both curves labeled C and P coincide with this reference line at time T = 0.

Only the first 8 seconds of response are reported herein as this initial time period contains the critical response. No additional information of value would be presented if the response at later times were included.

The displacement u_g corresponding with the El Centro acceleration function as prescribed in the analysis is shown in each case in Figs. 49-54. It should be noted that these displacement values are not too accurate due to the well known difficulties of double-integrating, with accuracy,

a highly oscillatory acceleration function. However, the relative displacements of all curves identified by C and P with respect to a vertical reference axis through the moving base are quite accurate, as the above mentioned difficulties do not arise in their evaluation.

The clay yield shear strains of 0.0045 and 0.0090 are shown for Clay Systems Nos. 1 and 2, respectively, on the appropriate figures by a sloping dashed line from the base to the surface of the clay medium at T = 2.0 seconds. By comparing the absolute value of slopes along all curves labeled C with corresponding slopes of the dashed lines representing yield strain, one can easily see the amounts and locations of yielding which takes place in the clay medium as it responds to the base motion. This comparison shows that Clay System No. 1 undergoes a considerable amount of yielding at various depths, thus absorbing considerable amounts of energy. However, this same comparison for Clay System No. 2 shows rather small amounts of yielding. The yielding which does occur in this case is seen to take place in more restricted locations and also during much shorter periods of time than in the case of Clay System No. 1. Thus, Clay System No. 2 will respond with much more of the character of an elastic system than does Clay System No. 1. This basic difference is the reason for the differences in accelerations produced by these two media as previously noted.

Examining now the interaction displacements, i.e. the horizontal displacements between curves C and P, one generally observes these displacements to be small in comparison with the total displacements as measured from a vertical reference through the moving base. However, these interaction displacements are not insignificant as they have an

appreciable effect on the curvatures produced in the piles. The pile yield radius of curvature is indicated on each of Figs. 49-54. This radius of curvature is based on the classical linear flexure theory and has been calculated on the basis of a maximum flexure strain of 1.00×10^{-3} inches per inch. This strain corresponds to a concrete modulus of elasticity of 4.5×10^{6} psi and a maximum concrete flexure stress of 4.5×10^{3} psi. One will note that in general the response in Figs. 49-54 indicates maximum pile curvatures which are of the same order of magnitude as their yield curvatures. Comparing the actual curvatures produced in the 36" O.D. piles with those produced in the 54" O.D.piles, one finds that they are considerably larger. However, the ratios of the actual maximum curvatures for these two sizes are about the same as the ratio of their yield curvatures. Therefore, it is difficult to say whether one pile size is more critical than the other. If one carried this reasoning to smaller and smaller pile diameters, of course, one would reach a point where the curvatures in the piles coincide with the curvatures represented by the clay displacement curves C. In such a limiting case the curvatures would be controlled entirely by the response of the clay medium and therefore any further reduction in pile diameter would indeed represent a reduction in the maximum flexural stress produced. Note that the flexural stresses as referred to here do not reflect the direct stress as produced by the axial loads.

The maximum curvatures shown in Fig. 54 for the single row 36" pile grouping are believed to be somewhat larger than the actual curvatures which would be produced in this case. This statement is based on the belief that the higher mode oscillation producing these curvatures seems

somewhat unrealistic. This higher mode effect did not appear to this extent in the other cases studied and therefore does not reflect any general error. Further studies could, of course, clarify this isolated unexplainable behavior.

It needs to be pointed out that the displacements described above were plotted automatically and that because the computer calculated these displacements only at the 18 discrete levels, the plotter cannot accurately show these displacements at levels between these discrete locations. Since the plotter operates on a linear variation basis between points, some of the largest curvatures as shown by the above described plots are too large. When interpreting these data, one should visualize smooth curves drawn through the 19 data points ($n = 0, 1, 2, \ldots, 18$) rather than the straight line segments between points as produced by the plotter.

Total Force Distribution Along Pile Groupings

The total force intensity per unit of vertical dimension for the entire pile grouping is shown as a function of vertical location in the clay medium in Figs. 55-60 for the various systems analyzed. These force intensity plots need little explanation as one readily sees that they vary through the depth of the clay medium as one would expect from an examination of the corresponding interaction displacements shown in Figs. 49-54.

However, one very significant observation should be made in Figs. 55-60. Note that the maximum force intensities in all of these figures are very much below the so-called "yield intensity" given on each figure. This yield intensity is that force intensity at which the pile grouping would start to cut its way through the clay medium. Since the

force intensities could have reached their largest maximum values at times intermediate between those shown in Figs. 55-60, the computer program was written so that the maximum positive and negative values as selected from those calculated at 0.0025 second intervals could be obtained. These maximum force intensities along with the times at which they occurred are shown in Fig. 61. Again it is quite apparent that the maximum interaction force intensities developed were far below the yield intensities.

One would conclude from the above observation that standard size piles will never cut their way through a deforming clay medium. Remember that the above force intensities are sufficient to produce curvatures of the order of magnitude of the yield curvatures. As far as the authors are aware, this conclusion is not in conflict with field observations of embankment failures where piles have been in place.

Evaluation of Clay Effective Masses M_i^e

The analytical method of evaluating the clay effective masses M_i^e was presented in considerable detail in a previous section of this report. Because of the approximate way in which these masses are evaluated, it was considered desirable to check the sensitivity of the calculated pile displacements to possible errors in the evaluation of these effective masses. To carry out this check, a complete dynamic analysis of the entire bridge structural system using 54 inch piles and using Clay System No. 2 was performed. For this particular analysis, however, all clay effective masses M_i^e ($i = 1, 2, \ldots, 18$) were arbitrarily increased by 25 percent. A comparison of some of the results obtained from this solution with corresponding results obtained from the previous solution not having this arbitrary increase can be seen in Figs. 62 and 63. These figures show lateral displacement time histories of the multiple row

pile grouping and lateral displacement time histories of the clay medium (without interaction) which are identified by the letters P and C, respectively. Only those displacement time histories at the clay surface and at depths of 40 and 80 feet are shown.

First comparing the displacement functions for the pile grouping with the displacement functions for the clay medium, one can easily see how the pile grouping moves essentially with the clay medium in the earlier critical stages. During this period of time the interaction displacements, i.e., the differences in ordinates of the above functions, are quite small. During the later stages the interaction displacements are considerably larger. This observation holds for all cases in Figs. 62 and 63, i.e. for all levels and for both the solution using the regular effective clay masses and the solution using a 25 percent increase in effective masses.

Now comparing the results of the two solutions, one finds the increase in effective masses had little effect on the response in the earlier critical stages. However significant effects are noted in the later stages where higher frequency components are observed in the response. These higher frequency components correspond to higher mode effects which are undoubtedly more sensitive to errors in the effective mass evaluation.

Generally however the results of Figs. 62 and 63 would indicate that the method developed herein to evaluate effective masses is satisfactory from a standpoint of predicting maximum response.

Lower Boundary Condition of Piles

A pinned boundary condition has been assumed for all piles at the base of the clay medium. This boundary condition is in reality incorrect

as such piles must be driven sufficiently into the base medium to develop the necessary point bearing capacity. If the base medium below the clay layer has much higher stiffness and strength characteristics than the clay medium and if the piles are driven an appreciable distance into this medium, a rather bad situation is created at the interface of these two media. In other words the large discontinuity in soil shear strains at this point would likely cause curvatures in the piles which far exceed their yield values; thus, in effect plastic hinges would be developed in the piles at this location. The designer should recognize this situation and design the piles in this region so that their vertical load carrying capacities are not lost when such yielding occurs.

If the penetration distances of the piles into the base medium are sufficiently small such pile failures at this location would not occur since local soil failures would occur instead.

It should be recognized that assuming pinned lower boundary conditions in the general analysis does not lead to any general error in response of the entire system. Such errors involved are only in the immediate vicinity of the base of the piles.

Stability of Piles

The idealized structural model shown in Fig. 4 represents the interaction effects between piles and clay medium by linkages, each of which consists of a damping dashpot in parallel with a non-linear interaction spring which in turn are placed in series with a creep dashpot. All creep dashpot coefficients calculated by the methods previously presented were sufficiently high for the clay systems studied so that the creep displacements developed during the short period of the prescribed earthquake

were small compared with the total interaction displacements $U_i^r - u_i^r$. In fact they have been found to be sufficiently small during this short transient period so that they could have been neglected without any great loss in accuracy of the general solution.

Under static loads of long duration the above mentioned interaction linkages would, of course, give no lateral support to the piles because of the presence of the creep dashpots. Therefore while the idealized model used is a satisfactory one in calculating the transient response during an earthquake, it could not be used in the static case.

The clay medium does possess a certain permanent elasticity even though it may be small. This permanent elasticity could be represented in the model by an elastic spring placed in parallel with the creep dashpot. This spring would of course be much less stiff than the spring placed in parallel with the damping dashpot. Therefore, in view of the large creep dashpot coefficients this additional spring would transfer very little of the total interaction load during the transient period of an earthquake but would transfer all of the interaction load under static conditions.

Considering now the lateral stability of a single pile under static conditions, one needs to know the elastic spring constant k, i.e., the interaction force per unit of length per unit of lateral displacement, which the clay medium can provide permanently in giving lateral support to the pile. No attempt has been made to establish this spring constant in the general investigation reported herein. The experienced soil engineer can however give the designer some basis for establishing this constant.

Once the above spring constant has been established, the flexural stiffness EI of the pile can be selected to be of sufficient magnitude that

the vertical loads can be carried without lateral stability being a problem. The designer will need to recall in this case the theory of buckling of a uniform beam on an elastic foundation. If such a beam is of infinite length, has a flexural stiffness EI, and is supported by a Winkler type elastic foundation having a uniform spring constant k, it can be shown that the critical axial load P is given by the expression

$$P_{cr} = 2\sqrt{k\ EI} \tag{87}$$

and that the beam buckles as a sine wave having full wave lengths λ as given by the relation

$$\lambda = 2\pi\ (EI/k)^{1/4} \tag{88}$$

This theory shows that even a very flexible foundation, relatively speaking, is very effective in shortening the wave length λ and thus increasing the critical load.

CONCLUSIONS AND RECOMMENDATIONS

The basic theory presented in this report provides a rational approach for investigating seismic effects on bridges which are supported on long piles extending through deep sensitive clays. Solutions based on this theory can be obtained by digital computer with sufficient accuracy that the dynamic behavior of the entire bridge structural system, including the piles, is adequately defined for design purposes.

Before applying the above general theory to a specific structural system, it is necessary that all required clay medium properties be established. Based on the results of the soil testing program reported herein, it appears that the basic idealized model selected for this material can provide an adequate representation of its stress-deformation characteristics during the period of an earthquake. The testing procedures utilized in the investigation appear to provide an adequate means for determining these clay medium properties.

The application of the above methods in determining the dynamic response of the proposed Elkhorn Slough bridge structural system has produced results on which the following specific conclusions and recommendations are based:

(1) A deep clay layer can be expected to greatly filter the higher frequency components of a typical earthquake acceleration input at its base before such accelerations reach the surface. However, those lower frequency components which are near the fundamental shear mode frequency of the clay layer are likely to be amplified if the clay system has sufficient strength. In such cases structures built on the surface and having fundamental

frequencies which match or nearly match the fundamental frequency of the clay layer will experience greater peak response than if excited directly by the earthquake acceleration. The proposed Elkhorn Slough bridge shows a somewhat greater peak response in this respect when the NS component of El Centro earthquake acceleration is the prescribed input, i.e., the peak bridge deck acceleration is approximately 1.2g when considering the entire clay-pile-bridge superstructure system and is approximately 0.9 g when considering only the bridge superstructure system.

(2) The bridge superstructure, including attachments to piles, should be designed with full recognition of the importance of providing ductility so that large amounts of energy can be absorbed during the period of a very strong earthquake.

(3) The deformations which could be expected in the clay medium at the Elkhorn Slough site, if subjected at its base to an earthquake similar to that recorded at El Centro, would produce curvatures in the piles of the same order of magnitude as their yield curvatures. Such piles should therefore be designed so that they can withstand a considerable amount of inelastic deformation without losing their vertical load carrying capacity.

(4) It is quite apparent that standard size piles will never "cut" their way through a moving clay medium of the Elkhorn Slough type. Rather, such piles will be forced to deform essentially with the clay medium and will be given only relatively small relief by the interaction displacements. This type of behaviour means that considerably more control is placed on pile curvatures than on pile moments; therefore, standard or possibly somewhat smaller

than standard diameter piles would have an advantage over the larger diameter piles as far as flexural stresses are concerned. Of course, one must use a larger number of smaller size piles than larger size piles because of their lower vertical load carrying capacities.

(5) If the piles are driven to a considerable depth in the highly compacted sand layer just below the clay medium, very large curvatures should be expected to develop in the piles at the interface of these two layers during a strong earthquake. In such a case the piles should be designed with the necessary ductility in this region so that their vertical load carrying capacities are maintained.

(6) Further investigation is recommended to establish the existing "permanent elastic" moduli for the Elkhorn Slough clay medium which can be used to study the lateral stability of the piles under static conditions. Lateral stability of the piles is, of course, not a problem during the short period of transient excitation produced by an earthquake.

(7) Since the phase relations of the dynamic response of the bridge deck will differ from one section to the next, adequate separation should be provided in the expansion joints so that one section of bridge deck will not "pound" against the adjacent sections during the period of a strong earthquake.

It should be fully recognized that the specific analytical results obtained and conclusions drawn therefrom in this study apply only to the specific structural systems analyzed when subjected to an excitation

corresponding with the NS component of the 1940 El Centro earthquake. While these results and conclusions are considered extremely helpful when designing similar structures for future earthquakes, one must always recognize the many parameters involved which could differ appreciably, thus producing significant changes in the dynamic response characteristics of such systems.

APPENDIX A

"Step by Step" Matrix Procedures - Dynamic Response of Clay Medium

Basic Equations

$$m_i \ddot{u}_i^r + c_i^d \dot{u}_i^s - c_{i+1}^d \dot{u}_{i+1}^s + k_i u_i^s - k_{i+1} u_{i+1}^s = -m_i \ddot{u}_g \tag{1}$$

$$c_i^c (\dot{u}_i^r - \dot{u}_{i-1}^r - \dot{u}_i^s) - c_i^d \dot{u}_i^s - k_i u_i^s = 0 \tag{2}$$

$$c_i^c = \left[c_i^{co} + c_i^{c'} |\dot{u}_i^r - \dot{u}_{i-1}^r - \dot{u}_i^s| + c_i^{c''} (\dot{u}_i^r - \dot{u}_{i-1}^r - \dot{u}_i^s)^2 \right] f_i (t/T) \tag{3}$$

$$c_i^d = \left[c_i^{do} + c_i^{d'} |\dot{u}_i^s| \right] g_i (t/T) \tag{4}$$

$$k_i = k_{ie} h_i (t/T), \text{ or } k_i = k_{ip} h_i (t/T) \text{ see Fig. 2} \tag{5}$$

where $f_i (t/T)$, $g_i (t/T)$, and $h_i (t/T)$ will be of the form

$$y (t/T) = a_1 + (1 - a_1) (1 - t/T)^{a_3} \tag{6}$$

Notation

Let

$( )_o$ indicate value at the beginning of time interval Δt

$( )_t$ indicate value at the end of time interval Δt

Assumptions

(1) Acceleration $\ddot{u}_i^r$, $\ddot{u}_i^s$ are linear through time interval

(2) c_i^c, c_i^d, k_i given by Eqs. 2 - 5, respectively, remain constant during small time increment Δt

Method of Solution

By Assumption 1)

$$(\dot{u}_i^r)_t = (\dot{u}_i^r)_o + \frac{\Delta t}{2}(\ddot{u}_i^r)_o + \frac{\Delta t}{2}(\ddot{u}_i^r)_t \tag{7}$$

$$(u_i^r)_t = (u_i^r)_o + \Delta t\,(\dot{u}_i^r)_o + \frac{\Delta t^2}{3}(\ddot{u}_i^r)_o + \frac{\Delta t^2}{6}(\ddot{u}_i^r)_t \tag{8}$$

Similarly,

$$(\dot{u}_i^s)_t = (\dot{u}_i^s)_o + \frac{\Delta t}{2}(\ddot{u}_i^s)_o + \frac{\Delta t}{2}(\ddot{u}_i^s)_t \tag{9}$$

$$(u_i^s)_t = (u_i^s)_o + \Delta t\,(\dot{u}_i^s)_o + \frac{\Delta t^2}{3}(\ddot{u}_i^s)_o + \frac{\Delta t^2}{6}(\ddot{u}_i^s)_t \tag{10}$$

From Eq. 9

$$\frac{\Delta t}{2}(\ddot{u}_i^s)_t = (\dot{u}_i^s)_t - (\dot{u}_i^s)_o - \frac{\Delta t}{2}(\ddot{u}_i^s)_o \tag{11}$$

Substituting value of $(\ddot{u}_i^s)_t$ into Eq. 10) gives

$$(u_i^s)_t = (u_i^s)_o + \Delta t\,(\dot{u}_i^s)_o + \frac{\Delta t^2}{3}(\ddot{u}_i^s)_o + \frac{\Delta t}{3}\left((\dot{u}_i^s)_t - (\dot{u}_i^s)_o - \frac{\Delta t}{2}(\ddot{u}_i^s)_o\right) \tag{12}$$

Substituting Eqs. 7 and 12 into Eqs. 1 and 2, two equations are obtained containing $(\dot{u}^s)_t$ and $(\ddot{u}^r)_t$ which can be solved simultaneously. These equations are

$$c_i^c \frac{\Delta t}{2}(\ddot{u}_i^r)_t - c_i^c \frac{\Delta t}{2}(\ddot{u}_{i-1}^r)_t - (c_i^c + c_i^d)(\dot{u}_i^s)_t - k_i \frac{\Delta t}{3}(\dot{u}_i^s)_t$$

$$= -c_i^c\left[(\dot{u}_i^r)_o + \frac{\Delta t}{2}(\ddot{u}_i^r)_o\right] + c_i^c\left[(\dot{u}_{i-1}^r)_o + \frac{\Delta t}{2}(\ddot{u}_{i-1}^r)_o\right]$$

$$+ k_i \left[(u_i^s)_o + \Delta t\, (\dot{u}_i^s)_o + \frac{\Delta t^2}{3} (\ddot{u}_i^s)_o - \frac{\Delta t}{3}\left[(\dot{u}_i^s)_o + \frac{\Delta t}{2} (\ddot{u}_i^s)_o \right] \right]$$

and

$$m_i\, (\ddot{u}_i^r)_t + c_i^d\, (\dot{u}_i^s)_t + k_i \frac{\Delta t}{3} (\dot{u}_i^s)_t - c_{i+1}^d\, (\dot{u}_{i+1}^s)_t - k_{i+1} \frac{\Delta t}{3} (\dot{u}_{i+1}^s)_t$$

$$= -m_i\, \ddot{u}_g - k_i \left[(u_i^s)_o + \Delta t\, (\dot{u}_i^s)_o + \frac{\Delta t^2}{3} (\ddot{u}_i^s)_o - \frac{\Delta t}{3} \left[(\dot{u}_i^s)_o + \frac{\Delta t}{2} (\ddot{u}_i^s)_o \right] \right]$$

$$+ k_{i+1} \left[(\dot{u}_{i+1}^s) + \Delta t\, (\dot{u}_{i+1}^s)_o + \frac{\Delta t^2}{3} (\ddot{u}_{i+1}^s)_o - \frac{\Delta t}{3} \left[(\dot{u}_{i+1}^s)_o + \frac{\Delta t}{2} (\ddot{u}_{i+1}^s)_o \right] \right]$$

Let, $$B_i = (u_i^s)_o + \Delta t\, (\dot{u}_i^s)_o + \frac{\Delta t^2}{3} (\ddot{u}_i^s)_o - \frac{\Delta t}{3} \left[(\dot{u}_i^s)_o + \frac{\Delta t}{2} (\ddot{u}_i^s)_o \right]$$

$$E_i = (\dot{u}_i^r)_o + \frac{\Delta t}{2} (\ddot{u}_i^r)_o$$

Then,

$$(c_i^c \frac{\Delta t}{2})\, (\ddot{u}_i^r)_t - (c_i^c \frac{\Delta t}{2})\, (\ddot{u}_{i-1}^r)_t - (c_i^c + c_i^d + k_i \frac{\Delta t}{3})\, (\dot{u}_i^s)_t$$

$$= c_i^c\, (-E_i + E_{i-1}) + k_i\, B_i \qquad (13)$$

$$m_i\, (\ddot{u}_i^r)_t + (c_i^d + k_i \frac{\Delta t}{3})\, (\dot{u}_i^s)_t - (c_{i+1}^d + k_{i+1} \frac{\Delta t}{3})\, (\dot{u}_{i+1}^s)_t$$

$$= -m_i\, \ddot{u}_g - k_i\, B_i + k_{i+1}\, B_{i+1} \qquad (14)$$

From Eq. 13

$$(\dot{u}_i^s)_t = \frac{(c_i^c \frac{\Delta t}{2})\, (\ddot{u}_i^r)_t - (c_i^c \frac{\Delta t}{2})\, (\ddot{u}_{i-1}^r)_t - c_i^c\, (-E_i + E_{i-1}) - k_i\, B_i}{(c_i^c + c_i^d + k_i \frac{\Delta t}{3})}$$

Similarly,

$$(\dot{u}_{i+1}^s)_t = \frac{(c_{i+1}^c \frac{\Delta t}{2})(\ddot{u}_{i+1}^r)_t - (c_{i+1}^c \frac{\Delta t}{2})\, (\ddot{u}_i^r)_t - c_{i+1}^c\, (-E_{i-1} + E_i) - k_{i+1} B_{i+1}}{(c_{i+1}^c + c_{i+1}^d + k_{i+1} \frac{\Delta t}{3})}$$

Substituting the latter two values in Eq. 14 gives

$$m_i (\ddot{u}^r_i)_t + \frac{(c^d_i + k_i \frac{\Delta t}{3}) \left[(c^c_i \frac{\Delta t}{2}) (\ddot{u}^r_i)_t - (c^c_i \frac{\Delta t}{2}) (\ddot{u}^r_{i-1})_t\right]}{c^c_i + c^d_i + k_i \frac{\Delta t}{3}}$$

$$- \frac{(c^d_{i+1} + k_{i+1} \frac{\Delta t}{3}) \left[(c^c_{i+1} \frac{\Delta t}{2}) (\ddot{u}^r_{i+1})_t - (c^c_{i+1} \frac{\Delta t}{2}) (\ddot{u}^r_i)_t\right]}{c^c_{i+1} + c^d_{i+1} + k_{i+1} \frac{\Delta t}{3}}$$

$$= -m_i \ddot{u}_g - k_i B_i + k_{i+1} B_{i+1}$$

$$+ (c^d_i + k_i \frac{\Delta t}{3}) \left[c^c_i (-E_i + E_{i-1}) + k_i B_i\right] / (c^c_i + c^d_i + k_i \frac{\Delta t}{3})$$

$$- (c^d_{i+1} + k_{i+1} \frac{\Delta t}{3}) \left[c^c_{i+1} (-E_{i+1} + E_i) + k_{i+1} B_{i+1}\right] / (c^c_{i+1} + c^d_{i+1} + k_{i+1} \frac{\Delta t}{3})$$

$$= L_i$$

Let $P_i \equiv (c^d_i \frac{\Delta t}{2} + k_i \frac{\Delta t^2}{6}) / (c^c_i + c^d_i + k_i \frac{\Delta t}{3})$

Then,

$$-c^c_i P_i (\ddot{u}^r_{i-1})_t + (m_i + c^c_i P_i + c^c_{i+1} P_{i+1}) (\ddot{u}^r_i)_t - c^c_{i+1} P_{i+1} (\ddot{u}^r_{i+1})_t = L_i$$

Let $D_i = B_i / (c^c_i + c^d_i + k_i \frac{\Delta t}{3})$

Then,

$$L_i = -m_i \ddot{u}_g - c^c_i D_i k_i + c^c_{i+1} D_{i+1} K_{i+1}$$

$$+ \frac{2c^c_i}{\Delta t} (-E_i + E_{i-1}) P_i - \frac{2c^c_{i+1}}{\Delta t} (-E_{i+1} + E_i) P_{i+1}$$

or

$$\left[A\right] \left\{\ddot{u}^r\right\}_t = \left\{L\right\}$$

where

$\left[A\right]$ is a symmetric band matrix.

Summary Equations

$$B_i = (u_i^s)_o + \frac{2\Delta t}{3} (\dot{u}_i^s)_o + \frac{\Delta t^2}{6} (\ddot{u}_i^s)_o$$

$$E_i = (\dot{u}_i^r)_o + \frac{\Delta t}{2} (\ddot{u}_i^r)_o$$

$$P_i = \left(c_i^d \frac{\Delta t}{2} + k_i \frac{\Delta t^2}{6} \right) / \left(c_i^c + c_i^d + k_i \frac{\Delta t}{3} \right)$$

$$D_i = B_i / \left(c_i^c + c_i^d + k_i \frac{\Delta t}{3} \right)$$

$$L_i = -m_i \ddot{u}_g - c_i^c D_i k_i + c_{i+1}^c D_{i+1} k_{i+1} + \frac{2c_i^c}{\Delta t} P_i (-E_i + E_{i-1}) - \frac{2c_{i+1}^c}{\Delta t} (-E_{i+1} + E_i) P_{i+1}$$

$$\left\{\ddot{u}^r\right\}_t = \left[A\right]^{-1} \left\{L\right\}$$

$$A_{i,\, i-1} = -c_i^c P_i$$

$$A_{i,\, i+1} = -c_{i+1}^c P_{i+1}$$

$$A_{i,i} = m_i - A_{i,\, i-1} - A_{i,\, i+1}$$

$$(\dot{u}_i^r)_t = (\dot{u}_i^r)_o + \frac{\Delta t}{2} (\ddot{u}_i^r)_o + \frac{\Delta t}{2} (\ddot{u}_i^r)_t = E_i + \frac{\Delta t}{2} (\ddot{u}_i^r)_t$$

$$(u_i^r)_t = (u_i^r)_o + \Delta t (\dot{u}_i^r)_o + \frac{\Delta t^2}{3} (\ddot{u}_i^r)_o + \frac{\Delta t^2}{6} (\ddot{u}_i^r)_t$$

$$(\dot{u}_i^s)_t = \frac{c_i^c \frac{\Delta t}{2} \left[(\ddot{u}_i^r)_t - (\ddot{u}_{i-1}^r)_t \right] - c_i^c (-E_i + E_{i-1}) - k_i B_i}{\left(c_i^c + c_i^d + k_i \frac{\Delta t}{3} \right)}$$

$$(\ddot{u}_i^s)_t = \frac{2}{\Delta t} \left[(\dot{u}_i^s)_t - (\dot{u}_i^s)_o - \frac{\Delta t}{2} (\ddot{u}_i^s)_o \right]$$

$$(u_i^s)_t = (u_i^s)_o + \Delta t (\dot{u}_i^s)_o + \frac{\Delta t^2}{3} (\ddot{u}_i^s)_o + \frac{\Delta t^2}{6} (\ddot{u}_i^s)_t$$

APPENDIX B

"Step by Step" Procedures - Clay Medium-Bridge Structure Interaction

General

Displacements and velocities expressed in terms of accelerations

$$x_t = x_o + \Delta t\, \dot{x}_o + \frac{\Delta t^2}{3}\, \ddot{x}_o + \frac{\Delta t^2}{6}\, \ddot{x}_t$$

$$\dot{x}_t = \dot{x}_o + \frac{\Delta t}{2}\, \ddot{x}_o + \frac{\Delta t}{2}\, \ddot{x}_t$$

Spring and dashpot forces are estimated by constant acceleration method, thereby reducing the degrees of freedom to $(2n + 2m + 1)$.

Pier damping force $C_i^b\ (\dot{u}_i^b - \dot{u}_n^r)$ is calculated on the basis of $\dot{u}_i^b$ and $\dot{u}_n^r$ of the previous cycle.

Reduced Equations

Pile Mass

Let

$$\overline{FORCE}_i = \overline{K}_i \left[(\overline{U}_i^s)_o + \Delta t\, (\dot{\overline{U}}_i^s)_o + \frac{\Delta t^2}{2}\, (\ddot{\overline{U}}_i^s)_o \right] - \overline{COF}_i + \overline{C}_i^d \left[(\dot{\overline{U}}_i^s)_o + \Delta t\, (\ddot{\overline{U}}_i^s)_o \right]$$

$$\overline{F3}_i = (\overline{U}_i^r)_o + \Delta t\, (\dot{\overline{U}}_i^r)_o + \frac{\Delta t^2}{3} (\ddot{\overline{U}}_i^r)_o$$

$$\overline{F2}_i = (\dot{\overline{U}}_i^r)_o + \frac{\Delta t}{2}\, (\ddot{\overline{U}}_i^r)_o$$

$$\left[\overline{M}_i\right] \left\{\ddot{\overline{U}}_i^r\right\} + \frac{\Delta t^2}{6}\left[\overline{k}_{ij}^a\right] \begin{Bmatrix} \ddot{\overline{U}}_j^r \\ \ddot{\theta} \end{Bmatrix} + \frac{\Delta t^2}{6}\left[\overline{T}_i\, \ddot{\overline{U}}_{i-1}^r - (T_i + T_{i+1})\, \ddot{\overline{U}}_i^r + \overline{T}_{i+1}\, \ddot{\overline{U}}_{i+1}^r\right] = \left\{AL_i\right\} \qquad (1)$$

where

$$AL_i = -\ddot{u}_g \bar{M}_i^p + \ddot{u}_i^r \bar{M}_i^e - \overline{FORCE}_i - \left[\bar{k}_{ij}^a\right] \begin{Bmatrix} \overline{F3}_i \\ \overline{03} \end{Bmatrix} - \left[\bar{T}_i \overline{F3}_{i-1} - (\bar{T}_i + \bar{T}_{i+1}) \overline{F3}_i + \bar{T}_{i+1} \overline{F3}_{i+1}\right]$$

Top Mass in Pile

$$\bar{M}_n \ddot{U}_n^r + \frac{\Delta t^2}{6} \langle \bar{k}_{nj}^a \rangle \begin{Bmatrix} \ddot{U}_j^r \\ \ddot{\theta} \end{Bmatrix} + \frac{\Delta t^2}{6} \langle k_{ij}^b \rangle \begin{Bmatrix} \ddot{U}_n^r \\ \ddot{\theta} \\ \ddot{U}_k^b \end{Bmatrix} + \frac{\Delta t^2}{6} \left[\bar{T}_n \ddot{U}_{n-1}^r - (\bar{T}_n + \bar{S}_1) \ddot{U}_n^r + \bar{S}_1 \ddot{U}_1^b\right] = -\ddot{u}_g \bar{M}_n^p + \ddot{u}_n^r \bar{M}_n^e - \overline{FORCE}_n - \langle \bar{k}_{nj}^a \rangle \begin{Bmatrix} \overline{F3}_j \\ \overline{03} \end{Bmatrix} - \langle \bar{k}_{1j}^b \rangle \begin{Bmatrix} \overline{F3}_n \\ \overline{03} \\ \overline{H3}_k \end{Bmatrix} - \left[\bar{T}_n \overline{F3}_{n-1} - (\bar{T}_n + \bar{S}_1) \overline{F3}_n + \bar{S}_1 \overline{H3}_1\right] \quad (1a)$$

where

$$\overline{03} = \bar{\theta}_o + \Delta t \, \dot{\bar{\theta}}_o + \frac{\Delta t^2}{3} \ddot{\bar{\theta}}_o$$

$$\overline{02} = \dot{\bar{\theta}}_o + \frac{\Delta t}{2} \ddot{\bar{\theta}}_o$$

$$\overline{H3}_j = \bar{U}_j^b + \Delta t \, \dot{\bar{U}}_j^b + \frac{\Delta t^2}{3} \ddot{\bar{U}}_j^b$$

$$\overline{H2}_j = \dot{\bar{U}}_j^b + \frac{\Delta t}{2} \ddot{\bar{U}}_j^b$$

Pile Cap Rotation

$$\bar{I}_n \ddot{\bar{\theta}} + \frac{\Delta t^2}{6} \langle \bar{k}_{2j}^b \rangle \begin{Bmatrix} \ddot{U}_n^r \\ \ddot{\theta}_b \\ \ddot{U}_k^b \end{Bmatrix} + \frac{\Delta t^2}{6} \langle \bar{k}_{n+1,j}^a \rangle \begin{Bmatrix} \ddot{U}_j^r \\ \ddot{\theta} \end{Bmatrix} + \frac{\Delta t^2}{6} \bar{k}_\theta \ddot{\bar{\theta}} + \frac{\Delta t}{2} \bar{C}_\theta \ddot{\bar{\theta}}$$

$$= -\langle \bar{k}_{2j}^b \rangle \begin{Bmatrix} \overline{F3}_n \\ \overline{03} \\ \overline{H3}_k \end{Bmatrix} - \langle \bar{k}_{n+1,j}^a \rangle \begin{Bmatrix} \overline{F3}_j \\ \overline{03} \end{Bmatrix} - \bar{K}_\theta \, \overline{03} - \bar{C}_\theta \, \overline{02} \quad (2)$$

Pier Mass

$$\left[\bar{M}^b_i\right]\left\{\ddot{\bar{U}}^b_i\right\} + \frac{\Delta t^2}{6}\left[\bar{k}^b_{i+2,j}\right]\begin{Bmatrix}\ddot{\bar{U}}^r_n\\ \ddot{\theta}_b\\ \ddot{\bar{U}}^b_k\end{Bmatrix} + \frac{\Delta t^2}{6}\left[\bar{S}_i\,\ddot{\bar{U}}^b_{i-1} - (\bar{S}_i + \bar{S}_{i+1})\,\ddot{\bar{U}}^b_i + \bar{S}_{i+1}\,\ddot{\bar{U}}^b_{i+1}\right] = -\ddot{u}_g\left[\bar{M}^b_i\right] - \left[\bar{k}^b_{i+2,j}\right]\begin{Bmatrix}\overline{F3}_n\\ \overline{03}\\ \overline{H3}_k\end{Bmatrix} - \bar{C}^b_i\left[\dot{\bar{U}}^b_i - \dot{\bar{U}}^r_n\right] - \left[\bar{S}_i\,\overline{H3}_{i-1} - (\bar{S}_i + \bar{S}_{i+1})\,\overline{H3}_i + \bar{S}_{i+1}\,\overline{H3}_{i+1}\right] \tag{3}$$

Bridge Deck

Adding Eq. 3 for i=m for single pile grouping to Eq. 3 for i=m for multiple pile row grouping, will yield the equation of motion for bridge deck. Eqs. 1, 2, and 3 have constant elements on their left hand side. Hence, a matrix may be formed, inverted, and multiplied by a force vector to yield the accelerations given by Eq. 4.

$$\left[A\right]\left\{\ddot{U}\right\} = \left\{AL\right\}$$

$$\begin{Bmatrix}\ddot{U}\end{Bmatrix} = \begin{Bmatrix}\ddot{\bar{U}}^r_1\\ \vdots\\ \ddot{\bar{U}}^r_m\\ \ddot{\theta}\\ \ddot{\bar{U}}^b_1\\ \vdots\\ \ddot{\bar{U}}^b_m = \ddot{\bar{U}}^b_m\end{Bmatrix} \tag{4}$$

$$\ddot{\bar{U}}^b_{m-1}\quad \ddot{\bar{U}}^b_1\quad \ddot{\theta}\quad \ddot{\bar{U}}^r_n\quad \ddot{\bar{U}}^r_1$$

Having found accelerations, velocities and displacements may be found by substituting value of acceleration into "Step by Step" equations for velocity and displacement. $\ddot{\bar{U}}^s$ and $\ddot{\bar{U}}^c$ may be found by substituting $\ddot{\bar{U}}^r$ into the interaction equations.

Interaction Equations

Let $\overline{G2}_i = (\dot{\bar{U}}^r_i)_o + \frac{\Delta t}{2}(\ddot{\bar{U}}^s_i)_o$

$\overline{G3}_i = (\bar{U}^s_i)_o + \Delta t\,(\dot{\bar{U}}^r_i)_o + \frac{\Delta t^2}{3}(\ddot{\bar{U}}^r_i)_o$

$\overline{E2}_i = (\dot{\bar{U}}^c_i)_o + \frac{\Delta t}{2}(\ddot{\bar{U}}^c_i)_o$

$\overline{E3}_i = (\bar{U}^c_i)_o + \Delta t\,(\dot{\bar{U}}^c_i)_o + \frac{\Delta t^2}{3}(\ddot{\bar{U}}^c_i)_o$

$\bar{U}^s_i + \bar{U}^c_i = \bar{U}^r_i - (u^r_i)_{clay}$

$\bar{k}_i \bar{U}^s_i - \overline{COF}_i + \bar{C}^d_i \dot{\bar{U}}^s_i = \bar{C}^c_i \dot{\bar{U}}^c_i$

Substituting for $\bar{U}^s_i$ in terms of $\bar{U}^c_i$ gives

$$\bar{k}_i\left[\bar{U}^r_i - (u^r_i)_{clay} - \bar{U}^c_i\right] - \overline{COF}_i + \bar{C}^d_i\left[\dot{\bar{U}}^r_i - (\dot{u}^r_i)_{clay} - \dot{\bar{U}}^c_i\right] = \bar{C}^c_i \dot{\bar{U}}^c_i$$

$$(\bar{C}^c_i + \bar{C}^d_i)\dot{\bar{U}}^c_i + \bar{k}_i \bar{U}^c_i = -\overline{COF}_i + \bar{k}_i\left[\bar{U}^r_i - (u^r_i)_{clay}\right] + \bar{C}^d_i\left[\dot{\bar{U}}^r_i - (\dot{u}^r_i)_{clay}\right]$$

$$\bar{U}^c_i = \frac{\Delta t^2}{6}\ddot{\bar{U}}^c_i + \overline{E3}_i$$

$$\dot{\bar{U}}^c_i = \frac{\Delta t}{2}\ddot{\bar{U}}^c_i + \overline{E2}_i$$

$$\ddot{\bar{U}}^c_i = \frac{-\overline{COF}_i + \bar{k}_i\left[\bar{U}^r_i - u^r_i\right] + \bar{C}^d_i\left[\dot{\bar{U}}^r_i - \dot{u}^r_i\right] - \left[\bar{C}^c_i + \bar{C}^d_i\right]\overline{E2}_i - \bar{k}_i\,\overline{E3}_i}{(\bar{C}^c_i + \bar{C}^d_i)\frac{\Delta t}{2} + \bar{k}_i\frac{\Delta t^2}{6}}$$

APPENDIX C

Description and Notation of Interaction Program

Chain Link 1 has the following programs:

1. INTAC1
2. PSTFNS
3. STIFFM
4. INDCO1
5. INDCO3
6. INDCO4
7. SUBMAT
8. BIGINV
9. SYMINV
10. PRNTIM

Chain Link 2 has the following programs:

1. INTAC2
2. STIFCO
3. VARCO1
4. VARCO2
5. VARCO3
6. VARCO4
7. RESPON
8. WRITAP
9. REDTAP
10. SOLEQU

Chain Link 1

In the first chain link most of the data are read in, stiffness matrices $\bar{k}^a$, $\bar{\bar{k}}^a$, $\bar{k}^b$, and $\bar{\bar{k}}^b$ are generated, and finally the structural stiffness matrix AC is generated.

1. INTAC1: This is the main program in which data are read in, printed, values initialized, and matrices are printed.
2. PSTFNS: This is a program which puts stiffness matrices for piles and piers calculated by STIFFM program into their proper locations. Estimation of rows and columns corresponding to reaction or known displacement is done here.

3. STIFFM: This is a general program to develop stiffness matrix for all translational degrees of freedom and rotational degrees of freedom at one or both ends. An elastic moment spring of stiffness "ST" at the bottom end of the member is also incorporated and stiffness matrix developed accordingly.

4. INDCO1: This program develops structural stiffness matrix $\left[AC\right]$ for Method 1. As there are no variable elements to be added later this matrix is inverted in INTAC1.

5. INDCO3: This program develops structural stiffness matrix $\left[AC\right]$ for Method 3. This matrix is for points which have masses, i.e. of size $\left[2\,(N - JM) + 2M + 1\right]$. $\left[AC\right]$ is inverted in INTAC1.

6. INDCO4: This program develops structural stiffness matrix $\left[AC\right]$ for Methods 2 and 4. Methods 2 and 4 have the same approach except for the treatment of variable elements due to interaction springs and dashpots. In Method 2, interaction force is estimated by eliminating variable elements. $\left[AC\right]$ is inverted in INTAC1. In Method 4, variable elements are calculated in VARCO4 of Chain Link 2, and equations are solved for each cycle and hence no inversion of matrix $\left[AC\right]$.

7. SUBMAT: This program is used only in the case of Method 3. It modifies $\left[SA\right]$ matrix for points with and without masses as explained in writeup for Method 3.

8. BIGINV: This is SYMINV with dimension 53 x 53.
9. SYMINV: This is an inversion routine with dimension 21 x 21.
10. PRINTTM: This is a program to print three dimensional array.

Chain Link 2

In this link integration is carried out, response calculated, clay system response is accepted for input and output tape is generated. Most of the program is executed every cycle.

1. INTAC2: This is the main program in which subroutines are called and at the end of each cycle it is checked for overflow and SAVE exits.

2. REDTAP: This is a program in which clay system response is read from TAPE 5 at the end of a prescribed number of cycles and values are assigned to u_g, $\dot{u}_g$, $\ddot{u}_g$, u_i, $\dot{u}_i$, $\ddot{u}_i$ at every cycle. There are two different programs.

   (a) N = KN, DT = DT1: equal number of masses in both the systems and same time interval.

   (b) N = KN, DT < DT1 and DT1/DT = INTEGER: Tape is read in as in Program a but values for intermediate cycles are interpolated and then assigned.

3. STIFCO: C^c, C^d, k, COF are calculated. Interaction force $\left[k_i U_i^s - COF_i + C_i^d \dot{U}_i^s\right]$ is estimated and used later in the case of Methods 1, 2 and 3 and ingored in the case of Method 4. Other values F2, F3, G2, G3, etc. as defined earlier are calculated. There are two channels. One channel is for Methods 2, 3, and 4 where F2, F3, etc. have the same meaning and the other channel is for Method 1 where F2, F3 have different formula.

4. VARCO1: This program develops force vector $\{AL\}$ for Method 1 and multiplies $[AC]^{-1}$ by $\{AL\}$ to give displacements which are again multiplied by "SCALE".

5. VARCO2: This program develops force vector $\{AL\}$ for Method 2 and multiplies $[AC]^{-1}$ by $\{AL\}$ to obtain accelerations which are again multiplied by "SCALE".

6. VARCO3: This program calculates force vector for every point, then modifies it to get force vector for points with masses as shown in the writeup for Method 3. $\left[AC\right]^{-1}$ is multiplied by $\left\{AL\right\}$ to get accelerations of points with masses. Note that at this stage acceleration of points with zero numbers are not known.

7. VARCO4: It calculates force vector $\left\{AL\right\}$ for every point. Variable elements are generated to which constant elements are added. SOLEQU is called in the main program to solve the equations.

8. RESPON: It calculates remaining values, i.e., velocities and accelerations in the case of Method 1 and velocities and displacements in the case of Methods 2, 3, and 4. For Method 3 displacements are calculated for no mass points from the displacement of points with mass as shown in writeup for Method 3. Having determined U^r, $\dot{U}^r$, $\ddot{U}^r$ for all points, spring values U^s, $\dot{U}^s$, $\ddot{U}^s$ and creep dashpot values U^c, $\dot{U}^c$, $\ddot{U}^c$ are calculated at the discrete points in the pile.

9. WRITAP: Puts 2N + 3 (4N + 2M + 1) values for every cycle into a location called URS which is dimensioned for 4000. At the end of 4000/ (2N + 3 (4N + 2M + 1))cycles, Tape 6 is written in binary form. Response is printed according to K1(L) values, i.e., every $K1(1)^{th}$ cycle is printed up to $K1\ (2)^{th}$ cycle, then every $K1\ (3)^{th}$ cycle is printed up to $K1\ (4)^{th}$ cycle, etc.

10. SOLEQU: This program solves symmetrical simultaneous linear equations with dimension statement $\left[53 \times 53\right]$. This program is used in the case of Method 4 only.

Interaction Program

Notations: J = 1 for multiple row grouping

J = 2 for single row grouping

JOB NO.: Any number less than 5 digits.

METHOD 1: Backward difference procedure

METHOD 2: Step by step procedure with estimation of interaction forces

METHOD 3: Step by step procedure with estimation and modification for zero mass points

METHOD 4: Step by step procedure without estimation and modification

N = number of masses in pile (including cap)

M = number of masses in pier (including deck)

Kl (1,3,5,7,9,11)
Kl (2,4,6,8,10,12) } = every Kl $(J)^{th}$ cycle is printed up to Kl $(J+1)^{th}$ cycle (J = 1,3,5,7,9, and 11)

DT = time interval of integration

TC = duration of earthquake

U2DG = ground acceleration at t=0 in inch/sec^2 for initialization

SCALE = to scale down the structural stiffness matrix $\left[A\right]$ to obtain accurate inversion.Force matrix is multiplied by the same scale. Equal to 1 if no scaling is required (SHOULD NOT BE ZERO).

USM (J,I) = $(U_m^s)_i$

UCM (J,I) = $(U_m^c)_i$

UDM (J,I) = $(U_m^d)_i$

USF (J,I) = Maximum spring force

UCF (J,I) = Maximum creep dashpot force

UDF (J,I) = Maximum damping dashpot force

EIS = E times moment of inertia of piers

E (I) = height of mass i in pier above pile cap

WS (J,I) = $\bar{M}_i^b$ = pier mass i

CB (J,I) = $\bar{C}_i^b$ = damping in pier

S(J,I) = axial force in the segment between i and i-1 divided by the length of the segment between i and i-1.

RM (J) = I_n = rotational moment of inertia of the pile cap.

SKO = $\bar{k}_\theta$ = rotational spring constant of the pile cap.

CBO (J) = C_θ^b = damping coefficient of pile cap (rotational)

EI (J) = E times the moment of inertia of piles (for whole group and not for one pile)

ST = stiffness of moment spring at bottom of pile which equals zero if hinged.

D (J,I) = height of i^{th} mass in pile from the bottom (later changed to length of segment between i and i-1)

W (J,I) = M_i^p = pile mass i

WE (J,I) = M_i^e = clay mass i

TO (J,I) = K_{ie} = first slope of bilinear interaction spring

T1 (J,I) = K_{ip} = second slope of bilinear interaction spring

RT1 (J,I)
RT2 (J,I)

for $h_i(\frac{t}{T}) = RT2 + (1 - RT2)\,(1 - \frac{t}{T})^{RT1}$

CO (J,I) = C_i^{co}
C1 (J,I) = C_i^{c1}
C2 (J,I) = C_i^{c2}
RC1 (J,I) = RC1
RC2 (J,I) = RC2

for

$$C_i^c = \left[C_i^{co} + C_i^{c1}\,|\dot{U}_i^c| + C_i^{c2}\,(\dot{U}_i^c)^2\right] \quad f_i\,(t/T)$$

where

$$f_i\,(t/T) = RC2 + (1 - RC2)\,(1 - t/T)^{RC1}$$

$$\left.\begin{aligned} DO\ (J,I) &= C_i^{do} \\ D1\ (J,I) &= C_i^{d1} \\ RD1\ (J,I) &= RD1 \\ RD2\ (J,I) &= RD2 \end{aligned}\right\} \quad \text{for} \quad C_i^d = \left[C_i^{do} + C_i^{d1} \left|\dot{U}_i^s\right|\right] g_i\ (t/T)$$

where

$$g_i\ (t/T) = RD2 + (1 - RD2)\ (1 - t/T)^{RD1}$$

T (J,I) = axial force between segments i and i-1 divided by the length of the segment between i and i-1

U (J,I) = U_i^r , i.e., $\overline{U}_i^r$ and $\overline{\overline{U}}_i^r$

UD (J,I) = $\dot{U}_i^r$

U2D (J,I) = $\ddot{U}_i^r$

UR (I) = $(u_i^r)_{clay}$

UDR (I) = $(\dot{u}_i^r)_{clay}$

U2DR (I) = $(\ddot{u}_i^r)_{clay}$

US (J,I) = U_i^s

UDS (J,I) = $\dot{U}_i^r$

U2DS (J,I) = $\ddot{U}_i^s$

UC (J,I) = U_i^c

UDC (J,I) = $\dot{U}_i^c$

U2DC (J,I) = $\ddot{U}_i^c$

UB (J,I) = U_i^b

UDB (J,I) = $\dot{U}_i^b$

U2DB (J,I) = $\ddot{U}_i^b$

O (J) = θ

OD (J) = $\dot{\theta}$

O2D (J) = $\ddot{\theta}$

OM1 (J) = $\theta_{t-2\Delta t}$

OM2 (J) = $\theta_{t-3\Delta t}$

UM1 (J,I) = $(U^r_{t-2\Delta t})_i$

UM2 (J,I) = $(U^r_{t-3\Delta t})_i$

UBM1 (J,I) = $(U^b_{t-2\Delta t})_i$

UB2 (J,I) = $(U^b_{t-3\Delta t})_i$

} USED IN BACKWARD DIFFERENCE METHOD

NT = 2N + 2M + 1

AC (I,J) = structural stiffness matrix

SA (J,I,K) = Pile stiffness matrix k^a_{ij}

SB (J,I,K) = Pier stiffness matrix k^b_{ij}

NOMASS (K) = number of points in the pile which has zero mass, i.e.

NOMASS (K) = 6 implies 6 point has zero mass.

JM = Total number of points with no mass

NN = 2 (N - JM) + 2M + 1

F2 (J,I) = $(\dot{U}^r_i)_{t-\Delta t} + (\Delta t/2)\ (\ddot{U}^r_i)_{t-\Delta t}$ ----- (Step by Step)

= $4.0\ (U^r_i)_{t-\Delta t} - (U^r_i)_{t-2\Delta t}$ ----- (Backward Difference)

F3 (J,I) = $(U^r_i)_{t-\Delta t} + \Delta t\ (\dot{U}^r_i)_{t-\Delta t} + \frac{\Delta t^2}{3}\ (\ddot{U}^r_i)_{t-\Delta t}$ ----- (Step by Step)

= $5.0\ (U^r_i)_{t-\Delta t} - 4.0\ (U^r_i)_{t-2\Delta t} + (U^r_i)_{t-3\Delta t}$ ----- (Backward Difference)

$$O2(J) = \dot{\theta}_{t-\Delta t} + \frac{\Delta t}{2}\ddot{\theta}_{t-\Delta t} \quad \text{----- (Step by Step)}$$

$$= 4.0\,\theta_{t-\Delta t} - \theta_{t-\Delta t} \quad \text{----- (Backward Difference)}$$

$$O3(J) = \theta_{t-\Delta t} + \Delta t\,\dot{\theta}_{t-\Delta t} + \frac{\Delta t^2}{3}\ddot{\theta}_{t-\Delta t} \quad \text{----- (Step by Step)}$$

$$= 5.0\,\theta_{t-\Delta t} - 4.0\,\theta_{t-2\Delta t} + \theta_{t-3\Delta t} \quad \text{----- (Backward Difference)}$$

$COF(J,I) = COF_i$

$USPU(J,I) = U^s_{pu}$

$USPB(J,I) = U^s_{pb}$

$USPC(J,I) = U^s_{pc}$

TI = time value in seconds for current cycle of integration

M1 = number of the current cycle

M2 = number of cycles before which tape was last read

M3 = number of cycles before which tape was last written

K6 = number of cycles before which response was printed

U2DG = $\ddot{u}_g$ = ground acceleration at time TI

UDG = $\dot{u}_g$ = ground velocity at time TI

UG = u_g = ground displacement at time TI

N1 = N + 1

NK = 2N + 3 (4N + 2M + 2) = Total number of values to be put on the tape

URS (L) = location at which values are stored before the tape is written

UCHK5 = last value on tape read so far (Tape 5)

UCHK6 = last value on tape written so far (Tape 6)

EM (J,I) = Total interaction force

TSTOP = time in seconds after which it is desired to stop execution temporarily

ISTOP = TSTOP/DT

FORCE (J,I) = first used to calculate estimated force ($K_i U_i^s - COF_i + C_i^d \dot{U}_i^s$)

in Methods 1, 2 and 3. Later this notation designates the spring force, i.e. ($K_i U_i^s - COF_i$), for the print out.

X (J,I) = used as temporary location in VARCO3 and RESPON for Method 3 and used as temporary location in VARCO4 for Method 4.

KN = number of masses in clay system

NM (K) = number of masses common to clay and interaction systems

DT1 = time interval used in clay system $\geq$DT and (DT1/DT); must be an integer

I2 = 10000/3(N+1) = number of cycles stored in location URR(10000) REDTAP

= 4000/3(N+1) = number of cycles stored in URS (4000) WRITAP

APPENDIX D

Computer Program Listings

```
*************************************************
*     DYNAMIC  RESPONSE  OF  CLAY  MEDIUM       *
*************************************************


+++++++++++++++++++++++++++++++++++++++++++++++++
+     DYNAMIC  RESPONSE  OF  CLAY  MEDIUM       +
+++++++++++++++++++++++++++++++++++++++++++++++++
*     LABEL
*     FORTRAN
CCLYSYS
C     DYNAMIC  RESPONSE  OF  CLAY  MEDIUM
      DIMENSIONW(22),SO(22),S1(22),S2(22),RS1(22),RS2(22),CC0(22),CC1(22      2
     1),RC1(22),RC2(22),CD0(22),CD1(22),RD1(22),RD2(22),US(22),UDS(22),U      3
     22DS(22),UR(22),UDR(22),U2DR(22),CC(22),CD(22),S(22),U2DRT(22),AL(2      4
     .32),A(22,22),D(22),E(22),P(22),K(22),U(10000),B(22),CC2(22)
      DIMENSION USC(22),UDC(22),UCC(22),UCF(22),UDF(22),USF(22)
      DIMENSION COF(22),USPU(22),USPB(22),FORCE(22),FU(6400)
      DIMENSION UDC(22),U2DC(22)
      DIMENSION FMAX(22)
      COMMON JOBNO,N,DT,T,K,N1,N2,N8,I2,13,W,SO,S1,S2,RS1,RS2,CC0,CC1,
     1CC2,RC1,RC2,CD0,CD1,RD1,RD2,USC,UDC,UCC,UCF,UDF,USF,USPU,USPB,US,
     2UDS,U2DS,COF,UR,UDR,U2DR,U2DRT,UG,UDGT,U2DG,T1,M1,M2,M3,N3,N4,CC,
     3CD,S,TOT,B,U,FORCE,FU,I4
    1 FORMAT(15,I3,F7.4,F7.2,10I5)
    2 FORMAT(F7.3,3F13.3,F7.4,F7.2)
    3 FORMAT(5F13.3)
    7 FORMAT(28HINCORRECT  DIAGONAL  ELEMENT)
                                                                        BLANK
      REWIND 5
      REWIND 6
                                                                        BLANK
C     READ  DATA
   11 READ1,JOBNO,N,DT,T,(K(J),J=1,10)
      N1=N 1
      N2=N 2
      KKC=(T+.000001)/DT
C     CALCULATE NUMBER OF CYCLES  THAT CAN BE STORED IN LOCATION OF  )
C     THERE ARE 3*(N+1) OUTPUT VALUES FOR EACH CYCLE
      AN=N2+2*N+1
      N8=AN
      I2=1    .0/AN
      IF(KKC-I2) 300,300,301
  300 I2=KKC
  301 PRINT1,JOBNO,N,DT,T,(K(J),J=1,12)
      I3=I2*N8
      I4=2*I2*N
      READ 250,(FMAX(I),I=1,N1)
  250 FORMAT(9F8.2)
      PRINT 265,(FMAX(I),I=1,N1)
  265 FORMAT(9F12.4)
   12 DO14I=2,N1
      READ2,W(I),SO(I),S1(I),S2(I),RS1(I),RS2(I)
   13 READ 3,CC0(I),CC1(I),CC2(I),RC1(I),RC2(I)
      READ 3,CD0(I),CD1(I),RD1(I),RD2(I)
C     READ      CRITICAL VALUES OF VELOCITY AND DISPLACEMENT BEYOND
C     WHICH  CONSTANT  VALUE  OF  RESPECTIVE  FORCE WILL BE USED
      READ 3,USC(I),UDC(I)
      USPU(I)=USC(I)
      USPB(I)=-USC(I)
      PRINT2,W(I),SO(I),S1(I),S2(I),RS1(I),RS2(I)
      PRINT3,CC0(I),CC1(I),CC2(I),RC1(I),RC2(I)
      PRINT3,CD0(I),CD1(I),RD1(I),RD2(I)
   14 PRINT 3,USC(I),UDC(I)
      DO 3  I=2,N1
      UDF(I)=UDC(I)*(CD0(I)+CD1(I)*UDC(I))
   30 USF(I)=USC(I)*(SO(I)+S1(I)*USC(I)+S2(I)*USC(I)*USC(I))
C     INITIALISE
      DO151=1,N2
      US(I)=0.0
      COF(I)=0.0
      UDS(I)=0.0
      U2DS(I)=0.0
      UR(I)=0.0
      UDR(I)=0.0
      U2DRT(I)=0.0
   15 U2DR(I)=0.0
      T1=0.0
      M1=0
      M2=0
      M3=0
      N3=1
      N4=1
C     IT IS CONVINIENT TO WORK WITH INDEX 2 TO N1 INSTEAD OF 1 TO N
   16 W(1)=0.0
      W(N2)=0.0
      S(1)=0.0
      S(N2)=0.0
      CC(1)=0.0
   17 CC(N2)=0.0
      CD(1)=0.0
      USPU(1)=0.0
      USPU(N2)=0.0
      USPB(1)=0.0
      USPB(N2)=0.0
      CD(N2)=0.0
C     CALCULATION  OF  CONSTANTS  THROUGH TIME INT.  DT
   18 TOT=T1/T
      CALL CONCOE
      T1=T1+DT
      M1=M1+1
      M2=M2+1
      M3=M3+1
      CALL GRNDAC
C     FORMATION  OF  MATRICES
      DO 173 I=2,N1
  171 D(I)=1./(CC(I)+CD(I)+S(I)*DT/3.)
      P(I)=.5*DT*(CD(I)+S(I)*DT/3.)*D(I)
  173 E(I)=UDR(I)+.5*DT*U2DR(I)
  174 DO 177 I=2,N1
  175 AL(I)=-W(I)*U2DG-CC(I)*D(I)*(B(I)-COF(I))+CC(I+1)*D(I+1)*(B(I+1)-C
     1OF(I 1))
     2+2./DT*(CC(I)*P(I)*(-E(I)+E(I-1))-CC(I+1)*(-E(I+1)+E(I))*P(I+1))
  176 A(I,I-1)=-CC(I)*P(I)
      A(I,I+1)=-CC(I+1)*P(I+1)
  177 A(I,I)=W(I)-A(I,I-1)-A(I,I+1)
C     TRANSFER 2 TO N1 EQUATIONS TO 1 TO N AS REQUIRED BY SOLEQU ROUTINE
  178 DO179I=1,N
      AL(I)=AL(I+1)
      DO179J=1,N
  179 A(I,J)=A(I+1,J+1)
  272 IF DIVIDE CHECK 180,180
  180 CALL SOLSYB(A,N,AL)
  181 IF(AL(1,1))182,140,182
  182 PRINT7
      CALL EXIT
C     RESPONSE OF THE SYSTEM AT T1
  140 DO1401=2,N1
  141 U2DRT(I)=AL(I-1)
  142 DO144I=2,N1
  143 UDST=D(I)*(CC(I)*(0.5*DT*(U2DRT(I)-U2DRT(I-1))+E(I)-E(I-1))
     1 -B(I)+COF(I))
  144 U2DST=2.0*(UDST-UDS(I)-0.5*DT*U2DS(I))/DT
      UDRT=E(I)+0.5*DT*U2DRT(I)
  145 URT=UR(I)+DT*(    UDR(I)+DT*(U2DR(I)+U2DRT(I)/4.0)/3.0)
  146 UST=US(I)+DT*(    UDS(I)+DT*(U2DS(I)+U2DST/2.0)/3.0)
      U2DS(I)=U2DST
  147 UDS(I)=UDST
      US(I)=UST
      UDR(I)=UDRT
  148 UR(I)=URT
      CALL WRITAP(KKC)
  201 IF(M2-KKC) 18,91,91
   91 CALL EXIT
      END


+++++++++++++++++++++++++++
+     SUBROUTINE CONCOE     +
+++++++++++++++++++++++++++
*     LIST
*     LABEL
*     FORTRAN
C
      SUBROUTINE CONCOE
C     SUBROUTINE FOR COEFFICIENTS THROUGH TIME INTERVAL DT
      DIMENSIONW(22),SO(22),S1(22),S2(22,,RS1(22),RS2(22),CC0(22),CC1(22      2
     1),RC1(22),RC2(22),CD0(22),CD1(22),RD1(22),RD2(22),US(22),UDS(22),U      3
     22DS(22),UR(22),UDR(22),CC(22),CD(22),S(22),U2DRT(22),
     3K(22),U(10000),B(22),CC2(22),U2DR(22)
      DIMENSION COF(22),USPU(22),USPB(22),FORCE(22),FU(6400),S1P(22)
      DIMENSION USC(22),UDC(22),UCC(22),UCF(22),UDF(22),USF(22),USPC(22)
      COMMON JOBNO,N,DT,T,K,N1,N2,N8,I2,13,W,SO,S1,S2,RS1,RS2,CC0,CC1,
     1CC2,RC1,RC2,CD0,CD1,RD1,RD2,USC,UDC,UCC,UCF,UDF,USF,USPU,USPB,US,
     2UDS,U2DS,COF,UR,UDR,U2DR,U2DRT,UG,UDGT,U2DG,T1,M1,M2,M3,N3,N4,CC,
     3CD,S,TOT,B,U,FORCE,FU,I4
    1 FORMAT(6F12.4)
      IF(M2)2,2,3
    2 READ 1,(S1P(I),I=2,N1)
      PRINT1,(S1P(I),I=2,N1)
      DO 14 I=1,N2
   14 USPC(I)=0.0
    3 DO 4 2 I=2,N1
      EF=RC2(I)+(1.0-RC2(I))*(1.0-TOT)**RC1(I)
      EG=RD2(I)+(1.0-RD2(I))*(1.0-TOT)**RD1(I)
      EH=RS2(I)+(1.0-RS2(I))*(1.0-TOT)**RS1(I)
   21 F1=ABSF(UDR(I)-UDR(I-1)-UDS(I))
      G1=ABSF(UDS(I))
   22 CC(I)=EF*(CC0(I)+CC1(I)*F1)
  301 IF(G1-UDC(I))214,214,213
  213 CD(I)=EG*UDF(I)/G1
      GOTO 302
  214 CD(I)=EG*(CD0(I)+CD1(I)*G1)
  302 IF(S1(I))303,304,303
  303 H1=ABSF(US(I))
      COF(I)=0.0
      IF(H1-USC(I))23,23,215
  215 S(I)=EH*USF(I)/H1
      GOTO 306
   23 S(I)=EH*(SO(I)+S1(I)*H1+S2(I)*H1*H1)
      GOTO 306
  304 IF(US(I)-USPU(I))307,305,305
  307 IF(US(I)-USPB(I))309,309,308
  308 S(I)=SO(I)*EH
      COF(I)=S(I)*USPC(I)
      GOTO 306
  305 USPU(I)=US(I)
      USPB(I)=US(I)-2.0*USC(I)
      USPC(I)=USPU(I)-(USF(I)+(USPU(I)-USC(I))*S1P(I))/SO(I)
      IF(UDS(I))308,308,401
  401 S(I)=S1P(I)*EH
      COF(I)=S(I)*USC(I)-USF(I)*EH
      GOTO 306
  309 USPB(I)=US(I)
      USPU(I)=US(I)+2.0*USC(I)
      USPC(I)=USPU(I)-(USF(I)+(USPU(I)-USC(I))*S1P(I))/SO(I)
      IF(UDS(I))403,308,308
  403 S(I)=S1P(I)*EH
      COF(I)=-S(I)*USC(I)+USF(I)*EH
  306 B(I)=(US(I)+2.*DT*UDS(I)/3.+DT*DT*U2DS(I)/6.)*S(I)
  402 CONTINUE
      RETURN
      END


+++++++++++++++++++++++++++
+     SUBROUTINE GRNDAC     +
+++++++++++++++++++++++++++
*     LIST
*     LABEL
*     FORTRAN
CGRNDAC
      SUBROUTINE GRNDAC
      DIMENSIONW(22),SO(22),S1(22),S2(22),RS1(22),RS2(22),CC0(22),CC1(22      2
     1),RC1(22),RC2(22),CD0(22),CD1(22),RD1(22),RD2(22),US(22),UDS(22),U      3
     22DS(22),UR(22),UDR(22),U2DR(22),CC(22),CD(22),S(22),U2DRT(22),AL(2      4
     32),A(22,22),D(22),E(22),P(22),K(22),U(10000),B(22),CC2(22)
      DIMENSION UDC(22),U2DC(22)
      DIMENSION USC(22),UDC(22),UCC(22),UCF(22),UDF(22),USF(22)
      DIMENSION COF(22),USPU(22),USPB(22),FORCE(22),FU(6400)
      DIMENSION TW(800),UM(800)
      COMMON JOBNO,N,DT,T,K,N1,N2,N8,I2,13,W,SO,S1,S2,RS1,RS2,CC0,CC1,
     1CC2,RC1,RC2,CD0,CD1,RD1,RD2,USC,UDC,UCC,UCF,UDF,USF,USPU,USPB,US,
     2UDS,U2DS,COF,UR,UDR,U2DR,U2DRT,UG,UDGT,U2DG,T1,M1,M2,M3,N3,N4,CC,
     3CD,S,TOT,B,U,FORCE,FU,I4
    5 FORMAT(I3,4(F8.4,F9.6))
  150 IF(M2-1)151,151,158
  151 UDG0=0.0
```

```
      UG0= .0
  152 DO155J=1,200
  153 READ5,IM,TM(4*J-3),UM(4*J-3),TM(4*J-2),UM(4*J-2),TM(4*J-1),UM(4*J-
     1),TM(4*J),UM(4*J)
  154 IF(TM(4*J)-T)155,156,156
  155 CONTINUE
  156 I1=1
      IF(M2-1)162,162,157
  162 U2DG=386.0*UM(1)
      U2DG =U2DG
      U2DS(2)=-CC(2)*U2DG/(CC(2)+CD(2))
      DO 163 I=2,N1
  163 U2DR(I)=-U2DG
  157 U2DG2=386.4*UM(I1)
      T2=TM(I1)
  158 DT2=T2-T1
      IF(DT2)159,160,160
  159 I1=I1+1
      T3=T2
      U2DG1=U2DG2
      IF(I1-800)157,157,152
  160 U2DG=U2DG2-(U2DG2-U2DG1)*DT2/(T2-T3)
      UDGT=UDG0+.5*DT*(U2DG0+U2DG)
      UG=UG0+DT*(UDG0+DT*U2DG0/3.0+DT*U2DG/6.0)
      UG0=UG
  161 U2DG =U2DG
      UDG0=UDGT
      RETURN
      END
```

```
++++++++++++++++++++++++++++++++++
+     SUBROUTINE SOLSYB(A,N,AL)    +
++++++++++++++++++++++++++++++++++
*     FORTRAN
*     LABEL
C     SOLUTION OF SYMMETRICAL LINEAR BAND (THREE ELEMENTS) EQUATIONS
      SUBROUTINE SOLSYB(A,N,AL)
      DIMENSION A(22,22),AL(22)
    1 FORMAT(41H1  BAD INVERSE   ZERO ON DIAGONAL    ROW = I3)
      M=0
C     REDUCTION OF M TH EQUATION
   50 M=M+1
      MM=M 1
      AL(M)=AL(M)/A(M,M)
      IF(M N)70,130,70
   70 A(M,MM)=A(M,MM)/A(M,M)
      IF DIVIDE CHECK 200,71
C     SUBSTITUTION INTO REMAINING EQUATIONS
   71 A(MM,MM)=A(MM,MM)-A(MM,M)*A(M,MM)
      AL(MM)=AL(MM)-A(MM,M)*AL(M)
      GOTO 50
C     BACK SUBSTITUTION
  130 M=M-1
      MM=M 1
      AL(M)=AL(M)-A(M,MM)*AL(MM)
      IF(M 1)130,150,130
  150 A=0.
      GOTO 131
  200 PRINT 1,M




      A=2.
  131 RETURN
      END
```

```
++++++++++++++++++++++++++++++
+     SUBROUTINE WRITAP(KKC)   +
++++++++++++++++++++++++++++++
*     LABEL
*     FORTRAN
C
      SUBROUTINE WRITAP(KKC)
      DIMENSIONW(22),S0(22),S1(22),S2(22),RS1(22),RS2(22),CC0(22),CC1(22
     1),RC1(22),RC2(22),CD0(22),CD1(22),RD1(22),RD2(22),US(22),UDS(22),U
     2DS(22),UR(22),UDR(22),CC(22),CD(22),S(22),U2DRT(22),
     3K(22),U(10000),B(22),CC2(22),U2DH(22)
      DIMENSION USC(22),UDC(22),UCL(22),UCF(22),UDF(22),USF(22)
      DIMENSION COF(22),USPU(22),USPS(22),FUNCE(22),FU(6400)
      COMMON JOBNO,N,DT,T,K,N1,N2,N8,IZ,I3,W,S0,S1,S2,RS1,RS2,CC0,CC1,
     1CC2,RC1,RC2,CD0,CD1,RD1,RD2,USC,UDC,UCC,UCF,UDF,USF,USPU,USPB,US,
     2UDS,U2DS,COF,UR,UDR,U2DR,U2DRT,UG,UDGT,U2DG,T1,M1,M2,M3,N3,N4,CC,
     3CD,S,TOT,8,U,FORCE,FU,I4
    4 FORMAT(1HO,10X,6H MASS ,F20.8,2F19.8,F11.3)
    5 FORMAT(1HO,10X,6HSPRING,F20.8,2F19.8,F11.3)
    6 FORMAT(15H1TIME INTERVAL=,F8.3,3F15.8)
    9 FORMAT(7HOCOEFFT,I4,3F20.8)
C     PUT CALCULATED VALUES INTO U(  ) LOCATION, PRINT ETC.
      J=(M3-1)*N8+1
      U(J)=UG
      U(J+1)=UDGT
      U(J+2)=U2DG
   81 DO83I=2,N1
   82 U2DR(I)=U2DRT(I)
      J=(M3-1)*N8+3*I-2
      FORCE(I)=S(I)*US(I)-COF(I)
      LJ=2*(M3-1)*N+2*I-3
      FU(LJ)=FORCE(I)
      FU(LJ+1)=US(I)
      U(J)=UR(I)
      U(J+1)=UDR(I)
   83 U(J+2)=U2DR(I)
   84 IF(M3-I2)86,85,85
   85 WRITE TAPE 5,(U(J),J=1,I3)
      WRITE TAPE 6,(FU(J),J=1,I4)
      M3=0
   86 IF(M1-K(N4))90,87,87
   87 PRINT6,T1,UG,UDGT,U2DG
      DO 92 I=2,N1
      IM1=I-1
      PRINT9,IM1,S(I),CC(I),CD(I)
      PRINT 5,US(I),UDS(I),U2DS(I),FORCE(I)
   92 PRINT4,UR(I),UDR(I),U2DR(I)
      M1=0
   88 IF(M2-K(N4+1))90,89,89
   89 N3=N3+1
      N4=2*N3-1
   90 CONTINUE
      IF(M2-KKC) 18,91,91
   91 I3=M3*N8
      I4=2*M3*N
      WRITE TAPE 5,(U(J),J=1,I3)
      PRINT 130,M3,I2,I3,N,M2
  130 FORMAT(5I10)
      PRINT 140,(U(J),J=1,100)
  140 FORMAT(8E10.3)
      WRITE TAPE 6,(FU(J),J=1,I4)
      CALL EOF(5)
      CALL REWUNL(5)
      CALL EOF(6)
      CALL REWUNL(6)
   18 RETURN
      END
```

```
**************************************************
*     INTERACTION COEFFICIENTS MAIN PROGRAM      *
**************************************************


++++++++++++++++++++++++++++++++++++++++++++++++++
+     INTERACTION COEFFICIENTS MAIN PROGRAM      +
++++++++++++++++++++++++++++++++++++++++++++++++++
CKCCMCD
C     INTERACTION COEFFICIENTS MAIN PROGRAM
      DIMENSION X(16),Y(16),NS(16),XN(16),KCCCDM(3,20)
      COMMON X,Y,XN,NS,KCCCDM,N1,N,DN,RAD,ANK,H,RAD2,N2,Q,AN,AI,C,CQ,TOC
      COMMON J1,ALFA,BETA,AK,CC1,CC2,C1,C12,C2,C22,ALFA2,BETA2,CQ21,CQ22,
     1,CQ41,CQ42,CQ4,CC26,CC16,C4,CBI,CAI,C4B,C4A,CQ2,UMAX
    1 FORMAT(2I4,3F12.3)
  101 FORMAT(26H1 INTERACTION COEFFICIENTS)
  102 FORMAT(18H0 PILE LAYOUT DATA)
    2 FORMAT(I4,2F12.3)
  104 FORMAT(21H0 SINGLE ROW GROUPING)
  105 FORMAT(23H0 MULTIPLE ROW GROUPING)
  103 FORMAT(10H0 PILE NO.,12X1HX,12X1HY)
  107 FORMAT(I7,F20.4,F13.4)
  108 FORMAT(25H0 HEIGHT OF CLAY MEDIUM  =,F20.4)
  109 FORMAT(25H0 NUMBER OF POINTS       =,F20.4)
  110 FORMAT(25H0 RADIUS OF PILES        =,F20.4)
    4 FORMAT(72I1)
      READ 1,N1,N,DN,RAD,ANK
      PRINT 1,N1,N,DN,RAD,ANK
      AN=N
      PRINT 101
      PRINT 102
      READ2, (NS(I),X(I),Y(I),I=1,N1)
      PRINT 2,(NS(I),X(I),Y(I),I=1,N1)
      N2=N1
      J1=0.0
      DO 11 J=1,N1
      IF(NS(J)-1) 13,13,12
   12 N2=N2+1
      Y(N2)=-Y(J)
      X(N2)=X(J)
   13 IF(Y(J)) 11,14,11
   14 IF(X(J)) 11,11,15
   15 XN(J1)=X(J)-RAD
      J1=J 1
   11 CONTINUE
      IF(ANK-2.1) 16,16,17
   16 PRINT 105
      GO TO 18
   17 PRINT 104
   18 PRINT 103
      DO 19 I=1,N2
   19 PRINT 107,I,X(I),Y(I)
      PRINT 108,DN
      PRINT 109,AN
      PRINT 110,RAD
      RAD2=RAD*RAD
      Q=N2
      H=DN/AN*.5
      READ 4,((KCCCDM(J,I),J=1,3),I=1,N)
      PRINT 4,((KCCCDM(J,I),J=1,3),I=1,N)



      DO 2  I=1,N
      AI=I
      C=2.*H*(AN-AI)
      TOC=2.0*C
      CQ=C*C
      DO 21 J=1,3
      IF(KCCCDM(J,I)) 21,21,22
   22 GO TO (23,24,25),J
   23 CALL KINTAC(I)
      GO TO 21
   24 CALL CCINTA(I)
      GO TO 21
   25 CALL CDINTA(I)
   21 CONTINUE
   20 CONTINUE
      CALL EXIT
      END


++++++++++++++++++++++++++++++++++
+     SUBROUTINE CCINTA(I)       +
++++++++++++++++++++++++++++++++++
*     LIST
*     LABEL
*     FORTRAN
C
      SUBROUTINE CCINTA(I)
C     CALCULATION OF CC VALUES
      DIMENSION X(16),Y(16),NS(16),XN(16),KCCCDM(3,20)
      DIMENSION CC(10),V8(10),SL(10),DX(10),DEL(10)
      COMMON X,Y,XN,NS,KCCCDM,N1,N,DN,RAD,ANK,H,RAD2,N2,Q,AN,AI,C,CQ,TOC
      COMMON J1,ALFA,BETA,AK,CC1,CC2,C1,C12,C2,C22,ALFA2,BETA2,CQ21,CQ22,
     1,CQ41,CQ42,CQ4,CC26,CC16,C4,CBI,CAI,C4B,C4A,CQ2,UMAX
    2 FORMAT(I4,5F13.5)
  101 FORMAT(19H0 DATA FOR CC VALUE)
  102 FORMAT(8H0 OUTPUT)
   34 FORMAT(3E16.7)
  103 FORMAT(3H S=,E15.7,4X9HS SQUARE=,E15.7,4X7HS CUBE=,E15.7)
  104 FORMAT(11H0 CC AND V8)
      PRINT 101
  106 FORMAT(4H DX=,F12.3,8H UPTO X=,F12.3)
      READ 2,N3,ALFA,BETA,D1,D2,D3
      PRINT 99,N3,ALFA,BETA,D1,D2,D3
   99 FORMAT(I4,5E15.4)
      READ 5,NET,(DEL(J),J=1,NET)
      PRINT5,NET,(DEL(J),J=1,NET)
      READ 23,(DX(J),J=1,NET)
      PRINT23,(DX(J),J=1,NET)
      IF(KCCCDM(1,I))50,50,51
   50 PRINT 52
   52 FORMAT(49H0K NOT CALCULATED FOR THIS LEVEL SO CC IS SKIPPED)
      GOTO 54
   51 CQ2=2.0*CQ
      C4A=4.0*C-ALFA
      C4B=4.0*C+BETA
      CAI=C-ALFA
      CBI=C+BETA
      C1=TOC-ALFA
      C2=TOC+BETA
      C12=C1*C1
      C22=C2*C2
      CC1=C*C1
      CC2=C*C2
      ALFA2=ALFA*ALFA
      BETA2=BETA*BETA
      CQ21=2.0*CQ*C1
      CQ22=2.0*CQ*C2
      CQ41=4.0*CQ*C1
      CQ42=4.0*CQ*C2
      CQ4=4.0*CQ
      CC26=6.0*CC2
      CC16=6.0*CC1
      C4=4.0*C
    5 FORMAT(I4,11F6.3)
   23 FORMAT(6F12.3)
      ST=0.0
      ST2=0.0
      ST3=0.0
      XI=RAD+0.001
      M1=1
      KL=1
      DX1=DX(1)
      CALL SSTAR(DX1,M1,XI,ST,ST2,ST3,S)
      PRINT 105,XI,S
  105 FORMAT(17H VALUE OF S(AT X=,F8.3,2H)=E15.7)
      DO 17 J=1,NET
   17 SL(J)=ABSF(S*DEL(J))
   16 DX1=DX(KL)
      XI=XI+DX1
      CALL SSTAR(DX1,M1,XI,ST,ST2,ST3,S)
      S=ABSF(S)
      IF(S SL(KL))18,18,16
   18 KL=KL+1
      PRINT 106,DX1,XI
      IF(KL-NET)16,16,30
   30 H2Q=2.0*H*Q
      HQ=D1*ST/12.56637
      SKI=AK*1.15*UMAX/(H2Q*5.)
      H1Q=D2*ST2/157.91365
      H3Q=D3*ST3/1984.4014
      DO 22 J=1,5
      AJ=J
      PJ=SKI*AJ
      VB(J)=(HQ+H1Q*PJ+H3Q*PJ*PJ*PJ
   22 CC(J)=(ALFA + BETA)*ANK*Q*PJ/VB(J)
      PRINT 102
      PRINT 103,ST,ST2,ST3
      PRINT 104
      PRINT 35,(CC(J),VB(J),J=1,5)
   35 FORMAT(2E16.7)
   54 RETURN
      END


++++++++++++++++++++++++++
+     SUBROUTINE AKC     +
++++++++++++++++++++++++++
*     LABEL
*     FORTRAN
C
      SUBROUTINE AKC



      DIMENSION X(16),Y(16),NS(16),XN(16),KCCCDM(3,20)
      COMMON X,Y,XN,NS,KCCCDM,N1,N,DN,RAD,ANK,H,RAD2,N2,Q,AN,AI,C,CQ,TOC
      COMMON J1,ALFA,BETA,AK,CC1,CC2,C1,C12,C2,C22,ALFA2,BETA2,CQ21,CQ22,
     1,CQ41,CQ42,CQ4,CC26,CC16,C4,CBI,CAI,C4B,C4A,CQ2,UMAX
      C1=2.*C-ALFA
      C12=C1*C1
      C2=2.*C+BETA
      C22=C2*C2
      ALFA2=ALFA*ALFA
      BETA2=BETA*BETA
      CC1=C*C1
      CC2=C*C2
      CQ21=2.0*CQ*C1
      CQ22=2.0*CQ*C2
      CQ41=4.0*CQ*C1
      CQ42=4.0*CQ*C2
      SUM=.
      DO 11 I=1,N2
      DO 11 J=1,N2
      IF(I J) 10,11,10
   10 XRS=X(I)-X(J)
      YRS=Y(I)-Y(J)
      XRS2=XRS*XRS
      YRS2=YRS*YRS
      R=XRS2+YRS2
      RQ=R**.5
      A=(R ALFA2)**.5
      B=(R BETA2)**.5
      A1=(R+C12)**.5
      B1=(R+C22)**.5
      AL=(C2+B1)*(BETA+B1)*(ALFA+A1)/((C1*A1)*R)
      D1=LOGF(AL)
      D2=XRS2/R*(TOC*(R+CC2)/(B1**3)+CQ42/(R*B1)+BETA/B+ALFA/A-TOC*(R+CC
     11)/(A1**3)-CQ41/(R*A1))-(CQ22+YRS2*TOC-BETA*XRS2)/(B1*R)+(CQ21+YRS
     22*TOC-ALFA*XRS2)/(A1*R)
      SUM=SUM+D1+D2
   11 CONTINUE
      D1=(RAD2+C12)**.5
      D2=(RAD2+C22)**.5
      D3=(RAD2+ALFA2)**.5
      D4=(RAD2+BETA2)**.5
      D5=(C2+D2)*(BETA+D4)*(ALFA+D3)/((C1+D1)*RAD2)
      D5=LOGF(D5)
      D5=D5+1.3333*C*((RAD2+CC2)/(D2**3)-(RAD2+CC1)/(D1**3))+0.66666*
     1(BETA/D4+ALFA/D3+((CQ*C2-RAD2*(C-BETA))/D2-(CQ*C1-RAD2*(C+ALFA))/D
     21)/RAD2)
      D5=D5*Q
      SUM=SUM+D5
      AK=Q/SUM
      PRINT 15,AK
   15 FORMAT(6HOFTA =,F20.8)
      RETURN
      END


++++++++++++++++++++++++++++++++++
+     SUBROUTINE KINTAC(I)       +
++++++++++++++++++++++++++++++++++
*     LIST
*     LABEL
*     FORTRAN
C
```

```
      SUBROUTINE KINTAC(I)
      DIMENSION X(16),Y(16),NS(16),XN(16),KCCCDM(3,20)
      COMMON X,Y,XN,NS,KCCCDM,N1,N,DN,RAD,ANK,H,RAD2,N2,Q,AN,AI,C,CQ,TOC
      COMMON J1,ALFA,BETA,AK,CC1,CC2,C1,C12,C2,C22,ALFA2,BETA2,CQ21,CQ22,
     1,CQ41,CQ42,CQ4,CC26,CC16,C4,CBI,CAI,C4B,C4A,CQ2,UMAX
    2 FORMAT(4F15.5)
    5 FORMAT(1HO,9X,2HE=F15.5/9X,3HCS=F15.5/9X3HNC=F15.5/1HO,9X,2HK=,
     1F15.5/1HO,6X,5HUMAX=,F15.5)
    6 FORMAT(26HOINTERACTION SPRING VALUES)
    7 FORMAT(1H1,8HLEVEL NO,I5)
      ALFA=C
      BETA=2.*H*AI
      READ 2,E,CS,ANC
      QU=H*ANK*Q*E*16.7551608
      QP=4.*RAD*H*Q
      CALL AKC
      AK=AK*QU
      IF(I N) 3,4,4
    4 AK=AK/2.
    3 UMAX = ANC*CS*QP*ANK/AK
      PRINT 7,I
      PRINT 6
      PRINT 5,E,CS,ANC,AK,UMAX
      RETURN
      END


++++++++-+++++++++++++++++++++++++
+     SUBROUTINE CDINTA(I)      +
++++++++++++++++++++++++++++++++++
*     FORTRAN
*     LABEL
CCDINTA
      SUBROUTINE CDINTA(I)
      DIMENSION X(16),Y(16),NS(16),XN(16),KCCCDM(3,20)
      DIMENSION DEL(101),DK(10),DY(10),SQL(10)
      COMMON X,Y,XN,NS,KCCCDM,N1,N,DN,RAD,ANK,H,RAD2,N2,Q,AN,AI,C,CQ,TOC
      COMMON J1,ALFA,BETA,AK,CC1,CC2,C1,C12,C2,C22,ALFA2,BETA2,CQ21,CQ22,
     1,CQ41,CQ42,CQ4,CC26,CC16,C4,CBI,CAI,C4B,C4A,CQ2,UMAX
    4 FORMAT(1H1,8HLEVEL NO,I5)
    5 FORMAT(3F10.5)
    7 FORMAT(5HORHO=F12.4,3X5HALFA=F12.4,3X5HBETA=F12.4)
    8 FORMAT(6HOMASS=F15.5)
   12 FORMAT(F15.8)
   13 FORMAT(1HO,13X,2HC*,12X,2HCD)
   14 FORMAT(4X,2F15.8)
   23 FORMAT(6F12.3)
  106 FORMAT(2F15.5,2F16.8)
  107 FORMAT(I4,11F6.3)
  108 FORMAT(1HO7X1HX,14X1HY,13X2HSQ,14X4HGAMA)
  109 FORMAT(18HOINTERACTION FIELD)
  110 FORMAT(4HOSQ=F15.5,5X6HAT EDGE OF CENTRAL PILE ALONG X AXIS)
  200 FORMAT(10HOCDSTAR = ,F10.3/23HODAMPING COEFFICIENT = ,F10.4)
      IF(KCCCDM(1,I))1,1,2
    1 IF(KCCCDM(2,I))3,3,2
    3 PRINT 4,I
    2 READ 5,RHO,ALFA,BETA
      PRINT 5,RHO,ALFA,BETA
      IF(I N)20,21,21
   21 C=H/2.0


   20 PRINT 6
    6 FORMAT(19HOMASS AND CD VALUES)
      GAM2=0.0
      GAMA=0.0
      AREA=0.0
      AMZ= .0
      CALL AKC
      CQ4=4.0*CQ
      CC26=6.0*CC2
      CC16=6.0*CC1
      C4=4.0*C
      READ 107,NET,(DEL(J),J=1,NET)
      PRINT 107,NET,(DEL(J),J=1,NET)
      READ 23,(DX(J),DY(J),J=1,NET)
      PRINT23,(DX(J),DY(J),J=1,NET)
      BD=RAD*0.01
      CALL SYXYZ(BD,0.0,GAM,SYX,SYY,SYZ)
      SQ=SYX*SYX+SYY*SYY+SYZ*SYZ
      PRINT 110,SQ
      DO 15 J=1,NET
   15 SQL(J)=DEL(J)*SQ
      DY1=DY(1)/2.0
      PRINT 109
      PRINT 108
      YI=DY1
      NDEY=1
  116 XI=0.0
      NDEX=NDEY
      DX1=DX(NDEX)/2.0
      DXY=4.0*DX1*DY1
  117 XI=XI+DX1
      CALL SYXYZ(XI,YI,GAM,SYX,SYY,SYZ)
      AREA=AREA+DXY
      GAMA=GAMA+GAM*DXY
      GAM2=GAM2+GAM*GAM*DXY
      SQ=SYX*SYX+SYY*SYY+SYZ*SYZ
      CALL FTMOPT(7,10,0)
      AMZ=AMZ+SQ*DXY
       XI=XI+DX1
      DO 56 MMT=1,NET
      IF(SQ-SQL(MMT))56,56,57
   56 CONTINUE
      MMT=NET+1
   57 IF(NDEX-MMT)118,117,118
  118 NDEX=MMT
      IF(NDEX-NET)119,119,120
  119 DX1=DX(NDEX)/2.0
      DXY=4.0*DX1*DY1
      GOTO 117
  120 PRINT 106,XI,YI,SQ,GAM
      YI=YI+2.0*DY1
      CALL SYXYZ(BD,YI,GAM,SYX,SYY,SYZ)
      SQ=SYX*SYX+SYY*SYY+SYZ*SYZ
      DO 58 MMT=1,NET
      IF(SQ-SQL(MMT))58,58,59
   58 CONTINUE
      MMT=NET+1
   59 IF(NDEY-MMT)60,116,60
   60 NDEY=MMT
      IF(NDEY-NET)112,112,113
  112 YI=YI-DY1
      DY1=DY(NDEY)/2.0


      DXY=4.0*DX1*DY1
      YI=YI+DY1
      GOTO 116
  113 AME=8.0*ANK*H*AK*AK*RHO*AMZ
      GAM2=GAM2*8.0*H*ANK*(2.0*AK/3.0)**2.0
      GAMA=2.0*AK*GAMA/(3.0*AREA)
      IF(I N) 70,22,22
   22 AME=AME/2.0
      GAM2=GAM2/2.0
   70 PRINT8,AME
      READ 12, CSTLA
      CD = CSTLA*GAMZ
      PRINT 200, CSTLA, CD
      RETURN
      END


++++++++++++++++++++++++++++++++++++++++++++++++++
+     SUBROUTINE SSTAR(DX1,M1,XI,ST,ST2,ST3,S)     +
++++++++++++++++++++++++++++++++++++++++++++++++++
*     LABEL
*     FORTRAN
C
      SUBROUTINE SSTAR(DX1,M1,XI,ST,ST2,ST3,S)
      DIMENSION X(16),Y(16),NS(16),XN(16),KCCCDM(3,20)
      COMMON X,Y,XN,NS,KCCCDM,N1,N,DN,RAD,ANK,H,RAD2,N2,Q,AN,AI,C,CQ,TOC
      COMMON J1,ALFA,BETA,AK,CC1,CC2,C1,C12,C2,C22,ALFA2,BETA2,CQ21,CQ22,
     1,CQ41,CQ42,CQ4,CC26,CC16,C4,CBI,CAI,C4B,C4A,CQ2,UMAX
      S=0.
      DO 19 K=1,N2
      XS=XI-X(K)
      YS=Y(K)
      XS2=XS*XS
      YS2=YS*YS
      R=XS2+YS2
      A=(R ALFA2)**0.5
      B=(R BETA2)**0.5
      A1=(R+C12)**0.5
      B1=(R+C22)**0.5
      VS1=1.0/B1
      US1=1.0/A1
      VS3=VS1**3
      US3=US1**3
      TS1=1.0/B
      SS1=1.0/A
      R1=1.0/R
      R12=2.0*R1
      VS12=VS1*VS1
      US12=US1*US1
      D1=(CC26*CBI*VS3*VS12-CC16*CAI*US3*US12-C4B*VS3+C4A*US3-R12*C2*VS1
     1*(1.   CQ2*(VS12+R12))+R12*C1*US1*(1.0+CQ2*(US12+R12))-BETA*TS1*(TS
     21*TS1+R12)-ALFA*SS1*(SS1*SS1+R12))*(XS2-YS2)
      D2=YS2*8.00*C*(VS3-US3+CC2*VS1*R1*(VS12+R12)-CC1*US1*R1*(US12+R12))
     1)
      S=S+XS*R1*(D1+D2)
   19 CONTINUE
   41 IF(M1-J1)28,28,29
   28 IF(XI+DX1-XN(M1))29,27,27
   27 DX1=XN(M1)-XI
      XI=XN(M1)-DX1+2.0*B


      M1=M1+1
   29 ST=ST+S*DX1
      ST2=ST2+S*ABSF(S)*DX1
      ST3=ST3+S**3*DX1
      RETURN
      END


++++++++++++++++++++++++++++++++++++++++++++++++++
+     SUBROUTINE SYXYZ(XI,YI,GAM,SYX,SYY,SYZ)     +
++++++++++++++++++++++++++++++++++++++++++++++++++
*     LIST
*     LABEL
*     FORTRAN
C
      SUBROUTINE SYXYZ(XI,YI,GAM,SYX,SYY,SYZ)
      DIMENSION X(16),Y(16),NS(16),XN(16),KCCCDM(3,20)
      COMMON X,Y,XN,NS,KCCCDM,N1,N,DN,RAD,ANK,H,RAD2,N2,Q,AN,AI,C,CQ,TOC
      COMMON J1,ALFA,BETA,AK,CC1,CC2,C1,C12,C2,C22,ALFA2,BETA2,CQ21,CQ22,
     1,CQ41,CQ42,CQ4,CC26,CC16,C4,CBI,CAI,C4B,C4A,CQ2,UMAX
      GAM= .0
      SYX= .0
      SYY= .0
      SYZ= .0
      DO 1  I=1,N2
      XS=XI-X(I)
      YS=YI-Y(I)
      XS2=XS*XS
      YS2=YS*YS
    1 R=XS2+YS2
      R5=R**0.5
      A=(R ALFA2)**0.5
      B=(R BETA2)**0.5
      A1=(R-C12)**0.5
      B1=(R+C22)**0.5
      VS1=1.0/B1
      US1=1.0/A1
      VS3=VS1**3
      US3=US1**3
      TS1=1.0/B
      SS1=1.0/A
      R1=1.0/R
      R12=2.0*R1
      VS12=VS1*VS1
      US12=US1*US1
      D1=(C2+B1)*(BETA+B)*(ALFA+A)/((C1+A1)*R)
      D1=LOGF(D1)
      D2=R1*(XS2*(TOC*(R+CC2)*VS3+CQ42*VS1*R1+BETA*TS1-TOC*(R+CC1)*US3-C
     1Q41*US1*R1+ALFA*SS1)-VS1*(CQ22+TOC*YS2-BETA*XS2)+US1*(CQ21+TOC*YS2
     2+ALFA*XS2))
      SYX=SYX+D1+D2
      SYY=SYY+XS*YS*R1*(BETA*TS1+ALFA*SS1+R1*(R+CQ4)*(VS1*C2-US1*C1+
     1+TOC*(VS3*(R+CC2)-US3*(R+CC1)))
      SYZ=SYZ+XS*(TS1-SS1+VS1-US1+TOC*(VS3*(C+BETA)-US3*(C-ALFA)))
      GAM=GAM+XS*R1*(XS2*(CC26*(C+BETA)*VS3*VS12-CC16*(C-ALFA)*US3*US12
     1-BETA*TS1*(TS1*TS1+R12)-ALFA*(SS1*SS1+R12)*SS1)
     2+C4*(YS2-XS2)*(VS3-US3)-(3.0*XS2+2.0*YS2)*(BETA*VS3-ALFA*US3)
     3+R12*((YS2*(C2*VS1-C1*US1))+CQ*(3.0*YS2-XS2)*(C2*VS1*(VS12+R12)-
     4C1*US1*(US12+R12))))
   10 CONTINUE
      RETURN
      END
```

```
**********************
*     CHAIN (1,A4)     *
**********************


++++++++++++++++++++++++++++++++++++++++++++++++
+     CHAIN LINK 1 OF INTERACTION PROGRAM      +
++++++++++++++++++++++++++++++++++++++++++++++++
*     CHAIN (1,A4)
*     LABEL
*     FORTRAN
CINTAC1
C     CHAIN LINK 1 OF INTERACTION PROGRAM
      DIMENSION W(2,20),WE(2,20),WS(2,6),SA(2,21,21),SB(2,8,8),RM(2),
     1CB(2,6),CBO(2),T(2,20),S(2,6),AC(53,53)
      DIMENSION CO(2,20),C1(2,20),RC1(2,20),RC2(2,20),DO(2,20),D1(2,20),
     1RD1(2,20),RD2(2,20),TO(2,20),T1(2,20),RT1(2,20),RT2(2,20),CC(2,20)
     2,CD(2,20),SK(2,20),      E(20),C2(2,20),K1(20),O(2),OD(2),O2D(2),
     3U(2,20),UD(2,20),U2D(2,20),US(2,20),UDS(2,20),U2DS(2,20),UB(2,6),
     4UDB(2,6),U2DB(2,6),USM(2,20),UCM(2,20),UDM(2,20),USF(2,20),
     5UCF(2,20),UDF(2,20), AL(53),D(2,20),EI(2),UC(2,20),UDC(2,20),
     6U2DC(2,20),NOMASS(20)
      DIMENSION OM1(2),OM2(2),UM1(2,20),UM2(2,20),UBM1(2,6),UBM2(2,6)
      COMMON W,WE,WS,RM,CB,CBO,N,M,DT,NT,EI,D,SA,SB,T,S,SKO,DT2,DT3,DT6
      COMMON NOMASS,NN,JM
     ,COMMON CO,C1,RC1,RC2,DO,D1,RD1,RD2,TO,T1,RT1,RT2,CC,CD,SK,C2,K1,
     1O,OD,O2D,U,UD,U2D,US,UDS,U2DS,UB,UDB,U2DB,TC,USM,UCM,UDM,USF,UCF,
     2UDF,AC,AL,SCALE,METHOD,UC,UDC,U2DC,OM1,OM2,UM1,UM2,UBM1,UBM2
    1 FORMAT(6E12.5)
    2 FORMAT(14I5)
    3 FORMAT(1H ,E11.4,5E12.5)
    4 FORMAT(1H1,4HDATA)
    8 FORMAT(43H0ABOVE MATRICES ARE PILE STIFFNESS MATRICES)
    9 FORMAT(43H0ABOVE MATRICES ARE PIER STIFFNESS MATRICES)
   10 FORMAT(44H0ABOVE MATRIX IS STRUCTURAL STIFFNESS MATRIX)
   11 FORMAT(55H0ABOVE MATRIX IS INVERSE OF STRUCTURAL STIFFNESS MATRIX)
   32 FORMAT(31H0TIME AT COMPLETION OF CHAIN 1=,F15.5)
   57 FORMAT(11H0PILE GROUP,I6)
   58 FORMAT(10H0PILE MASS,I7)
   59 FORMAT(11H0PIER GROUP,I6)
   60 FORMAT(10H0PIER MASS,I7)
   53 FORMAT(27H1BACKWARD DIFFERENCE METHOD)
   54 FORMAT(54H1STEP BY STEP INTEGRATION WITH ESTIMATED SPRING FORCES)
   61 FORMAT(58H1MODIFIED STEP BY STEP METHOD WITH ESTIMATED SPRING FORC
     1ES)
   55 FORMAT(25H1STEP BY STEP INTEGRATION)
C
C     READ DATA
C
      PRINT 4
      READ 2,JOBNO,METHOD,N,M,(K1(I),I=1,10)
      PRINT 2,JOBNO,METHOD,N,M,(K1(I),I=1,10)
      READ 1,DT,TC,U2DG,SCALE
      PRINT 3,DT,TC,U2DG,SCALE
C
C     PILE AND SUPERSTRUCTURE COEFFICIENTS
C
      READ 1,CROSAD
      PRINT 1,CROSAD
      DO 14 J=1,2
      PRINT 57,J
      READ 1,EI(J),ST,(D(J,I),I=1,N)
      PRINT 3,EI(J),ST,(D(J,I),I=1,N)
      DO 12 I=1,N
      READ 1,W(J,I),WE(J,I),TO(J,I),T1(J,I),RT1(J,I),RT2(J,I)
      READ 1,CO(J,I),C1(J,I),C2(J,I),RC1(J,I),RC2(J,I)
      READ 1,DO(J,I),D1(J,I),RD1(J,I),RD2(J,I),T(J,I)
      READ 1,USM(J,I),UCM(J,I),UDM(J,I)
      USF(J,I)=TO(J,I)*USM(J,I)
      UCF(J,I)=(CO(J,I)+C1(J,I)*UCM(J,I)+C2(J,I)*UCM(J,I)**2)*UCM(J,I)
      UDF(J,I)=(DO(J,I)+D1(J,I)*UDM(J,I))*UDM(J,I)
      PRINT 58,I
      PRINT3,W(J,I),WE(J,I),TO(J,I),T(J,I),RT1(J,I),RT2(J,I)
      PRINT3,CO(J,I),C1(J,I),C2(J,I),RC1(J,I),RC2(J,I)
      PRINT3,DO(J,I),D1(J,I),RD1(J,I),RD2(J,I),T(J,I)
      PRINT3,USM(J,I),UCM(J,I),UDM(J,I)
      PRINT 3,USF(J,I),UCF(J,I),UDF(J,I)
   12 CONTINUE
      PRINT 59,J
      READ 1,EIS,(E(I),I=1,M)
      PRINT 3,EIS,(E(I),I=1,M)
      DO 13 I=1,M
      PRINT 60,I
      READ 1,WS(J,I),CB(J,I),S(J,I)
   13 PRINT3,WS(J,I),CB(J,I),S(J,I)
      CALL PSTFNS(J,EIS,ST,E,CROSAD)
   14 CONTINUE
      READ 1,RM(1),RM(2),SKO,CBO(1),CBO(2)
      PRINT3,RM(1),RM(2),SKO,CBO(1),CBO(2)
C
C     INITIALISE
C
      DT2=DT/2.0
      DT3=DT*DT/3.0
      DT6=DT*DT/6.0
      NP1=N+1
      MP2=M+2
      NT=2*N+2*M+1
      NN=NT
      WS(1,M)=WS(1,M)/2.0
      WS(2,M)=WS(1,M)
      CB(1,M) = CB(1,M) + CB(2,M)
      CB(2,M) = 0.0
      DO 23 I=1,2
      OM1(I)=0.0
      OM2(I)=0.0
      O(I)=0.0
      OD(I)=0.0
      O2D(I)=0.0
      DO 22 J=1,N
      NOMASS(J)=0
      UM1(I,J)=0.0
      UM2(I,J)=0.0
      U(I,J)=0.0
      UD(I,J)=0.0
      U2D(I,J)=-U2DG
      UC(I,J)=0.0
      UDC(I,J)=0.0
      U2DC(I,J)=0.0
      US(I,J)=0.0
      UDS(I,J)=0.0
   22 U2DS(I,J)=0.0
      DO 23 J=1,M
      UBM1(I,J)=0.0
      UBM2(I,J)=0.0
      UB(I,J)=0.0
      UDB(I,J)=0.0
   23 U2DB(I,J)=-U2DG
      DO 15 I=1,NT
      DO 15 J=1,NT
   15 AC(I,J)=0.0
      CALL PRNTTM(SA,2,NP1,NP1,2,21)
      PRINT 8
      CALL PRNTTM(SB,2,MP2,MP2,2,8)
      PRINT 9
      NINV=NT
      GOTO (50,51,62,52),METHOD
   50 PRINT 53
      CALL INDCO1(AC)
      GOTO 56
   51 PRINT 54
      CALL INDCO4(AC)
      GOTO 56
   62 PRINT 61
      CALL INDCO3(AC)
      NINV=NN
      GOTO 56
   52 PRINT 55
      CALL INDCO4(AC)
      CALL PRNTTM(AC,1,NT,NT,1,53)
      PRINT 10
      GOTO 17
   56 CALL PRNTTM(AC,1,NT,NT,1,53)
      PRINT 10
      DO 16 I=1,NT
      DO 16 J=1,NT
   16 AC(I,J)=AC(I,J)*SCALE
      CALL BIGINV(AC,NINV)
      CALL PRNTTM(AC,1,NT,NT,1,53)
      PRINT 11
   17 CALL TIME(CLOCK)
      PRINT 32,CLOCK
      CALL CHAIN(2,A4)
      END

++++++++++++++++++++++++++++++++++++++++++++++++++
+     SUBROUTINE PSTFNS(K1,EIS,ST,E,CROSAD)      +
++++++++++++++++++++++++++++++++++++++++++++++++++
*     LABEL
*     FORTRAN
C
      SUBROUTINE PSTFNS(K1,EIS,ST,E,CROSAD)
      DIMENSION W(2,20),WE(2,20),WS(2,6),SA(2,21,21),SB(2,8,8),RM(2),
     1CB(2,6),CBO(2)
      DIMENSION S11(22,22),D(2,20),E(20),EI(2),T(2,20),S(2,6),F(20)
      COMMON W,WE,WS,RM,CB,CBO,N,M,DT,NT,EI,D,SA,SB,T,S,SKO,DT2,DT3,DT6
      NC=N+2
      DO 3 I=2,N
      J=NC-I
      D(K1,J)=D(K1,J)-D(K1,J-1)
    3 F(J)=D(K1,J)
      F(1)=D(K1,1)
      EIP=EI(K1)
      CALL STIFFM(N,EIP,F,ST,S11,NC,CROSAD,K1)
      DO 2 I=2,NC
      I1=I-1
      DO 2 J=2,NC
      J1=J-1
    2 SA(K1,I1,J1)=S11(I,J)
      NC=M+3
      NC1=NC-1
      IF (M-1)10,10,11
   11 DO 5 I=2,M
      J=NC1-I
    5 E(J)=E(J-1)
   10 CONTINUE
      CALL STIFFM(M,EIS,E,0.0,S11,NC)
      SB(K1,1,1)=S11(1,1)
      SB(K1,1,2)=S11(1,NC1)
      SB(K1,2,1)=S11(NC1,1)
      SB(K1,2,2)=S11(NC1,NC1)
      DO 6 J=3,NC1
      J1=J-1
      SB(K1,1,J)=S11(1,J1)
      SB(K1,J,1)=S11(J1,1)
      SB(K1,2,J)=S11(NC1,J1)
      SB(K1,J,2)=S11(J1,NC1)
      DO 6 I=3,NC1
      I1=I-1
      SB(K1,J,I)=S11(J1,I1)
    6 CONTINUE
      RETURN
      END

++++++++++++++++++++++++++++++++++++++++++++++++++++++++++++++++
+     SUBROUTINE STIFFM(N,EI,AL,ST,S11,NC,CROSAD,K1)           +
++++++++++++++++++++++++++++++++++++++++++++++++++++++++++++++++
*     LABEL
*     FORTRAN
C
      SUBROUTINE STIFFM(N,EI,AL,ST,S11,NC,CROSAD,K1)
      DIMENSION S11(22,22),S12(20,20),S21(20,20),S22(21,21),AL(20),A(42,
     142),T(22,22),TM(22,22)
      EI=2.0*EI
      N1=N+1
      N12=2*N1
C
C     INITIALISE
C
      DO 2 I=1,42
      DO 2 J=1,42
    2 A(I,J)=0.0
      DO 50 I=1,22
      DO 50 J=1,22
      T(I,J)=0.0
   50 TM(I,J)=0.0
```

```
C
C     FORM STIFFNESS MATRIX
C
      DO 3 I=1,N
      J=I
      ALI=1.0/AL(J)
  201 AL6=6.0*ALI**3
      A(I,I)=A(I,I)+AL6
      A(I,I+1)=-AL6
      A(I+1,I+1)=AL6
      N1I=N1+I
      AL3=3.0*ALI*ALI
      A(I,N1I)=A(I,N1I)+AL3
      A(I,N1I+1)=AL3
      A(I+1,N1I+1)=-AL3
      A(I+1,N1I)=-AL3
      AL2=2.0*ALI
      A(N1I,N1I)=A(N1I,N1I)+AL2
      A(N1I,N1I+1)=ALI
      A(N1I+1,N1I+1)=AL2
    3 CONTINUE
      NMP=N12-1
      DO 5 I=1,NMP
      IP1=I+1
      DO 5 J=IP1,N12
    5 A(J,I)=A(I,J)
      A(N+2,N+2)=A(N+2,N+2)+ST/EI
C
C     CHANGE KNOWNS AND UNKNOWNS
C
      DO 6 I=1,N12
      AK=A(NC,I)
      A(NC,I)=A(N12,I)
    6 A(N12,I)=AK
      DO 7 I=1,N12
      AK=A(I,NC)
      A(I,NC)=A(I,N12)
    7 A(I,N12)=AK
      N2=NC
C
      DO 8I=1,N2
      DO 8 J=1,N2
    8 S11(I,J)=A(I,J)
      N3=N2+1
      IF(N3-N12)61,61,60
   60 DO 62 I=1,N2
      DO 62 J=1,N2
   62 S11(I,J)=S11(I,J)*EI
      GO TO 23
   61 DO 9 I=N3,N12
      II=I-N2
      DO 9 J=1,N2
      S21(II,J)=A(I,J)
    9 S12(J,II)=S21(II,J)
      DO 10 I=N3,N12
      II=I-N2
      DO 10 J=N3,N12
      J1=J-N2
   10 S22(I1,J1)=A(I,J)
      IF(K1-1) 40,42,40

   42 IF(N-4) 40,44,40
   44 S22(1,1)=S22(1,1)+CROSAD
   40 K=N12-N2
C
C     INVERSE
C
   21 CALL SYMINV(S22,K)
C     MULTIPLY S12  S22
      DO 11 I=1,N2
      DO 11 J=1,K
      DO 11 L=1,K
   11 T(I,J)=T(I,J)+S12(I,L)*S22(L,J)
C     FINAL MATRIX
      DO 13 I=1,N2
      DO 13 J=1,N2
      DO 12 L=1,K
   12 TM(I,J)=TM(I,J)+T(I,L)*S21(L,J)
   13 S11(I,J)=(S11(I,J)-TM(I,J))*EI
   23 RETURN
      END

++++++++++++++++++++++++++++++++++
+     SUBROUTINE INDC01(AC)      +
++++++++++++++++++++++++++++++++++
      SUBROUTINE INDC01(AC)
      DIMENSION W(2,20),WE(2,20),WS(2,6),RM(2),SB(2,6),CBO(2),AC(53,53)
      DIMENSION SA(2,21,21),SB(2,8,8),T(2,20),S(2,6),EI(2),D(2,20)
      COMMON W,WE,WS,RM,CB,CBO,N,M,DT,NT,EI,D,SA,SB,T,S,SKO,DT2,DT3,DT6
      DO 60 J1=1,2
      IF(J1-1) 43,43,42
   43 L1=1
      L2=0
      GOTO 44
   42 L1=-1
      L2=NT+1
   44 DO 51 J=1,N
      I=L2+L1*J
      AC(I,I)=(W(J1,J)+WE(J1,J))*2.0/(DT*DT)+SA(J1,J,J)-T(J1,J)
      L3=L2+L1*(N+1)
      AC(I,L3)=SA(J1,J,N+1)
      IF(J-N)45,46,46
   45 AC(I,I)=AC(I,I)-T(J1,J+1)
      IP1=J+1
      DO 47 K=IP1,N
      L3=L2+L1*K
   47 AC(I,L3)=SA(J1,J,K)
      L3=I+L1
      AC(I,L3)=AC(I,L3)+T(J1,J+1)
   46 CONTINUE
   51 CONTINUE
      AC(I,I)=AC(I,I)-S(J1,1)+SB(J1,1,1)
      L3=I+L1
      AC(I,L3)=AC(I,L3)+SB(J1,1,2)
      DO 48 J=1,M
      L3=I+L1*(J+1)
   48 AC(I,L3)=SB(J1,1,J+2)
      L3=I+2*L1
      AC(I,L3)=AC(I,L3)+S(J1,1)
      I=I+L1
      AC(I,I)=RM(J1)*2.0/(DT*DT)+1.5*CBO(J1)/DT+SKO+SA(J1,N+1,N+1)+SB(J1,2,
     1,2,2)
      DO 49 J=1,M
      L3=I+L1*J
   49 AC(I,L3)=SB(J1,2,J+2)
      DO 50 J=1,M
      I=L2+L1*(N+1+J)
      AC(I,I)=AC(I,I)+WS(J1,J)*2.0/(DT*DT)-S(J1,J)+SB(J1,J+2,J+2)
      IF(J-M) 52,50,50
   52 JP1=M-J
      DO 54 K=1,JP1
      L3=I+L1*K
      JK2=J+K+2
   54 AC(I,L3)=SB(J1,J+2,JK2)
      L3=I+L1
      AC(I,L3)=AC(I,L3)+S(J1,J+1)
      AC(I,I)=AC(I,I)-S(J1,J+1)
   50 CONTINUE
   60 CONTINUE
      NT1=(NT-1)/2
      NT2=(NT+1)/2
      DO 61 I=1,NT1
      IP1=I+1
      IK=NT2-1+I
      DO 61 J=IP1,NT2
      JK=NT2-1+J
      AC(IK,JK)=AC(JK,IK)
   61 AC(J,I)=AC(I,J)
      I=L2+L1*(N+1)
      AC(I,I)=AC(I,I)-SKO
      RETURN
      END

++++++++++++++++++++++++++++++++++
+     SUBROUTINE INDC03(AC)      +
++++++++++++++++++++++++++++++++++
*     LABEL
*     FORTRAN
C
      SUBROUTINE INDC03(AC)
      COMMON W,WE,WS,RM,CB,CBO,N,M,DT,NT,EI,D,SA,SB,T,S,SKO,DT2,DT3,DT6
      COMMON NOMASS,NN,JM
      DIMENSION W(2,20),WE(2,20),WS(2,6),SA(2,21,21),SB(2,8,8),RM(2),
     1CB(2,6),CBO(2),T(2,20),S(2,6),AC(53,53),NOMASS(20),EI(2),D(2,20)
      JM=1
      DO 24 J=1,N
      IF(W(1,J))25,25,24
   25 NOMASS(JM)=J
      JM=JM+1
   24 CONTINUE
      JM=JM-1
      LUMPM=N-JM
      NN=2*LUMPM+2*M+1
      LUMP1=LUMPM+1
      CALL SUBMAT(SA,N,JM,NOMASS)
      DO 60 J1=1,2
      NM=1
      IF(J1-1)43,43,42

   43 L1=1
      L2=0
      GOTO 44
   42 L1=-1
      L2=NN+1
   44 DO 51 J=1,N
      IF(J-NOMASS(NM))30,31,30
   31 NM=NM+1
      GOTO 51
   30 JR=J+1-NM
      I=L2+L1*JR
      AC(I,I)=W(J1,J)+WE(J1,J)+DT6*SA(J1,JR,JR)
      L3=L2+L1*LUMP1
      AC(I,L3)=DT6*SA(J1,JR,LUMP1)
      IF(JR-LUMPM)45,46,46
   45 IP1=JR+1
      DO 47 K=IP1,LUMPM
      L3=L2+L1*K
   47 AC(I,L3)=DT6*SA(J1,JR,K)
   46 CONTINUE
   51 CONTINUE
      AC(I,I)=AC(I,I)+DT6*SB(J1,1,1)
      L3=I+L1
      AC(I,L3)=AC(I,L3)+DT6*SB(J1,1,2)
      DO 48 J=1,M
      L3=I+L1*(J+1)
   48 AC(I,L3)=DT6*SB(J1,1,J+2)
      I=I+L1
      AC(I,I)=RM(J1)+DT2*CBO(J1)+DT6*SKO+DT6*(SA(J1,LUMP1,LUMP1)+
     1SB(J1,2,2))
      DO 49 J=1,M
      L3=I+L1*J
   49 AC(I,L3)=DT6*SB(J1,2,J+2)
      DO 50 J=1,M
      I=L2+L1*(LUMP1+J)
      AC(I,I)=AC(I,I)+WS(J1,J)+DT6*SB(J1,J+2,J+2)
      IF(J-M)52,50,50
   52 JP1=M-J
      DO 54 K=1,JP1
      L3=I+L1*K
      JK2=J+K+2
   54 AC(I,L3)=DT6*(SB(J1,J+2,JK2))
   50 CONTINUE
   60 CONTINUE
      NT1=(NN-1)/2
      NT2=(NN+1)/2
      DO 61 I=1,NT1
      IP1=I+1
      IK=NT2-1+I
      DO 61 J=IP1,NT2
      JK=NT2-1+J
      AC(IK,JK)=AC(JK,IK)
   61 AC(J,I)=AC(I,J)
      I=L2+L1*LUMP1
      AC(I,I)=AC(I,I)-DT6*SKO
      RETURN
      END
```

```
++++++++++++++++++++++++++++++++
+     SUBROUTINE INDCO4(AC)    +
++++++++++++++++++++++++++++++++
*     LABEL
*     FORTRAN
C
      SUBROUTINE INDCO4(AC)
      DIMENSION W(2,20),WE(2,20),WS(2,6),SA(2,21,21),SB(2,8,8),RM(2),
     1CB(2,6),CBO(2),T(2,20),S(2,6),AC(53,53),EI(2),DT(2,20)
      COMMON W,WE,WS,RM,CB,CBO,N,M,DT,NT,EI,D,SA,SB,T,S,SKO,DT2,DT3,DT6
      DO 60 J1=1,2
      IF(J1-1) 43,43,42
   43 L1=1
      L2=0
      GOTO 44
   42 L1=-1
      L2=NT+1
   44 DO 51 J=1,N
      I=L2+L1*J
      AC(I,I)=W(J1,J)+WE(J1,J)+DT6*(SA(J1,J,J)-T(J1,J))
      L3=L2+L1*(N+1)
      AC(I,L3)= DT6*SA(J1,J,N+1)
      IF(J-N)45,46,46
   45 AC(I,I)=AC(I,I)-DT6*T(J1,J+1)
      IP1=J+1
      DO 47 K=IP1,N
      L3=L2+L1*K
   47 AC(I,L3)= DT6*SA(J1,J,K)
      L3=I+L1
      AC(I,L3)=AC(I,L3)+DT6*T(J1,J+1)
   46 CONTINUE
   51 CONTINUE
      AC(I,I)=AC(I,I)-DT6*(S(J1,1)-SB(J1,1,1))
      L3=I+L1
      AC(I,L3)=AC(I,L3)+DT6*SB(J1,1,2)
      DO 48 J=1,M
      L3=I+L1*(J+1)
   48 AC(I,L3)= DT6*SB(J1,1,J+2)
      L3=I+2*L1
      AC(I,L3)=AC(I,L3)+DT6*S(J1,1)
      I=I+L1
      AC(I,I)=RM(J1)+DT2*CBO(J1)+DT6*SKO+DT6*(SA(J1,N+1,N+1)+SB(J1,2,2))
      DO 49 J=1,M
      L3=I+L1*J
   49 AC(I,L3)= DT6*SB(J1,2,J+2)
      DO 50 J=1,M
      I=L2+L1*(N+1+J)
      AC(I,I)=AC(I,I)+WS(J1,J)-DT6*(S(J1,J)-SB(J1,J+2,J+2))
      IF(J-M) 52,50,50
   52 JP1=M-J
      DO 54 K=1,JP1
      L3=I+L1*K
      JK2=J+K+2
   54 AC(I,L3)= DT6*(SB(J1,J+2,JK2))
      L3=I+L1
      AC(I,L3)=AC(I,L3)+DT6*S(J1,J+1)
      AC(I,I)=AC(I,I)-DT6*S(J1,J+1)
   50 CONTINUE
   60 CONTINUE
      NT1=(NT-1)/2



      NT2=(NT+1)/2
      DO 61 I=1,NT1
      IP1=I+1
      IK=NT2-1+I
      DO 61 J=IP1,NT2
      JK=NT2-1+J
      AC(IK,JK)=AC(JK,IK)
   61 AC(J,I)=AC(I,J)
      I=L2+L1*(N+1)
      AC(I,I)=AC(I,I)-DT6*SKO
      RETURN
      END


++++++++++++++++++++++++++++++++++++++++++++++++
+     SUBROUTINE SUBMAT(SA,N,JM,NOMASS)        +
++++++++++++++++++++++++++++++++++++++++++++++++
*     LABEL
*     FORTRAN
C
      SUBROUTINE SUBMAT(SA,N,JM,NOMASS)
      DIMENSION SA(2,21,21),NOMASS(20),STEMP(21,21)
  100 FORMAT(1H0,49HABOVE TWO MATRICES ARE MODIFIED MATRICES IN WHICH/79
     1H ROWS AND COLUMNS OF POINTS WITH NO MASS ARE STORED IN THE LOWER
     2PART OF MATRIX)
      N1=N+1
      LUMPM=N+1-JM
      DO 11 I=1,2
      NM=1
      DO 6 J=1,N1
      IF(J-NOMASS(NM))3,2,3
    2 LT=LUMPM+NM
      DO 4 K=1,N1
    4 STEMP(LT,K)=SA(I,J,K)
      NM=NM+1
      GOTO 6
    3 LS=J+1-NM
      DO 5 K=1,N1
    5 STEMP(LS,K)=SA(I,J,K)
    6 CONTINUE
      NM=1
      DO 7 J=1,N1
      IF(J-NOMASS(NM))8,9,8
    9 LT=LUMPM+NM
      DO 10 K=1,N1
   10  SA(I,K,LT)=STEMP(K,J)
      NM=NM+1
      GOTO 7
    8 LS=J+1-NM
      DO 12 K=1,N1
   12 SA(I,K,LS)=STEMP(K,J)
    7 CONTINUE
   11 CONTINUE
      CALL PRNTTM(SA,2,N1,N1,2,21)
      PRINT 100
      DO 22 I=1,2
      DO 13 J=1,JM
      NR=LUMPM+J
      DO 13 K=1,JM
      NC=LUMPM+K
      STEMP(J,K)=SA(I,NR,NC)
   13 CONTINUE
      CALL SYMINV(STEMP,JM)
      DO 14 J=1,JM
      NR=LUMPM+J
      DO 14 K=1,JM
      NC=LUMPM+K
      SA(I,NR,NC)=STEMP(J,K)
   14 CONTINUE
      DO 15 J=1,N1
      DO 15 K=1,N1
   15 STEMP(J,K)=0.0
      DO 16 J=1,JM
      NR=LUMPM+J
      DO 16 K=1,LUMPM
      DO 16 L=1,JM
      NC=LUMPM+L
      STEMP(J,K)=STEMP(J,K)+SA(I,NR,NC)*SA(I,NC,K)
   16 CONTINUE
      DO 17 J=1,JM
      NR=LUMPM+J
      DO 17 K=1,LUMPM
      SA(I,NR,K)=STEMP(J,K)
      STEMP(J,K)=0.0
   17 CONTINUE
      DO 19 J=1,LUNPM
      DO 19 K=1,LUMPM
      PS=0.0
      DO 20 L=1,JM
      NC=LUMPM+L
   20 PS=PS+SA(I,J,NC)*SA(I,NC,K)
      SA(I,J,K)=SA(I,J,K)-PS
   19 CONTINUE
      DO 21 J=1,LUMPM
      DO 21 K=1,JM
      NC=LUMPM+K
   21 SA(I,J,NC)=SA(I,NC,J)
   22 CONTINUE
      RETURN
      END


++++++++++++++++++++++++++++++++++++
+     SUBROUTINE BIGINV(A,NMAX)    +
++++++++++++++++++++++++++++++++++++
*     LABEL
*     FORTRAN
C
      SUBROUTINE BIGINV(A,NMAX)
C
C
      DIMENSION A(53,53)
C
      DO 5 N=1,NMAX
    5 A(N,1)=A(1,N)
      IF DIVIDE CHECK  20,20
C
   20 DO 160 N=1,NMAX
   30 PIVOT=A(N,N)



   40 A(N,N)=-1.0
   50 DO 60 J=1,NMAX
   60 A(N,J)=A(N,J)/PIVOT
C
   70 IF DIVIDE CHECK  260,80
   80 DO 145 I=1,NMAX
   90 IF (N-I) 95,145,95
   95 IF (A(I,N)) 100,145,100
  100 DO 140 J=1,NMAX
  110 IF (N-J) 120,140,120
  120 A(I,J)=A(I,J)-A(I,N)*A(N,J)
  130 A(J,I)=A(I,J)
  140 CONTINUE
  145 CONTINUE
C
  150 DO 160 I=1,NMAX
  160 A(I,N)=A(N,I)
C
  163 DO 165 I=1,NMAX
  164 DO 165 J=1,NMAX
  165 A(I,J)=-A(I,J)
C
  250 RETURN
C
  260 PRINT 280 ,N
  270 CALL EXIT
  280 FORMAT (25HOZERO DIAGONAL ELEMENT N=1I3)
C
      END


++++++++++++++++++++++++++++++++++++
+     SUBROUTINE SYMINV(A,NMAX)    +
++++++++++++++++++++++++++++++++++++
*     LABEL
*     FORTRAN
C
      SUBROUTINE SYMINV(A,NMAX)
C
C
      DIMENSION A(21,21)
C
      DO 5 N=1,NMAX
    5 A(N,1)=A(1,N)
      IF DIVIDE CHECK  20,20
C
   20 DO 160 N=1,NMAX
   30 PIVOT=A(N,N)
   40 A(N,N)=-1.0
   50 DO 60 J=1,NMAX
   60 A(N,J)=A(N,J)/PIVOT
C
   70 IF DIVIDE CHECK  260,80
   80 DO 145 I=1,NMAX
   90 IF (N-I) 95,145,95
   95 IF (A(I,N)) 100,145,100
  100 DO 140 J=1,NMAX
  110 IF (N-J) 120,140,120
  120 A(I,J)=A(I,J)-A(I,N)*A(N,J)
```

```
  130 A(J,I)=A(I,J)
  140 CONTINUE
  145 CONTINUE
C
  150 DO 160 I=1,NMAX
  160 A(I,N)=A(N,I)
C
  163 DO 165 I=1,NMAX
  164 DO 165 J=1,NMAX
  165 A(I,J)=-A(I,J)
C
  250 RETURN
C
  260 PRINT 280 ,N
  270 CALL EXIT
  280 FORMAT (25H0ZERO DIAGONAL ELEMENT N=113)
C
      END
```

```
++++++++++++++++++++++++++++++++++++++++++++++++++++++++
+     SUBROUTINE PRNTTM(A,NI,NR,NC,MAXI,MAXR)          +
++++++++++++++++++++++++++++++++++++++++++++++++++++++++
*     LABEL
*     FORTRAN
C
      SUBROUTINE PRNTTM(A,NI,NR,NC,MAXI,MAXR)
C     SUBROUTINE TO PRINT THREE DIMENSIONAL MATRIX
      DIMENSION A(1),NHED(8)
    2 FORMAT(1H1,6HMATRIX,I4)
    3 FORMAT(1H0,7X,I8,7I14)
    4 FORMAT(I4,4X,8E14.7)
      MXR=MAXR*MAXI
      DO 60 I=1,NI
      PRINT 2,I
      DO 50 J=1,NC,8
      II=NC-J+1
      IF(II-8)20,20,10
   10 II=8
   20 DO 30 K=1,II
   30 NHED(K)=J+K-1
      PRINT 3,(NHED(K),K=1,II)
      DO 50 K=1,NR
      KL=I+(K-1)*MAXI+(J-1)*MXR
      KH=KL+(II-1)*MXR
   50 PRINT 4,(K,(A(L),L=KL,KH,MXR))
   60 CONTINUE
      RETURN
      END
```

```
**************************
*     CHAIN (2,A4)       *
**************************


++++++++++++++++++++++++++++++++
+      INTERACTION PROGRAM     +
++++++++++++++++++++++++++++++++
*     CHAIN (2,A4)
*     LABEL
9     FORTRAN
CINTAC2
C     INTERACTION PROGRAM
      DIMENSION W(2,20),WE(2,20),WS(2,6),SA(2,21,21),SB(2,8,8),RM(2),
     1CB(2,6),CBO(2),T(2,20),S(2,6),AC(53,53)
      DIMENSION CO(2,20),C1(2,20),RC1(2,20),RC2(2,20),DO(2,20),D1(2,20),
     1RD1(2,20),RD2(2,20),TO(2,20),T1(2,20),RT1(2,20),RT2(2,20),CC(2,20)
     2,CD(2,20),SK(2,20),U2DC(2,20), C2(2,20),K1(20),O(2),OD(2),O2D(2),
     3U(2,20),UD(2,20),U2D(2,20),US(2,20),UDS(2,20),U2DS(2,20),UB(2,6),
     4UDB(2,6),U2DB(2,6),USM(2,20),UCM(2,20),UDM(2,20),USF(2,20),
     5UCF(2,20),UDF(2,20), AL(53),D(2,20),EI(2),UC(2,20),UDC(2,20)
      DIMENSION F2(2,20),F3(2,20),G2(2,20),G3(2,20),E2(2,20),E3(2,20),
     1H2(2,6),H3(2,6),O2(2),O3(2),USPU(2,20),USPB(2,20),USPC(2,20),
     2NOMASS(20),URS(4000),FORCE(2,20),BMMAX(2),BM(2,20),X(2,20),
     3UR(20),VDR(20),U2DR(20),COF(2,20),P(53)
      DIMENSION OM1(2),OM2(2),UM1(2,20),UM2(2,20),UBM1(2,6),UBM2(2,6)
      COMMON W,WE,WS,RM,CB,CBO,N,M,DT,NT,EI,D,SA,SB,T,S,SKO,DT2,DT3,DT6
      COMMON NOMASS,NN,JM
      COMMON CO,C1,RC1,RC2,DO,D1,RD1,RD2,TO,T1,RT1,RT2,CC,CD,SK,C2,K1,
     10,OD,O2D,U,UD,U2D,US,UDS,U2DS,UB,UDB,U2DB,TC,USM,UCM,UDM,USF,UCF,
     2UDF,AC,AL,SCALE,METHOD,UC,UDC,U2DC,OM1,OM2,UM1,UM2,UBM1,UBM2
      COMMON F2,F3,G2,G3,E2,E3,H2,H3,O2,O3,COF,USPU,USPB,USPC,TI,M1,M2,
     1M3,U2DG,UDG,UG,UR,U2DR,UDR,X,K6,N1,NK,URS,FORCE,UCHK6,BMMAX,ISTOP,
     2BM
    5 FORMAT(37H EXECUTION TERMINATED DUE TO OVERFLOW)
   30 FORMAT(24HOEXECUTION TERMINATED T=,F8.4/22HOLAST VALUE  ON TAPE 5,
     1F15.8/22HOLAST RECORD ON TAPE 6,F15.8)
   31 FORMAT(6F12.3)
   32 FORMAT(31HOTIME AT COMPLETION OF CHAIN 2=,F15.5)
      REWIND 6
      N1=N+1
      TI=0.0
      M1=0
      M2=0
      M3=0
      K6=0
      READ 31,TSTOP
      ISTOP=TSTOP/DT
      DO 1 I=1,2
      DO 1 J=1,N
      USPC(I,J)=0.0
      USPU(I,J)=USM(I,J)
      USPB(I,J)=-USM(I,J)
    1 CONTINUE
      NK=3*(NT+1+2*N)+2*N
   10 M1=M1+1
      M2=M2+1
      M3=M3+1
      K6=K6+1
      F=RC2(J,I)+(1.0-RC2(J,I))*(1.0-TOT)**RC1(J,I)
      G=RD2(J,I)+(1.0-RD2(J,I))*(1.0-TOT)**RD1(J,I)
      H=RT2(J,I)+(1.0-RT2(J,I))*(1.0-TOT)**RT1(J,I)
   17 F1=ABSF(UDC(J,I))
   18 G1=ABSF(UDS(J,I))
      H1=ABSF(US(J,I))
      IF(F1-UCM(J,I))2,2,3
    3 CC(J,I)=F*UCF(J,I)/F1
      GOTO 4
    2 CC(J,I)=F*(CO(J,I)+C1(J,I)*F1*C2(J,I)*F1*F1)
    4 IF(G1-UDM(J,I))5,5,6
    5 CD(J,I)=G*(DO(J,I)+D1(J,I)*G1)
      GOTO 7
    6 CD(J,I)=G*UDF(J,I)/G1
    7 IF(US(J,I)-USPU(J,I))8,9,9
    8 IF(US(J,I)-USPB(J,I))11,11,10
   10 SK(J,I)=TO(J,I)*H
      COF(J,I)=SK(J,I)*USPC(J,I)
      GOTO 15
    9 USPU(J,I)=US(J,I)
      USPB(J,I)=US(J,I)-2.0*USM(J,I)
      USPC(J,I)=USPU(J,I)-(USF(J,I)+(USPU(J,I)-USM(J,I))*T1(J,I))/TO(J,I
     1)
      IF(UDS(J,I))10,10,12
   12 SK(J,I)=T1(J,I)*H
      COF(J,I)=SK(J,I)*USM(J,I)-USF(J,I)*H
      GOTO 15
   11 USPB(J,I)=US(J,I)
      USPU(J,I)=US(J,I)+2.0*USM(J,I)
      USPC(J,I)=USPU(J,I)-(USF(J,I)+(USPU(J,I)-USM(J,I))*T1(J,I))/TO(J,I
     1)
      IF(UDS(J,I))13,10,10
   13 SK(J,I)=T1(J,I)*H
      COF(J,I)=-SK(J,I)*USM(J,I)+USF(J,I)*H
   15 E2(J,I)=UDC(J,I)+DT2*U2DC(J,I)
      E3(J,I)=UC(J,I)+DT*UDC(J,I)+DT3*U2DC(J,I)
      G2(J,I)=UDS(J,I)+DT2*U2DS(J,I)
      G3(J,I)=US(J,I)+DT*UDS(J,I)+DT3*U2DS(J,I)
      FORCE(J,I)=-COF(J,I)+CD(J,I)*(G2(J,I)+DT2*U2DS(J,I))
     1+SK(J,I)*(G3(J,I)+DT6*U2DS(J,I))
      GOTO(101,102,102,102),METHOD
  101 CONTINUE
      F2(J,I)=(4.0*U(J,I)-UM1(J,I))
      F3(J,I)=(5.0*U(J,I)-4.0*UM1(J,I) +UM2(J,I))
      UM2(J,I)=UM1(J,I)
      UM1(J,I)=U(J,I)
      GOTO 19
  102 CONTINUE
      F2(J,I)=UD(J,I)+DT2*U2D(J,I)
      F3(J,I)=U(J,I)+DT*UD(J,I)+DT3*U2D(J,I)
   19 CONTINUE
      GOTO (104,105,105,105),METHOD
  104 DO 120 I=1,M
      H2(J,I)=(4.0*UB(J,I)-UBM1(J,I))
      H3(J,I)=(5.0*UB(J,I)-4.0*UBM1(J,I)+UBM2(J,I))
      UBM2(J,I)=UBM1(J,I)
  120 UBM1(J,I)=UB(J,I)
      O2(J)=(4.0*O(J)-OM1(J))
      O3(J)=(5.0*O(J)-4.0*OM1(J)+OM2(J))
      TI=TI+DT
      CALL REDTAP(M1,M2,N,TC,DT,UG,UDG,U2DG,UR,UDR,U2DR,UCHK5)
      CALL STIFCO
      GOTO (101,102,103,104),METHOD
  101 CALL VARCO1(P)
      GOTO 25
  102 CALL VARCO2(P)
      GOTO 25
  103 CALL VARCO3(P)
      GOTO 25
  104 CALL VARCO4(P)
      CALL SOLEQU(AC,NT,AL)
   25 CALL RESPON
      CALL WRITAP
      IF ACCUMULATOR OVERFLOW 15,16
   16 IF(M1-ISTOP)10,21,21
   21 PRINT 30,TI,UCHK5,UCHK6
      CALL TIME(CLOCK)
      PRINT 32,CLOCK
      CALL SAVEXT
      READ 31,TSTOP
      ISTOP=TSTOP/DT
      GOTO 10
   15 PRINT 5
      CALL EXIT
      END


++++++++++++++++++++++++++++
+     SUBROUTINE STIFCO      +
++++++++++++++++++++++++++++
*     LABEL
*     FORTRAN
C
      SUBROUTINE STIFCO
C     STIFFNESS COEFFICIENTS CC,CD,K
      DIMENSION W(2,20),WE(2,20),WS(2,6),SA(2,21,21),SB(2,8,8),RM(2),
     1CB(2,6),CBO(2),T(2,20),S(2,6),AC(53,53)
      DIMENSION CO(2,20),C1(2,20),RC1(2,20),RC2(2,20),DO(2,20),D1(2,20),
     1RD1(2,20),RD2(2,20),TO(2,20),T1(2,20),RT1(2,20),RT2(2,20),CC(2,20)
     2,CD(2,20),SK(2,20),U2DC(2,20), C2(2,20),K1(20),O(2),OD(2),O2D(2),
     3U(2,20),UD(2,20),U2D(2,20),US(2,20),UDS(2,20),U2DS(2,20),UB(2,6),
     4UDB(2,6),U2DB(2,6),USM(2,20),UCM(2,20),UDM(2,20),USF(2,20),
     5UCF(2,20),UDF(2,20), AL(53),D(2,20),EI(2),UC(2,20),UDC(2,20)
      DIMENSION F2(2,20),F3(2,20),G2(2,20),G3(2,20),E2(2,20),E3(2,20),
     1H2(2,6),H3(2,6),O2(2),O3(2),USPU(2,20),USPB(2,20),USPC(2,20),
     2NOMASS(20),URS(4000),FORCE(2,20),BMMAX(2),BM(2,20),X(2,20),
     3UR(20),VDR(20),U2DR(20),COF(2,20)
      DIMENSION OM1(2),OM2(2),UM1(2,20),UM2(2,20),UBM1(2,6),UBM2(2,6)
      COMMON W,WE,WS,RM,CB,CBO,N,M,DT,NT,EI,D,SA,SB,T,S,SKO,DT2,DT3,DT6
      COMMON NOMASS,NN,JM
      COMMON CO,C1,RC1,RC2,DO,D1,RD1,RD2,TO,T1,RT1,RT2,CC,CD,SK,C2,K1,
     10,OD,O2D,U,UD,U2D,US,UDS,U2DS,UB,UDB,U2DB,TC,USM,UCM,UDM,USF,UCF,
     2UDF,AC,AL,SCALE,METHOD,UC,UDC,U2DC,OM1,OM2,UM1,UM2,UBM1,UBM2
      COMMON F2,F3,G2,G3,E2,E3,H2,H3,O2,O3,COF,USPU,USPB,USPC,TI,M1,M2,
     1M3,U2DG,UDG,UG,UR,U2DR,UDR,X,K6,N1,NK,URS,FORCE,UCHK6,BMMAX,ISTOP,
     2BM
      TOT=TI/TC
   22 DO 40 J=1,2
      DO 19 I=1,N
      OM2(J)=OM1(J)
      OM1(J)=O(J)
      GOTO 40
  105 DO 20 I=1,M
      H2(J,I)=UDB(J,I)+DT2*U2DB(J,I)
   20 H3(J,I)=UB(J,I)+DT*UDB(J,I)+DT3*U2DB(J,I)
      O3(J)=O(J)+DT*OD(J)+DT3*O2D(J)
      O2(J)=OD(J)+DT2*O2D(J)
   40 CONTINUE
  103 RETURN
      END


++++++++++++++++++++++++++++++
+     SUBROUTINE VARCO1(P)     +
++++++++++++++++++++++++++++++
*     LABEL
*     FORTRAN
C
      SUBROUTINE VARCO1(P)
      DIMENSION W(2,20),WE(2,20),WS(2,6),SA(2,21,21),SB(2,8,8),RM(2),
     1CB(2,6),CBO(2),T(2,20),S(2,6),AC(53,53)
      DIMENSION CO(2,20),C1(2,20),RC1(2,20),RC2(2,20),DO(2,20),D1(2,20),
     1RD1(2,20),RD2(2,20),TO(2,20),T1(2,20),RT1(2,20),RT2(2,20),CC(2,20)
     2,CD(2,20),SK(2,20),U2DC(2,20), C2(2,20),K1(20),O(2),OD(2),O2D(2),
     3U(2,20),UD(2,20),U2D(2,20),US(2,20),UDS(2,20),U2DS(2,20),UB(2,6),
     4UDB(2,6),U2DB(2,6),USM(2,20),UCM(2,20),UDM(2,20),USF(2,20),
     5UCF(2,20),UDF(2,20), AL(53),D(2,20),EI(2),UC(2,20),UDC(2,20)
      DIMENSION F2(2,20),F3(2,20),G2(2,20),G3(2,20),E2(2,20),E3(2,20),
     1H2(2,6),H3(2,6),O2(2),O3(2),USPU(2,20),USPB(2,20),USPC(2,20),
     2NOMASS(20),URS(4000),FORCE(2,20),BMMAX(2),BM(2,20),X(2,20),
     3UR(20),VDR(20),U2DR(20),COF(2,20),P(53)
      DIMENSION OM1(2),OM2(2),UM1(2,20),UM2(2,20),UBM1(2,6),UBM2(2,6)
      COMMON W,WE,WS,RM,CB,CBO,N,M,DT,NT,EI,D,SA,SB,T,S,SKO,DT2,DT3,DT6
      COMMON NOMASS,NN,JM
      COMMON CO,C1,RC1,RC2,DO,D1,RD1,RD2,TO,T1,RT1,RT2,CC,CD,SK,C2,K1,
     10,OD,O2D,U,UD,U2D,US,UDS,U2DS,UB,UDB,U2DB,TC,USM,UCM,UDM,USF,UCF,
     2UDF,AC,AL,SCALE,METHOD,UC,UDC,U2DC,OM1,OM2,UM1,UM2,UBM1,UBM2
      COMMON F2,F3,G2,G3,E2,E3,H2,H3,O2,O3,COF,USPU,USPB,USPC,TI,M1,M2,
     1M3,U2DG,UDG,UG,UR,U2DR,UDR,X,K6,N1,NK,URS,FORCE,UCHK6,BMMAX,ISTOP,
     2BM
      DO 20 I=1,NT
   20 AL(I)=0.0
      L1=1
      L2=0
      DO 14 J=1,2
      IF(J-2)1,2,2
    2 L1=-1
      L2=NT+1
    1 M5=L2+L1*N1
      DO 7 K=1,N
      I=L2+L1*K
      AL(I)=-W(J,K)*U2DG+WE(J,K)*U2DR(K)-FORCE(J,K)+
     1(W(J,K)+WE(J,K))*F3(J,K)/(DT*DT)
    7 CONTINUE
      AL(M5)=RM(J)*O3(J)/(DT*DT)+CBO(J)*O2(J)/(2.0*DT)
      DO 12 K=1,M
      I=L2+L1*(N1+K)
      AL(I)=AL(I)-WS(J,K)*U2DG-CB(J,K)*(UDB(J,K)-UD(J,N1)+
     1WS(J,K)*H3(J,K))/(DT*DT)
```

```
   12 CONTINUE
   14 CONTINUE
      DO 15 I=1,NT
      P(I)=0.0
      DO 15 J=1,NT
   15 P(I)=P(I)+AC(I,J)*AL(J)
      DO 16 I=1,NT
   16 AL(I)=P(I)*SCALE
      RETURN
      END


+++++++++++++++++++++++++++++++++
+     SUBROUTINE VARCO2 (P)     +
+++++++++++++++++++++++++++++++++
*     LABEL
*     FORTRAN
C
      SUBROUTINE VARCO2 (P)
      DIMENSION W(2,20),WE(2,20),WS(2,6),SA(2,21,21),SB(2,8,8),RM(2),
     1CB(2,6),CBO(2),T(2,20),S(2,6),AC(53,53)
      DIMENSION CO(2,20),C1(2,20),RC1(2,20),RC2(2,20),DO(2,20),D1(2,20),
     1RD1(2,20),RD2(2,20),TO(2,20),T1(2,20),RT1(2,20),RT2(2,20),CC(2,20)
     2,CD(2,20),SK(2,20),U2DC(2,20), C2(2,20),K1(20),O1(2),OD(2),O2D(2),
     3U(2,20),UD(2,20),U2D(2,20),US(2,20),UDS(2,20),U2DS(2,20),UB(2,6),
     4UDB(2,6),U2DB(2,6),USM(2,20),UCM(2,20),UDM(2,20),USF(2,20),
     5UCF(2,20),UDF(2,20), AL(53),D(2,20),EI(2),UC(2,20),UDC(2,20)
      DIMENSION F2(2,20),F3(2,20),G2(2,20),G3(2,20),E2I2,20),E3(2,20),
     1H2(2,6),H3(2,6),O2(2),O3(2),USPU(2,20),USPB(2,20),USPC(2,20),
     2NOMASS(20),URS(4000),FORCE(2,20),BMMAX(2),BM(2,20),X(2,20),
     3UR(20),UDR(20),U2DR(20),COF(2,20),P(53)
      DIMENSION OM1(2),OM2(2),UM1(2,20),UM2(2,20),UBM1(2,6),UBM2(2,6)
      COMMON W,WE,WS,RM,CB,CBO,N,M,DT,NT,EI,D,SA,SB,T,S,SKO,DT2,DT3,DT6
      COMMON NOMASS,NN,JM
      COMMON CO,C1,RC1,RC2,DO,D1,RD1,RD2,TO,T1,RT1,RT2,CC,CD,SK,C2,K1,
     1O,OD,O2D,U,UD,U2D,US,UDS,U2DS,UB,UDB,U2DB,TC,USM,UCM,UDM,USF,UCF,
     2UDF,AC,AL,SCALE,METHOD,UC,UDC,U2DC,OM1,OM2,UM1,UM2,UBM1,UBM2
      COMMON F2,F3,G2,G3,E2,E3,H2,H3,O2,O3,COF,USPU,USPB,USPC,TI,M1,M2,
     1M3,U2DG,UDG,UG,UR,U2DR,UDR,X,K6,N1,NK,URS,FORCE,UCHK6,BMMAX,ISTOP,
     2BM
      DO 20 I=1,NT
      AL(I)=0.0
   20 CONTINUE
      L1=1
      L2=0
      DO 14 J=1,2
      IF(J-2)1,2,2
    2 L1=-1
      L2=NT+1
    1 M5=L2+L1*N1
      DO 7 K=1,N
      AL(M5)=AL(M5)-SA(J,N1,K)*F3(J,K)
      PT=-FORCE(J,K)-W(J,K)*U2DG*WE(J,K)*U2DR(K)
     1+T(J,K)*F3(J,K)-SA(J,K,N1)*O3(J)
      IF(K-1)32,32,33
   33 PT=PT-T(J,K)*F3(J,K-1)
   32 IF(K-N)34,35,35
   34 PT=PT+T(J,K+1)*(F3(J,K)-F3(J,K+1))
   35 DO 38 I=1,N
```

```
   38 PT=PT-SA(J,K,I)*F3(J,I)
      I=L2+L1*K
      AL(I)=PT
    7 CONTINUE
      AL(I)=AL(I)-SB(J,1,1)*F3(J,N)-SB(J,1,2)*O3(J)
     1+S(J,1)*(F3(J,N)-H3(J,1))
      AL(M5)=AL(M5)-SA(J,N1,N1)*O3(J)-CBO(J)*O2(J)
     1-SB(J,2,1)*F3(J,N)-SB(J,2,2)*O3(J)
      IF(J-1)100,100,101
  100 AL(M5)=AL(M5)-SKO*O3(J)
  101 CONTINUE
      M4=1
      DO 12 K=1,M
      AL(M5)=AL(M5)-SB(J,2,K+2)*H3(J,K)
      AL(M4)=AL(M4)-SB(J,1,K+2)*H3(J,K)
      I=L1*(N1+K)+L2
      PT = -U2DG*WS(J,K)-CB(J,K)*(UDB(J,K)-UD(J,N))
     1         - SB(J,K+2,1)*F3(J,N)-SB(J,K+2,2)*O3(J)+S(J,K)*H3(J,K)
      DO 9 L=1,M
    9 PT=PT-SB(J,K+2,L+2)*H3(J,L)
      IF(K-1)10,10,11
   11 PT=PT-S(J,K)*H3(J,K-1)
      GOTO 50
   10 PT=PT-S(J,K)*F3(J,N)
   50 IF(K-M)13,12,12
   13 PT=PT-S(J,K+1)*H3(J,K+1)
     1+S(J,K+1)* H3(J,K)
   12 AL(I)=AL(I)+PT
   14 CONTINUE
      DO 15 I=1,NN
      P(I)=0.0
      DO 15 J=1,NN
   15 P(I)=P(I)+AC(I,J)*AL(J)
      DO 16 I=1,NN
   16 AL(I)=P(I)*SCALE
      RETURN
      END


+++++++++++++++++++++++++++++++++
+     SUBROUTINE VARCO3(P)      +
+++++++++++++++++++++++++++++++++
*     LABEL
*     FORTRAN
C
      SUBROUTINE VARCO3(P)
      DIMENSION W(2,20),WE(2,20),WS(2,6),SA(2,21,21),SB(2,8,8),RM(2),
     1CB(2,6),CBO(2),T(2,20),S(2,6),AC(53,53)
      DIMENSION CO(2,20),C1(2,20),RC1(2,20),RC2(2,20),DO(2,20),D1(2,20),
     1RD1(2,20),RD2(2,20),TO(2,20),T1(2,20),RT1(2,20),RT2(2,20),CC(2,20)
     2,CD(2,20),SK(2,20),U2DC(2,20), C2(2,20),K1(20),O1(2),OD(2),O2D(2),
     3U(2,20),UD(2,20),U2D(2,20),US(2,20),UDS(2,20),U2DS(2,20),UB(2,6),
     4UDB(2,6),U2DB(2,6),USM(2,20),UCM(2,20),UDM(2,20),USF(2,20),
     5UCF(2,20),UDF(2,20), AL(53),D(2,20),EI(2),UC(2,20),UDC(2,20)
      DIMENSION F2(2,20),F3(2,20),G2(2,20),G3(2,20),E2(2,20),E3(2,20),
     1H2(2,6),H3(2,6),O2(2),O3(2),USPU(2,20),USPB(2,20),USPC(2,20),
     2NOMASS(20),URS(4000),FORCE(2,20),BMMAX(2),BM(2,20),X(2,20),
     3UR(20),UDR(20),U2DR(20),COF(2,20),P(53)
      DIMENSION OM1(2),OM2(2),UM1(2,20),UM2(2,20),UBM1(2,6),UBM2(2,6)
      COMMON W,WE,WS,RM,CB,CBO,N,M,DT,NT,EI,D,SA,SB,T,S,SKO,DT2,DT3,DT6
      COMMON NOMASS,NN,JM
      COMMON CO,C1,RC1,RC2,DO,D1,RD1,RD2,TO,T1,RT1,RT2,CC,CD,SK,C2,K1,
     1O,OD,O2D,U,UD,U2D,US,UDS,U2DS,UB,UDB,U2DB,TC,USM,UCM,UDM,USF,UCF,
     2UDF,AC,AL,SCALE,METHOD,UC,UDC,U2DC,OM1,OM2,UM1,UM2,UBM1,UBM2
      COMMON F2,F3,G2,G3,E2,E3,H2,H3,O2,O3,COF,USPU,USPB,USPC,TI,M1,M2,
     1M3,U2DG,UDG,UG,UR,U2DR,UDR,X,K6,N1,NK,URS,FORCE,UCHK6,BMMAX,ISTOP,
     2BM
      LUMPM=N-JM
      LUMP1=LUMPM+1
      DO 20 I=1,NN
   20 AL(I)=0.0
      L1=1
      L2=0
      DO 14 J=1,2
      NM=1
      IF(J-2)1,2,2
    2 L1=-1
      L2=NN+1
    1 DO 31 K=1,N
      PT=-FORCE(J,K)-W(J,K)*U2DG*WE(J,K)*U2DR(K)
     1+T(J,K)*(F3(J,K)+DT6*U2D(J,K))
      IF(K-1)32,32,33
   33 PT=PT-T(J,K)*(F3(J,K-1)+DT6*U2D(J,K-1))
   32 IF(K-N)34,35,35
   34 PT=PT+T(J,K+1)*(F3(J,K)+DT6*U2D(J,K)-F3(J,K+1)-DT6*U2D(J,K+1))
   35 IF(K-NOMASS(NM))36,37,36
   37 IN=LUMPM+NM
      X(J,IN)=PT
      NM=NM+1
      GOTO 31
   36 IN=K+1-NM
      X(J,IN)=PT-SA(J,IN,LUMP1)*O3(J)
      KM=1
      DO 38 I=1,N
      IF(I-NOMASS(KM))39,40,39
   39 ID=I+1-KM
      X(J,IN)=X(J,IN)-SA(J,IN,ID)*F3(J,I)
      GOTO 38
   40 KM=KM+1
   38 CONTINUE
   31 CONTINUE
      M5=L2+L1*LUMP1
      NM=1
      DO 7 K=1,N
      IF(K-NOMASS(NM))41,42,41
   42 ID=LUMPM+NM
      AL(M5)=AL(M5)-SA(J,LUMP1,ID+1)*X(J,ID)
      NM=NM+1
      GOTO 7
   41 ID=K+1-NM
      I=L2+L1*ID
      AL(I)=X(J,ID)
      KM=1
      DO 43 L=1,N
      IF(L-NOMASS (KM))43,45,43
   45 IN=LUMP1+KM
      AL(I)=AL(I)-SA(J,ID,IN)*X(J,IN-1)
      KM=KM+1
   43 CONTINUE
```

```
    7 CONTINUE
      AL(I)=AL(I)-SB(J,1,1)*F3(J,N)-SB(J,1,2)*O3(J)
     1+S(J,1)*(F3(J,N)+DT6*U2D(J,N)-H3(J,1)-DT6*U2DB(J,1))
      AL(M5)=AL(M5)-SA(J,LUMP1,LUMP1)*O3(J)-CBO(J)*O2(J)-SKO*O3(J)
     1-SB(J,2,1)*F3(J,N)-SB(J,2,2)*O3(J)
      M4=I
      DO 12 K=1,M
      AL(M5)=AL(M5)-SB(J,2,K+2)*H3(J,K)
      AL(M4)=AL(M4)-SB(J,1,K+2)*H3(J,K)
      I=L1*(LUMP1+K)+L2
      PT=      -U2DG*WS(J,K)-CB(J,K)*(UDB(J,K)-UD(J,N))-SB(J,K+2,1)*
     1 F3(J,N)-SB(J,K+2,2)*O3(J)+S(J,K)*(H3(J,K)+DT6*U2DB(J,K))
      DO 9 L=1,M
    9 PT=PT-SB(J,K+2,L+2)*H3(J,L)
      IF(K-1)10,10,11
   11 PT=PT      -S(J,K)*(H3(J,K-1)+DT6*U2DB(J,K-1))
      GOTO 50
   10 PT=PT      -S(J,K)*(F3(J,N)+DT6*U2D(J,N))
   50 IF(K-M)13,12,12
   13 PT=PT      -S(J,K+1)*(H3(J,K+1)+DT6*U2DB(J,K+1))
     1+S(J,K+1)*(H3(J,K)+DT6*U2DB(J,K))
   12 AL(I)=AL(I)+PT
   14 CONTINUE
      I=L2+L1*LUMP1
      AL(I)=AL(I)+SKO*O3(J)
      DO 15 I=1,NN
      P(I)=0.0
      DO 15 J=1,NN
   15 P(I)=P(I)+AC(I,J)*AL(J)
      DO 16 I=1,NN
   16 AL(I)=P(I)*SCALE
      RETURN
      END


+++++++++++++++++++++++++++++++++
+     SUBROUTINE VARCO4(P)      +
+++++++++++++++++++++++++++++++++
*     LABEL
*     FORTRAN
C
      SUBROUTINE VARCO4(P)
C     COMPLETE STIFFNESS MATRIX A AND DISPLACEMENT VECTOR AL
      DIMENSION W(2,20),WE(2,20),WS(2,6),SA(2,21,21),SB(2,8,8),RM(2),
     1CB(2,6),CBO(2),T(2,20),S(2,6),AC(53,53)
      DIMENSION CO(2,20),C1(2,20),RC1(2,20),RC2(2,20),DO(2,20),D1(2,20),
     1RD1(2,20),RD2(2,20),TO(2,20),T1(2,20),RT1(2,20),RT2(2,20),CC(2,20)
     2,CD(2,20),SK(2,20),U2DC(2,20), C2(2,20),K1(20),O1(2),OD(2),O2D(2),
     3U(2,20),UD(2,20),U2D(2,20),US(2,20),UDS(2,20),U2DS(2,20),UB(2,6),
     4UDB(2,6),U2DB(2,6),USM(2,20),UCM(2,20),UDM(2,20),USF(2,20),
     5UCF(2,20),UDF(2,20), AL(53),D(2,20),EI(2),UC(2,20),UDC(2,20)
      DIMENSION F2(2,20),F3(2,20),G2(2,20),G3(2,20),E2(2,20),E3(2,20),
     1H2(2,6),H3(2,6),O2(2),O3(2),USPU(2,20),USPB(2,20),USPC(2,20),
     2NOMASS(20),URS(4000),FORCE(2,20),BMMAX(2),BM(2,20),X(2,20),
     3UR(20),UDR(20),U2DR(20),COF(2,20),P(53),A(53,53)
      DIMENSION OM1(2),OM2(2),UM1(2,20),UM2(2,20),UBM1(2,6),UBM2(2,6)
      COMMON W,WE,WS,RM,CB,CBO,N,M,DT,NT,EI,D,SA,SB,T,S,SKO,DT2,DT3,DT6
      COMMON NOMASS,NN,JM
      COMMON CO,C1,RC1,RC2,DO,D1,RD1,RD2,TO,T1,RT1,RT2,CC,CD,SK,C2,K1,
     1O,OD,O2D,U,UD,U2D,US,UDS,U2DS,UB,UDB,U2DB,TC,USM,UCM,UDM,USF,UCF,
```

```
     2UDF,AC,AL,SCALE,METHOD,UC,UDC,U2DC,OM1,OM2,UM1,UM2,UBM1,UBM2
      COMMON F2,F3,G2,G3,E2,E3,H2,H3,O2,O3,COF,USPU,USPB,USPC,TI,M1,M2,
     1M3,U2DG,UDG,UG,UR,U2DR,UDR,X,K6,N1,NK,URS,FORCE,UCHK6,BMMAX,ISTOP,
     2BM
        IF(M1-1)65,65,66
    65  DO 20 I=1,NT
        DO 20 J=1,NT
    20  A(I,J)=AC(I,J)
    66  DO 67 I=1,NT
        AL(I)=0.0
        DO 67 J=1,NT
    67  AC(I,J)=0.0
        L1=1
        L2=0
        DO 14 J=1,2
        IF(J-2)1,2,2
     2  L1=-1
        L2=NT+1
     1  M5=L2+L1*N1
        DO 7 K=1,N
        I=L2+L1*K
        AL(M5)=AL(M5)-SA(J,N1 ,K)*F3(J,K)
        X(J,K)=(CD(J,K)+DT*SK(J,K)/3.0)/(CC(J,K)+CD(J,K)+DT*SK(J,K)/3.0)
        AC(I,I)=CC(J,K)*DT2*X(J,K)
        PT=U2DR(K)*WE(J,K)-U2DG*W(J,K)+T(J,K)*F3(J,K)-SA(J,K,N1)*O3(J)
     1+CC(J,K)*(COF(J,K)+SK(J,K)*(UR(K)-F3(J,K)+E3(J,K)-E2(J,K)*DT/3.0)
     2+CD(J,K)*(UDR(K)-F2(J,K)))/(DT*SK(J,K)/3.0+CC(J,K)+CD(J,K))
        DO 3 L=1,N
     3  PT=PT-SA(J,K,L)*F3(J,L)
        IF(K-1)4,4,5
     5  PT=PT-T(J,K)*F3(J,K-1)
     4  IF(K-N)6,7,7
     6  PT=PT-T(J,K+1)*(F3(J,K+1)-F3(J,K))
     7  AL(I)=PT
        AL(I )=AL(I )-SB(J,1,1)*F3(J,N1-SB(J,1,2)*O3(J)+S(J,1)*(F3(J,N)-
     1H3(J,1))
        AL(M5)=AL(M5)-SA(J,N1,N1)*O3(J)
     1       -CBO(J)*O2(J)-SKO*O3(J)-SB(J,2,1)*F3(J,N)-SB(J,2,2)*O3(J)
        M4=I
        DO 12 K=1,M
        AL(M5)=AL(M5)-SB(J,2,K+2)*H3(J,K)
        AL(M4)=AL(M4)-SB(J,1,K+2)*H3(J,K)
        I=L2+L1*(N1+K)
        PT=          -U2DG*WS(J,K)-CB(J,K)*(UDB(J,K)-UD(J,N))-SB(J,K+2,1)*
     1F3(J,N)-SB(J,K+2,2)*O3(J)+S(J,K)*H3(J,K)
        DO 9 L=1,M
     9  PT=PT-SB(J,K+2,L+2)*H3(J,L)
        IF(K-1)10,10,11
    11  PT=PT-S(J,K)*H3(J,K-1)
        GOTO 50
    10  PT=PT-S(J,K)*F3(J,N)
    50  IF(K-M)13,12,12
    13  PT=PT       -S(J,K+1)*H3(J,K+1)+S(J,K+1)*H3(J,K)
    12  AL(I)=AL(I)+PT
    14  CONTINUE
        I=L2+L1*N1
        AL(I)=AL(I)+SKO*O3(J)
        DO 15 I=1,NT
        DO 15 J=1,NT
```

```
    15  AC(I,J)=AC(I,J)+A(I,J)
        RETURN
        END
```

```
++++++++++++++++++++++++++++++++++++++++++++++++++++++++
+     SUBROUTINE TO READ INPUT DATA FROM TAPE 5        +
++++++++++++++++++++++++++++++++++++++++++++++++++++++++
*     LIST
*     LABEL
*     FORTRAN
C
C     SUBROUTINE TO READ INPUT DATA FROM TAPE 5
C           FOR THE CASE IN WHICH DT = DT1
C
      SUBROUTINE REDTAP(M1,M2,N,TC,DT,UG,UDG,U2DG,UR,UDR,U2DR,UCHK5)
      DIMENSION URR(10000),UR(20),UDR(20),U2DR(20)
      IF(M1-1)1,1,2
    1 AN=3*(N+1)
      CALL REWIND (5)
      N6=AN
      I3=TC/DT
      I2=10000.0/AN
      IF(I3-I2) 100,100,101
  100 I2=I3
  101 I4=I2*N6
      GOTO 6
    2 IF(M2-I2)5,5,6
    6 CONTINUE
    7 I4=I2*N6
    8 I3=I3-I2
      READ TAPE 5,(URR(LT),LT=1,I4)
      UCHK5=URR(I4)
      M2=1
      IF(I3)3,3,5
    3 CALL REWUNL (5)
    5 K=(M2-1)*N6+1
      UG=URR(K)
      UDG=URR(K+1)
      K=K+2
      U2DG=URR(K)
      DO 9 I=1, N
      KR=K+(I-1)*3+1
      UR(I)=URR(KR)
      UDR(I)=URR(KR+1)
    9 U2DR(I)=URR(KR+2)
      RETURN
      END
```

```
++++++++++++++++++++++++++++++++++++++++++++++++++++++++
+     SUBROUTINE TO READ INPUT DATA FROM TAPE 5        +
++++++++++++++++++++++++++++++++++++++++++++++++++++++++
*     LABEL
*     FORTRAN
C
C     SUBROUTINE TO READ INPUT DATA FROM TAPE 5
C           FOR THE CASE IN WHICH DT = DT1/N , WHERE N IS AN INTEGER
C
      SUBROUTINE REDTAP(M1,M2,N,TC,DT,UG,UDG,U2DG,UR,UDR,U2DR,UCHK5)
      DIMENSION URR(10000),UR(20),UDR(20),U2DR(20)
   10 FORMAT(2F12.4)
      IF(M1-1)1,1,2
    1 AN=3*(N+1)
      N6=AN
      AX=1.0
      READ 10,DT1
      AT=DT1/DT
      I3=TC/DT1
      I2=10000.0/AN
      AI2=I2
      I4=I2*N6
      GOTO 6
    2 AM2=M2
      K=K
      AMX=AM2/AT
      IF(AMX-AI2)5,5,6
    6 IF(I3-I2)7,7,8
    7 I4=I3*N6
    8 I3=I3-I2
      READ TAPE 5,(URR(LT),LT=1,I4)
      UCHK5=URR(I4)
      M2=1
      K=3
      IF(I3)3,3,5
    3 CALL REWUNL(5)
    5 IF(AX-AT+0.00001)12,11,11
   12 A2DG=U2DG+(URR(K)-U2DG)/(AT-AX+1.0)
      ADG=UDG+DT/2.0*(A2DG+U2DG)
      AG=UG+DT*UDG+DT*DT/3.0*(U2DG+A2DG/2.0)
      U2DG=A2DG
      UDG=ADG
      UG=AG
      DO 14 I=1,N
      KR=K+(I-1)*3+1
      A2DG=U2DR(I)+(URR(KR+2)-U2DR(I))/(AT-AX+1.0)
      ADG=UDR(I)+DT/2.0*(A2DG+U2DR(I))
      AG=UR(I)+DT*UDR(I)+DT*DT/3.0*(U2DR(I)+A2DG/2.0)
      U2DR(I)=A2DG
      UDR(I)=ADG
      UR(I)=AG
   14 CONTINUE
      AX=AX+1.0
      GOTO 13
   11 AX=1.0
      U2DG=URR(K)
      UDG=URR(K-1)
      UG=URR(K-2)
      DO 15 I=1,N
      KR=K+(I-1)*3+1
      UR(I)=URR(KR)
      UDR(I)=URR(KR+1)
      U2DR(I)=URR(KR+2)
   15 CONTINUE
      K=K+N6
   13 RETURN
      END
```

```
++++++++++++++++++++++++++++++++++++
+     SUBROUTINE SOLEQU(A,N,X)     +
++++++++++++++++++++++++++++++++++++
*     LIST
*     LABEL
*     FORTRAN
C
      SUBROUTINE SOLEQU(A,N,X)
      DIMENSION A(53,53),X(53)
      NM=N-1
      DO 85 I=1,NM
      IP=I+1
      DO 25 J=IP,N
      A(I,J)=A(I,J)/A(I,I)
      IF DIVIDE CHECK 200,25
   25 CONTINUE
      DO 50 J=IP,N
      DO 45 K=J,N
      IF(A(I,J)) 35,50,35
   35 A(K,J)=A(K,J)-A(K,I)*A(I,J)
      A(J,K)=A(K,J)
   45 CONTINUE
   50 CONTINUE
      X(I)=X(I)/A(I,I)
      DO 75 K=IP,N
      X(K)=X(K)-A(K,I)*X(I)
   75 CONTINUE
   85 CONTINUE
      X(N)=X(N)/A(N,N)
      IF DIVIDE CHECK 200,100
  100 DO 125 II=1,NM
      I=N-II+1
      DO 125 K=1,N
      X(I-1)=X(I-1)-A(I-1,K)*X(K)
  125 CONTINUE
      A=.0
  130 RETURN
  200 PRINT 1,I
      A=2.0
      GO TO 130
    1 FORMAT(41H1  BAD INVERSE   ZERO ON DIAGONAL     ROW=I3)
      END
```

```
++++++++++++++++++++++++++++
+     SUBROUTINE RESPON    +
++++++++++++++++++++++++++++
*     LABEL
*     FORTRAN
C
      SUBROUTINE RESPON
      DIMENSION W(2,20),WE(2,20),WS(2,6),SA(2,21,21),SB(2,8,8),RM(2),
     1CB(2,6),CBO(2),T(2,20),S(2,6),AC(53,53)
      DIMENSION CO(2,20),C1(2,20),RC1(2,20),RC2(2,20),DO(2,20),D1(2,20),
     1RD1(2,20),RD2(2,20),TO(2,20),T1(2,20),RT1(2,20),RT2(2,20),CC(2,20)
     2,CD(2,20),SK(2,20),U2DC(2,20), C2(2,20),K1(20),U(2),OD(2),O2D(2),
     3U(2,20),UD(2,20),U2U(2,20),US(2,20),UUS(2,20),U2US(2,20),UB(2,6),
     4UDB(2,6),U2DB(2,6),USM(2,20),UUM(2,20),U2UM(2,20),USP(2,20),
     5UCF(2,20),UDF(2,20), AL(53),U(2,20),C1(2),UC(2,20),UUC(2,20)
      DIMENSION F2(2,20),F3(2,20),G2(2,20),G3(2,20),E2(2,20),E3(2,20),
```

```
     1H2(2,6),H3(2,6),O2(2),O3(2),USPU(2,20),USPB(2,20),USPC(2,20),
     2NOMASS(20),URS(4000),FORCE(2,20),BMMAX(2),BM(2,20),X(2,20),
     3UR(20),UDR(20),U2DR(20),COF(2,20)
      DIMENSION OM1(2),OM2(2),UM1(2,20),UM2(2,20),UBM1(2,6),UBM2(2,6)
      COMMON W,WE,WS,RM,CB,CBO,N,M,DT,NT,EI,D,SA,SB,T,S,SKO,DT2,DT3,DT6
      COMMON NOMASS,NN,JM
      COMMON CO,C1,RC1,RC2,DO,D1,RD1,RD2,TO,T1,RT1,RT2,CC,CD,SK,C2,K1,
     1O,OO,O2D,U,UD,U2D,US,UDS,U2DS,UB,UDB,U2DB,TC,USM,UCM,UDM,USF,UCF,
     2U2DF,AC,AL,SCALE,METHOD,UC,UDC,U2DC,OM1,OM2,UM1,UM2,UBM1,UBM2
      COMMON F2,F3,G2,G3,E2,E3,H2,H3,O2,O3,COF,USPU,USPB,USPC,TI,M1,M2,
     1M3,U2DG,UDG,UG,UR,U2DR,UDR,X,K6,N1,NK,URS,FORCE,UCHK6,BMMAX,ISTOP,
     2BM
      LUMPM=N-JM
      L3=(M3-1)*NK
      L1=1
      L2=0
      DO 6 J=1,2
      NM=1
      IF(J-1)2,2,3
    3 L1=-1
      L2=NN+1
    2 GO TO (101,102,102,102),METHOD
  102 DO 4 I=1,N
      IF(I-NOMASS(NM))10,11,10
   11 NM=NM+1
      GOTO 4
   10 ID=I+1-NM
      M5=L2+L1*ID
      U(J,I)=F3(J,I)+DT6* AL(M5)
      UD(J,I)=F2(J,I)+DT2*AL(M5)
      U2D(J,I)=AL(M5)
    4 CONTINUE
      M5=M5+L1
      O(J)=O3(J)+DT6*AL(M5)
      OD(J)=O2(J)+DT2*AL(M5)
      O2D(J)=AL(M5)
      DO 5 I=1,M
      M5=M5+L1
      UB(J,I)=H3(J,I)+DT6*AL(M5)
      UDB(J,I)=H2(J,I)+DT2*AL(M5)
      U2DB(J,I)=AL(M5)
    5 CONTINUE
      NM=1
      DO 20 I=1,N
      IF(I-NOMASS(NM))20,22,20
   22 ID=LUMPM+NM
      K=NOMASS(NM)
      PT=0.0
      KM=1
      DO 23 L=1,N
      IF(L-NOMASS(KM))24,25,24
   25 IN=KM+LUMPM
      PT=PT+SA(J,IU+L,IN+4)*X(J,IN)
      KM=KM+1
      GOTO 23
   24 IN=L+1-KM
      PT=PT-SA(J,ID+1,IN)*U(J,L)
   23 CONTINUE
      IF(M1-2)36,37,38
```

```
   36 UM2(J,I)=U(J,I)
      UM1(J,I)=PT
      GOTO 39
   37 UD(J,I)=(3.0*PT-4.0*UM1(J,I)+UM2(J,I))/(2.0*DT)
      U2D(J,I)=(UD(J,I)-F2(J,I))/DT2
      GOTO 40
   38 U2D(J,I)=(2.0*PT-5.0*U(J,I)+4.0*UM1(J,I)-UM2(J,I))/(DT*DT)
      UD(J,I)=(3.0*PT-4.0*U(J,I)+UM1(J,I))/(2.0*DT)
      UM2(J,I)=UM1(J,I)
      UM1(J,I)=U(J,I)
      GOTO 40
   39 U2D(J,I)=(PT-F3(J,I))/DT6
      UD(J,I)=F2(J,I)+DT2*U2D(J,I)
   40 U(J,I)=PT
      NM=NM+1
   20 CONTINUE
      GOTO 6
  101 DO 114 I=1,N
      M5=L2+L1*I
      U(J,I)=AL(M5)
      UD(J,I)=(3.0*U(J,I)-F2(J,I))/(2.0*DT)
      U2D(J,I)=(2.0*U(J,I)-F3(J,I))/(DT*DT)
  114 CONTINUE
      M5=M5+L1
      O(J)=AL(M5)
      OD(J)=(3.0*O(J)-O2(J))/(2.0*DT)
      O2D(J)=(2.0*O(J)-O3(J))/(DT*DT)
      DO 15 I=1,M
      M5=M5+L1
      UB(J,I)=AL(M5)
      UDB(J,I)=(3.0*UB(J,I)-H2(J,I))/(2.0*DT)
     U2DB(J,I)=(2.0*UB(J,I)-H3(J,I))/(DT*DT)
   15 CONTINUE
    6 CONTINUE
      DO 70 J=1,2
      NM1=N-1
      L1=1
      IF(J-1)32,32,33
   33 L1=-1
      L3=L3+NK+1
   32 DO 34 I=1,N
   21 U2DC(J,I)=(CD(J,I)*(UD(J,I)-UDR(I))+SK(J,I)*(U(J,I)-UR(I)-E3(J,I))
     1-COF(J,I)-E2(J,I)*(CC(J,I)+CD(J,I)))/
     2((CC(J,I)+CD(J,I))*DT2+DT6*SK(J,I))
      UDC(J,I)=E2(J,I)+DT2*U2DC(J,I)
      UC(J,I)=E3(J,I)+DT6*U2DC(J,I)
      US(J,I)=U(J,I)-UR(I)-UC(J,I)
      UDS(J,I)=UD(J,I)-UDR(I)-UDC(J,I)
      U2DS(J,I)=U2D(J,I)-U2DR(I)-U2DC(J,I)
      FORCE(J,I)=SK(J,I)*US(J,I)-COF(J,I)
      BM(J,I)=FORCE(J,I)+CD(J,I)*UDS(J,I)
      L4=L3+L1*6*(I-1)+L1
      URS(L4)=US(J,I)
      L4=L4+L1
      URS(L4)=UDS(J,I)
      L4=L4+L1
      URS(L4)=U2DS(J,I)
      L4=L4+L1
      URS(L4)=U(J,I)
```

```
      URS(L4)=UR(I)
      L4=L4+L1
      URS(L4) = U2D(J,I) + U2DG
   34 CONTINUE
      L4=L4+L1
      URS(L4) = U2DR(N) + U2DG
      L4=L4+L1
      URS(L4)=OD(J)
      L4=L4+L1
      URS(L4)=O2D(J)
      DO 35 I=1,M
      L4=L4+L1
      URS(L4)=UB(J,I)
      L4=L4+L1
      URS(L4)=UDB(J,I)
      L4=L4+L1
      URS(L4)=U2DB(J,I) + U2DG
   35 CONTINUE
      DO 31 I=1,N
      L4 = L4 + L1
   31 URS(L4)=BM(J,I)
   70 CONTINUE
      RETURN
      END
```

```
++++++++++++++++++++++++++++
+     SUBROUTINE WRITAP    +
++++++++++++++++++++++++++++
*     LIST
*     FORTRAN
*     LABEL
C
      SUBROUTINE WRITAP
      DIMENSION W(2,20),WE(2,20),WS(2,6),SA(2,21,21),SB(2,8,8),RM(2),
     1CB(2,6),CBO(2),T(2,20),S(2,6),AC(53,53)
      DIMENSION CO(2,20),C1(2,20),RC1(2,20),RC2(2,20),DO(2,20),D1(2,20),
     1RD1(2,20),RD2(2,20),TO(2,20),T1(2,20),RT1(2,20),RT2(2,20),CC(2,20)
     2,CD(2,20),SK(2,20),U2DC(2,20), C2(2,20),K1(20),O(2),OD(2),O2D(2),
     3U(2,20),UD(2,20),U2D(2,20),US(2,20),UDS(2,20),U2DS(2,20),UB(2,6),
     4UDB(2,6),U2DB(2,6),USM(2,20),UCM(2,20),UDM(2,20),USF(2,20),
     5UCF(2,20),U2DF(2,20), AL(53),OT(2,20),EI(2),UC(2,20),UDC(2,20)
      DIMENSION F2(2,20),F3(2,20),G2(2,20),G3(2,20),E2(2,20),E3(2,20),
     1H2(2,6),H3(2,6),O2(2),O3(2),USPU(2,20),USPB(2,20),USPC(2,20),
     2NOMASS(20),URS(4000),FORCE(2,20),BMMAX(2),BM(2,20),X(2,20),
     3UR(20),UDR(20),U2DR(20),COF(2,20)
      DIMENSION OM1(2),OM2(2),UM1(2,20),UM2(2,20),UBM1(2,6),UBM2(2,6)
      COMMON W,WE,WS,RM,CB,CBO,N,M,DT,NT,EI,D,SA,SB,T,S,SKO,DT2,DT3,DT6
      COMMON NOMASS,NN,JM
      COMMON CO,C1,RC1,RC2,DO,D1,RD1,RD2,TO,T1,RT1,RT2,CC,CD,SK,C2,K1,
     1O,OO,O2D,U,UD,U2D,US,UDS,U2DS,UB,UDB,U2DB,TC,USM,UCM,UDM,USF,UCF,
     2U2DF,AC,AL,SCALE,METHOD,UC,UDC,U2DC,OM1,OM2,UM1,UM2,UBM1,UBM2
      COMMON F2,F3,G2,G3,E2,E3,H2,H3,O2,O3,COF,USPU,USPB,USPC,TI,M1,M2,
     1M3,U2DG,UDG,UG,UR,U2DR,UDR,X,K6,N1,NK,URS,FORCE,UCHK6,BMMAX,ISTOP,
     2BM
   20 FORMAT(1H1,F9.4,3F15.8)
   22 FORMAT(19H0 PILE SYSTEM,I4)
   24 FORMAT(I4,3E20.8)
   25 FORMAT(4X,4F20.8)
```

```
   26 FORMAT(14H0 CAP ROTATION,I3,3F20.8)
   27 FORMAT(19H0 PIER SYSTEM,I4)
   32 FORMAT(31H0TIME AT COMPLETION OF CHAIN 2=,F15.5)
      IF(M3-1)1,1,2
    1 N3=1
      I2=4000/NK
      I4=I2*NK
      N4=2
      ISC=(TC+0.00000001)/DT
    2 IF(M3-I2)3,4,4
    4 WRITE TAPE 8,(URS(J),J=1,I4)
      M3=0
      UCHK6=URS(I4)
    3 N3=N3
      K6=K6
      N4=N4
      IF(K6-K1(N3))8,7,7
    7 K6=0
      PRINT 20,TI,UG,UDG,U2DG
      DO 21 J=1,2
      PRINT 22,J
      DO 23 I=1,N
      PRINT 24,I,SK(J,I),CC(J,T),CD(J,I)
      PRINT 25,UR(I),UDR(I),U2DR(I)
      PRINT 25,US(J,I),UDS(J,I),U2DS(J,I),FORCE(J,I)
      PRINT 25,U(J,I),UD(J,I),U2D(J,I),BM(J,I)
   23 CONTINUE
      PRINT 26,J,O(J),OD(J),O2D(J)
      PRINT 27,J
      DO 28 I=1,M
      PRINT 24,I,UB(J,I),UDB(J,I),U2DB(J,I)
   28 CONTINUE
   21 CONTINUE
    8 IF(M1-K1(N4))10,9,9
    9 N3=N3+2
      N4=N4+2
   10 IF(M1-ISC)5,6,6
    6 I4=M3*NK
      WRITE TAPE 8,(URS(J),J=1,I4)
      CALL TIME(CLOCK)
      PRINT 32,CLOCK
      CALL EOF(6)
      CALL REWUNL(6)
      CALL EXIT
    5 RETURN
      END
```

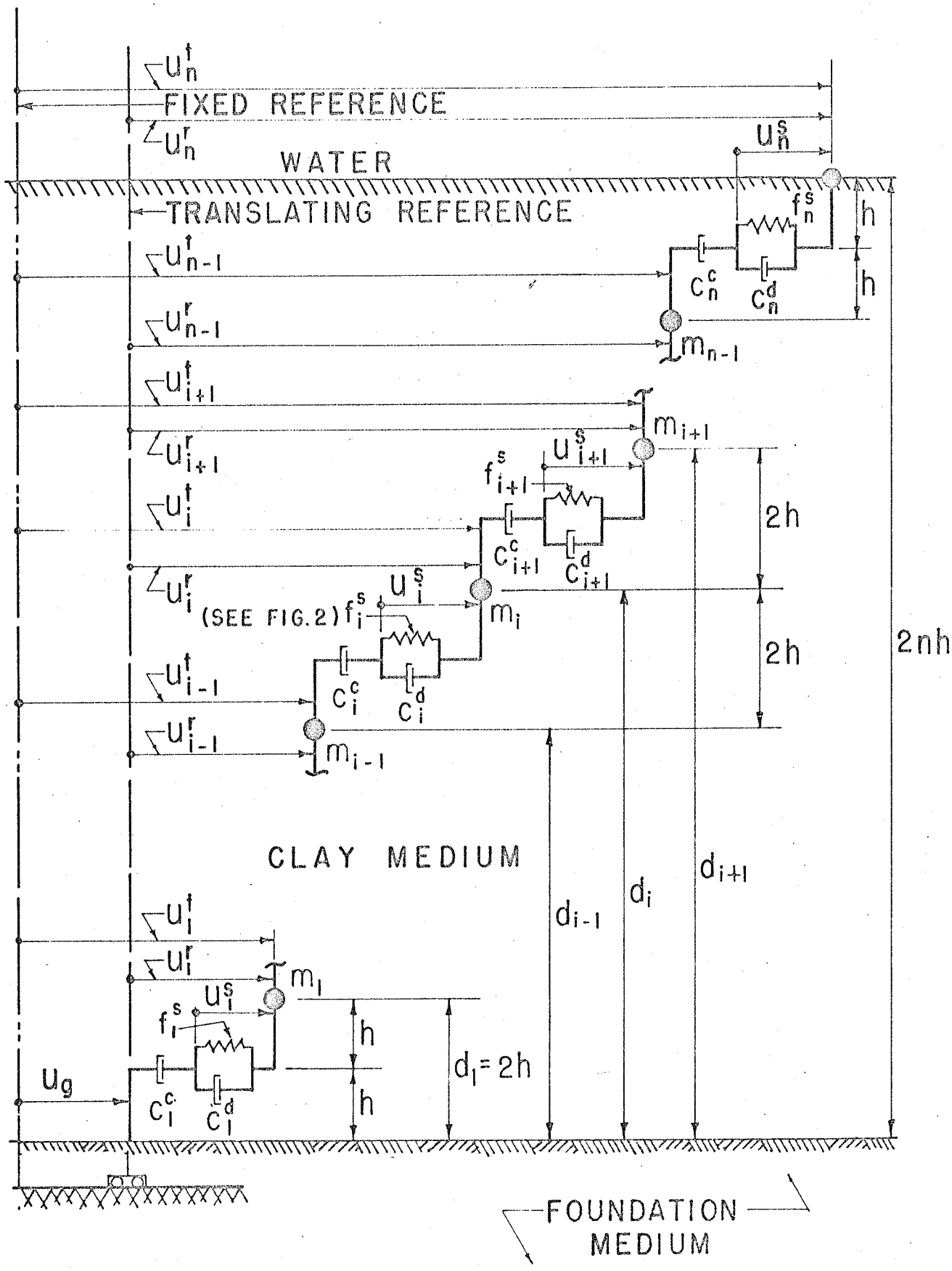

FIG. 1 IDEALIZED CLAY MEDIUM

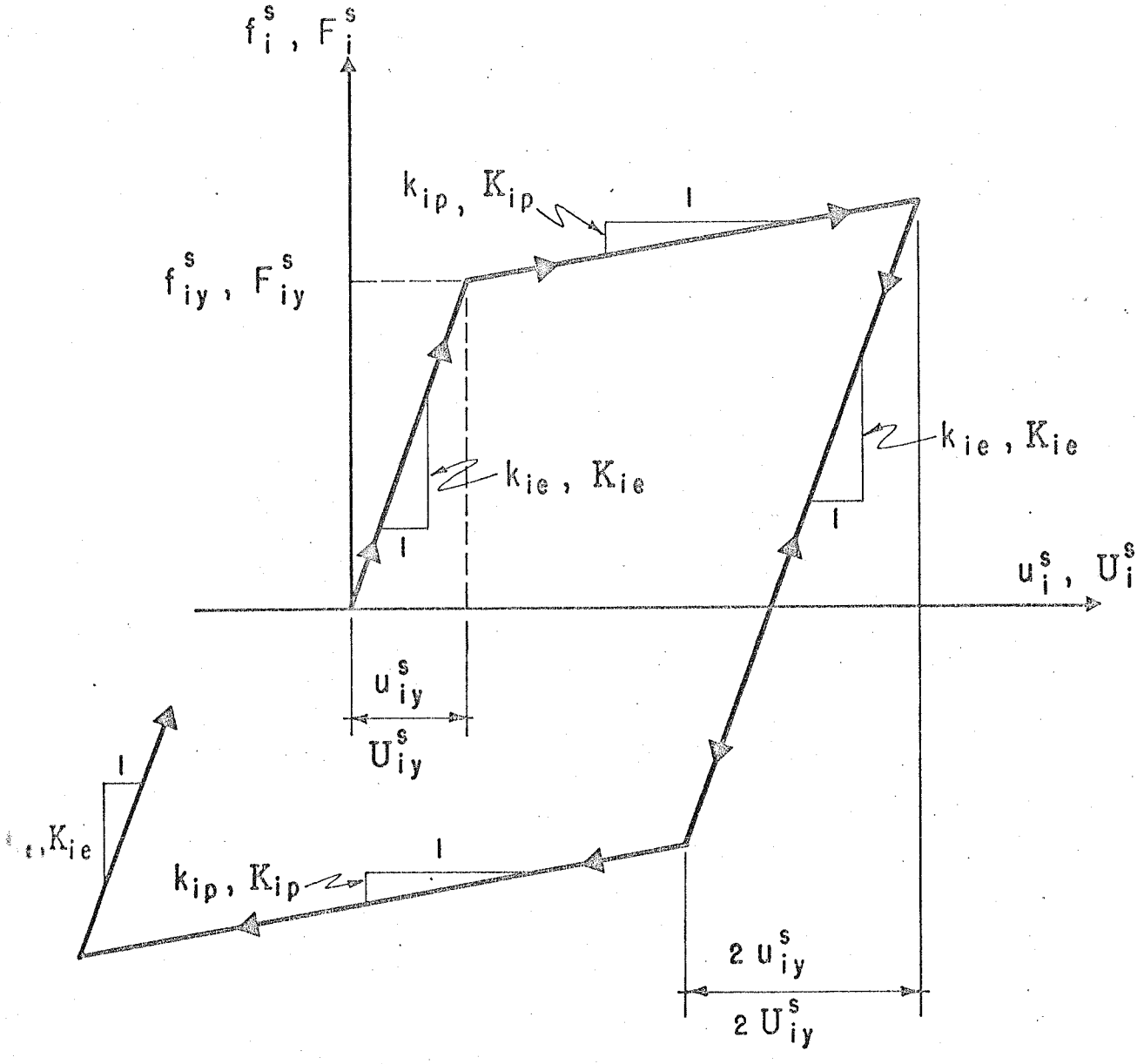

FIG. 2 FORCE-DISPLACEMENT CHARACTERISTICS OF SPRINGS.

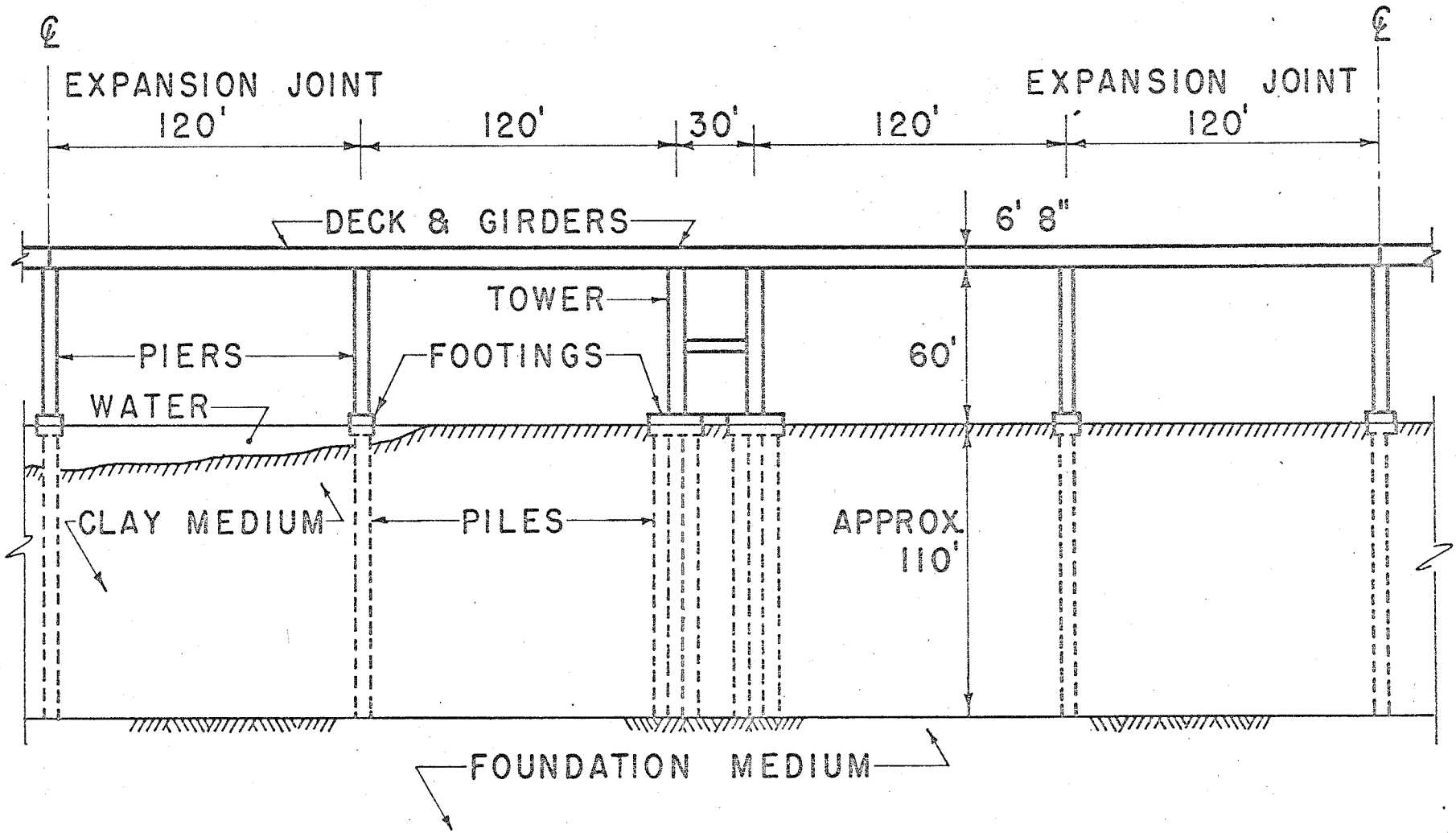

FIG. 3 BRIDGE STRUCTURAL SYSTEM

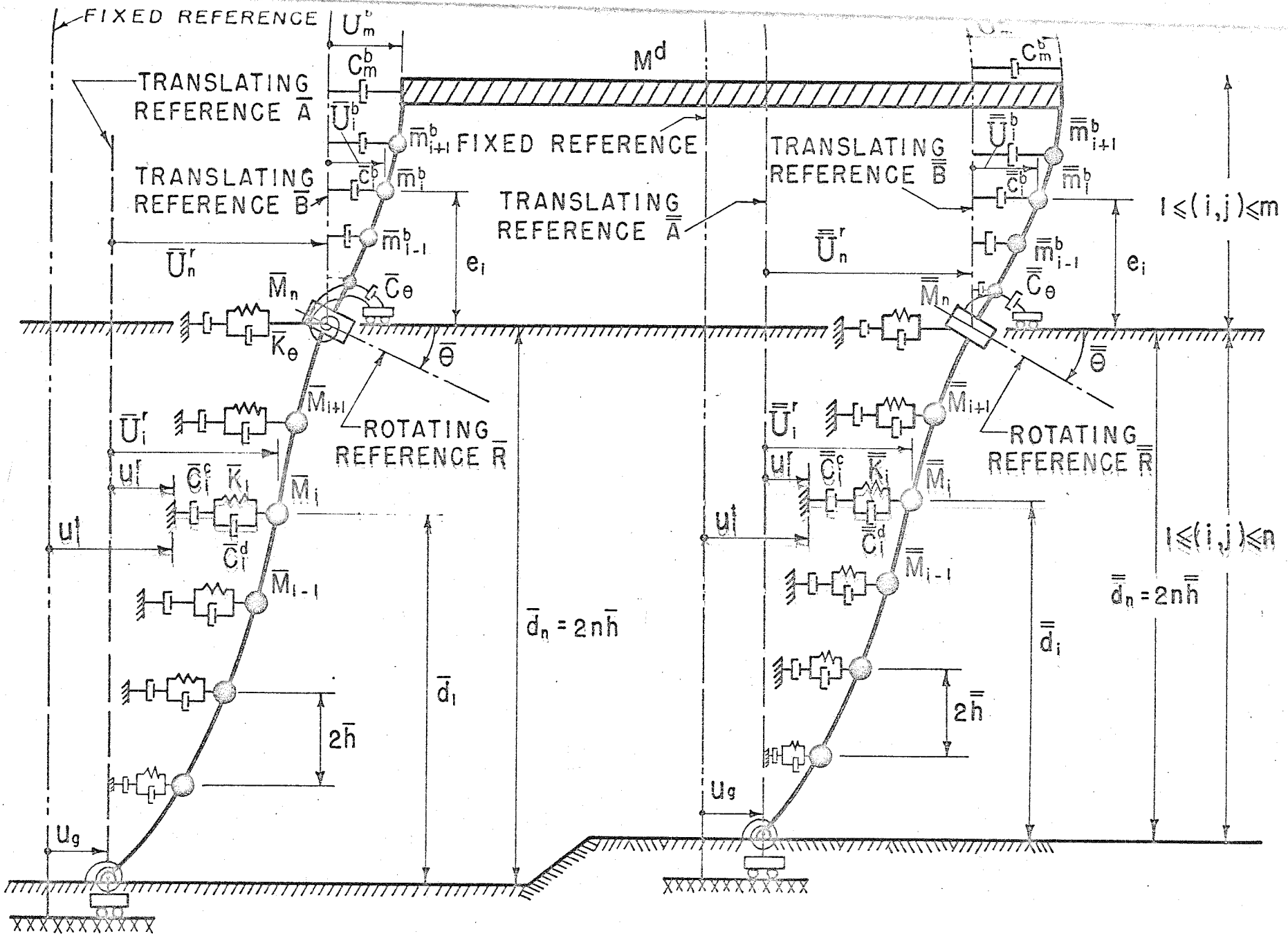

FIG. 4 IDEALIZED STRUCTURAL SYSTEM.

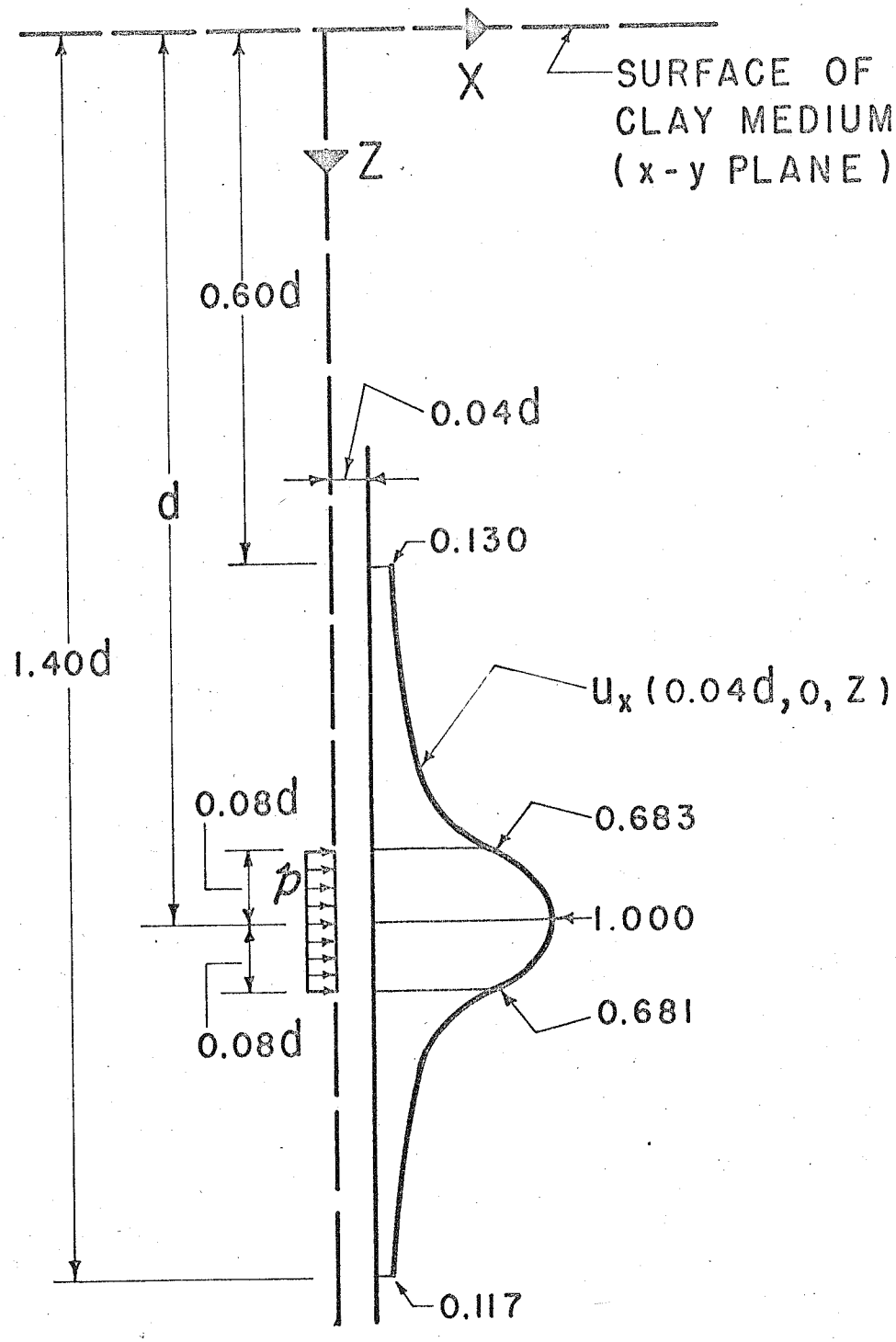

FIG. 5 VARIATION OF HORIZONTAL DISPLACEMENT ALONG A VERTICAL AXIS FOR UNIFORMLY DISTRIBUTED LOAD OF INTENSITY p.

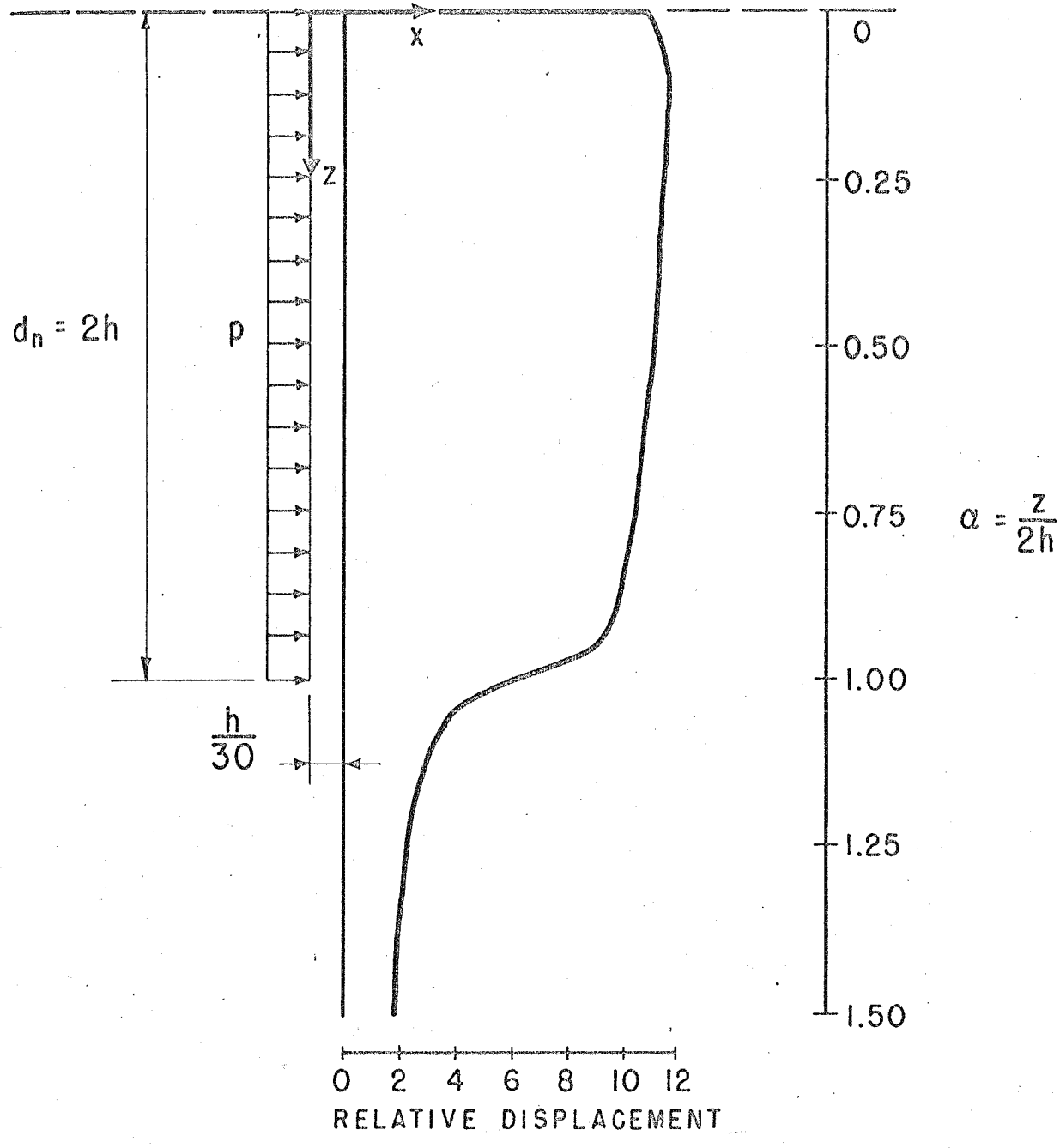

FIG. 6 VARIATION OF HORIZONTAL DISPLACEMENT FIELD FOR UNIFORMLY DISTRIBUTED LOAD FOR THE CASE OF $\bar{c} = h$.

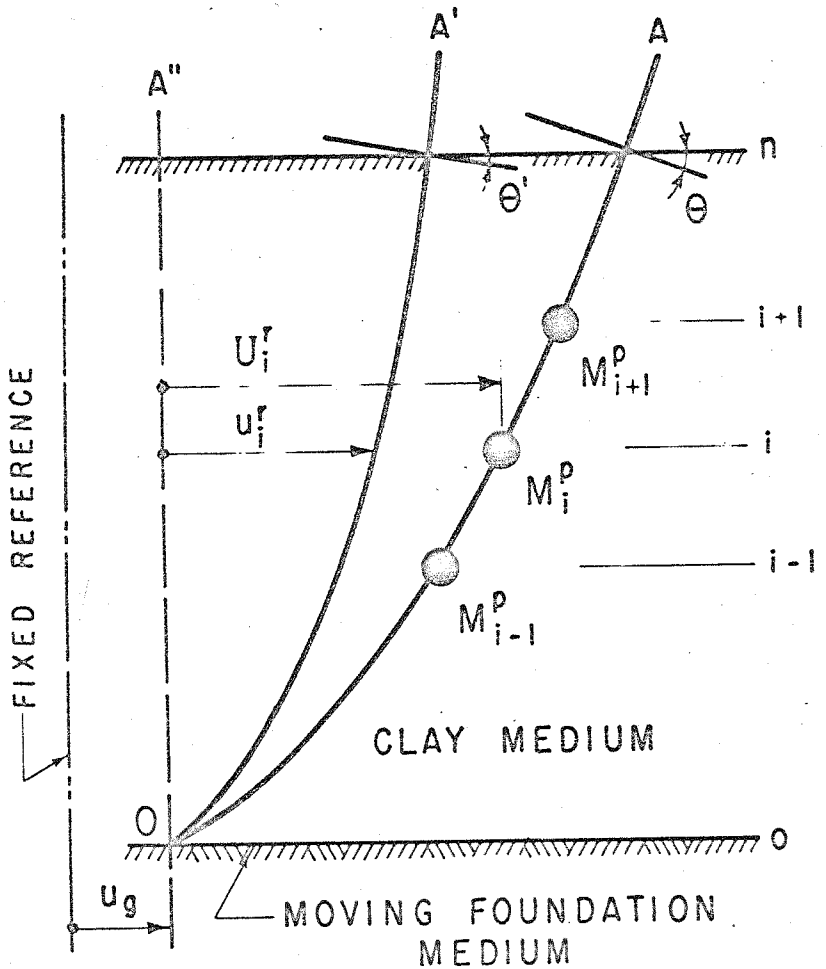

FIG. 7 TRUE MOTION OF STRUCTURAL SYSTEM.

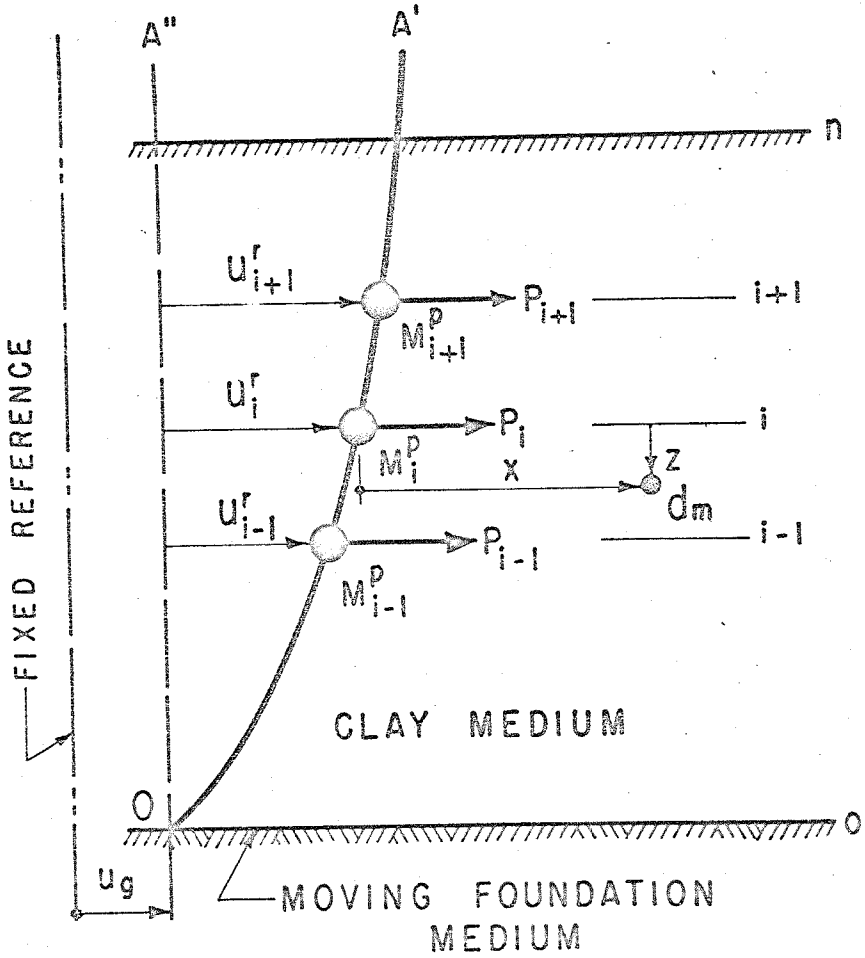

FIG. 8 FORCED MOTION OF STRUCTURAL SYSTEM WITH NO INTERACTION.

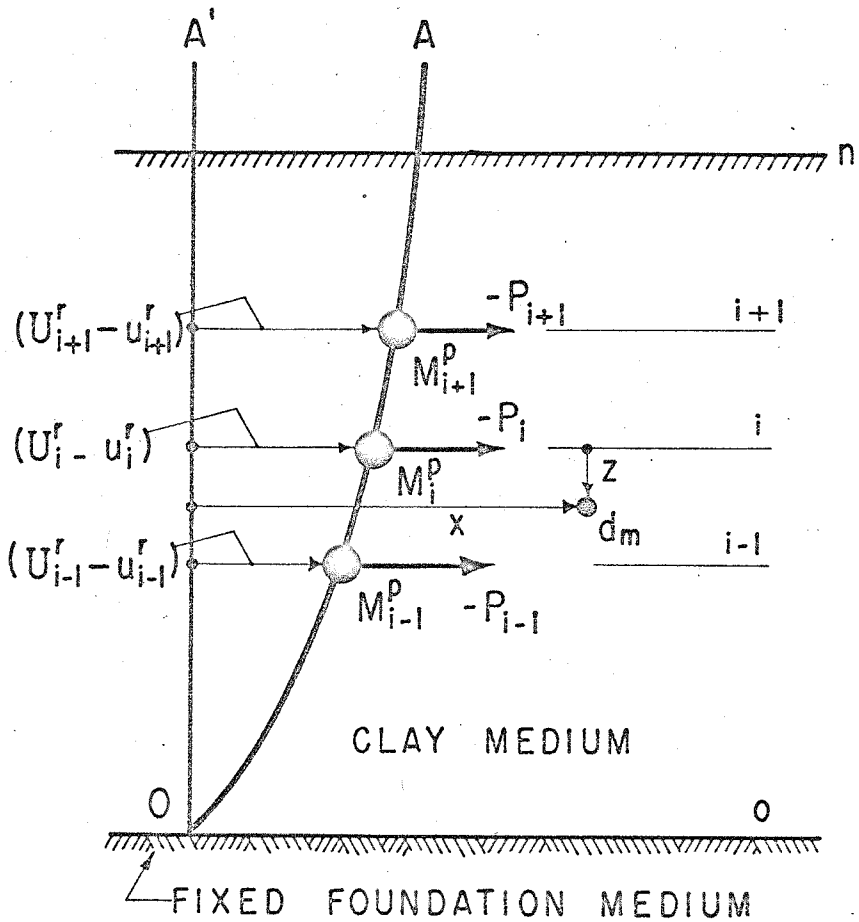

FIG. 9 FORCED MOTION OF REAL SYSTEM RELATIVE TO MOTION OF CLAY MEDIUM.

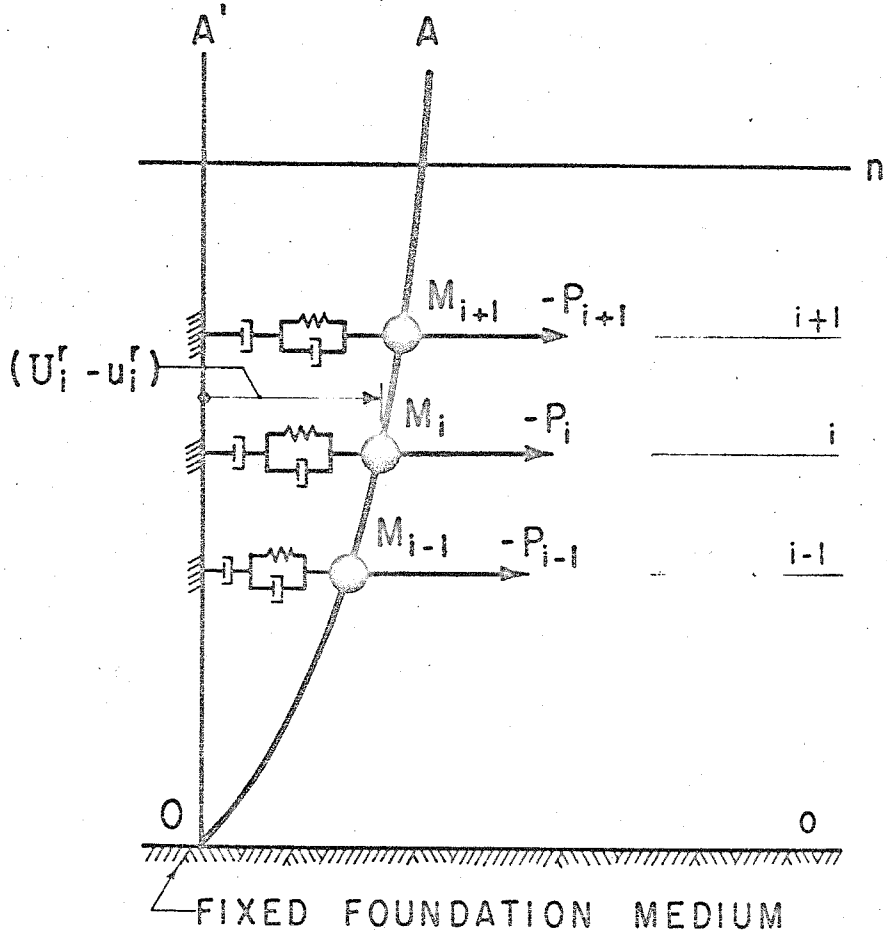

FIG. 10 MOTION OF IDEALIZED SYSTEM RELATIVE TO MOTION OF CLAY MEDIUM.

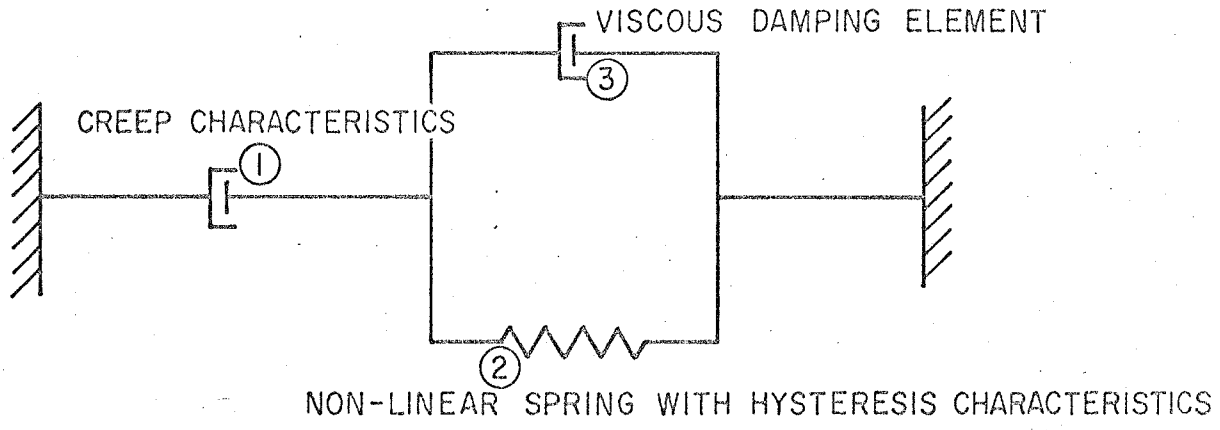

FIGURE 11. PROPOSED MODEL REPRESENTING STRESS-DEFORMATION CHARACTERISTICS OF CLAY UNDER SHORT-TERM CYCLIC LOADING

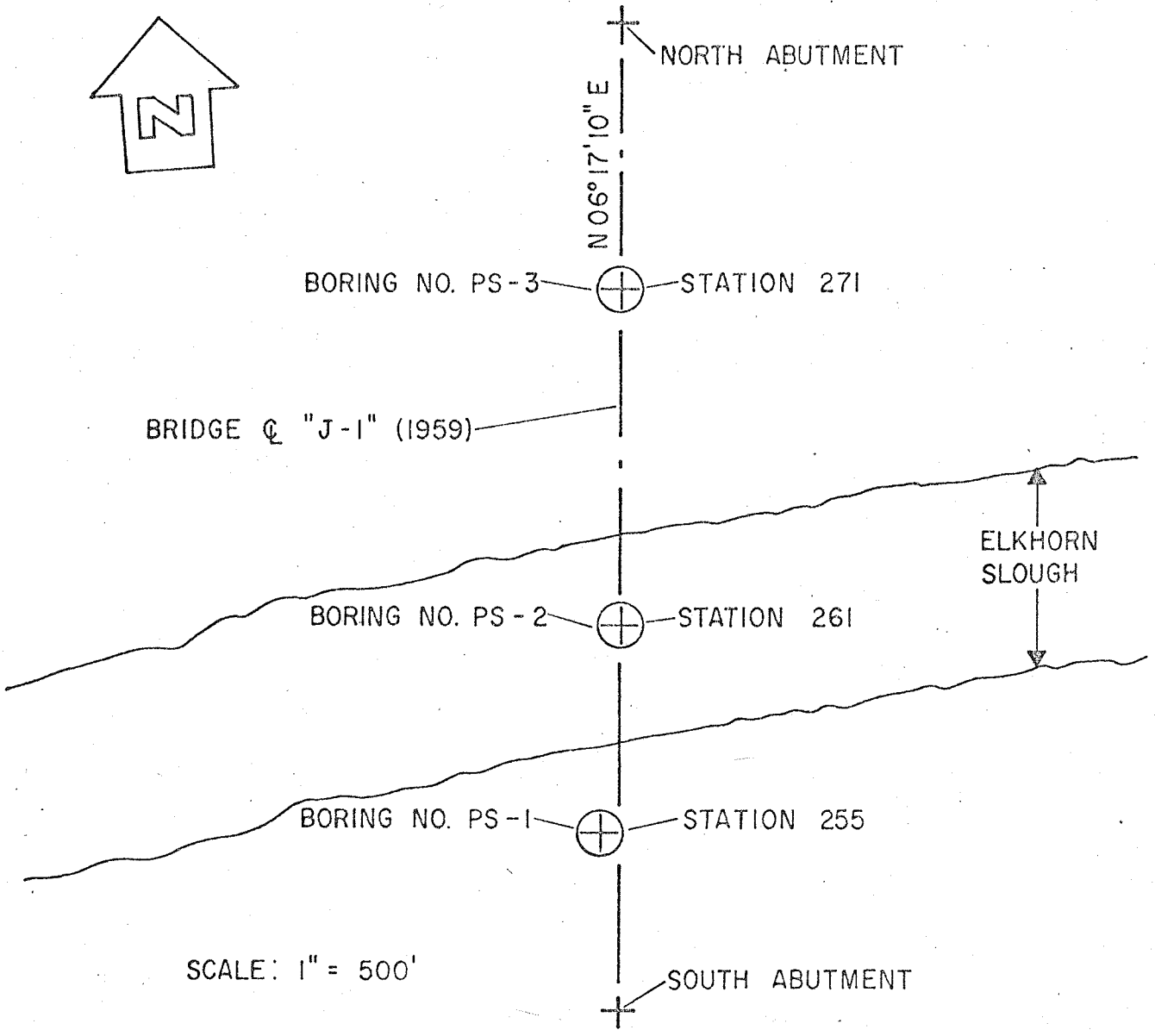

FIGURE 12. PLAN OF BORINGS

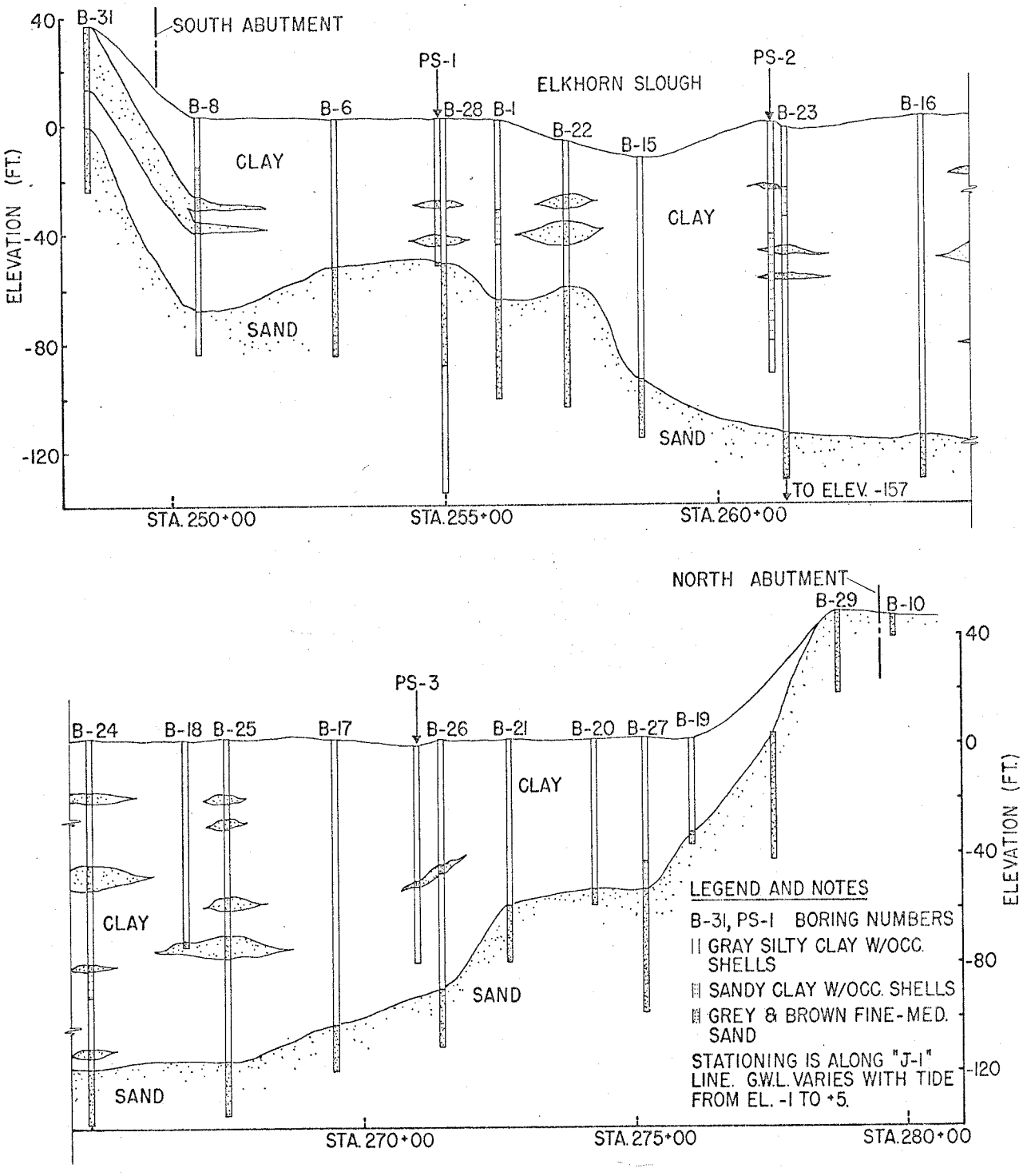

FIGURE 13. SOIL PROFILE

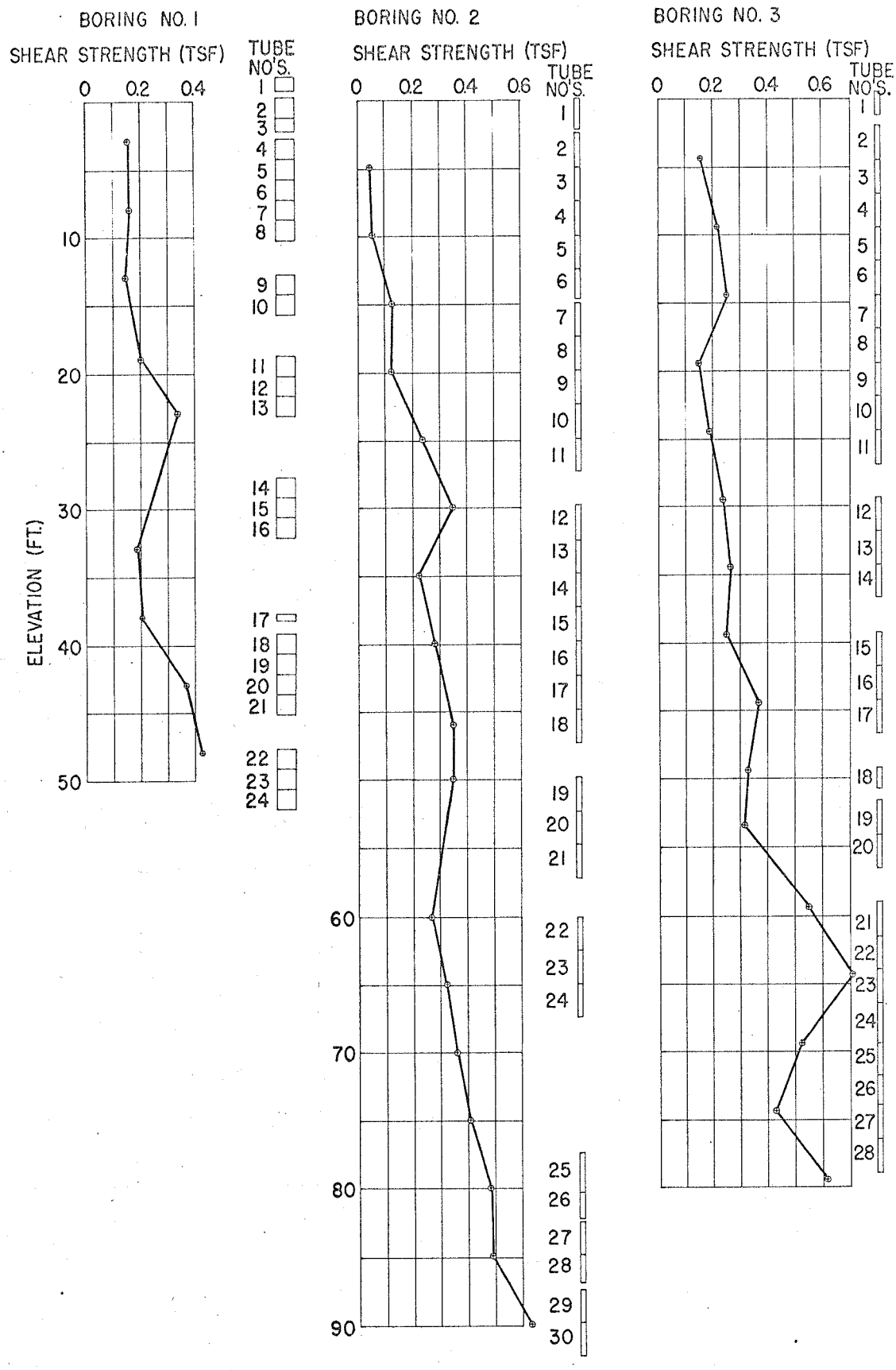

FIGURE 14. VANE SHEAR STRENGTHS AND SAMPLE ELEVATIONS

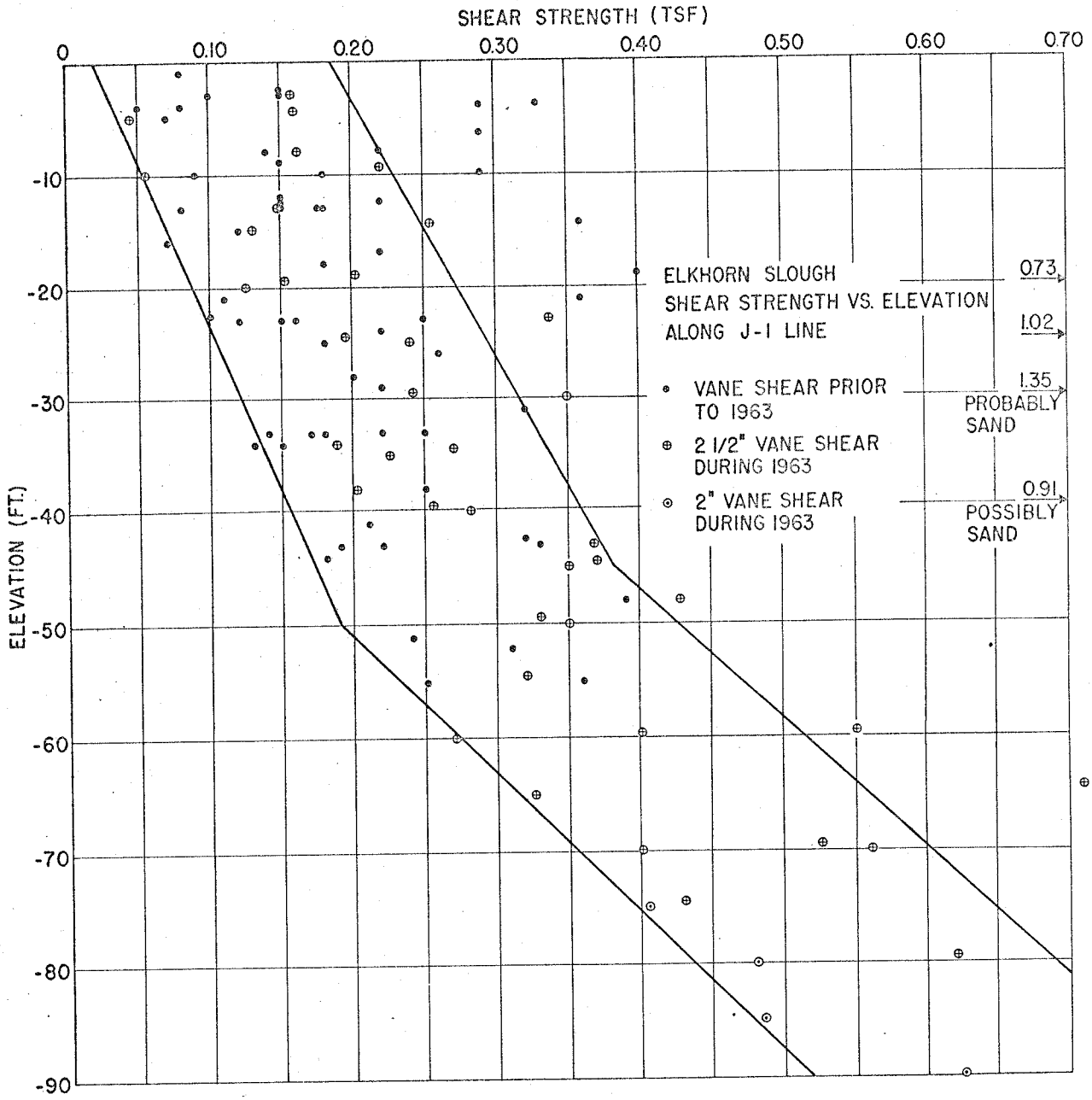

FIGURE 15. SUMMARY OF RESULTS OF VANE SHEAR TESTS

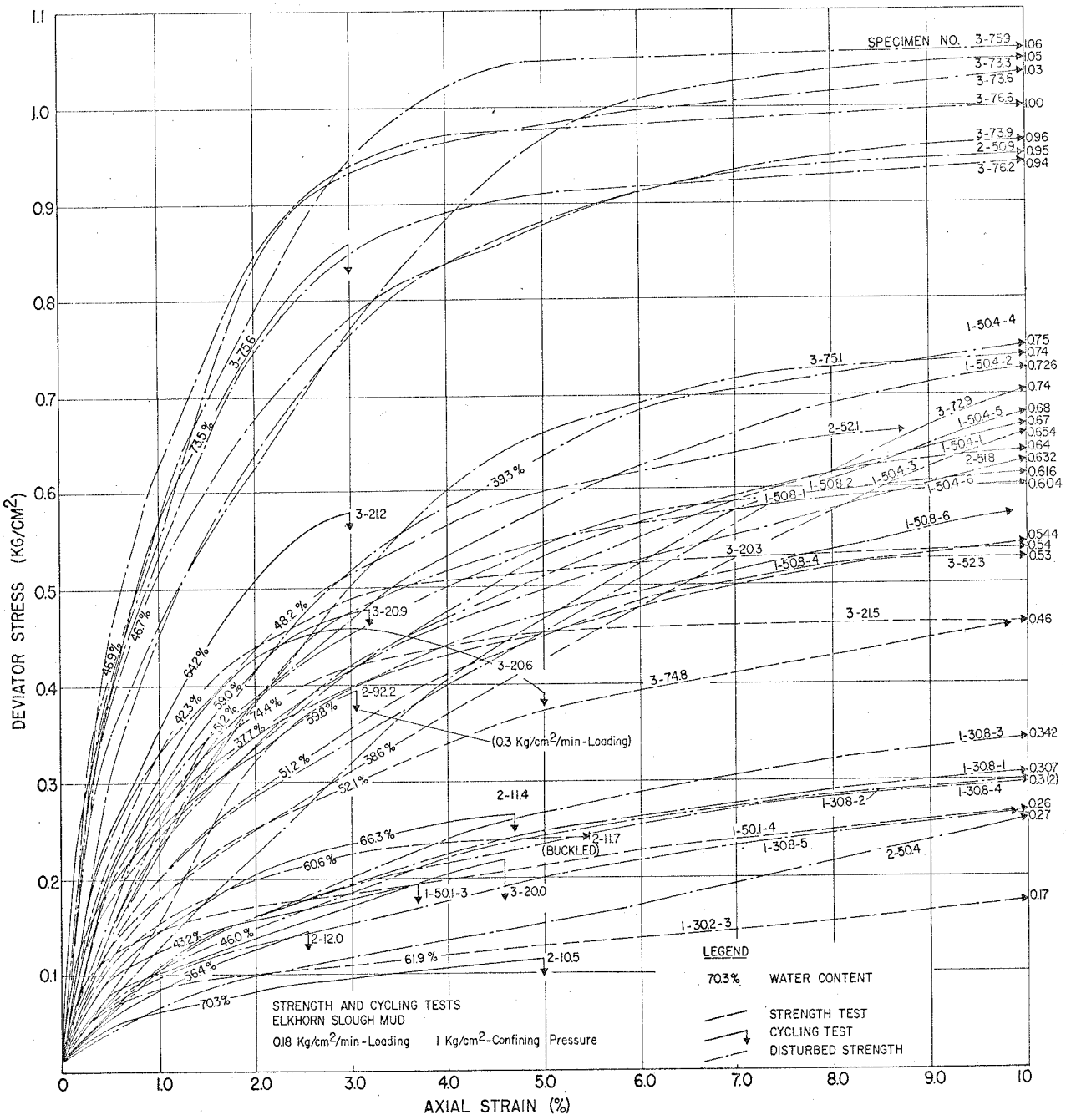

FIGURE 16. STATIC STRESS-STRAIN CURVES

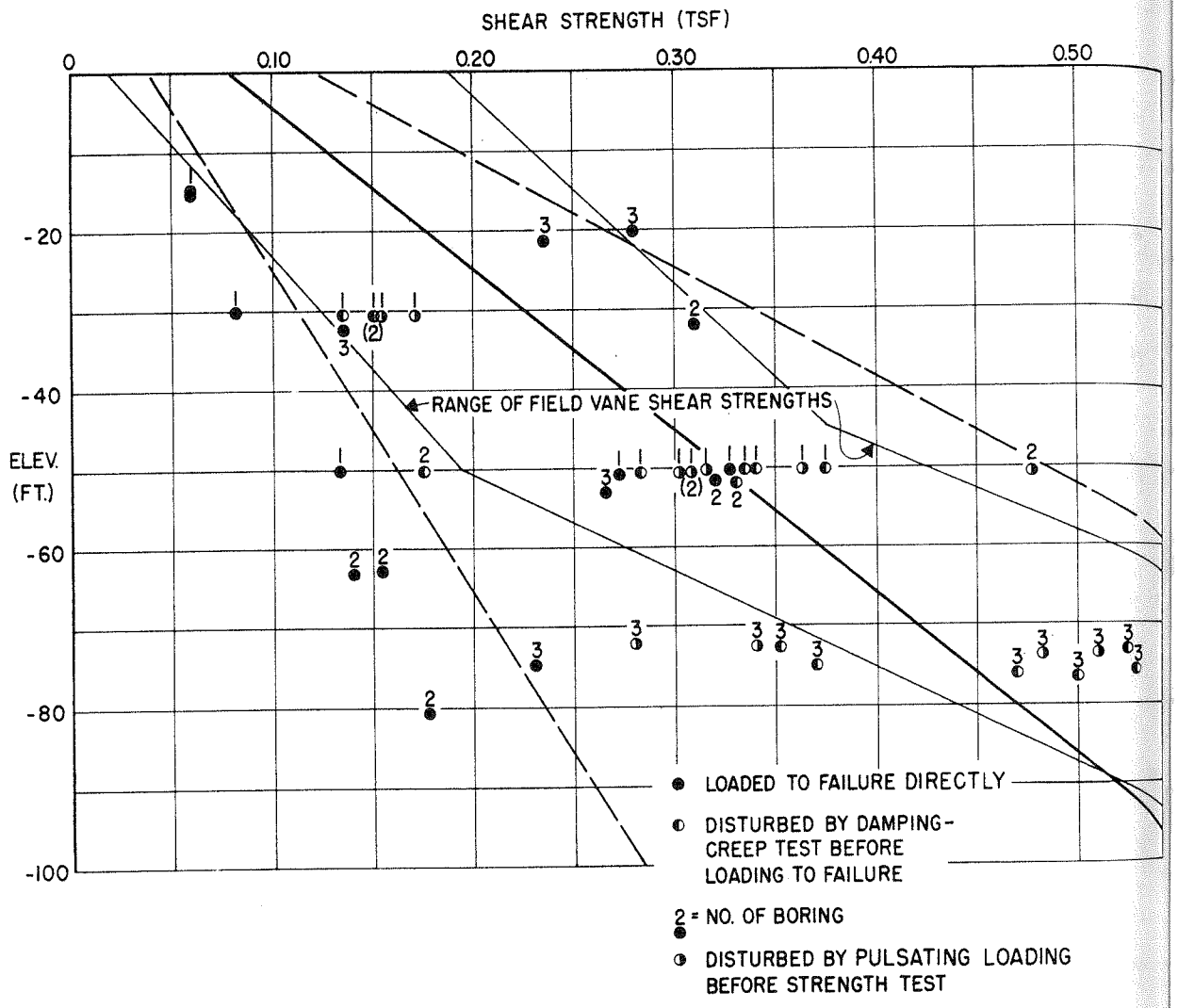

FIGURE 17. SHEAR STRENGTH VS. DEPTH

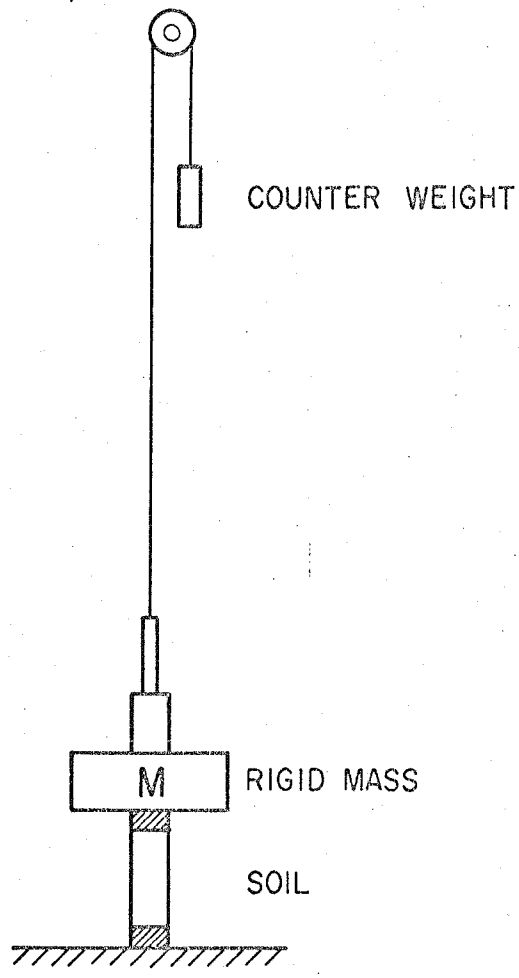

FIGURE 18. DYNAMIC TEST ARRANGEMENT

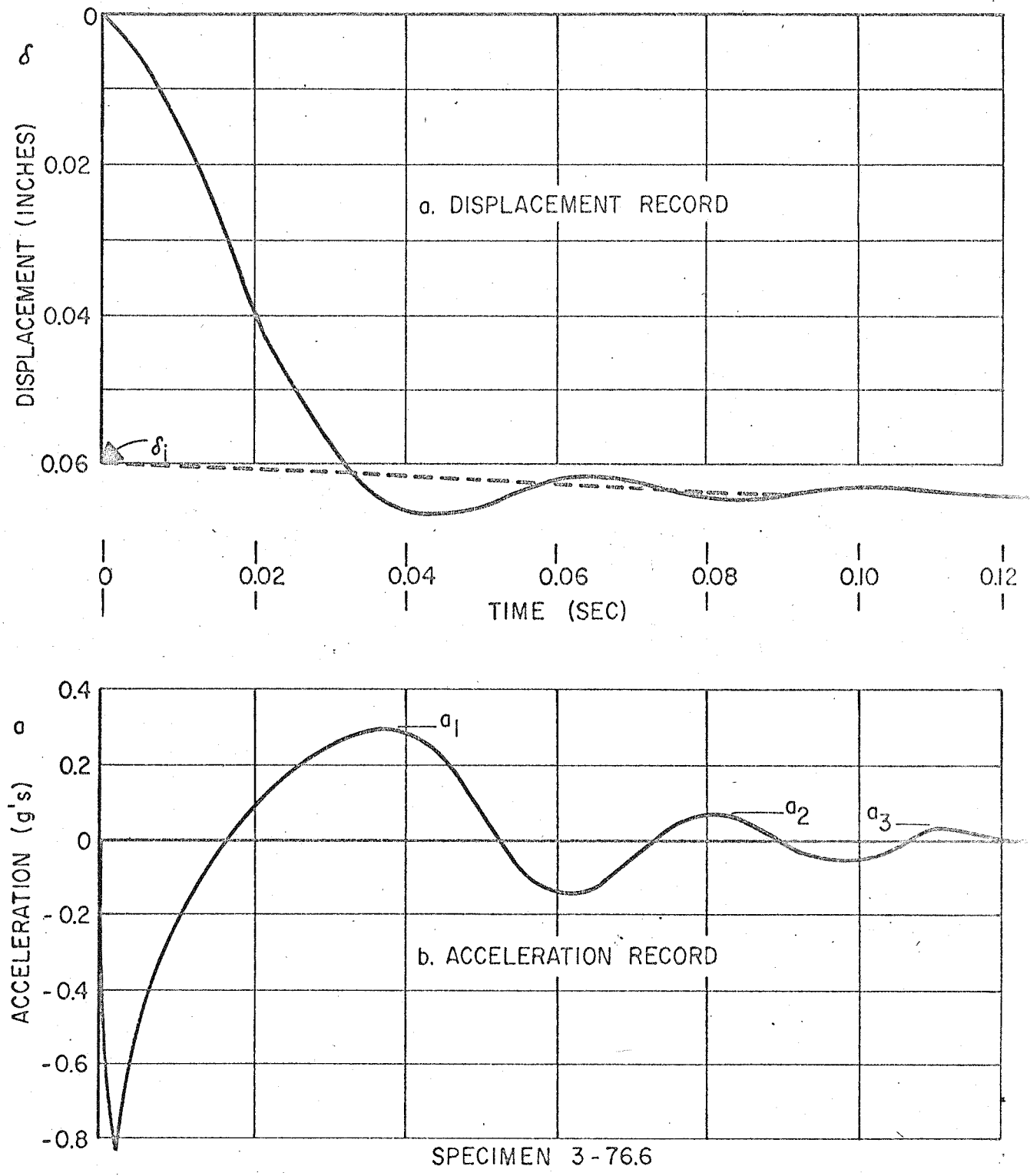

FIGURE 19. TYPICAL RECORDS OBTAINED FROM DYNAMIC TEST

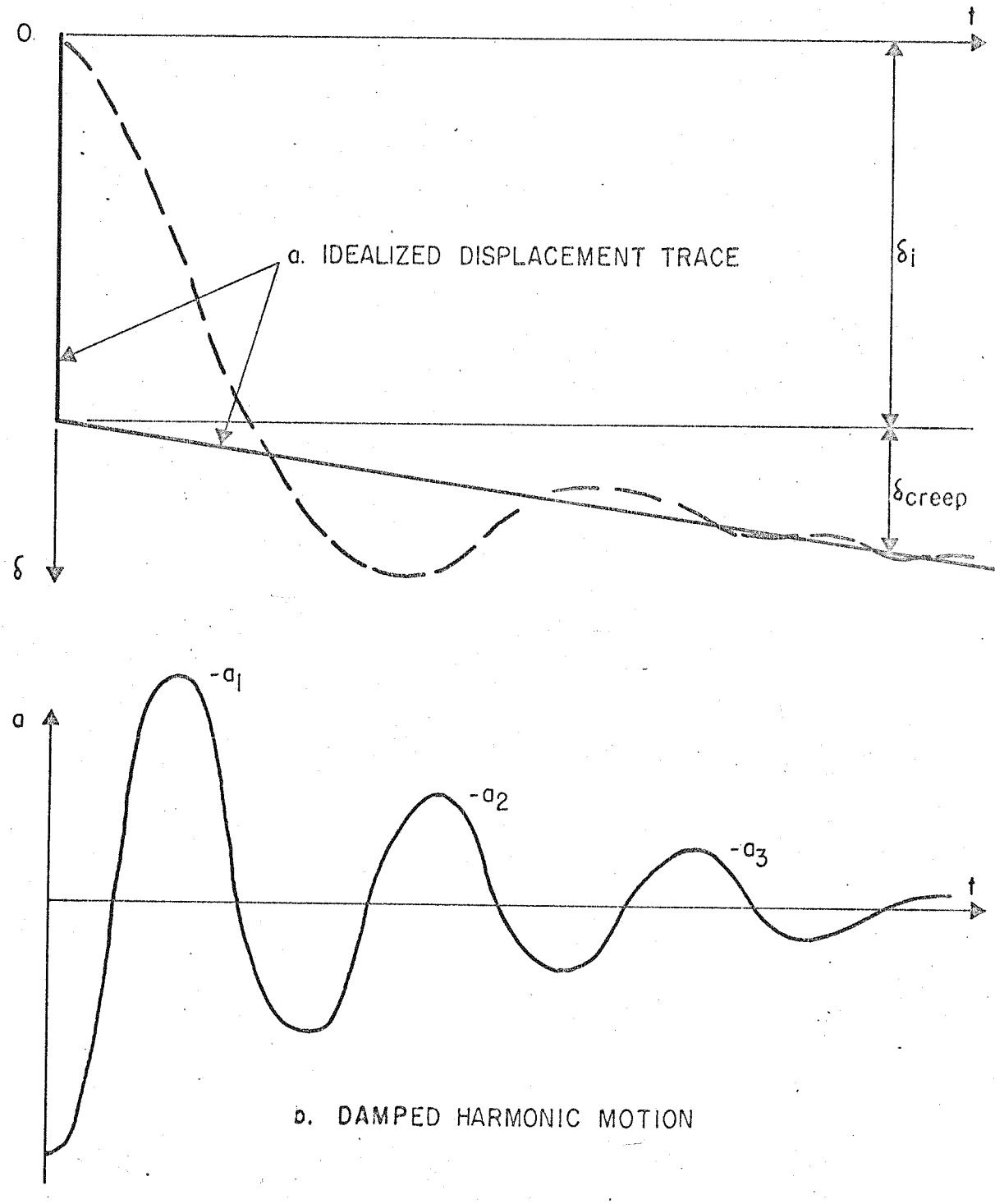

FIGURE 20. IDEALIZATIONS OF DYNAMIC TEST RESULTS

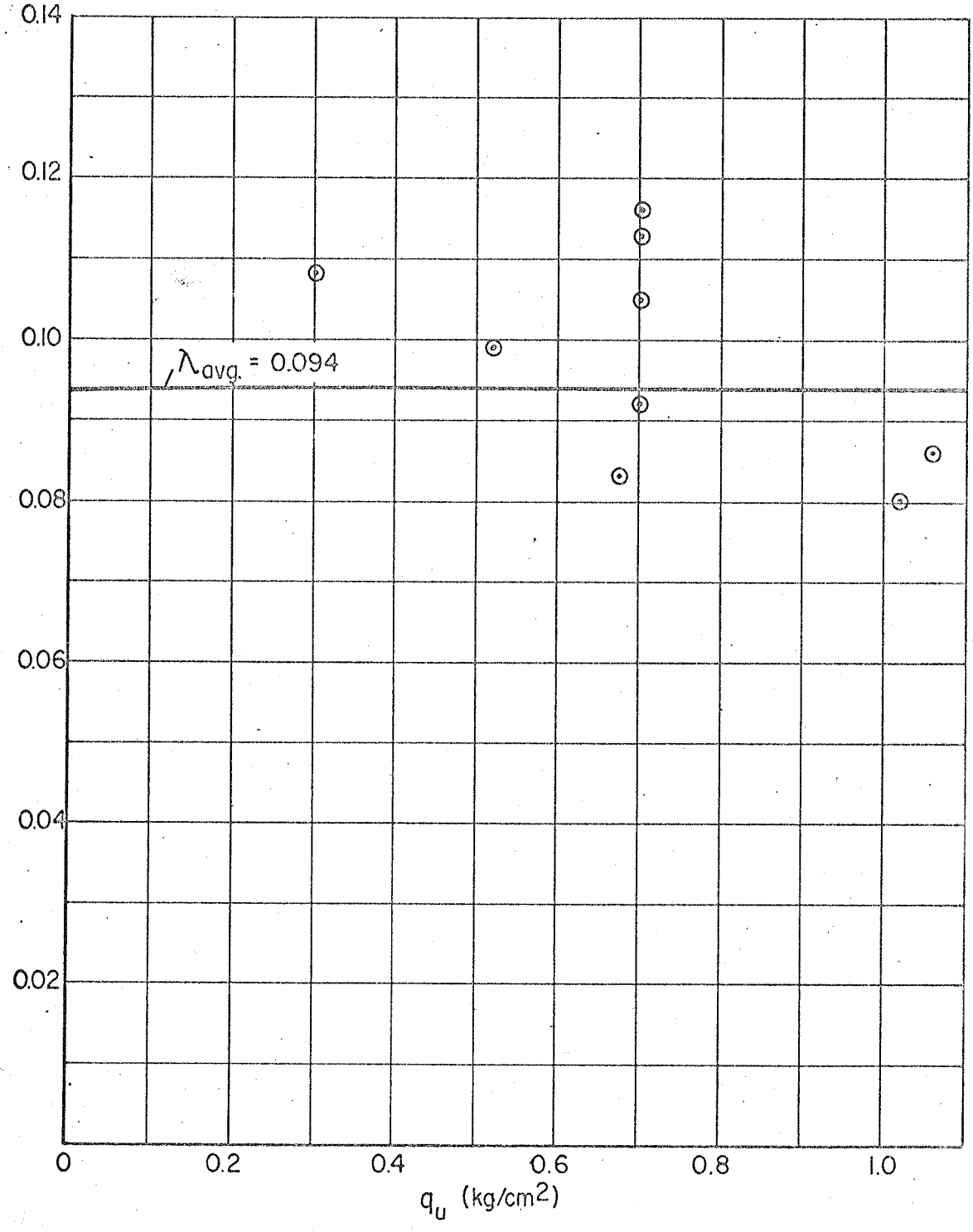

FIGURE 21. PERCENT CRITICAL DAMPING VS. COMPRESSIVE STRENGTH

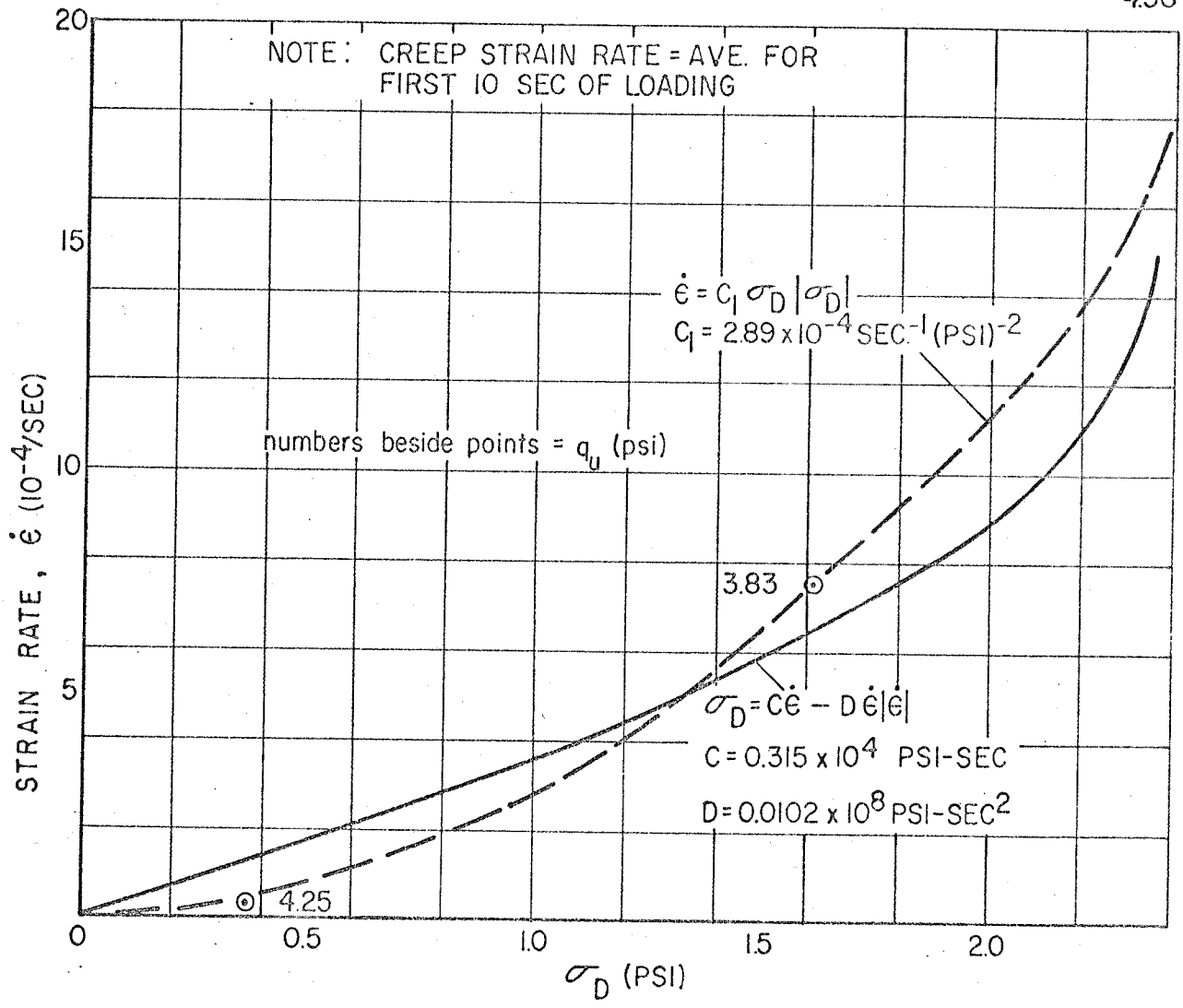

FIGURE 22. CREEP STRAIN RATE VS STRESS – SAMPLES OF 4 PSI STRENGTH

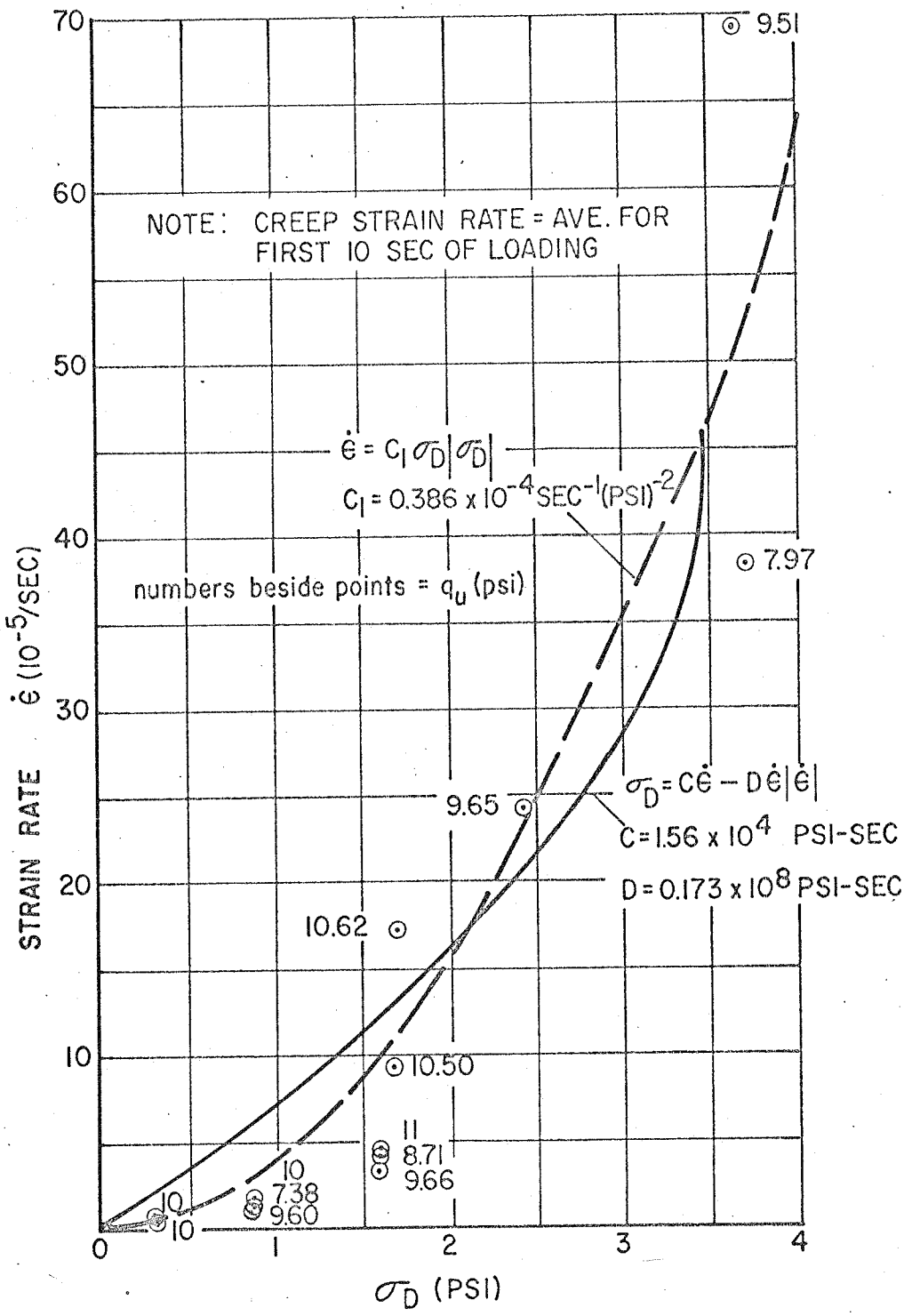

FIGURE 23. CREEP STRAIN RATE VS STRESS – SAMPLES OF 10 PSI STRENGTH

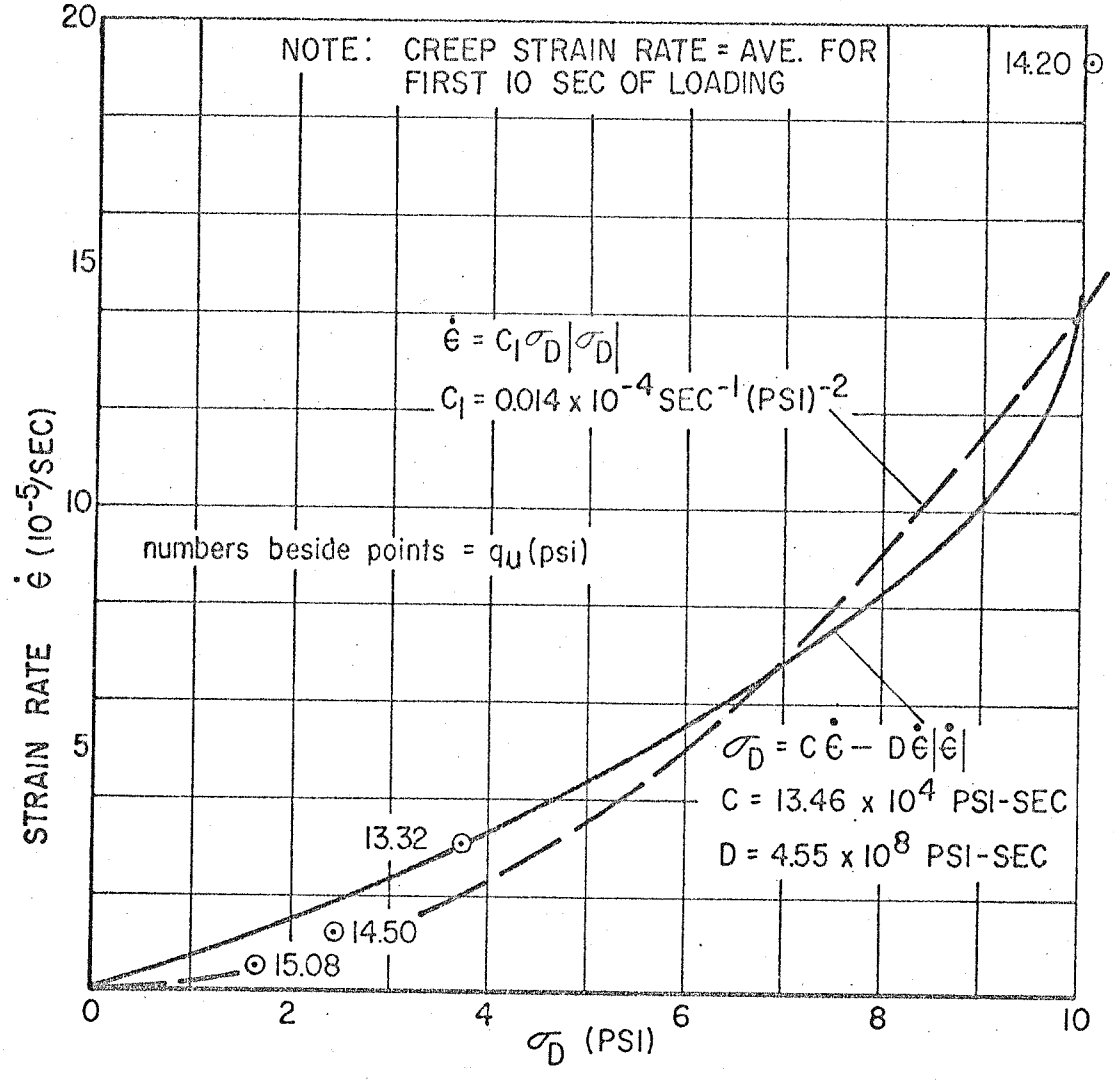

FIGURE 24. CREEP STRAIN RATE VS STRESS – SAMPLES OF 15 PSI STRENGTH

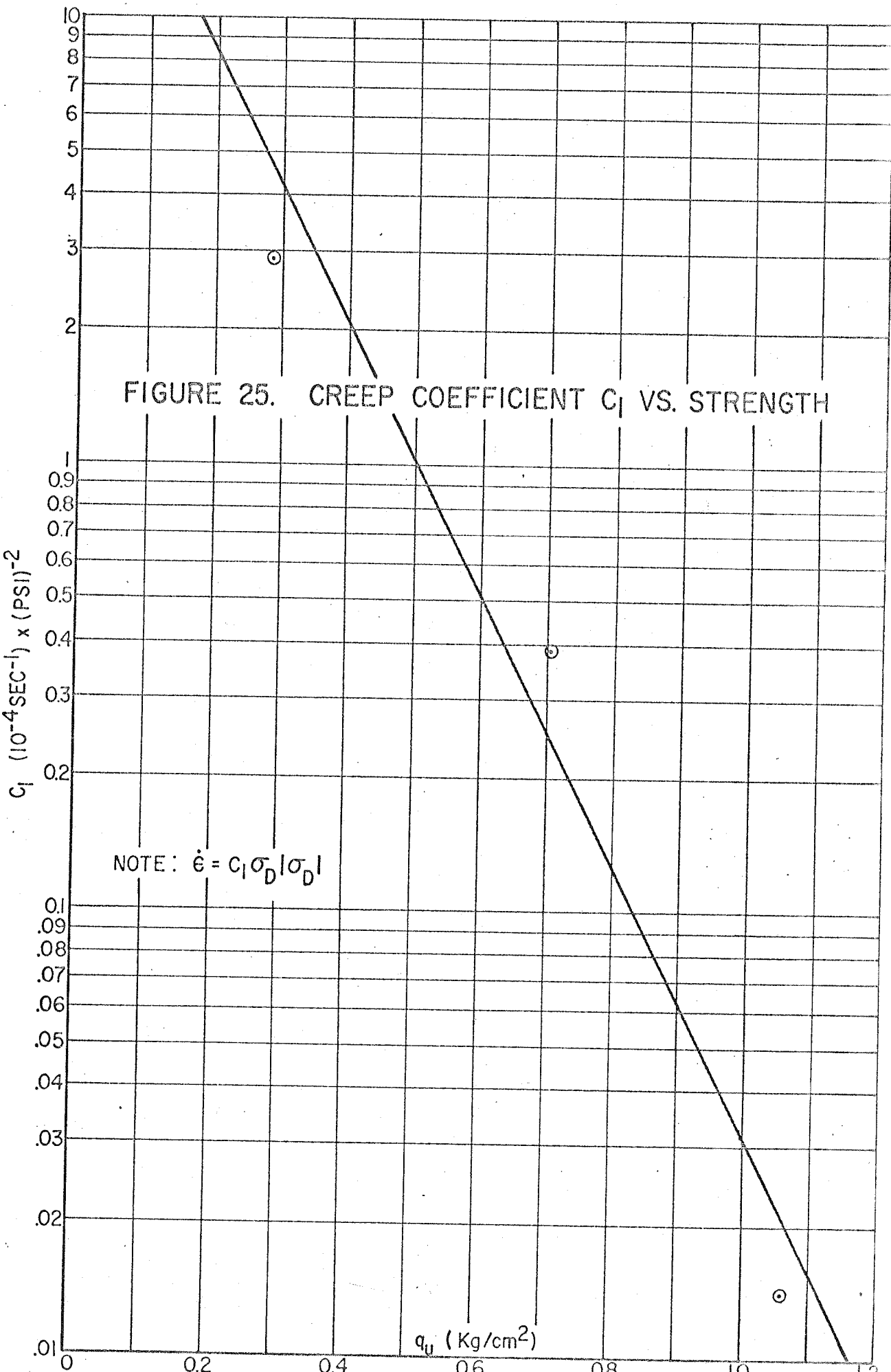

FIGURE 25. CREEP COEFFICIENT C_1 VS. STRENGTH

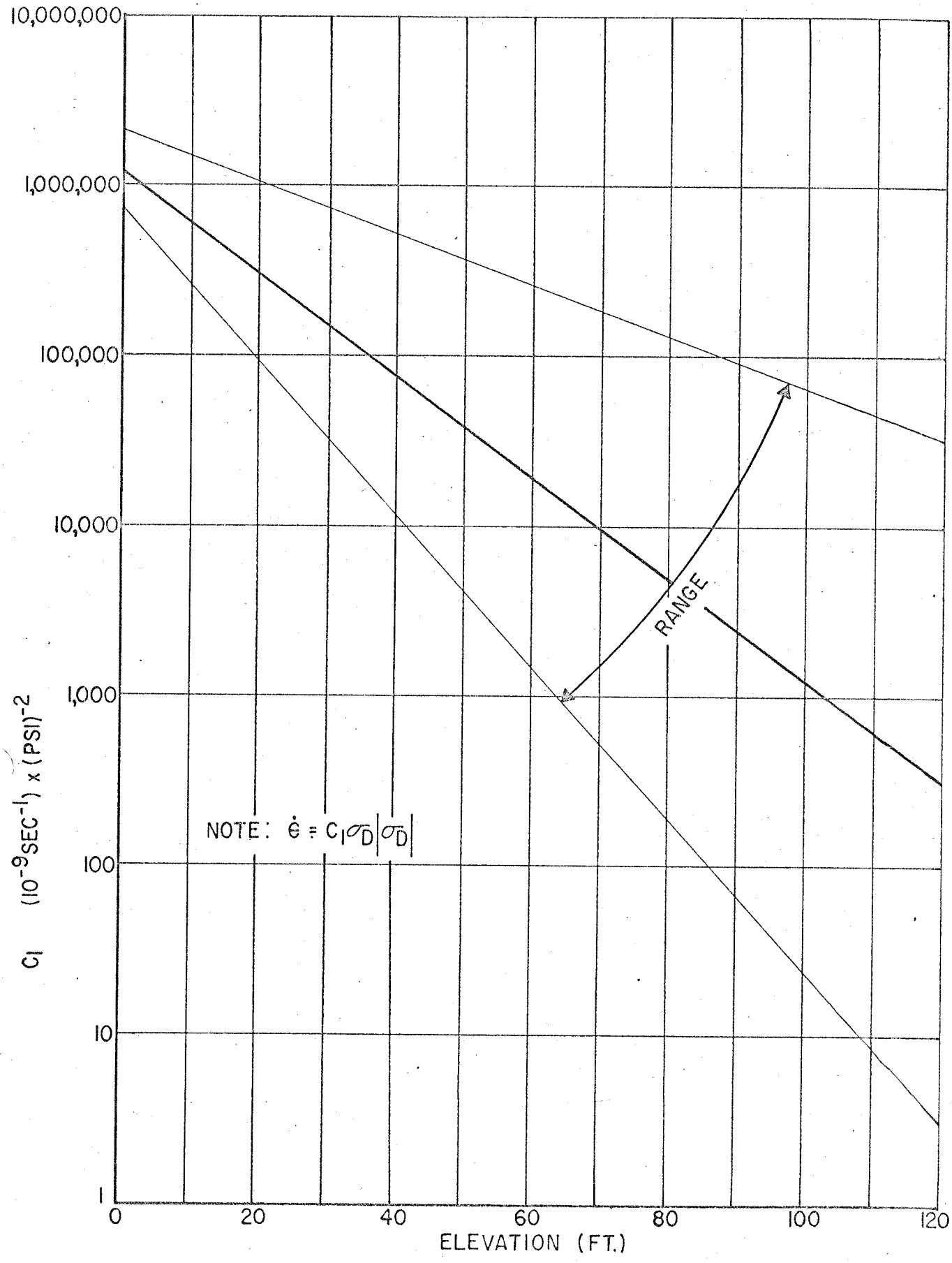

FIGURE 26. CREEP COEFFICIENT C_1 VS. ELEVATION

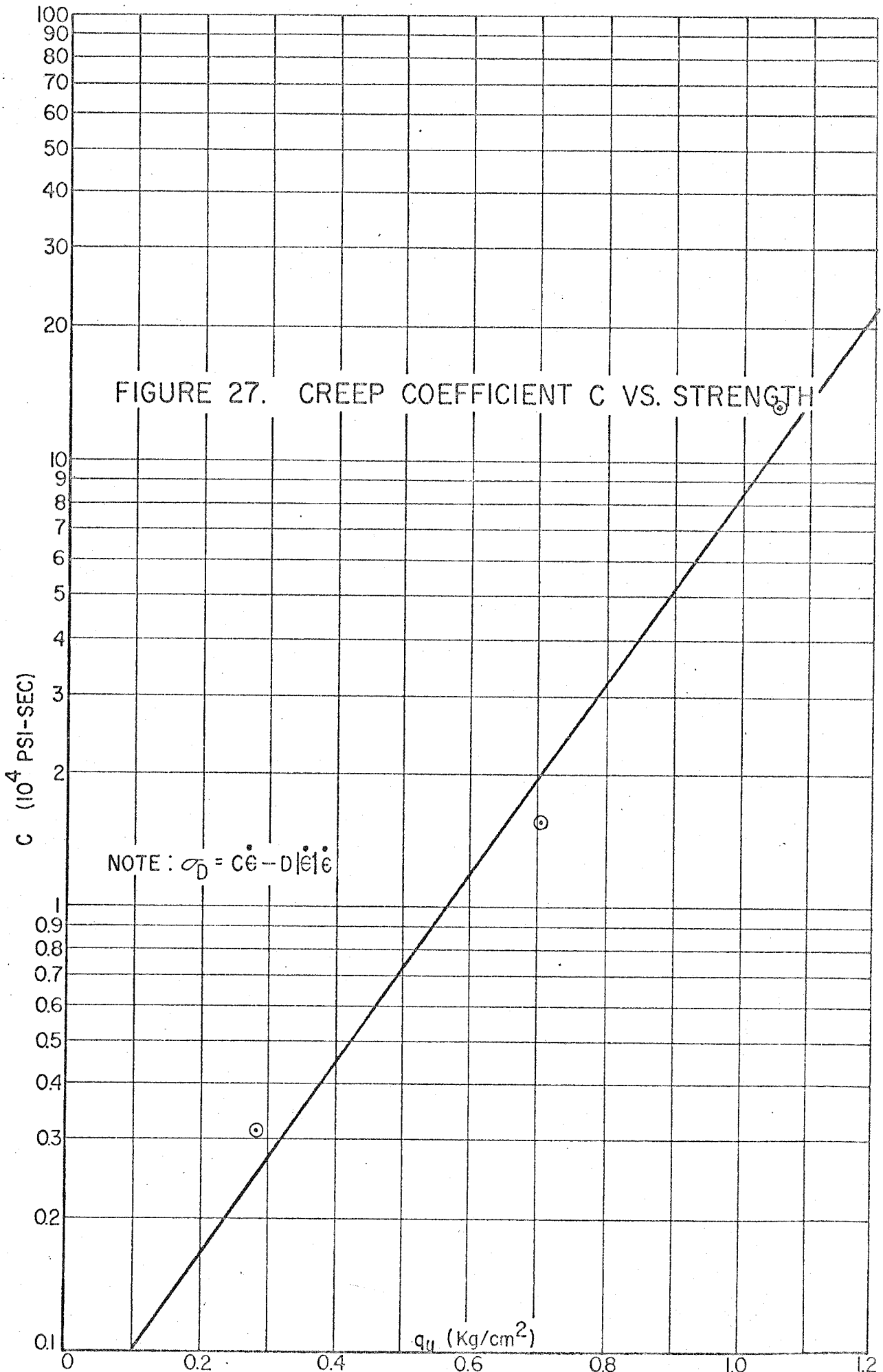

FIGURE 27. CREEP COEFFICIENT C VS. STRENGTH

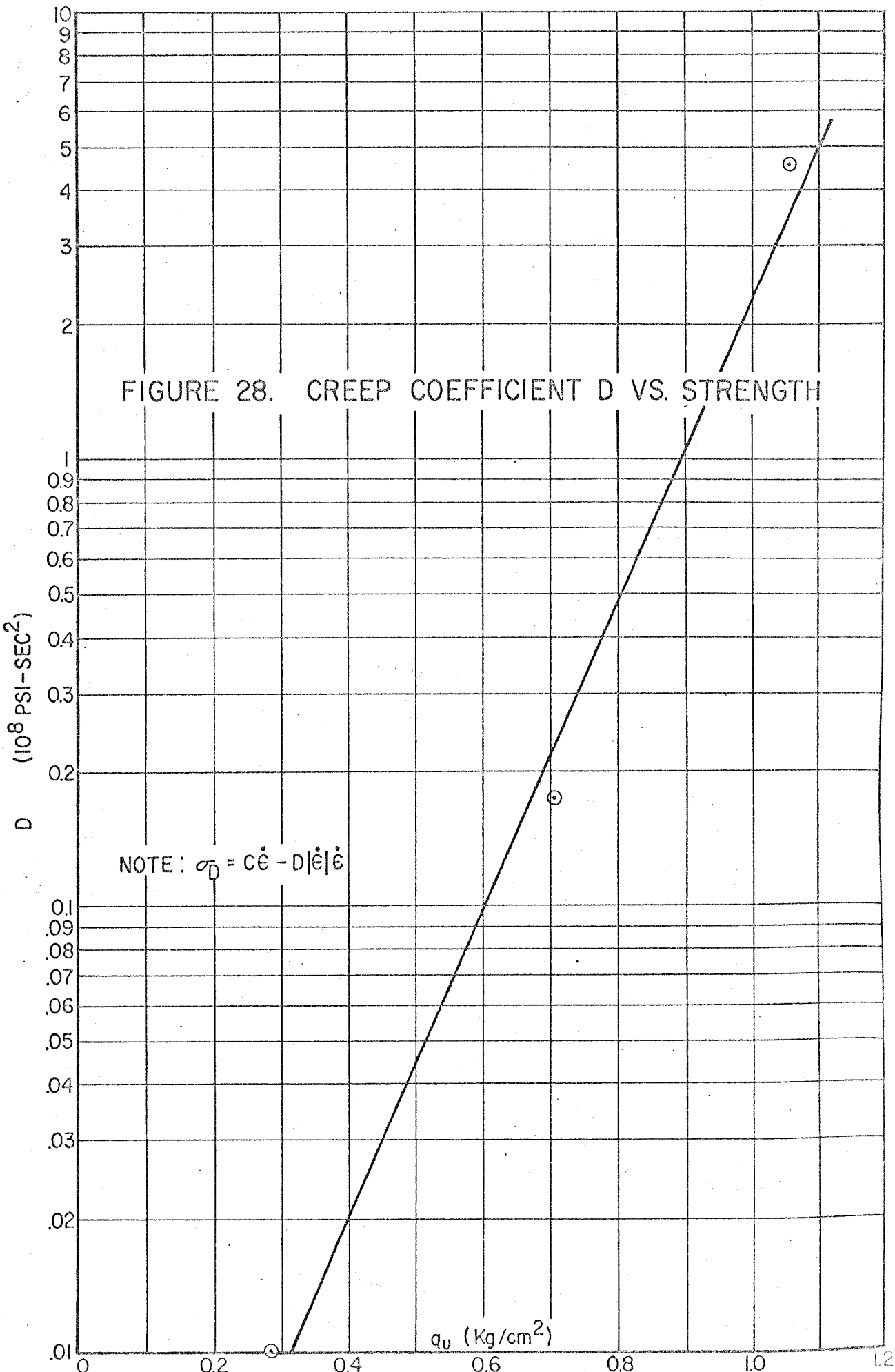

FIGURE 28. CREEP COEFFICIENT D VS. STRENGTH

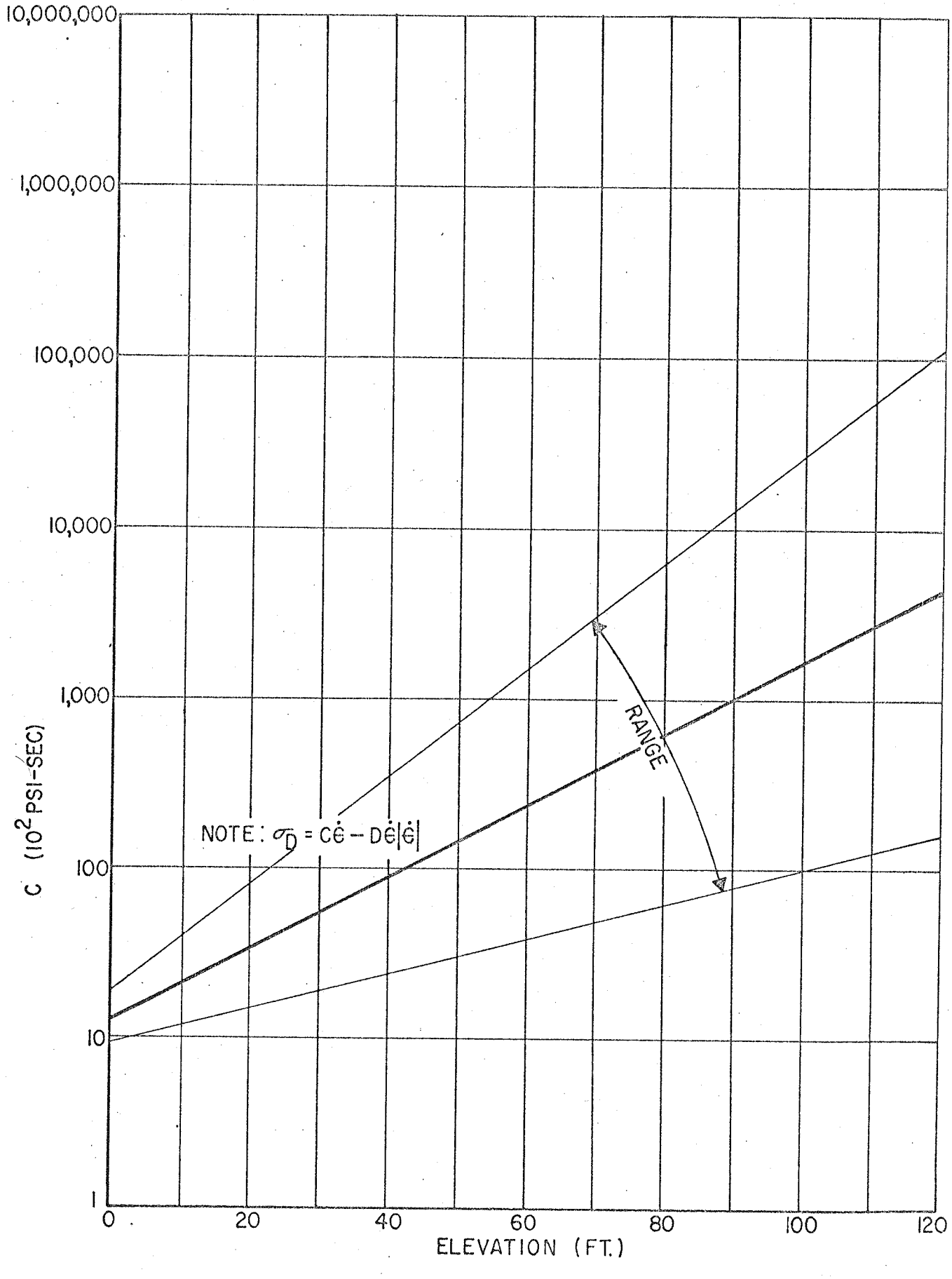

FIGURE 29. CREEP COEFFICIENT C VS. ELEVATION

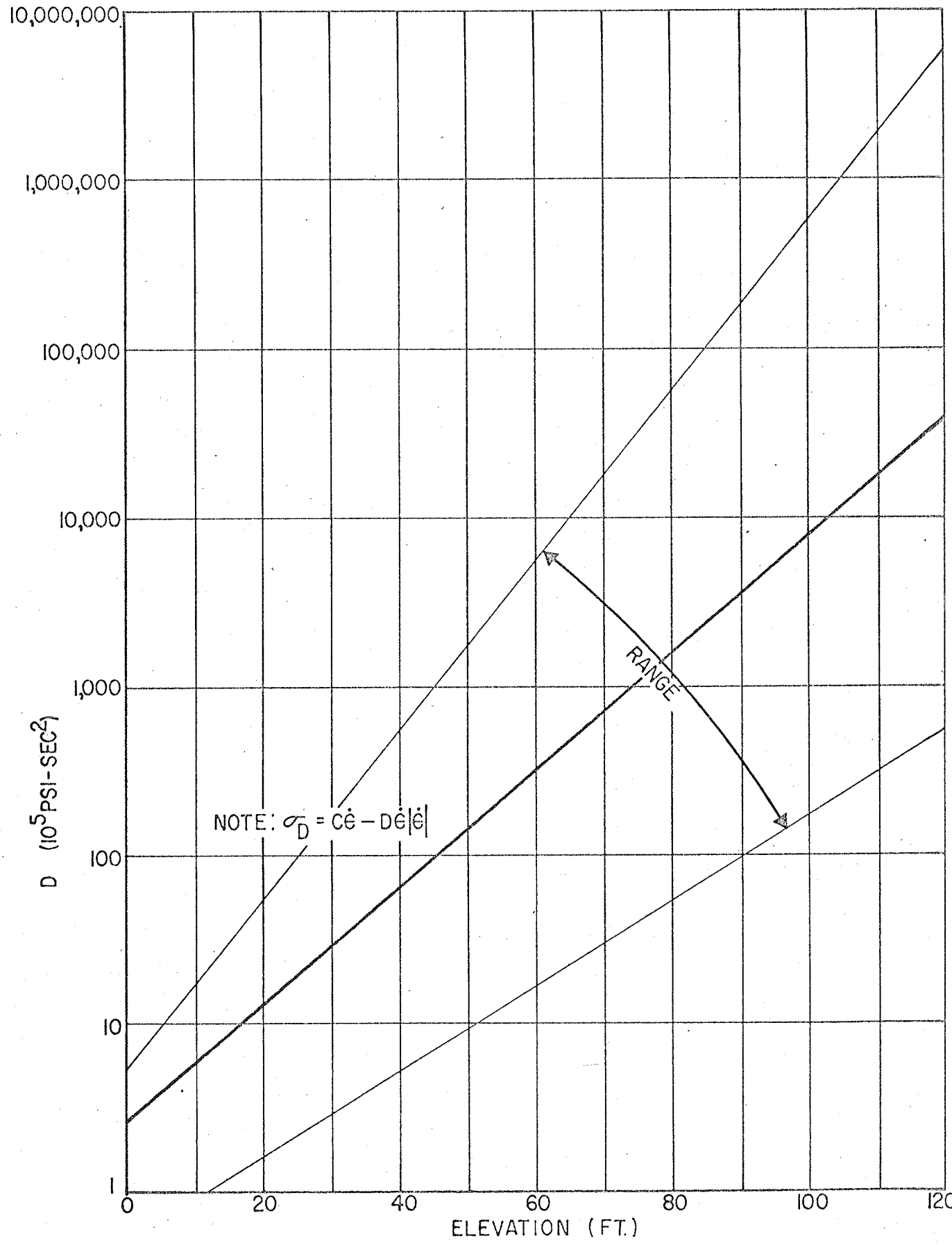

FIGURE 30. CREEP COEFFICIENT D VS. ELEVATION

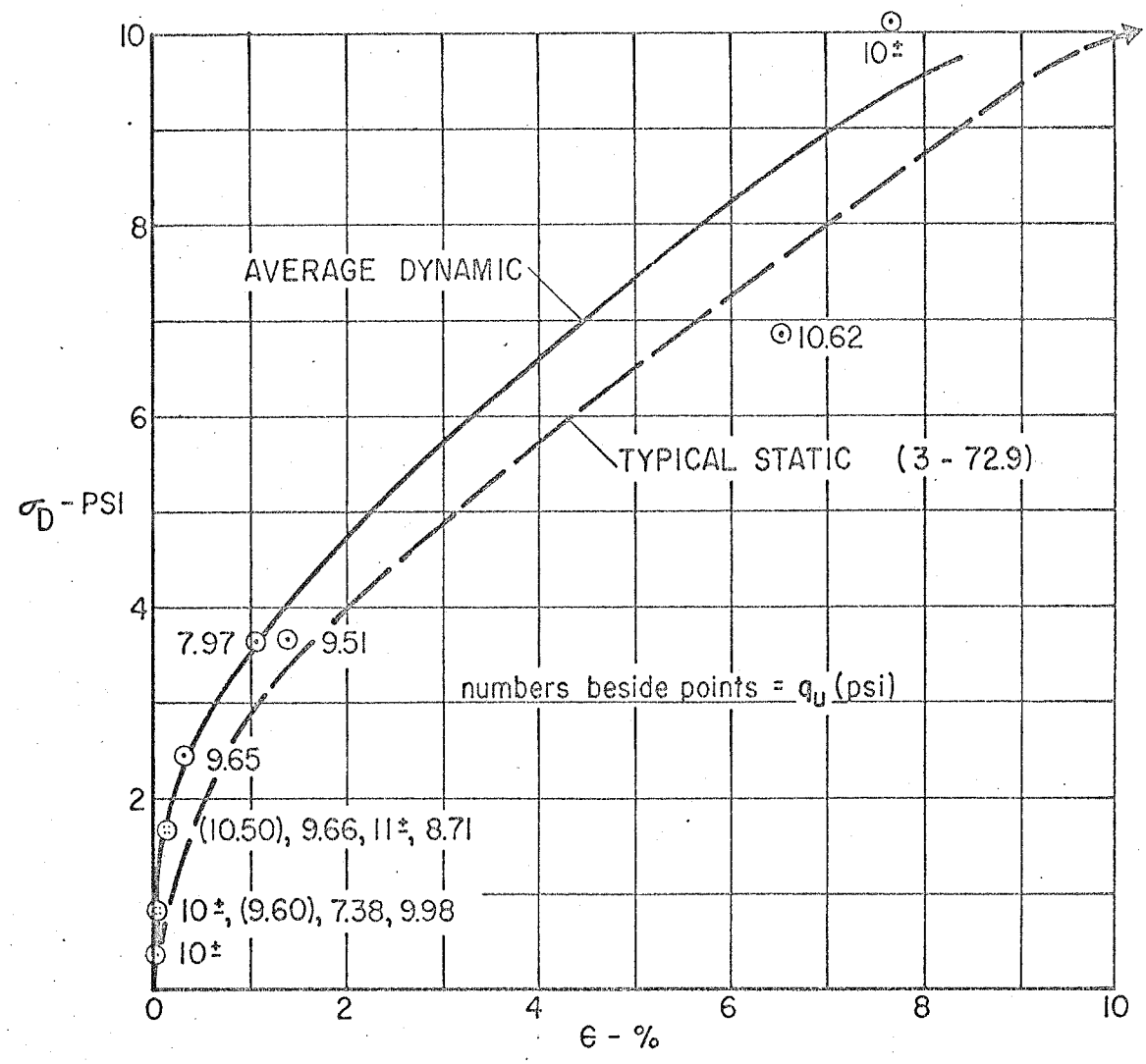

FIGURE 31. STRESS-STRAIN RELATIONS - SAMPLES OF 10 PSI STRENGTH

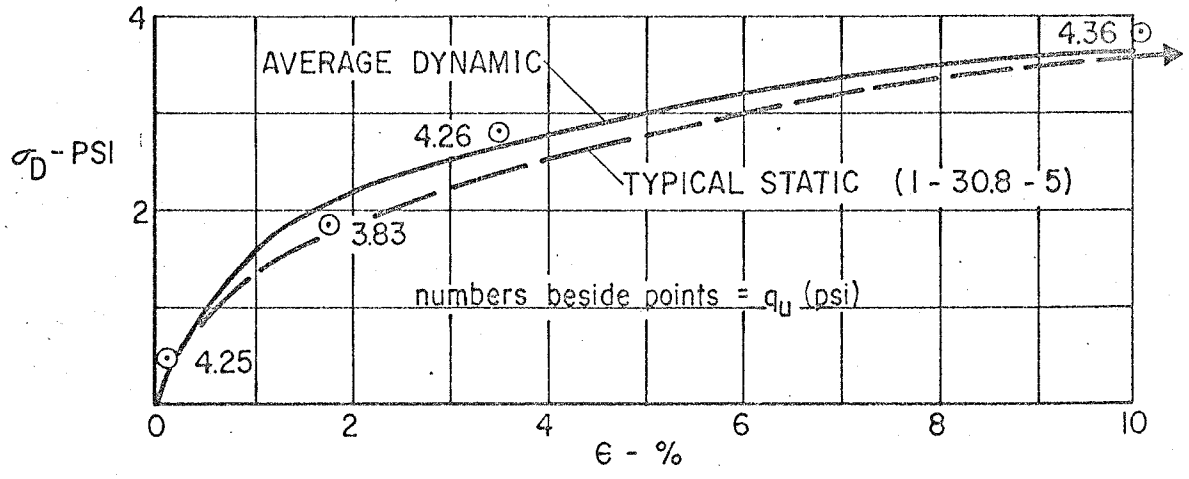

FIGURE 32. STRESS-STRAIN RELATIONS - SAMPLES OF 4 PSI STRENGTH

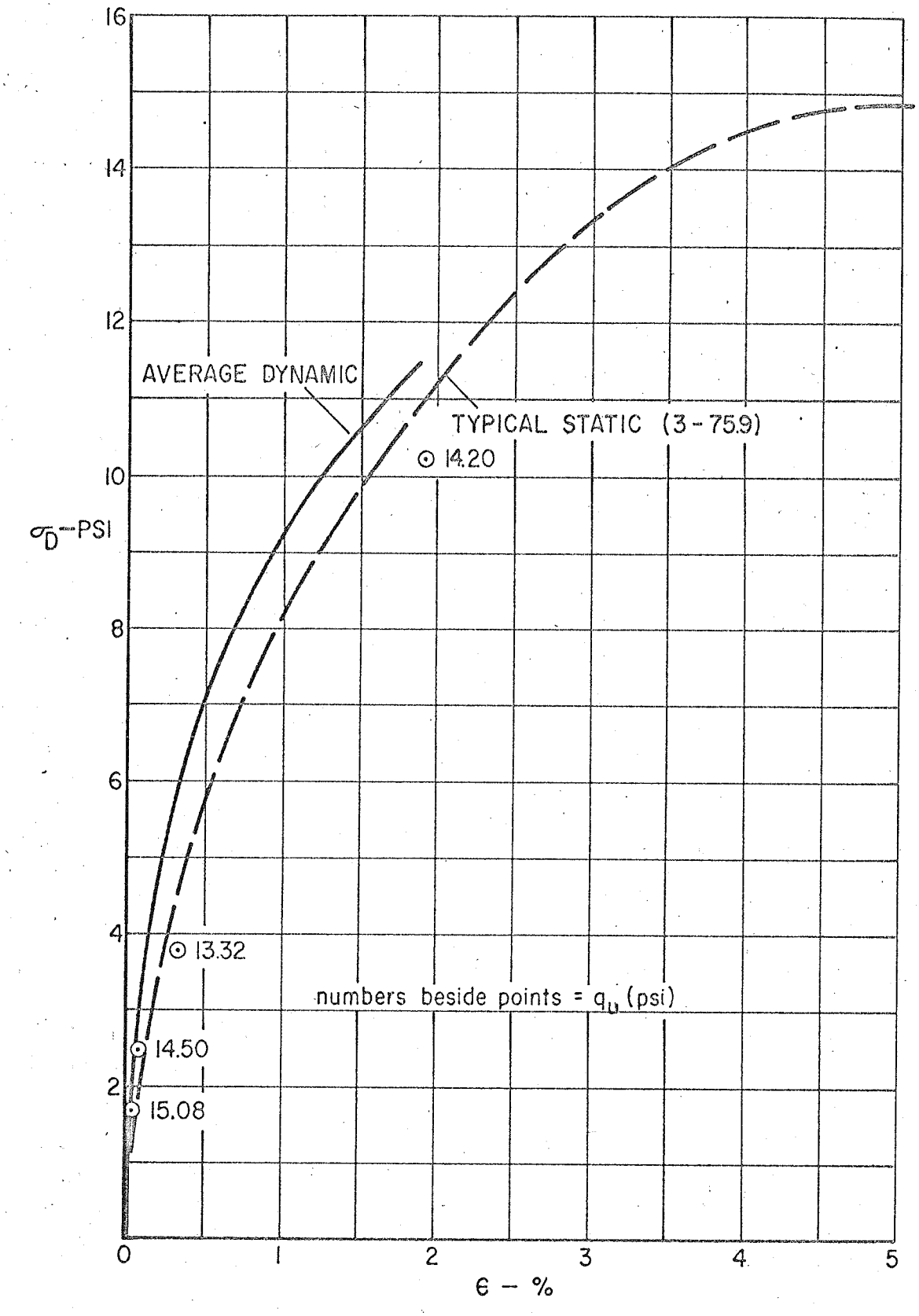

FIGURE 33. STRESS-STRAIN RELATIONS - SAMPLES OF 15 PSI STRENGTH

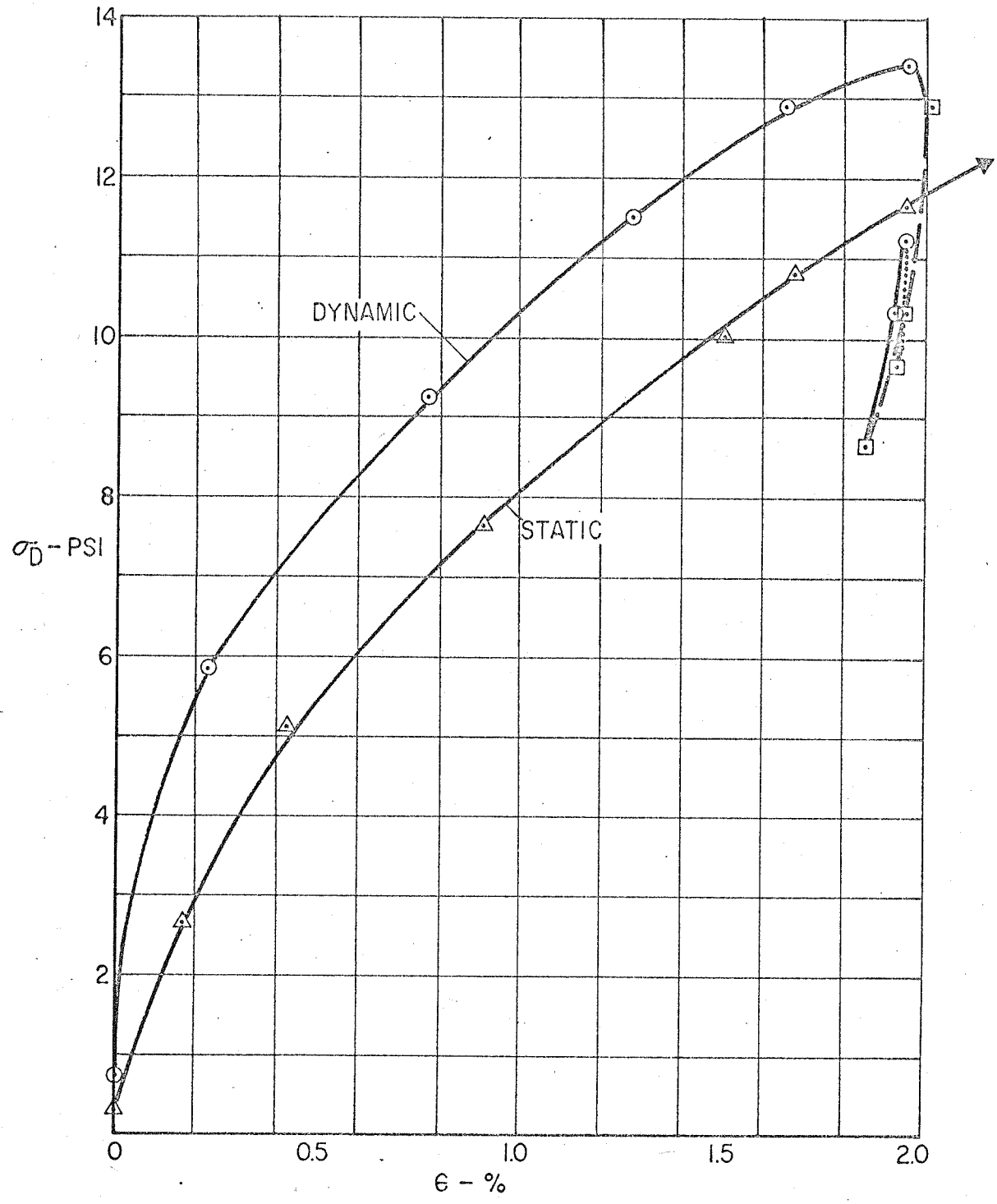

FIGURE 34. STRESS-STRAIN RELATIONS - SAMPLE 3 - 76.6 (q_u = 14.2 PSI)

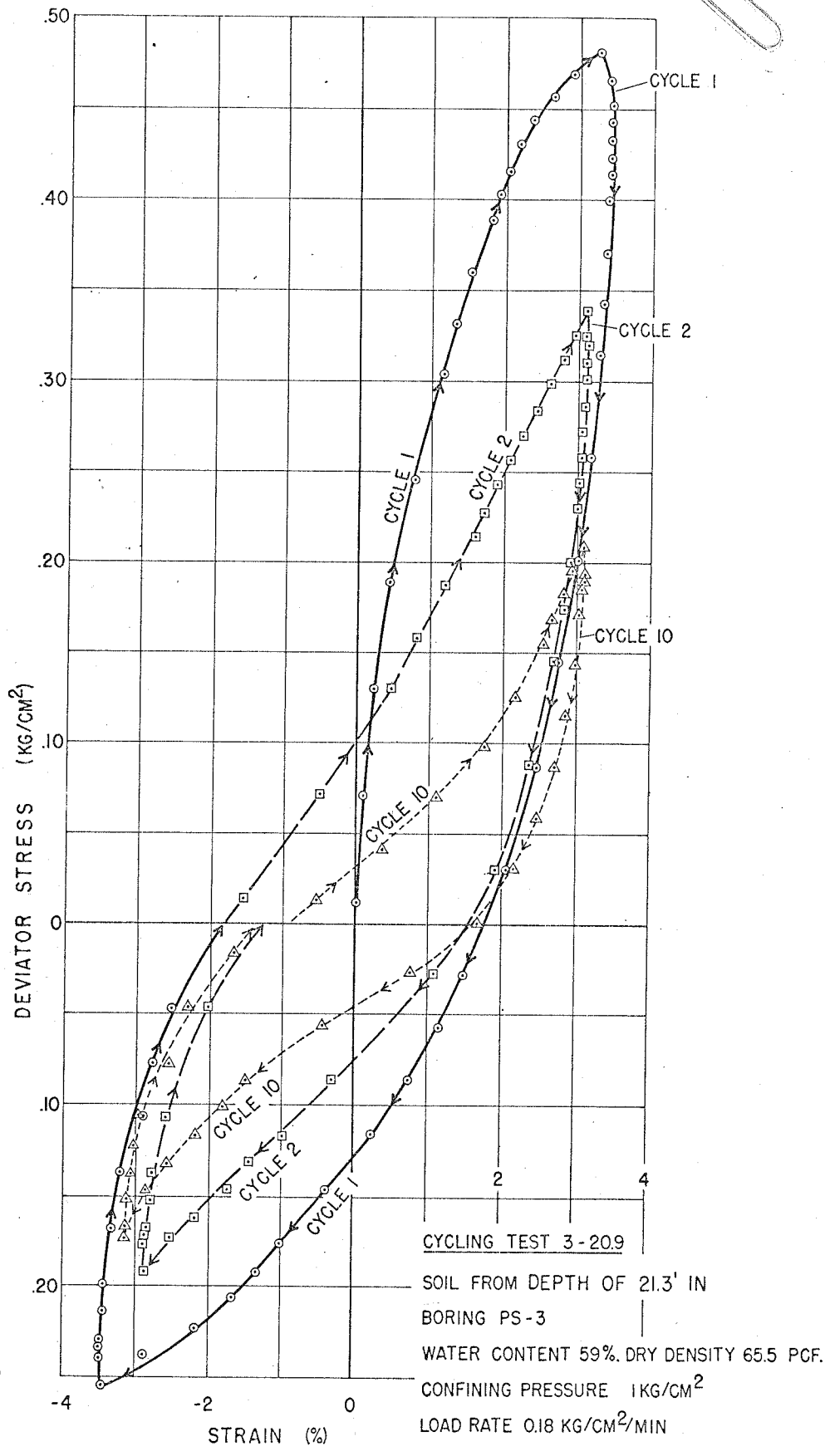

FIGURE 35. TYPICAL STRESS-STRAIN RELATIONSHIP IN CYCLIC LOADING TEST

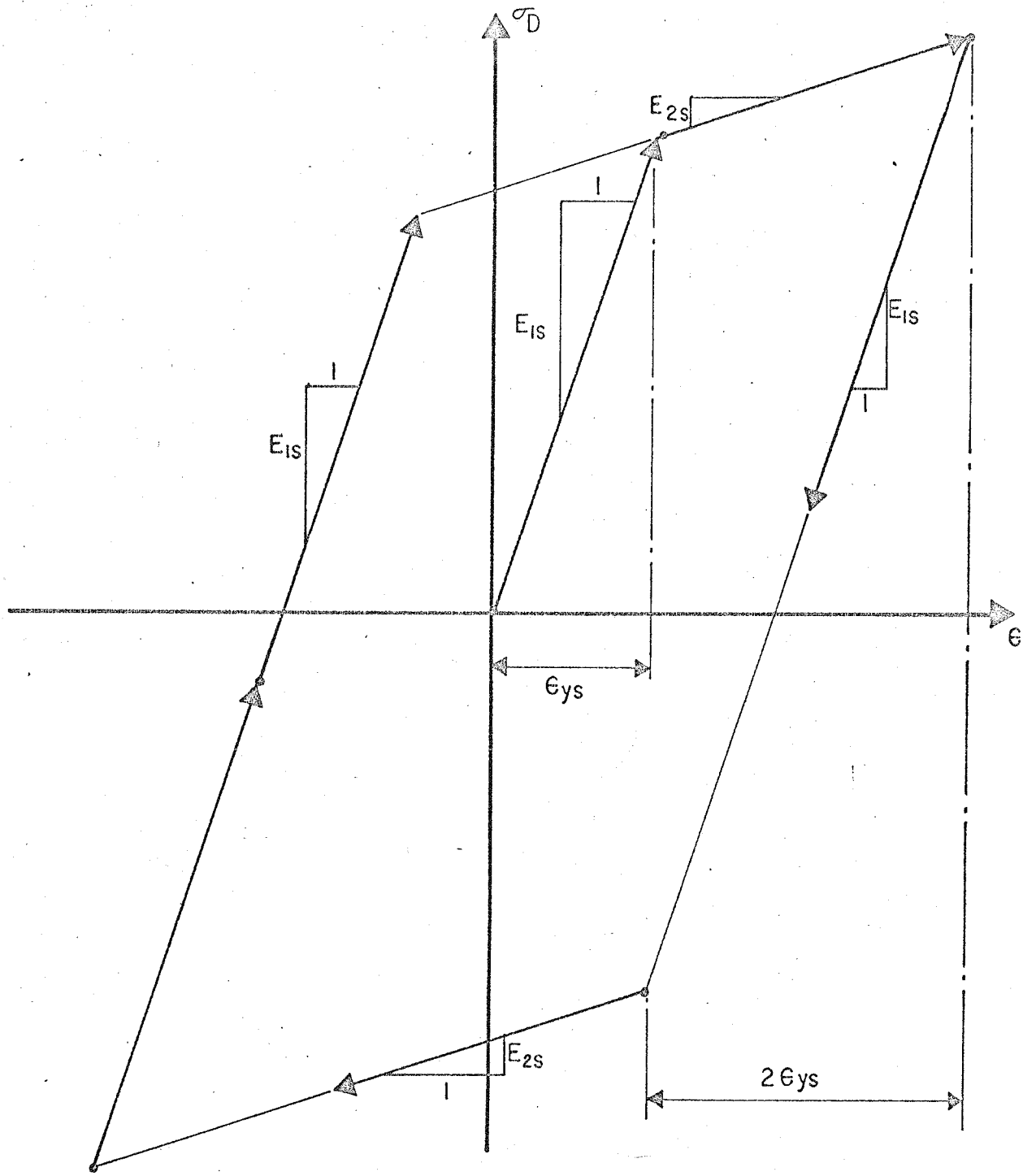

FIGURE 36. IDEALIZATION OF STRESS STRAIN RELATIONSHIP IN CYCLIC LOADING TEST

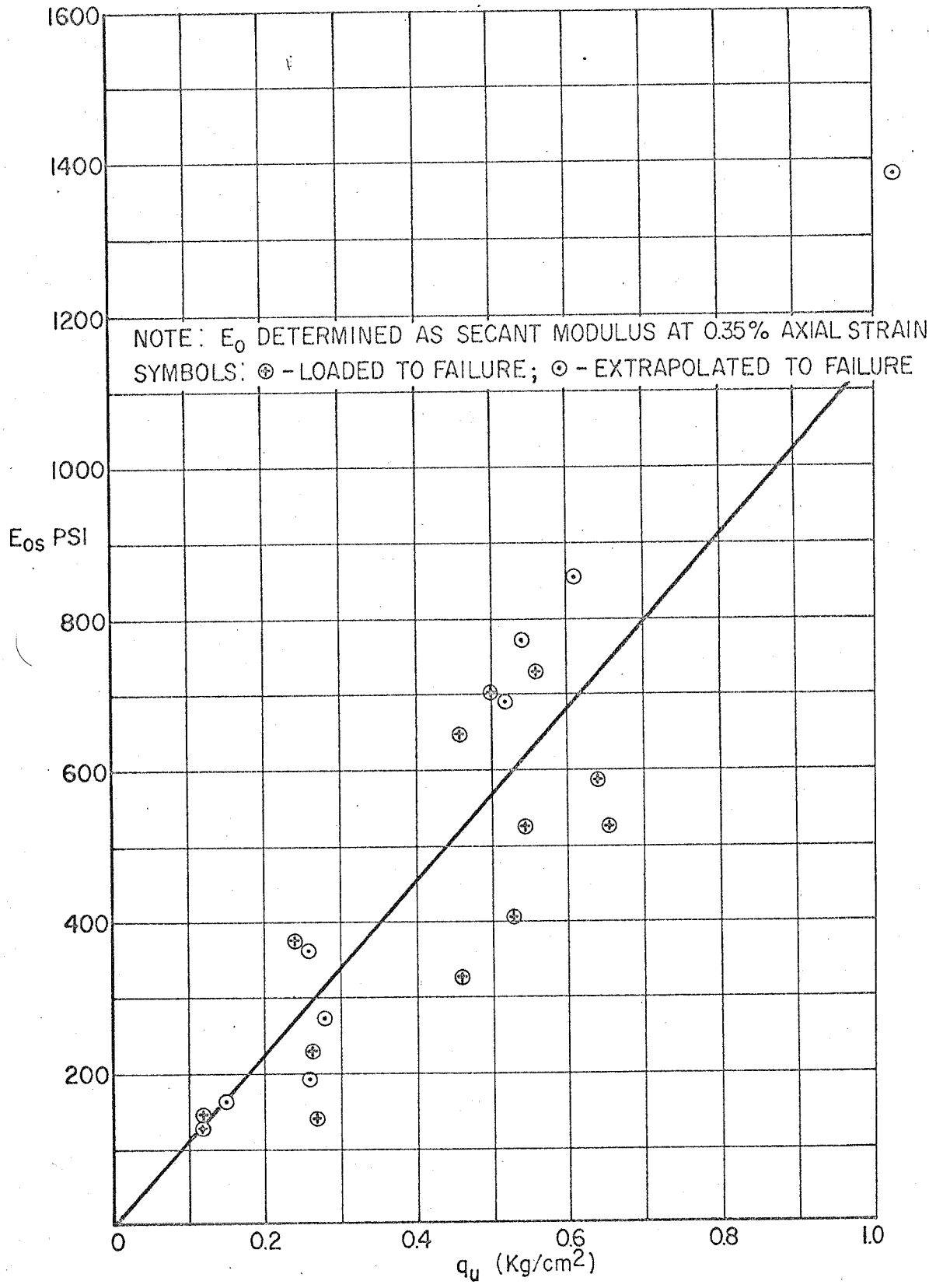

FIGURE 37. E_{os} VS. STRENGTH - STATIC LOADING

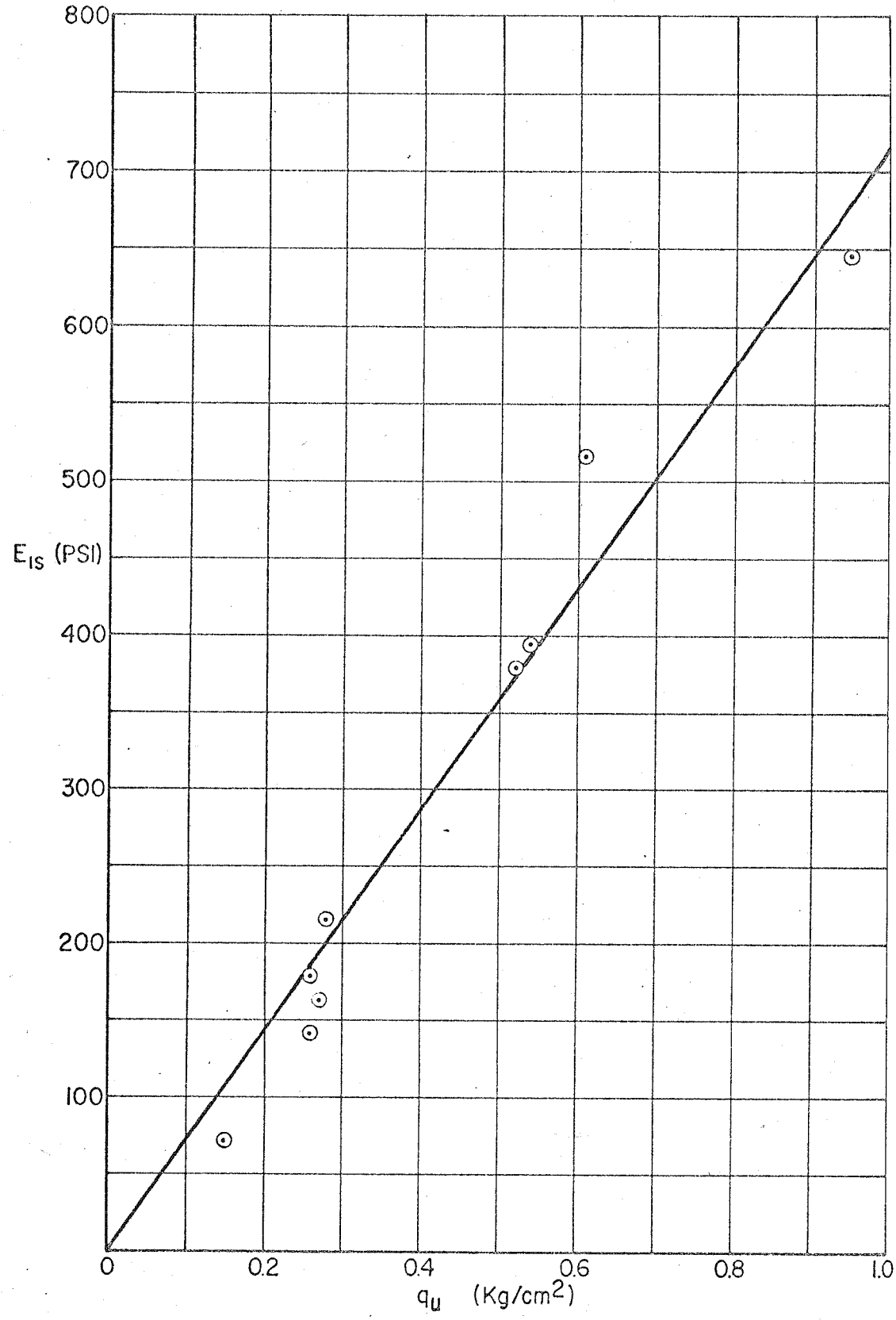

FIGURE 38. E_{IS} VS. STRENGTH – STATIC LOADING

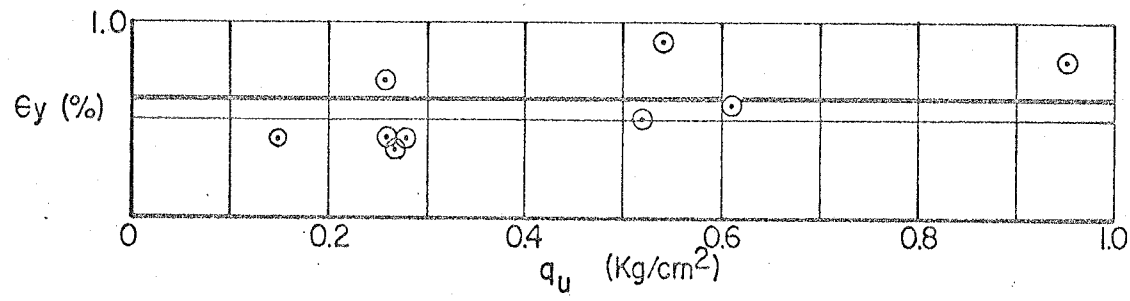

FIGURE 40. ϵ_y VS. STRENGTH – STATIC LOADING

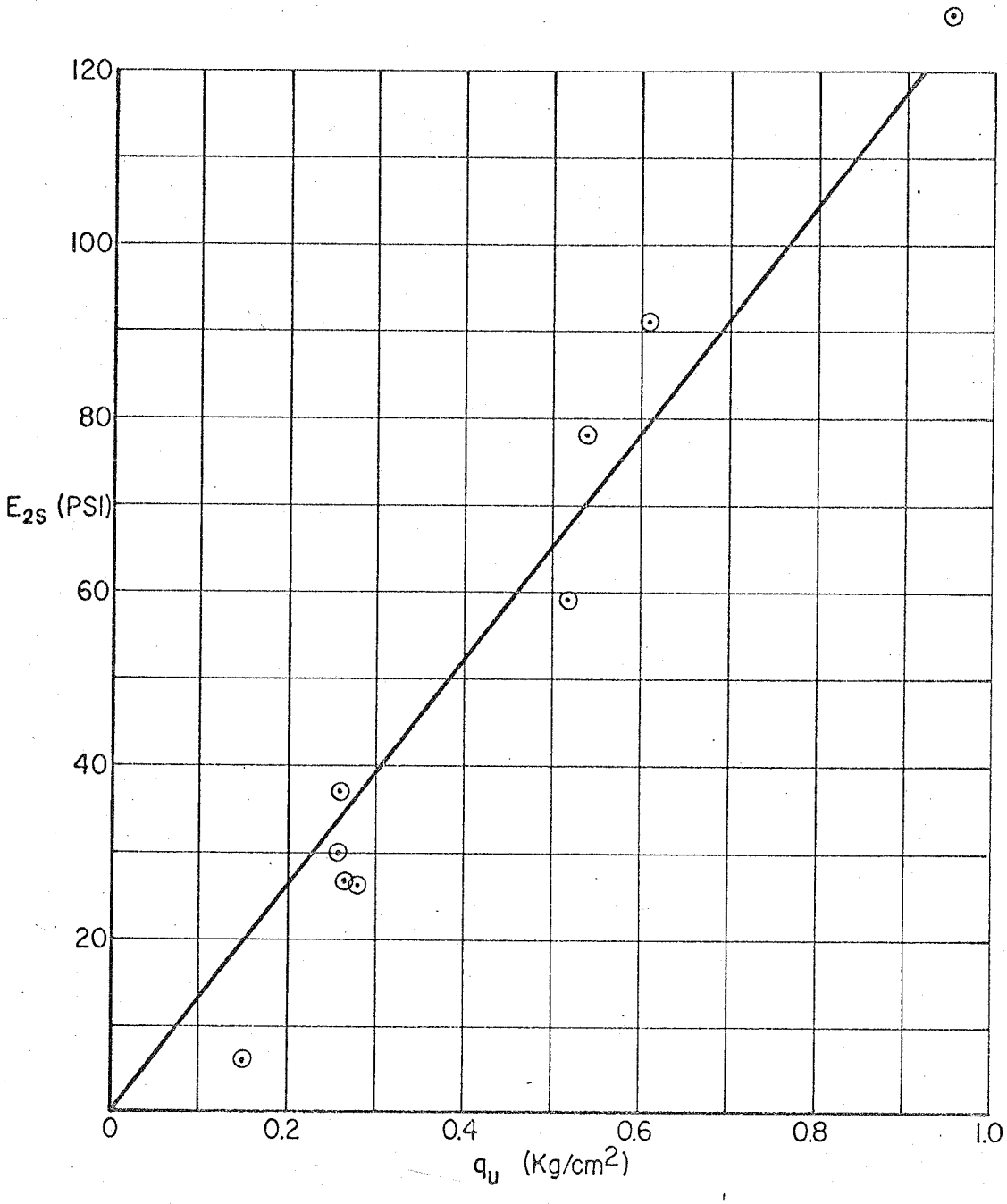

FIGURE 39. E_{2s} VS. STRENGTH – STATIC LOADING

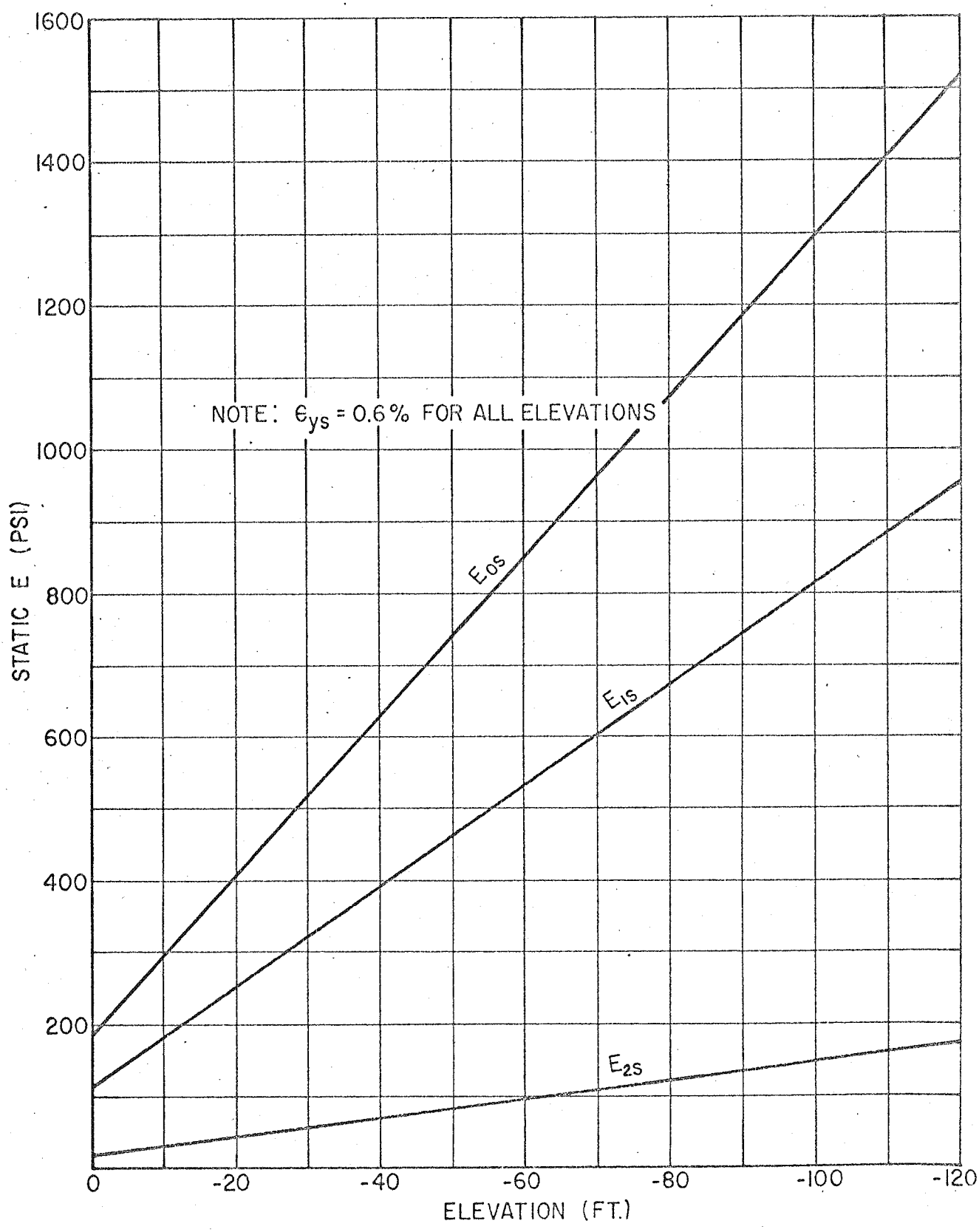

FIGURE 41. STATIC ELASTIC MODULI VS. ELEVATION

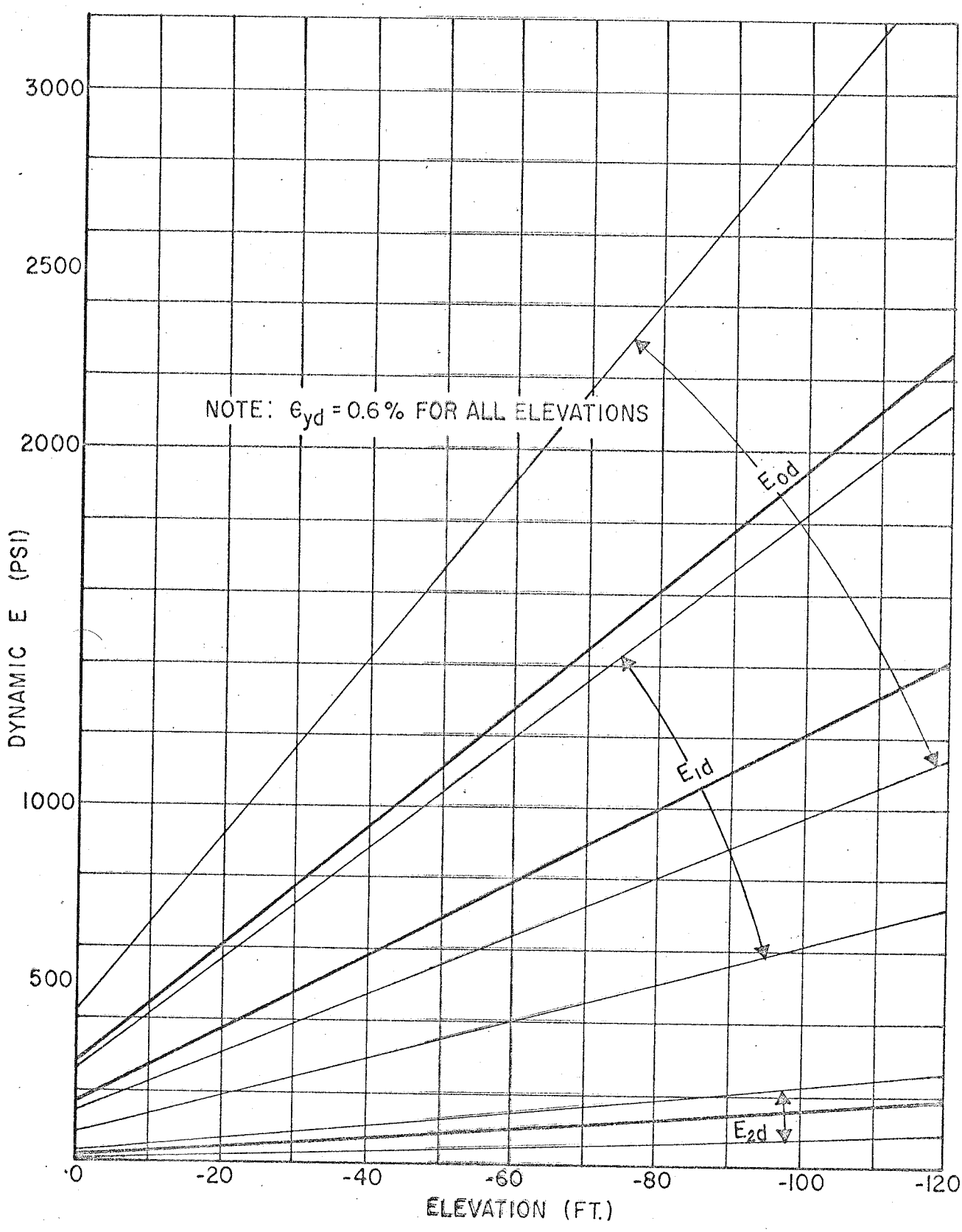

FIGURE 42. DYNAMIC ELASTIC MODULI VS. ELEVATION

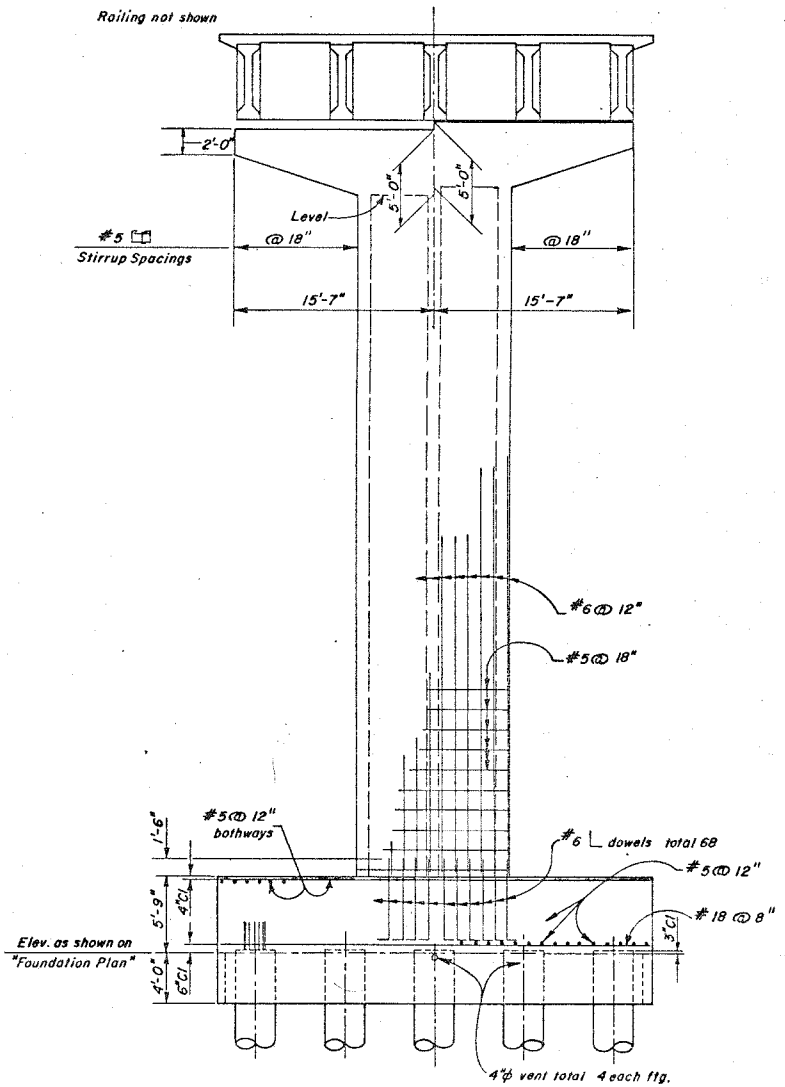

ELEVATION OF TYPICAL PIER
SCALE: 3/16" = 1'-0"

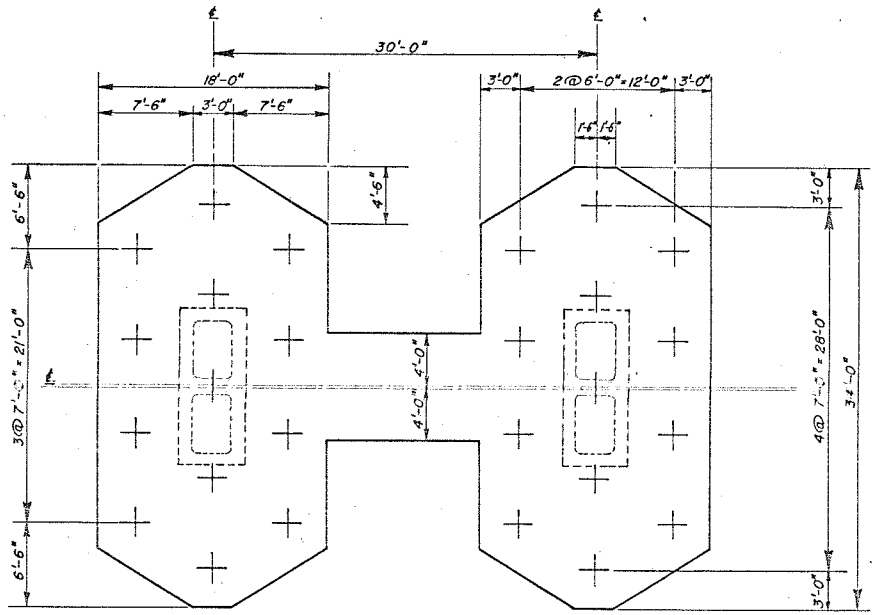

PLAN OF PILE CAP FOR THE TWO MULTIPLE ROW GROUPINGS
SCALE: 3/16" = 1'-0"

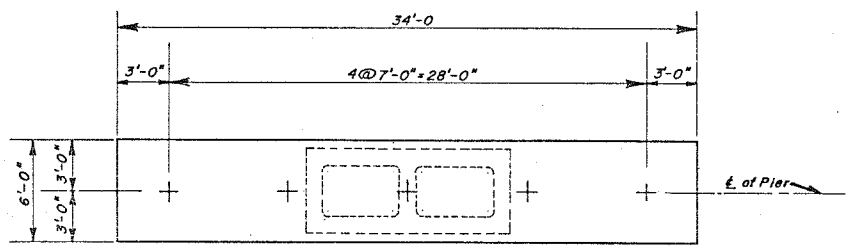

PLAN OF PILE CAP FOR SINGLE ROW GROUPING
SCALE: 1/4" = 1'-0"

Fig. 43-DETAILS OF BRIDGE STRUCTURE.

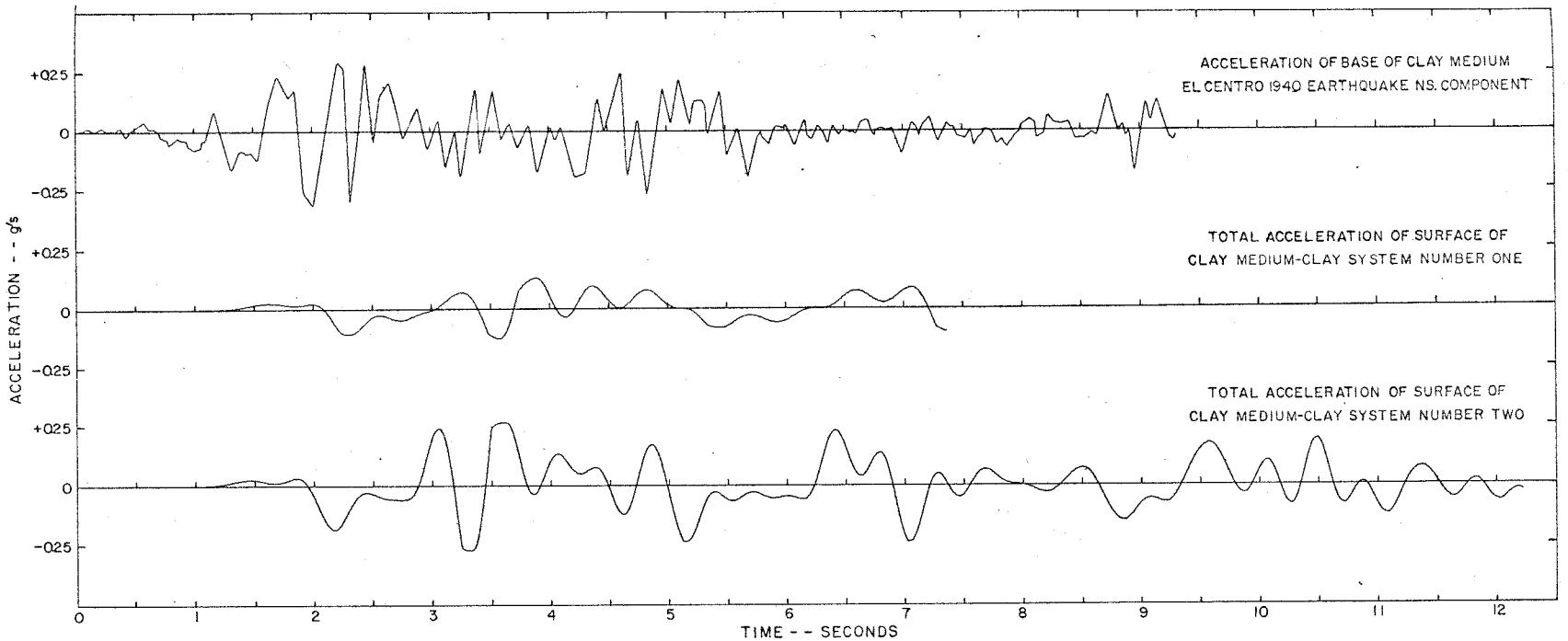

Fig. 44- ACCELERATION VS. TIME CURVES AT BASE AND SURFACE OF CLAY MEDIUMS.

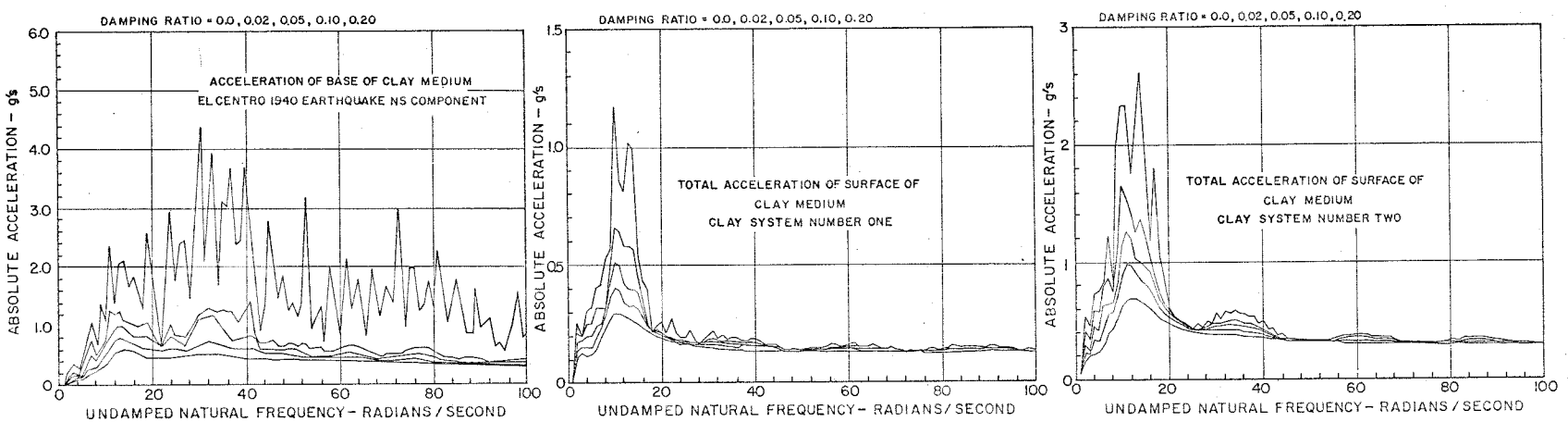

Fig. 45- ABSOLUTE ACCELERATION RESPONSE SPECTRA VS. UNDAMPED NATURAL FREQUENCY.

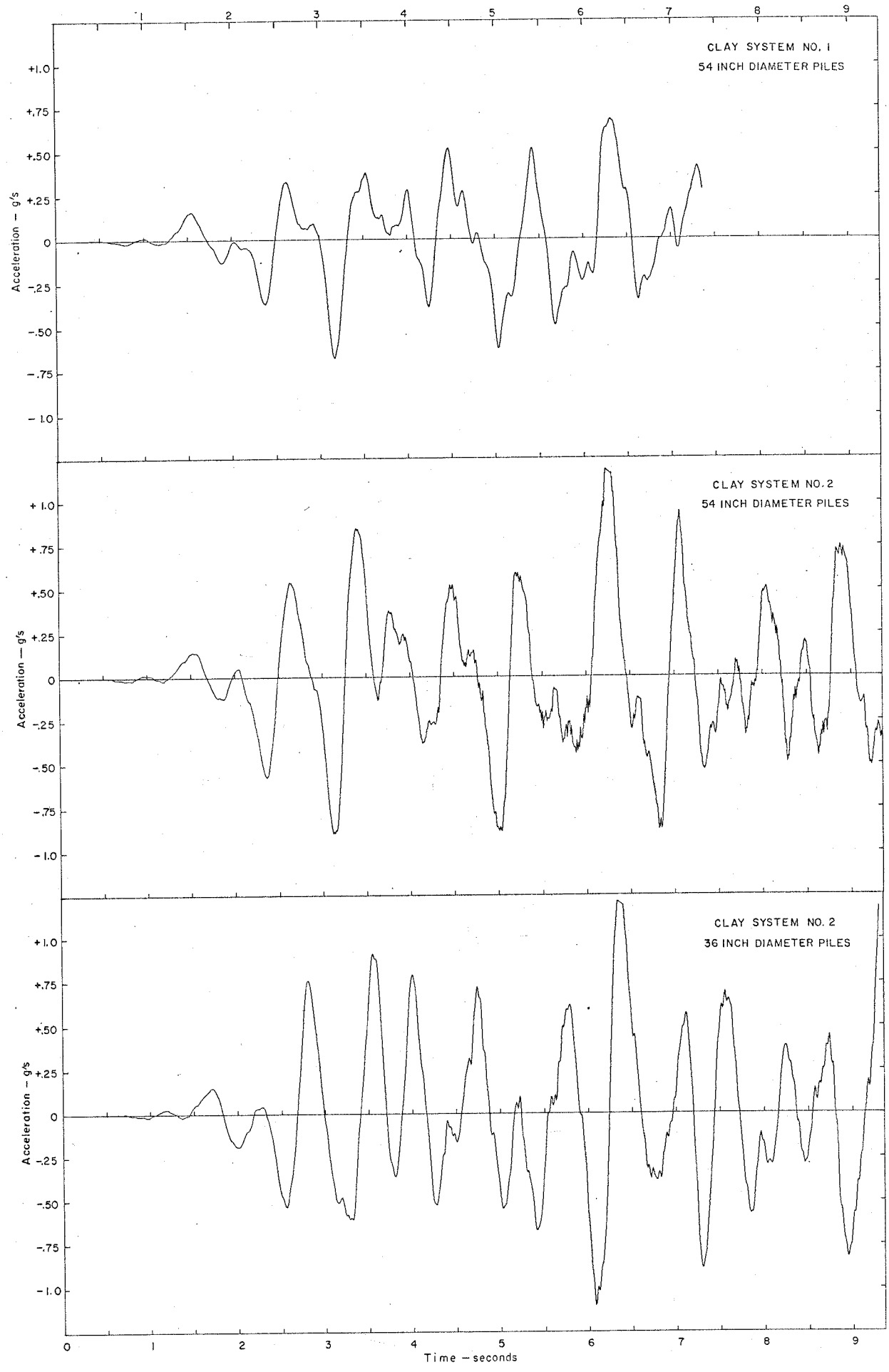

Fig. 46- TOTAL LONGITUDINAL ACCELERATION OF BRIDGE DECK.

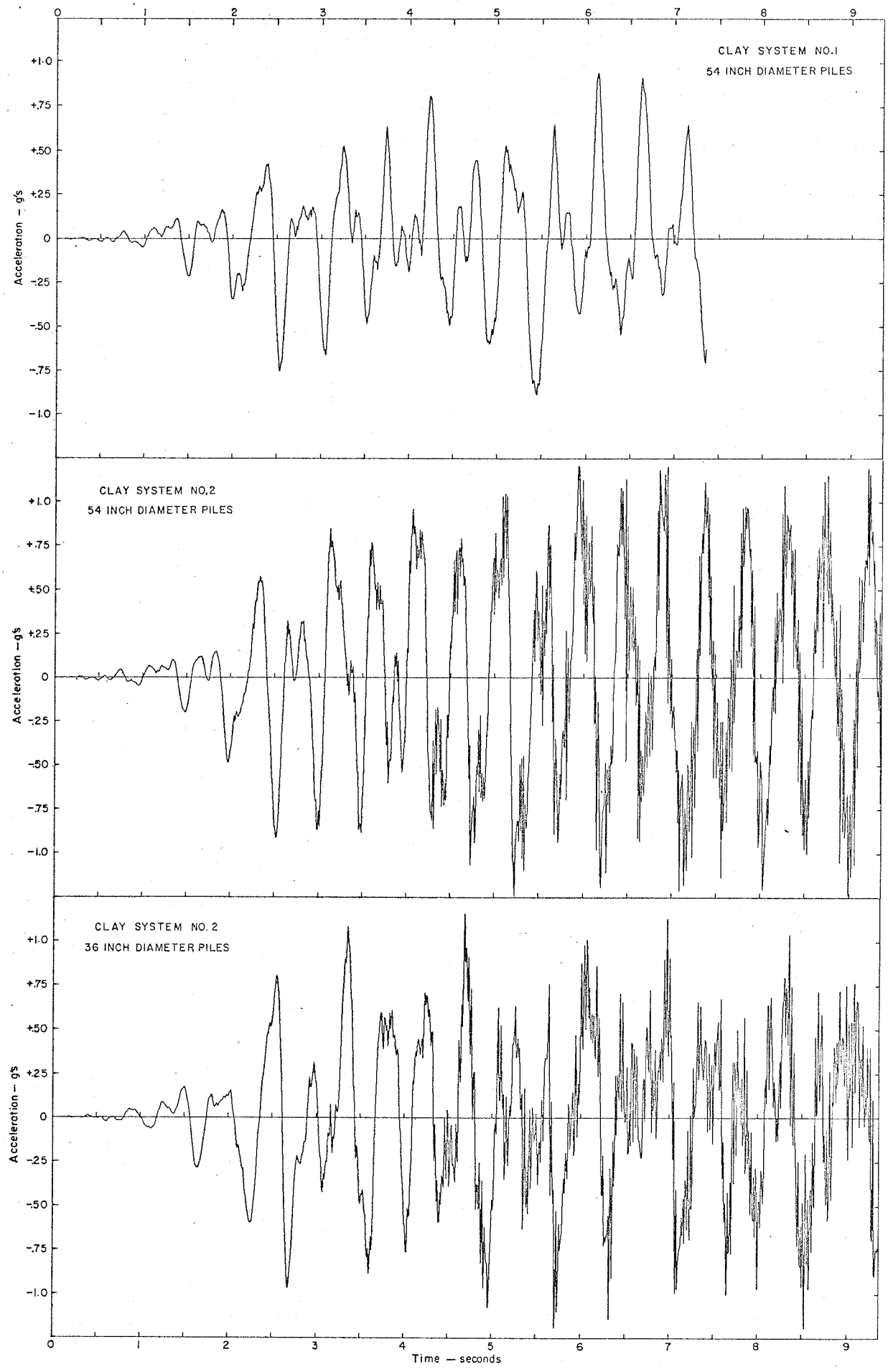

Fig. 47 – TOTAL LONGITUDINAL ACCELERATION OF PILE CAP -- MULTIPLE PILE ROW GROUPING.

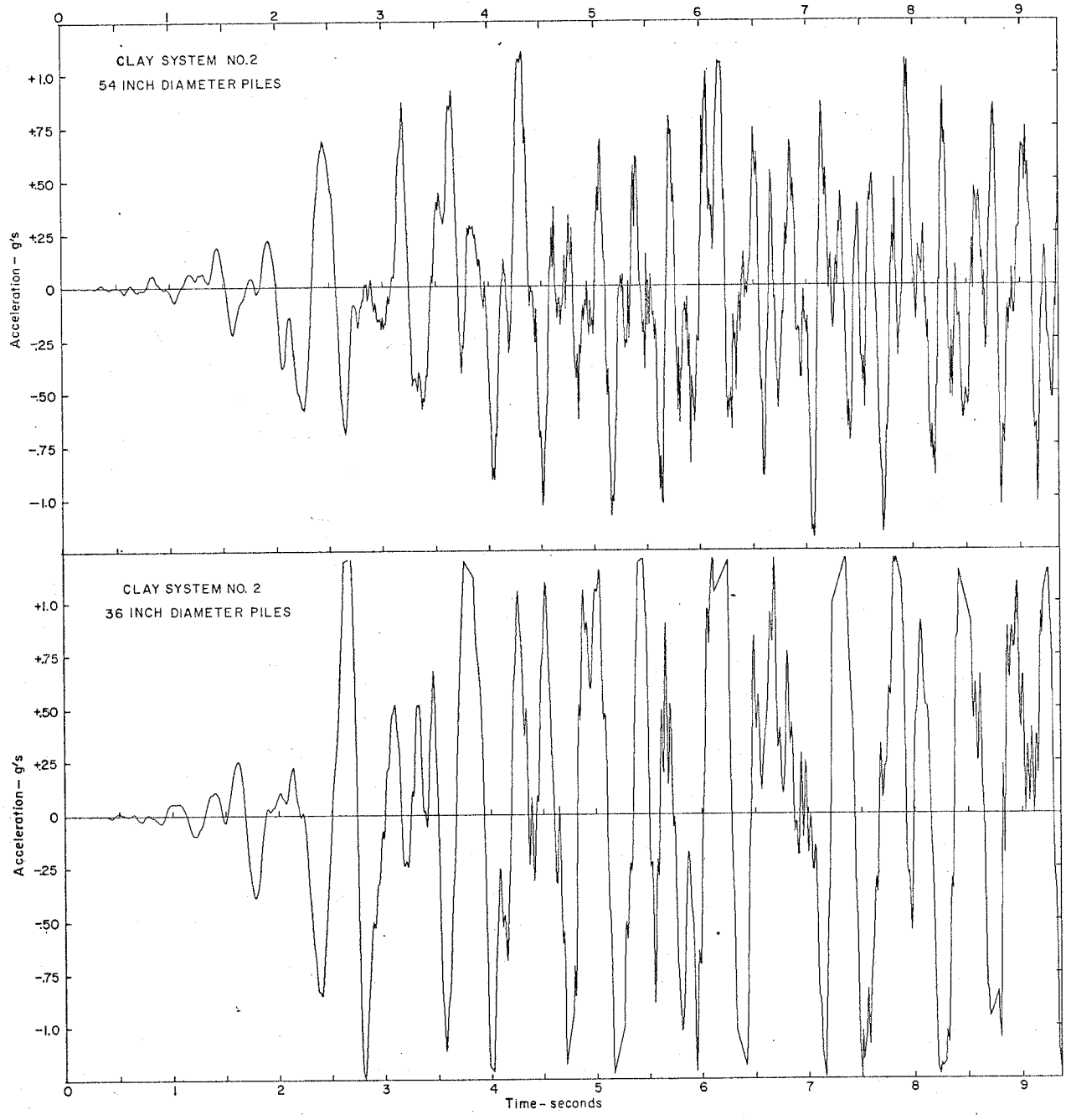

Fig. 48 - TOTAL LONGITUDINAL ACCELERATION OF PILE CAP -- SINGLE PILE ROW GROUPING.

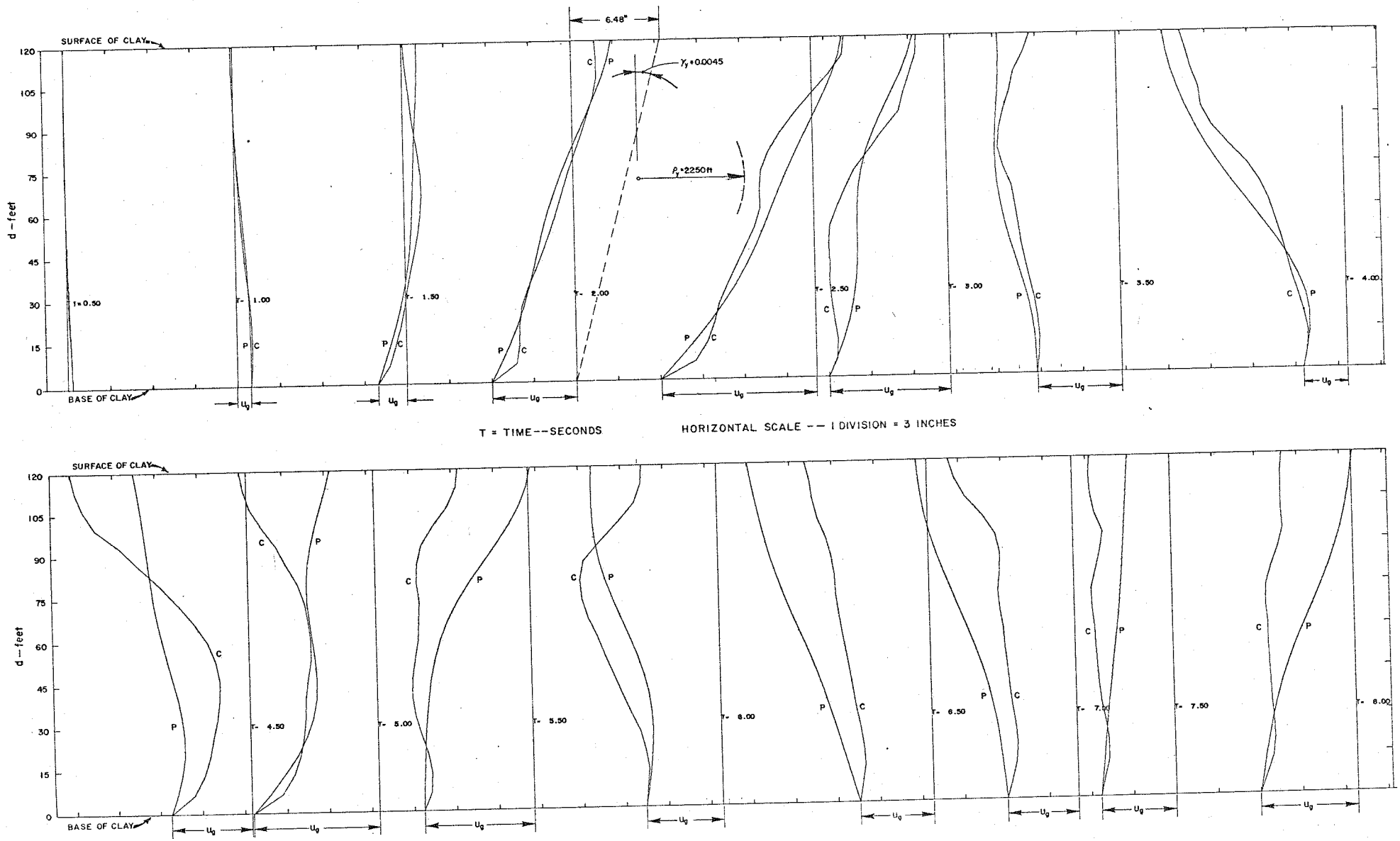

Fig. 49 - DEFLECTED SHAPES OF CLAY AND INTERACTION SYSTEMS
MULTIPLE ROW PILE GROUPING -- CLAY SYSTEM NO. 1 - 54 INCH PILES.

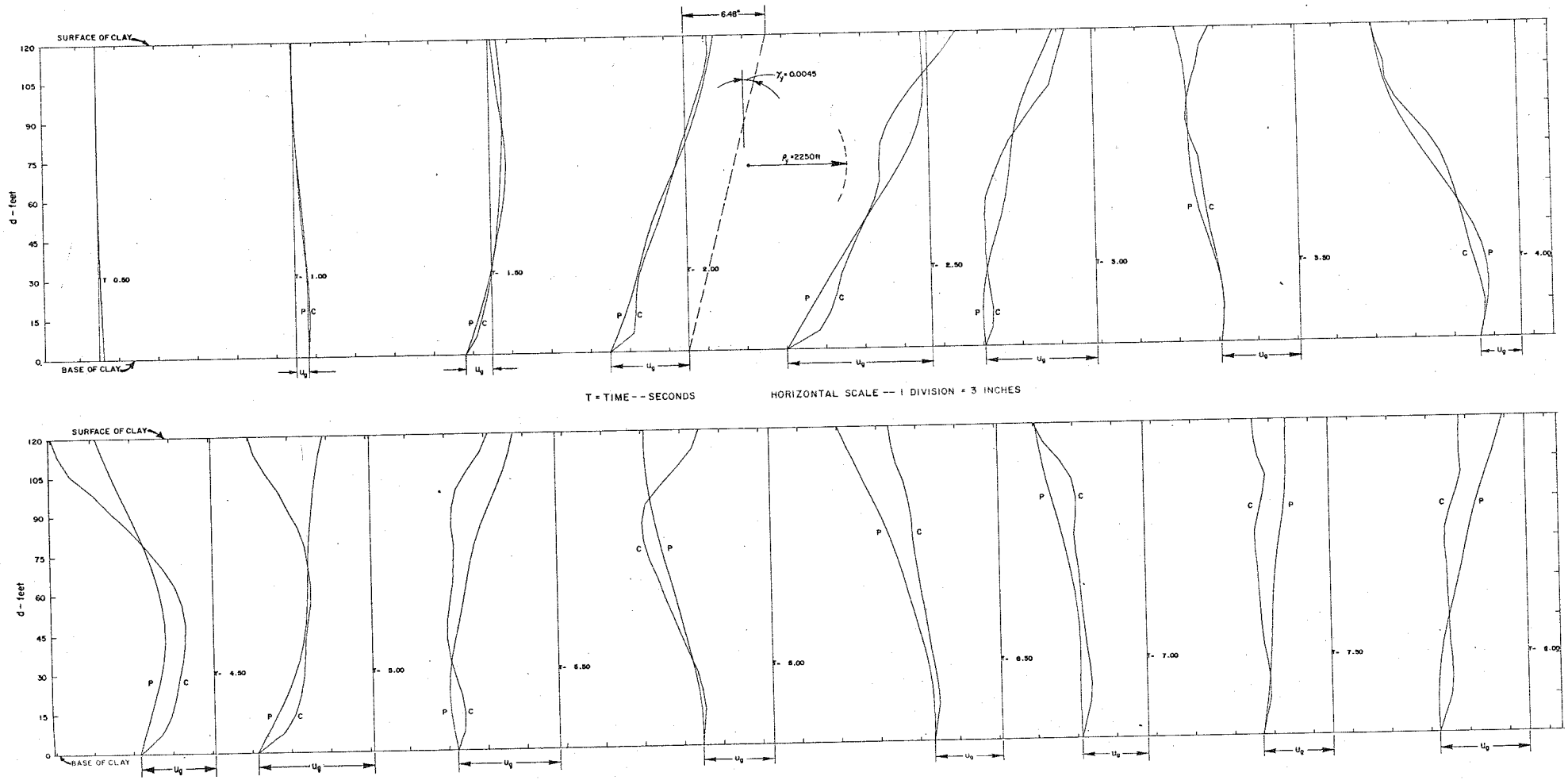

Fig. 50 - DEFLECTED SHAPES OF CLAY AND INTERACTION SYSTEMS
SINGLE ROW PILE GROUPING -- CLAY SYSTEM NO. 1 - 54 INCH PILES.

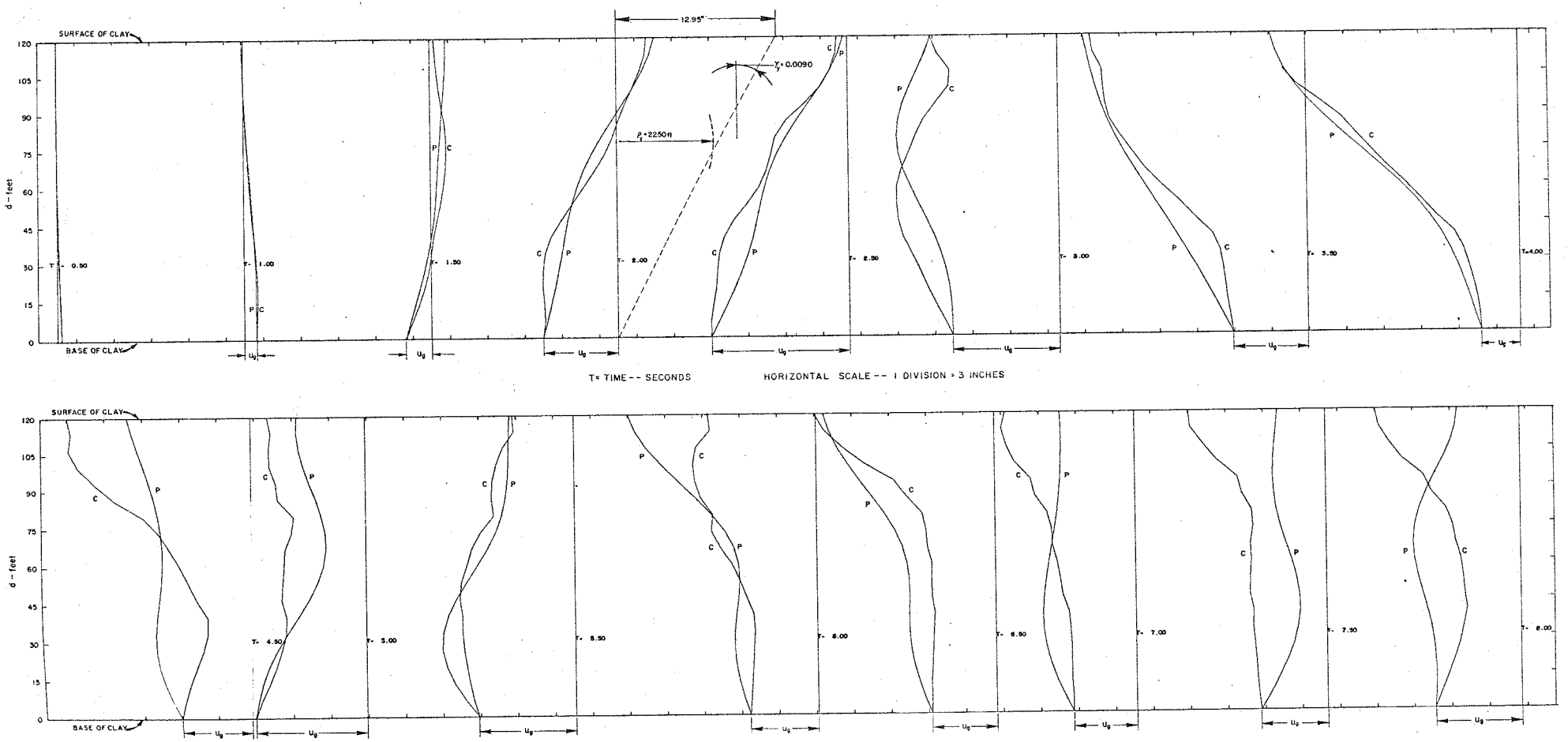

Fig. 51- DEFLECTED SHAPES OF CLAY AND INTERACTION SYSTEMS
MULTIPLE ROW PILE GROUPING -- CLAY SYSTEM NO. 2-54 INCH PILES.

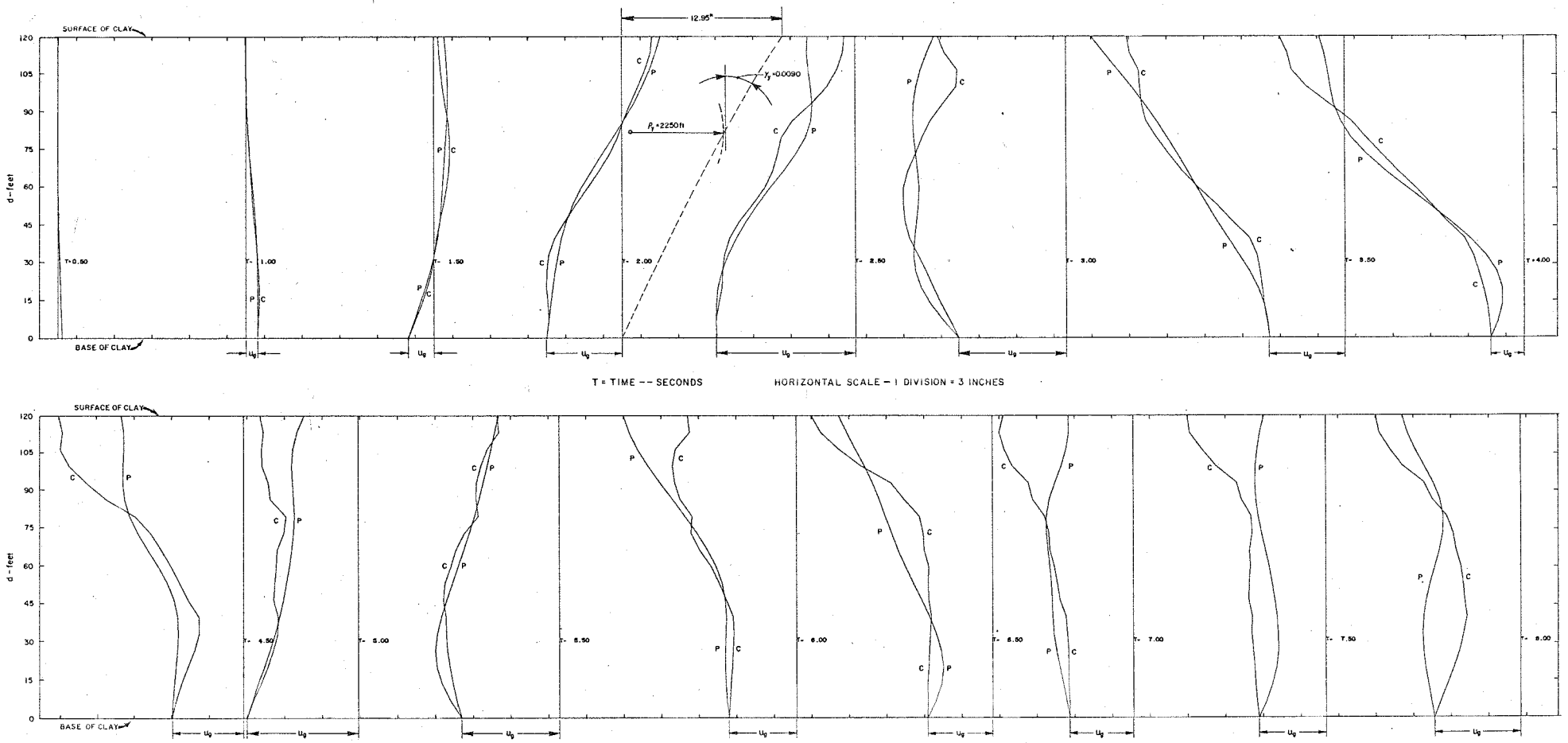

T = TIME -- SECONDS HORIZONTAL SCALE - 1 DIVISION = 3 INCHES

Fig.52-DEFLECTED SHAPES OF CLAY AND INTERACTION SYSTEMS
SINGLE ROW PILE GROUPING--CLAY SYSTEM NO.2 - 54 INCH PILES.

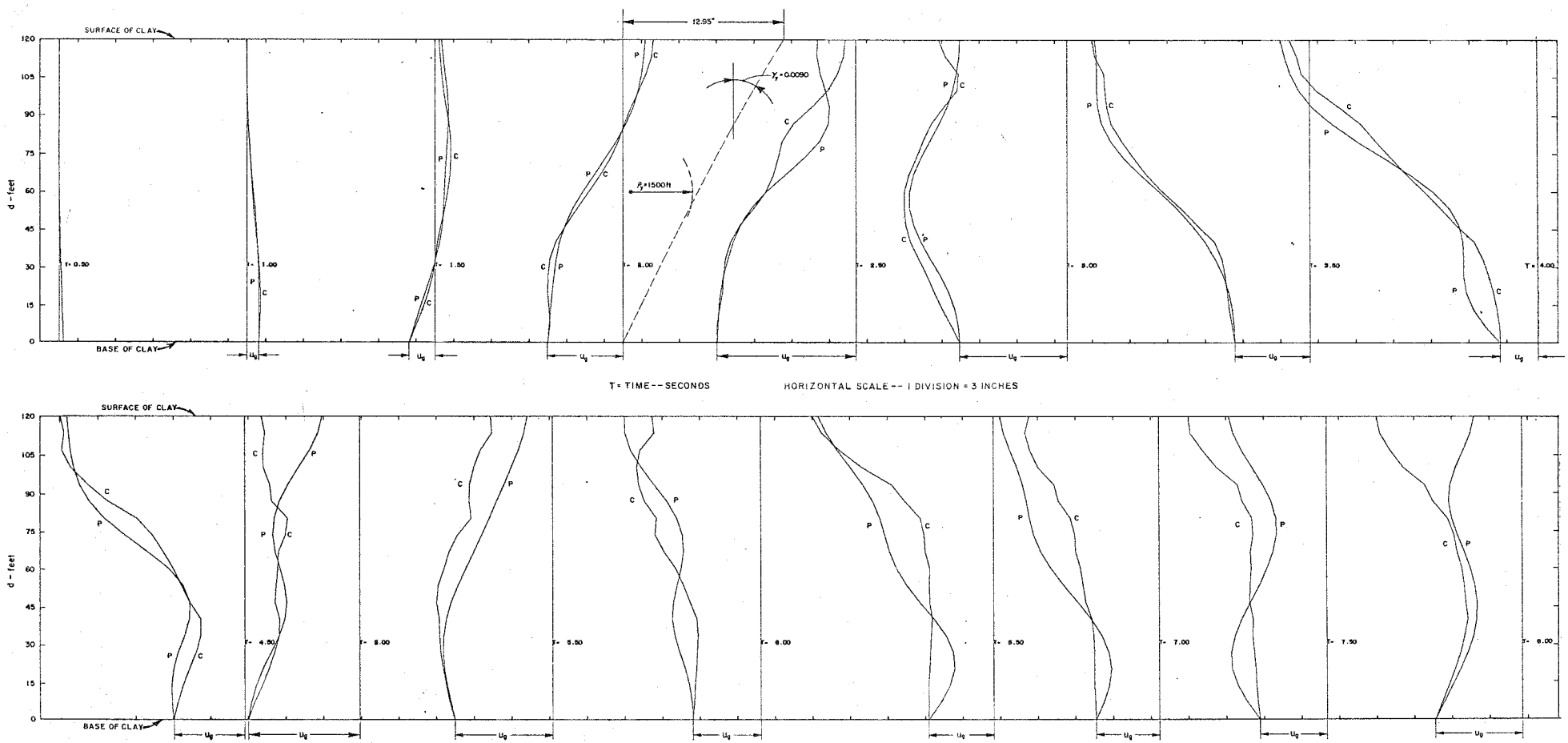

T = TIME -- SECONDS HORIZONTAL SCALE -- 1 DIVISION = 3 INCHES

Fig.53 – DEFLECTED SHAPES OF CLAY AND INTERACTION SYSTEMS
MULTIPLE ROW PILE GROUPING -- CLAY SYSTEM NO. 2 - 36 INCH PILES.

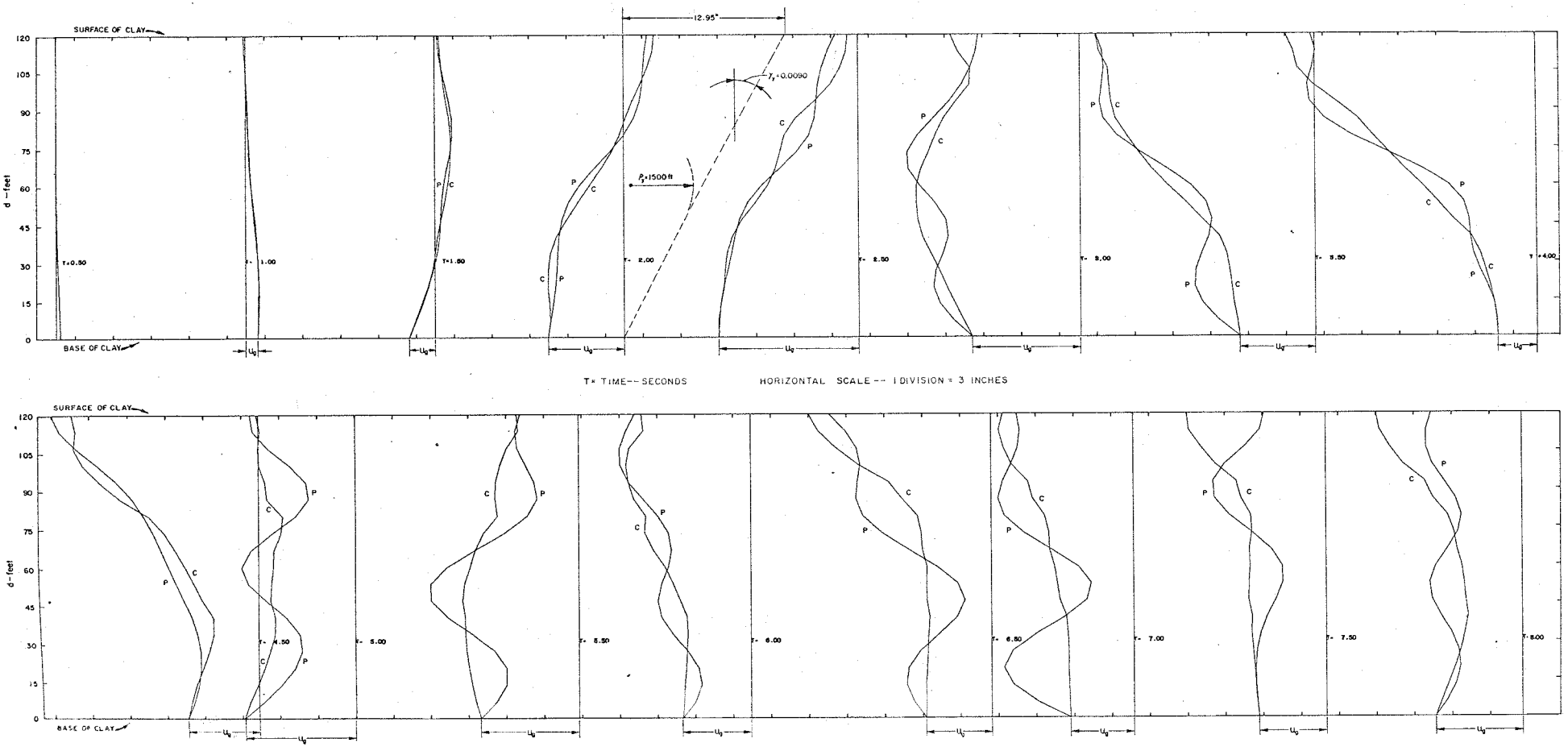

T = TIME -- SECONDS HORIZONTAL SCALE -- 1 DIVISION = 3 INCHES

Fig. 54 - DEFLECTED SHAPES OF CLAY AND INTERACTION SYSTEMS
SINGLE ROW PILE GROUPING - CLAY SYSTEM NO 2 - 36 INCH PILES.

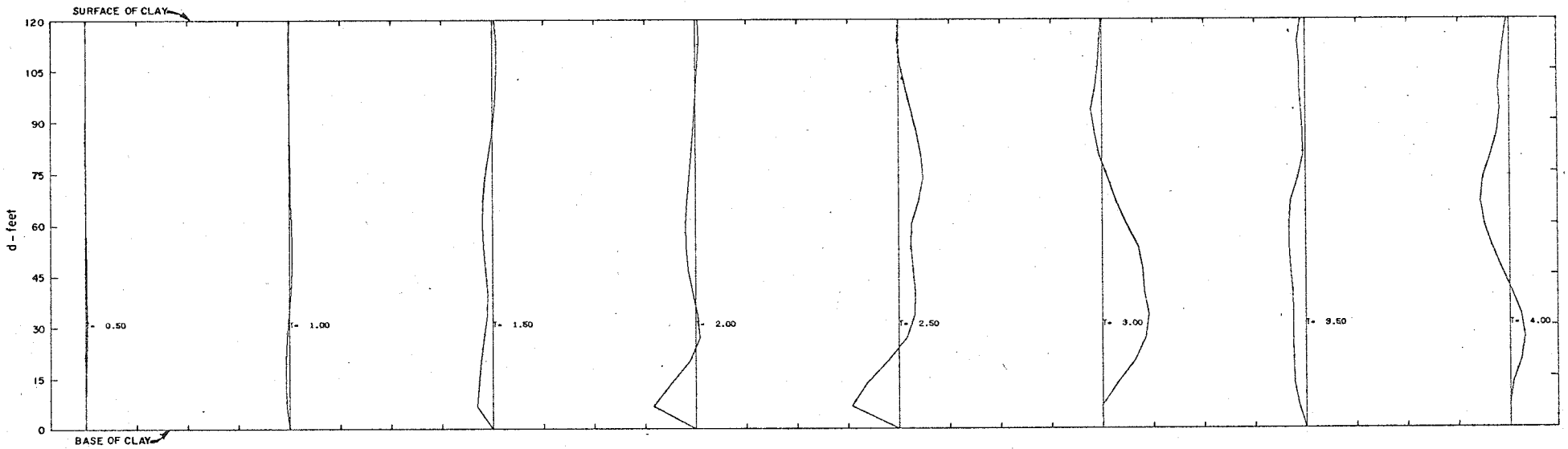

T = TIME -- SECONDS HORIZONTAL SCALE-- 1 DIVISION = 60 KIPS / FT

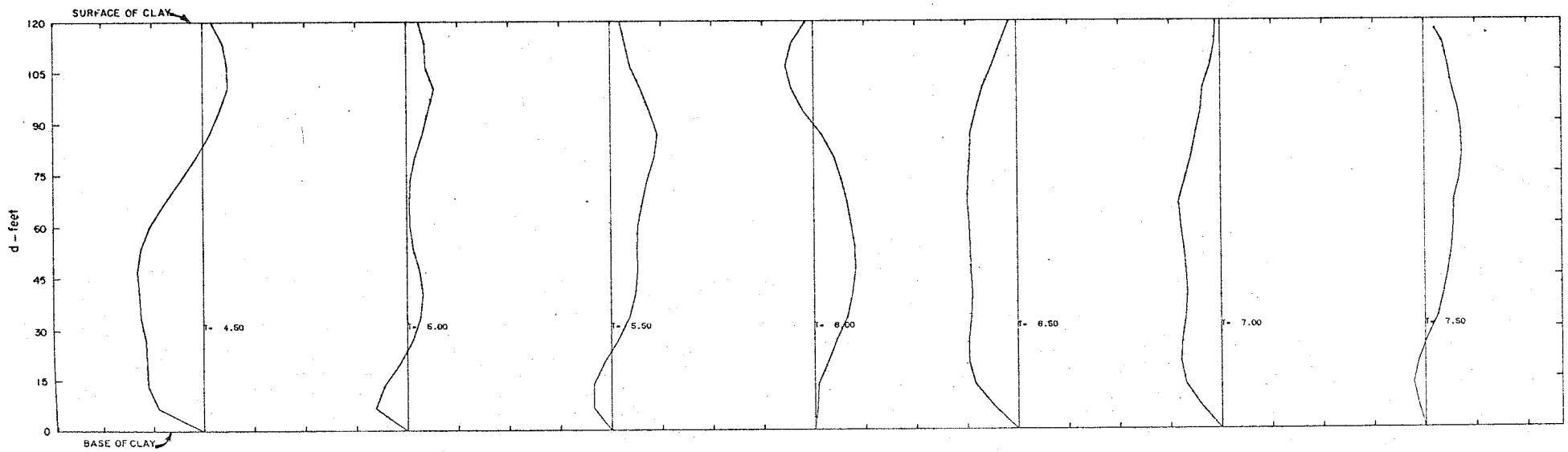

Fig.55-TOTAL FORCE DISTRIBUTION ALONG MULTIPLE ROW PILE GROUPING - - CLAY SYSTEM NO. 1 - 54 INCH PILES.

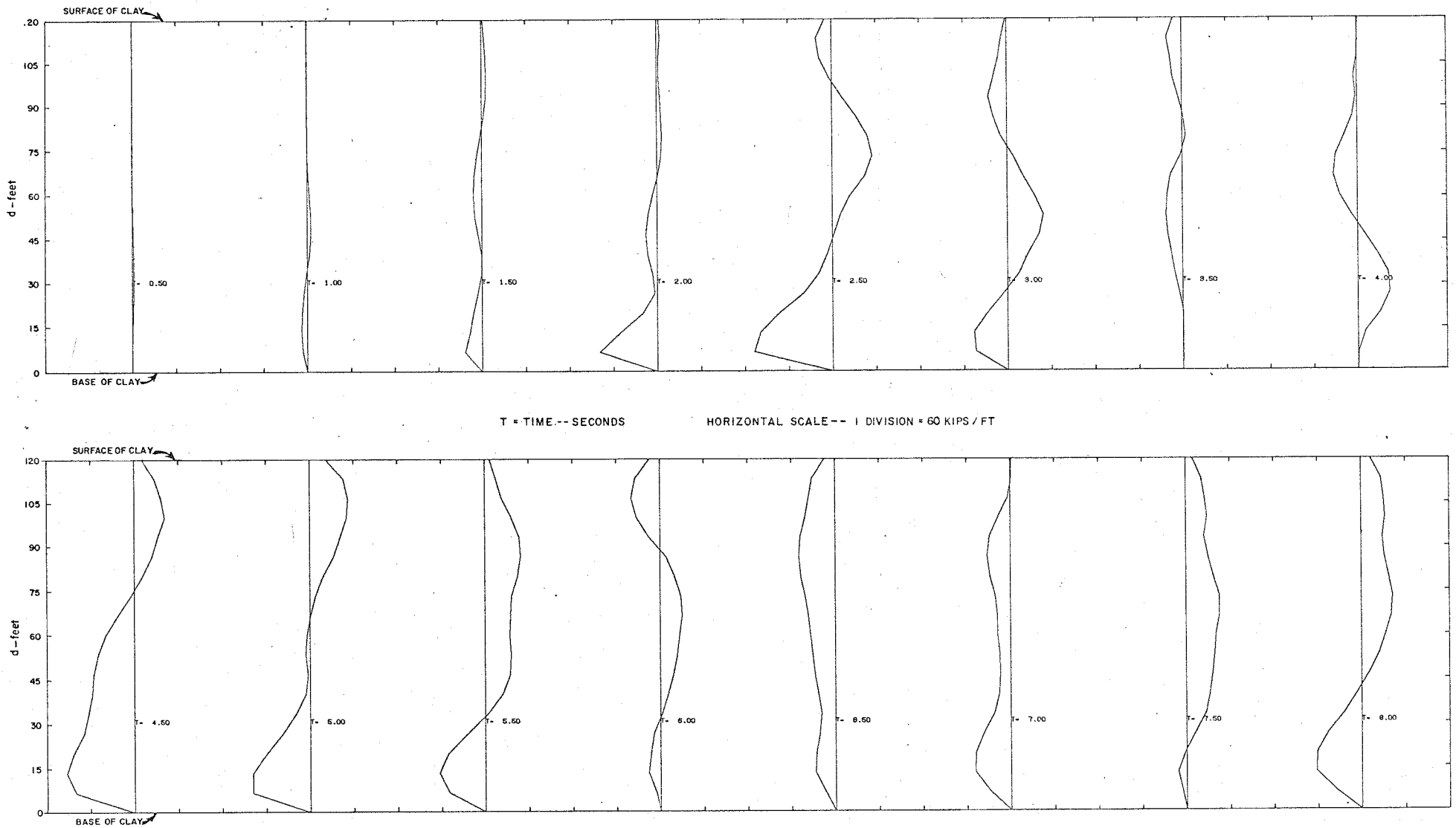

Fig. 56 - TOTAL FORCE DISTRIBUTION ALONG SINGLE ROW PILE GROUPING -- CLAY SYSTEM NO. 1 - 54 INCH PILES.

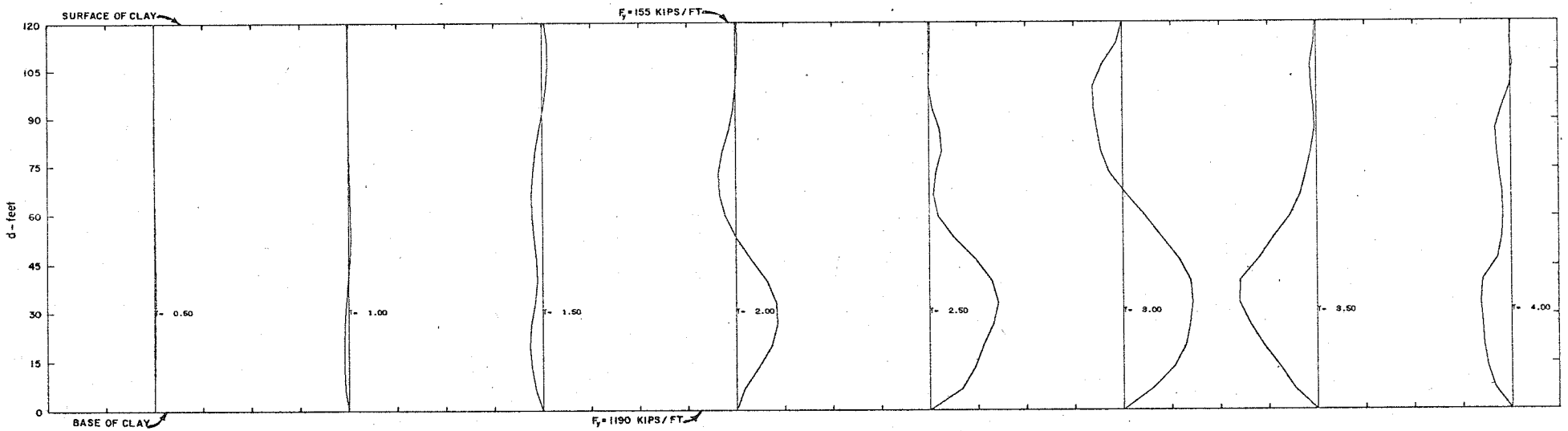

T = TIME -- SECONDS HORIZONTAL SCALE -- 1 DIVISION = 60 KIPS/FT

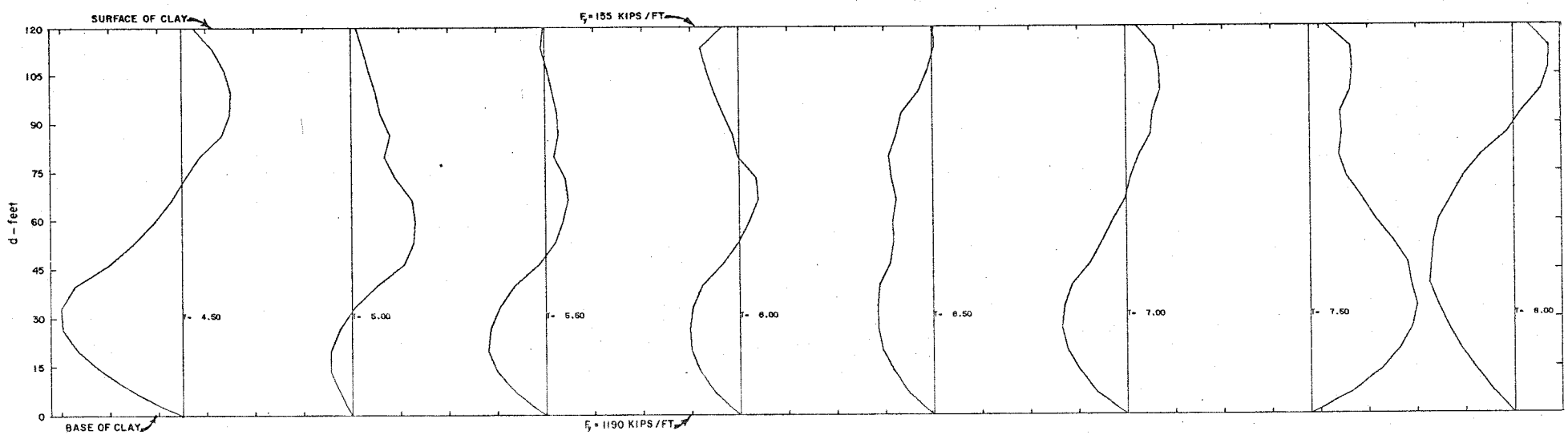

Fig. 57- TOTAL FORCE DISTRIBUTION ALONG MULTIPLE ROW PILE GROUPING -- CLAY SYSTEM NO. 2 - 54 INCH PILES.

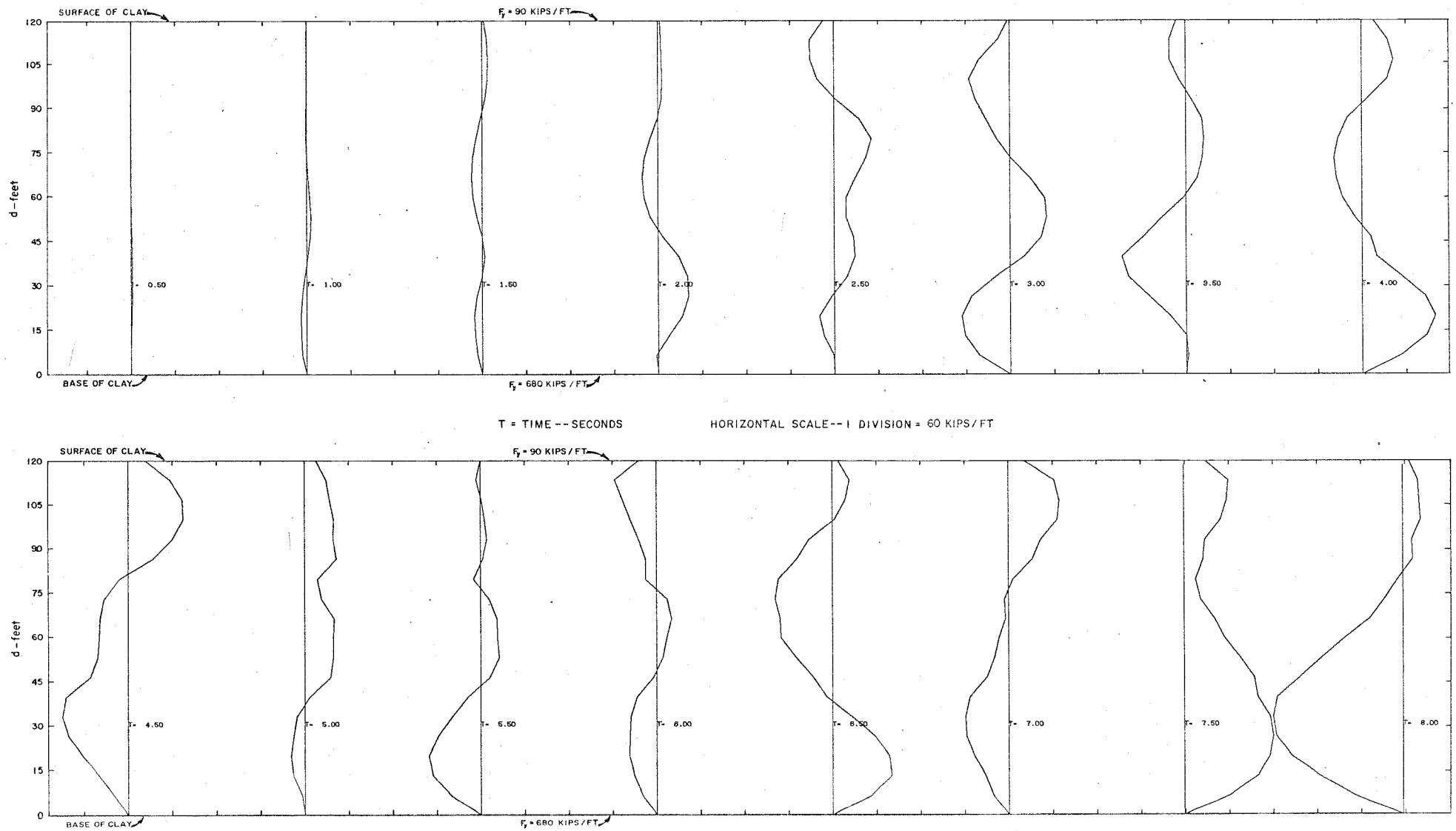

Fig. 58 - TOTAL FORCE DISTRIBUTION ALONG SINGLE ROW PILE GROUPING -- CLAY SYSTEM NO. 2 - 54 INCH PILES.

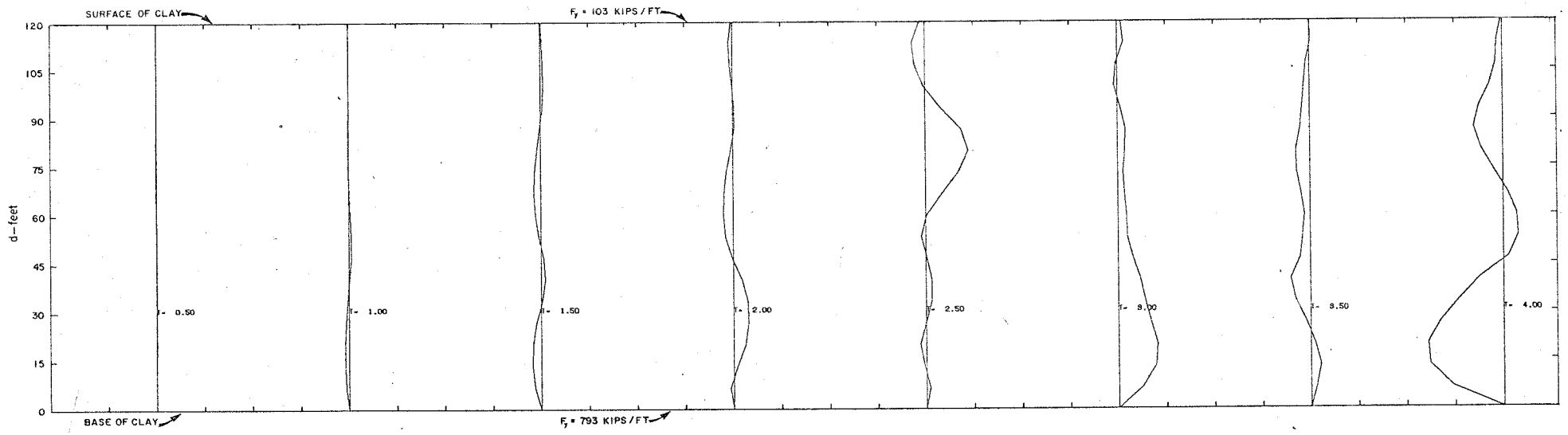

T = TIME--SECONDS HORIZONTAL SCALE-- 1 DIVISION = 60 KIPS/FT

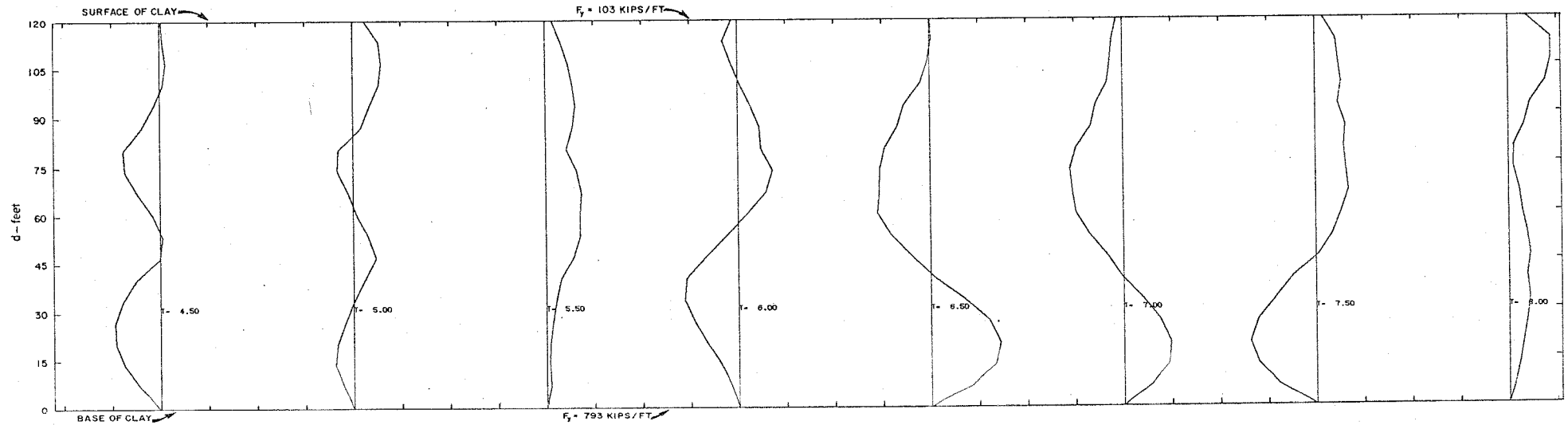

Fig. 59 - TOTAL FORCE DISTRIBUTION ALONG MULTIPLE ROW PILE GROUPING-- CLAY SYSTEM NO. 2 - 36 INCH PILES.

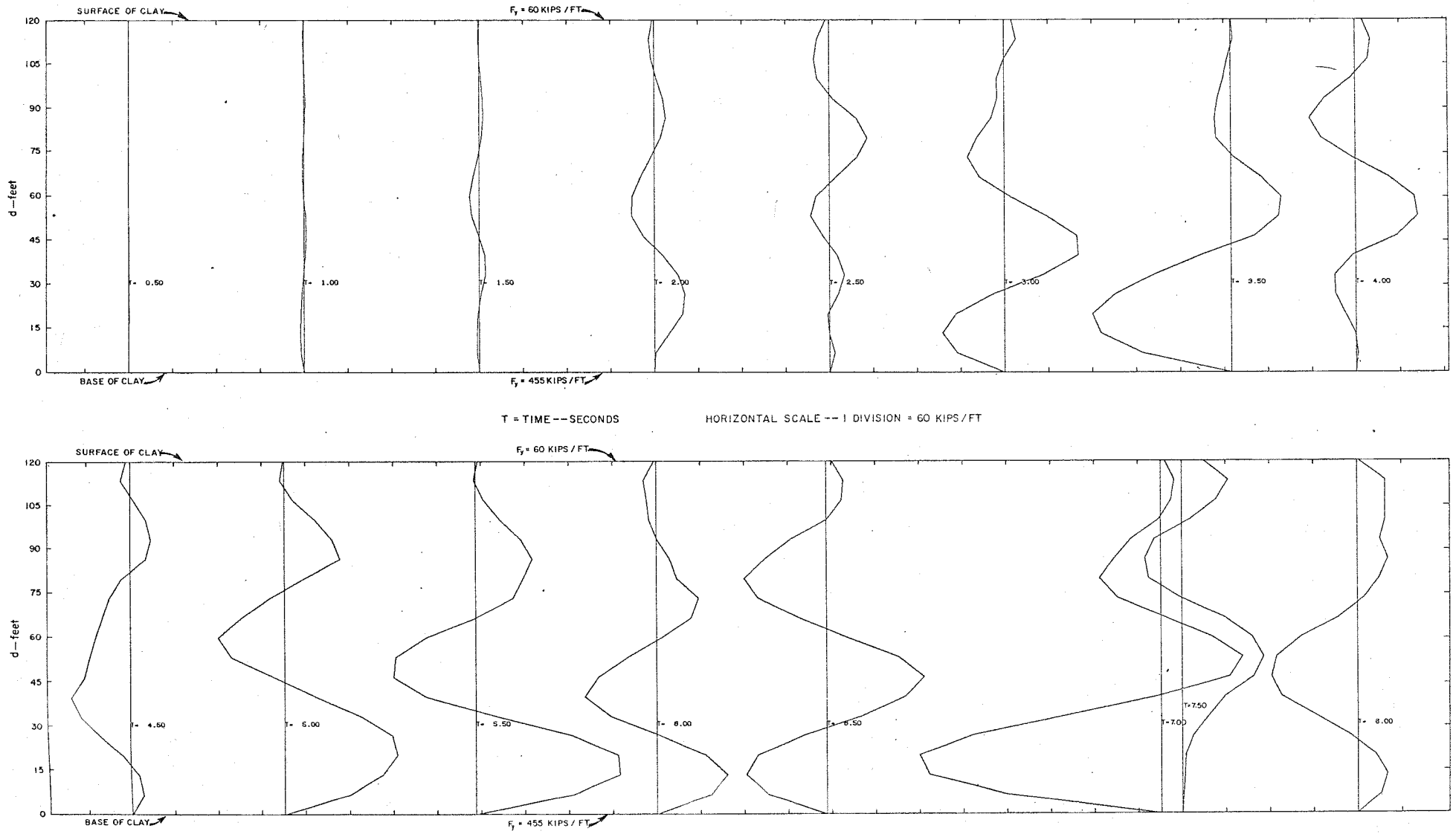

Fig. 60- TOTAL FORCE DISTRIBUTION ALONG SINGLE ROW PILE GROUPING -- CLAY SYSTEM NO. 2 - 36 INCH PILES.

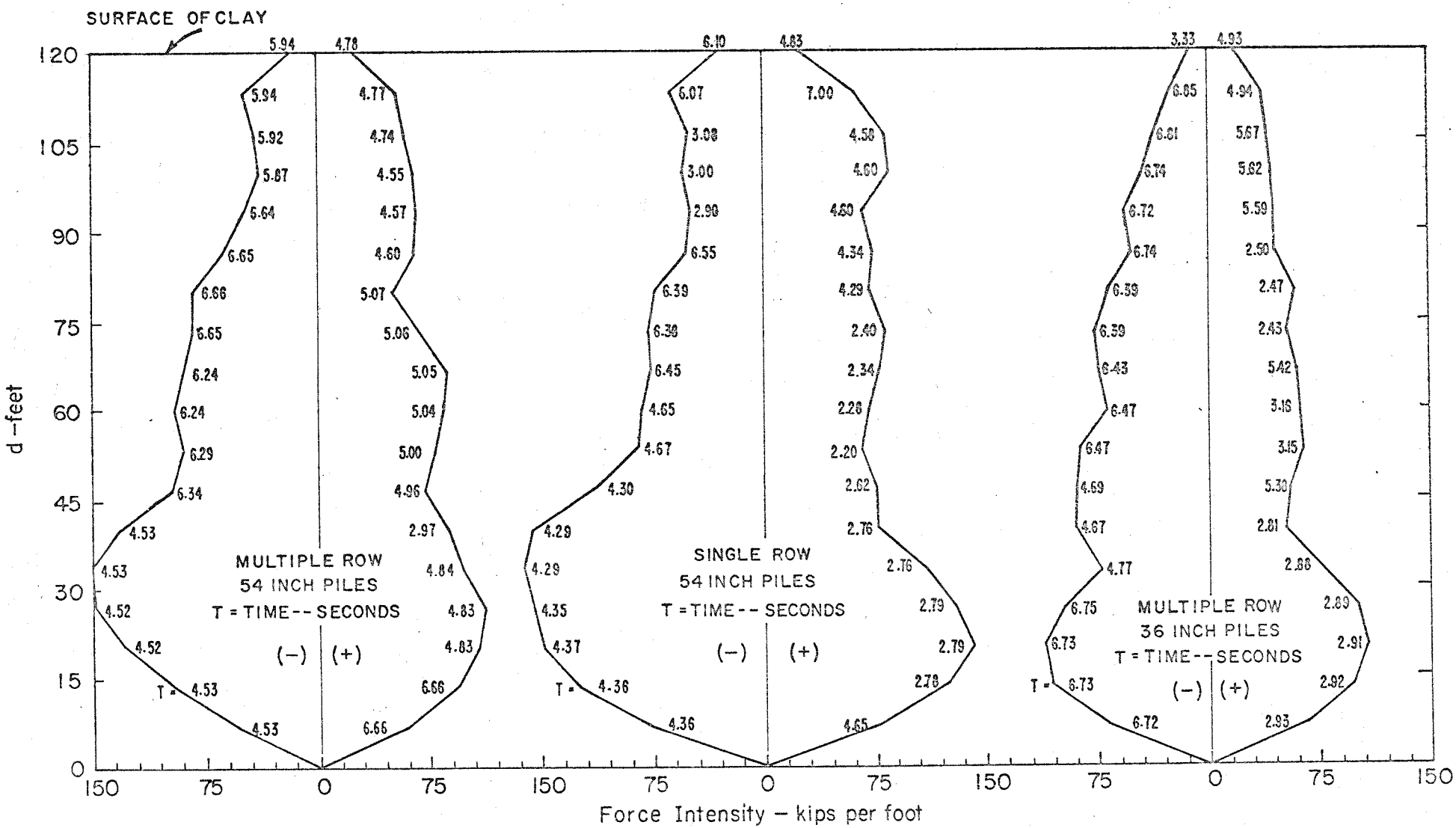

Fig.61 - MAXIMUM POSITIVE AND NEGATIVE FORCE INTENSITY ENVELOPE FOR PILE GROUPINGS -- KIPS PER FOOT.

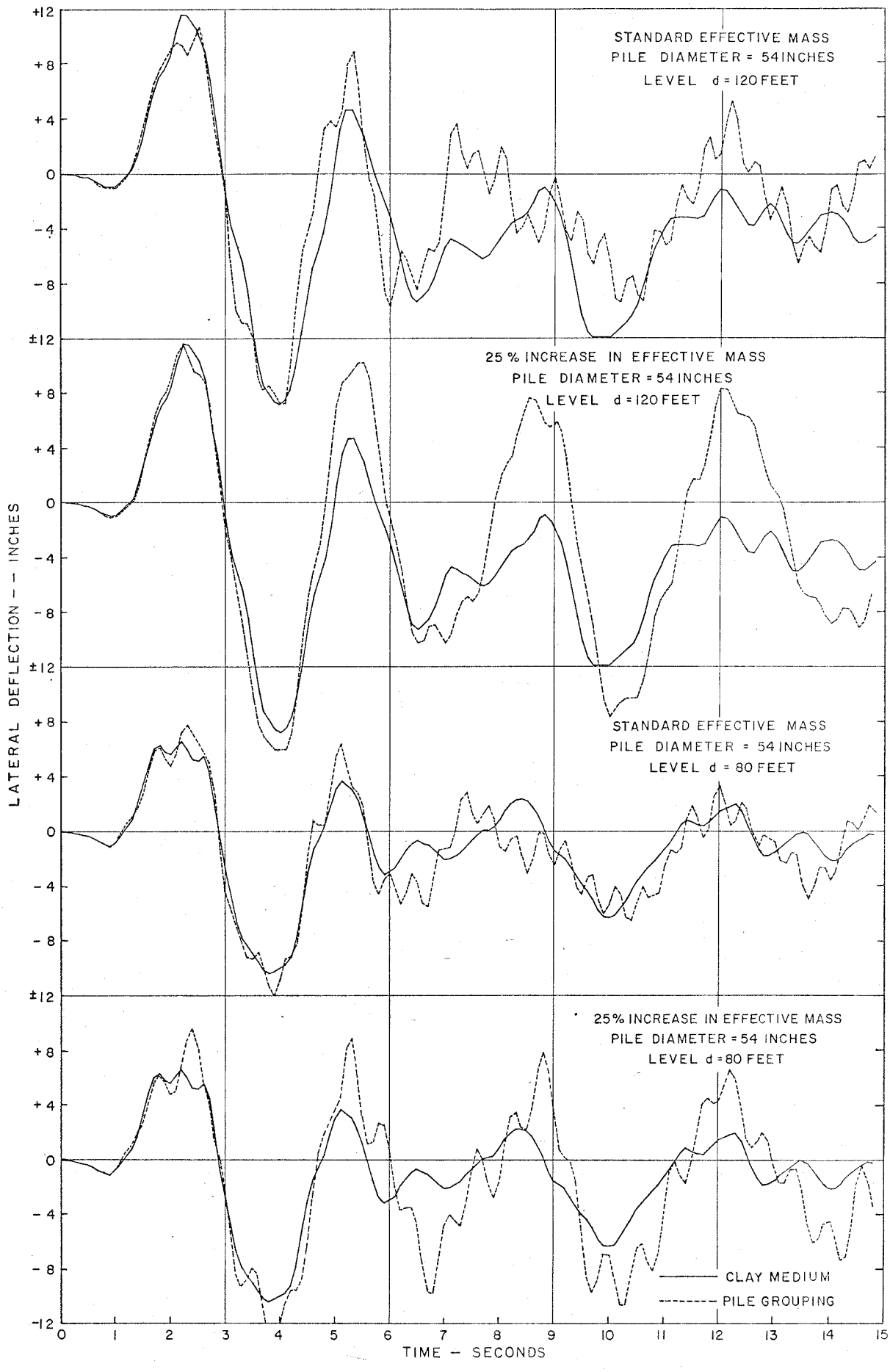

Fig. 62- LATERAL DEFLECTION OF CLAY MEDIUM AND MULTIPLE ROW PILE GROUPING WITH RESPECT TO MOVING BASE VS TIME.

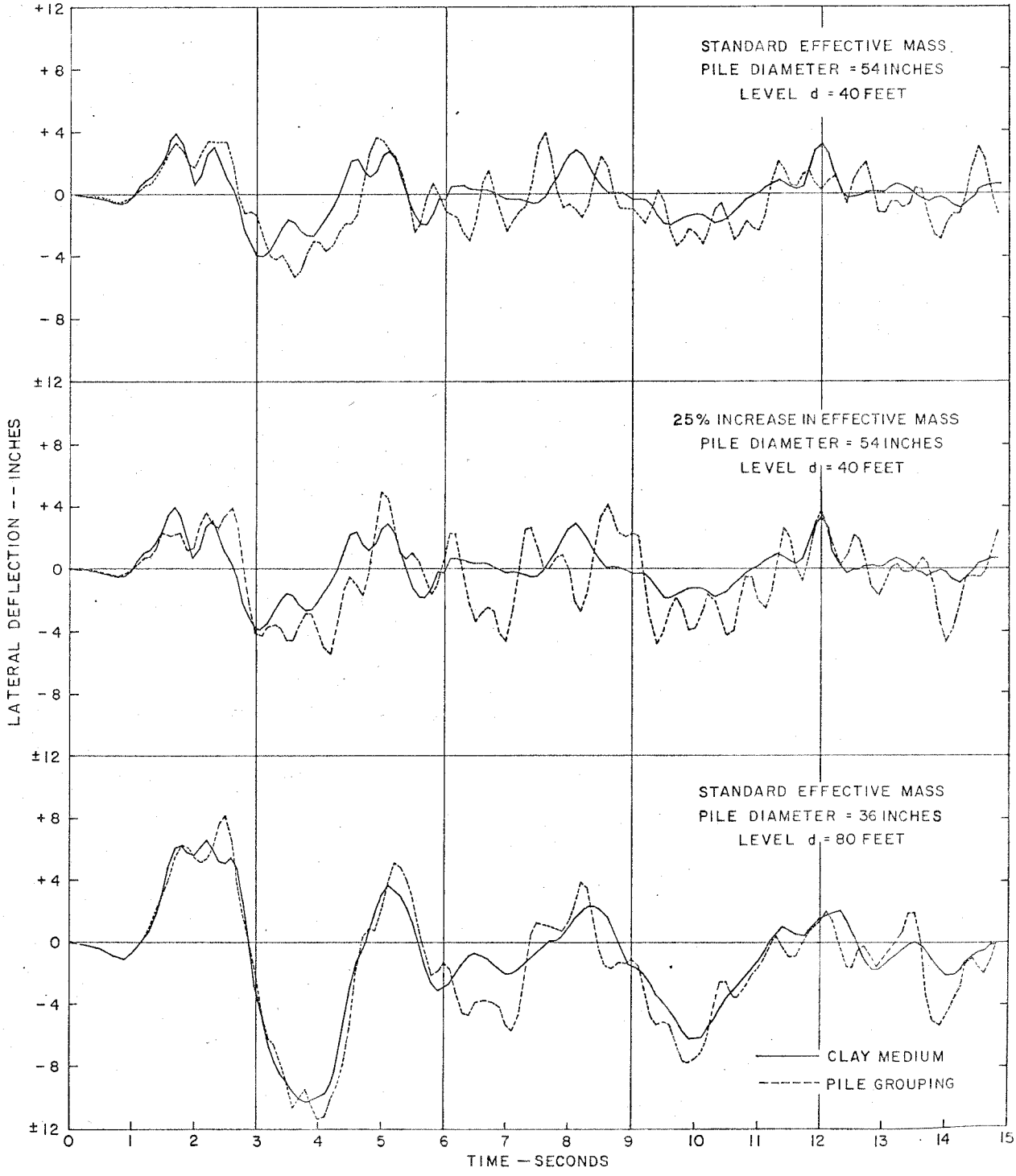

Fig. 63 - LATERAL DEFLECTION OF CLAY MEDIUM AND MULTIPLE ROW PILE GROUPING WITH RESPECT TO MOVING BASE VS. TIME.